DRI LAKE TAHOE SOURCE CHARACTERIZATION STUDY: FINAL REPORT

October 22, 2004

Prepared by:

Hampden Kuhns
M.-C. Oliver Chang
Judith C. Chow
Vic Etyemezian
Lung-Wen Antony Chen
Nicholas Nussbaum
Suresh Kumar K. Nathagoundenpalayam
Dana Trimble
Steve Kohl
Mary MacLaren
Mahmoud Abu-Aliban
Jack Gillies
Alan Gertler

(hkuhns@dri.edu)
Desert Research Institute
2215 Raggio Pky
Reno, NV 89512
Ph: (775) 674 7111
Fax: (775) 674 7060

Chris Damm
Cliff Denney
Candace Gallery
John Skotnik

Sierra Nevada College
999 Tahoe Boulevard
Incline Village, NV 89451-9500

Report prepared for:

Ash Lashgari
California Air Resources Board
1001 I Street
Sacramento, CA 95812
Ph: (916) 323-1506

EXECUTIVE SUMMARY

This study investigated the chemical composition and emission factors of selected particulate matter (PM) sources in the Lake Tahoe basin. PM is of interest because particles either by themselves or acting as nutrients or attachment points for algae are obscuring water clarity in the lake. Particulate matter (PM) samples directly relevant to major PM sources in Lake Tahoe were collected and analyzed as part of this study. Sources sampled included residential wood combustion, motor vehicle exhaust, and entrainment of road dust, traction control material, and road deicing material.

In addition, several new emission measurement technologies were applied during this study to investigate residential wood combustion, motor vehicle exhaust, and reentrained road dust.

The major chemical components of wood-burning PM emissions are organic carbon (OC) and elemental carbon (EC). Total carbon (TC) accounts for 15% to 74 % of PM2.5 mass. TC fractions of $PM_{2.5}$ mass from hardwood are generally higher than from softwood, and higher from fireplaces than from woodstoves. Crustal elements were found with high variability, probably contributed from ambient background during sample collection.

Measurements indicated that the between 40% to 90%of PM mass emissions from motor vehicles are composed of road dust material (i.e. silicon, aluminum, iron, and organic carbon). Road dust entrainment may be the dominant source of coarse organic carbon PM. The application of brine solution as a deicer on the roads produced downwind coarse particle (PM_{10} – $PM_{2.5}$) source profiles that were enriched with both sodium (21%) and chloride (22%). Motor vehicle exhaust was composed of organic (54%) and elemental carbon (15%), resulting in an elemental to total carbon ratio of 0.23. This is approximately a factor of two higher than the ratio observed in wood smoke.

Approximately ~2% of the fleet on local streets in Incline Village and on Highway 28 are heavy duty diesel vehicles (HDDV). For comparison 4% of the vehicle kilometers traveled (VKT) in Las Vegas are from HDDV. Fuel based emission factors were calculated by normalizing pollutants measured in emission plumes to the amount of excess carbon in the plume as CO_2, CO, and hydrocarbons. Fuel based emission factors have units of grams of pollutants per kilogram of fuel burned. Fleet average fuel-based emission factors of motor vehicle CO (23 g/kg fuel) and NO (1.6 g/kg fuel) were lower than recent remote sensing and tunnel studies by a factor of 3 or more. Both ammonia (0.33 g/kg fuel) and $PM_{0.59}$ (0.083 g/kg fuel) motor vehicle exhaust emission factors were in very good agreement with results from other studies.

Around the lake, road dust emissions varied by a factor of three from 0.5 g/vkt in early April to 0.17 g/vkt in mid-July. These reductions were associated with a decrease in precipitation and either a reduction in mud track-out onto road and/or a cessation of the application of traction control material.

A business survey identified 17 gas stations in the basin selling at total of 53600 Mg gasoline/year. The fuel sales were multiplied by the fuel based emission factors to estimate annual emissions of CO, NO, NH_3, and $PM_{0.59}$ as 1200 Mg/yr, 19 Mg/yr, 86 Mg/yr, and 4.4 Mg/yr, respectively. These estimates to not include contributions from cold starts, diesel vehicles, or fuel purchased outside of the basin. Previous studies have shown that cold starts may account for 20% or more of the total emissions from light duty motor vehicles. At only 2%

of the VKT in the basin, diesel vehicles may emit as much as 20% to 30% PM from mobile exhaust sources.

Measurements of road dust emission factors with the TRAKER vehicle consistently showed ~20%-30% higher PM emission factors in California than in Nevada. Differences in road maintenance practices based on jurisdiction may account for the variation in emission factors. Road dust emission factors from South Lake Tahoe, CA and Incline Village, NV were nearly equivalent. The largest emission factors were observed at the entrances to subdivisions and neighborhoods.

All measured emissions data from this study were compared with the CARB Tahoe Air Basin emission inventory scaled to the entire basin. The CARB emission estimates derived from the EMFAC model were 2 to 10 times greater than the measured on-road exhaust emissions based on estimated fuel consumption. Paved road dust, residential wood combustion, and campfire emissions were in general agreement with the CARB estimates. For particulate matter, the combined emission inventory indicates that residential wood combustion, unpaved road dust, and paved road dust are the largest sources.

ACKNOWLEDGEMENTS

We would like express our appreciation to the following individuals for their generous contributions of time and effort to this project. Thanks to:

Mark Kinter (*Elgin Sweeper*) for discussion of street sweeping practices in the Tahoe Basin.

Rita Whitney (*Tahoe Regional Planning Agency*) for supplying area public works Maintenance Efficiency Plans.

Rod Sevini and Janet Reck (Washoe County Public Works) for providing right of way permits and arranging for street sweeping, brine application, and traction control material application for roadside tests.

Robert Sawyer (U.C. Berkely) for the use of his cabin to conduct wood smoke testing.

TABLE OF CONTENTS

1. INTRODUCTION 1-1
1.1. Objectives 1-2
1.2. Guide to Report 1-2
2. MEASUREMENT METHODS 2-1
2.1 In-Plume Sampling System 2-1
2.1.1 Instrument Descriptions 2-3
2.1.2 Laboratory Sample Analysis 2-7
2.1.3 Data Processing 2-8
2.2 Flux Towers and Ambient Monitors 2-20
2.3 TRAKER Vehicle 2-23
2.3.1 Inlets 2-24
2.3.2 Instruments Used Onboard TRAKER 2-27
2.3.3 Data Acquisition and Measurement Documentation 2-27
2.3.4 TRAKER Data Processing 2-27
2.3.5 Relationship of TRAKER measurement to vehicle speed 2-30
2.4 Comparison of TRAKER with Flux Towers 2-32
3. RESIDENTIAL WOOD COMBUSTION (RWC) 3-1
3.1. Summary of wood burning appliances and wood fuels in the Lake Tahoe region 3-1
3.2. Source testing for RWC 3-1
3.3. Summary of Wood Burning Profiles 3-4
3.4. Fraction of Background in RWC Source Profile 3-17
3.5. Fuel-Based Emission Factor Calculation for RWC 3-18
4. MOTOR VEHICLE EXHAUST 4-1
4.1. Exhaust source profiles with soil subtraction 4-4
4.2. Fraction of Background in Motor Vehicle Exhaust Source Profile 4-14
4.3. Fuel Based Emission Factors for Motor Vehicle Exhaust 4-15
4.3.1. CO Emission Factors 4-15
4.3.2. NH_3 Emission Factors 4-16
4.3.3. PM Emission Factors 4-18
4.3.4. Emission Factors of NO 4-18
4.3.5. Emissions from Other Species 4-18
5. ROAD DUST 5-1
5.1. Flux Tower Location and Dates 5-1
5.1.1. Calculated Emission Factors 5-2
5.2. TRAKER Survey Routes and Dates 5-4
5.2.1. Summary of TRAKER measurements 5-5
5.3. Geological source profiles 5-12
6. BASIN WIDE EMISSIONS CALCULATIONS 6-1
6.1. Motor Vehicle Exhaust 6-1
6.1.1 Vehicle kilometers traveled in the basin 6-1
6.1.2 Fuel sales and basin exhaust emissions 6-1
6.1.3 Comparison of VKT with Fuel Sales 6-3
6.1.4 Annual Average Tahoe Basin Vehicle Exhaust Emissions 6-4
6.2. Road Dust Emissions 6-6

6.3. Wood Burning Emissions 6-6
6.4. Additional Sources 6-9
6.5. Emissions Summary 6-13
7. SUMMARY AND CONCLUSIONS 7-1
7.1. Source Profiles 7-1
7.2. Emission Factors 7-2
7.3. Emission Inventory 7-3
8. RECOMMENDATIONS 8-1
9. REFERENCES 9-1
10. APPENDICES 10-1
10.1. Daily Maps of TRAKER Routes 10-1

TABLE OF TABLES

Table 2-1. Instrumentation of In-Plume Sampling System. 2-3
Table 2-2. Gases analyzed using classical least squares analysis of infrared spectra from FTIR.2-4
Table 2-3. Emission factor results for vehicles associated with individual plumes. 2-16
Table 2-4. Validity criteria applied to each 1 sec TRAKER data point. 2-29
Table 3-1. Wood burning tests conducted at Lake Tahoe residences during November and December 2003. 3-2
Table 3-2. Availability of wood fuel at commercial stores in Lake Tahoe region. 3-3
Table 3-3. Summary of residential wood combustion profiles. All values are in percent of total mass. 3-5
Table 3-4. Summary of residential wood combustion profiles. All values are in percent of total mass. The grey column denote an invalid source sample. 3-6
Table 3-5. Intercomparisons among samples for each combination of wood fuel and residential wood combustion appliance. 3-11
Table 3-6. Composite of emission composition profiles for each combination of wood fuel type and RWC appliance. All values are in percent of total mass. 3-12
Table 3-7. Comparison of emission factors estimated from In-Plume Sampling System and AP-42 for RWC* study. 3-19
Table 4-1. Filter sampling data for vehicle exhaust filters collected in Incline Village, NV. 4-5
Table 4-2. Individual source profiles of the five motor vehicle exhausts collected in the Lake Tahoe Study. Values have units of percent of total mass measured on filter. 4-8
Table 4-3. Composite source profiles of motor vehicle exhausts at Lake Tahoe. 4-9
Table 4-4. Pair comparisons between motor vehicle profiles in the Lake Tahoe study. 4-10
Table 4-5. Measured emission factors for on road vehicles in Incline Village compared with published values from in-use vehicles. Negative value emission factors for NO_2, N_2O, Formaldehyde, and SO_2 are an artifact of the low signal to noise ratio for the measurement of these species with the FTIR. These values should be interpreted at below the detectable limits of the system and its configuration in the field. 4-17
Table 5-1. Samples collected and emission factors measured downwind of paved road on Highway 28 near Sand Harbor State Park. 5-3
Table 5-2. Schedule of TRAKER measurements conducted in the vicinity of Lake Tahoe. 5-4
Table 5-3. Chemical source profiles of grab samples collected in Incline Village, NV, between 7/26/03 and 7/29/03. Values shown are percentage of total aerosol mass collected on the filter. 5-14
Table 5-4. Chemical source profiles of roadside source samples collected in near Sand Harbor State Park, NV between 3/06/03 and 3/12/03. Values shown are percentage of total aerosol mass collected on the filter. 5-15
Table 5-5. Chemical source profiles of roadside source samples collected in near Sand Harbor State Park, NV, between 3/31/03 and 4/07/03. Values shown are percentage of total aerosol mass collected on the filter. 5-16
Table 5-6. Chemical source profiles of roadside source samples collected in near Sand Harbor State Park, NV, between 4/08/03 and 4/10/03. Values shown are percentage of total aerosol mass collected on the filter. 5-17
Table 6-1. Number of fuel pumps in the Lake Tahoe Basin. 6-2

Table 6-2. Traffic demand and forecasting model attribution of trips and VKT by trip purpose for base year 2003. 6-3
Table 6-3. Vehicle population, activity, and emissions for CARB Tahoe Air Basin and the entire Tahoe basin. Tahoe basin data are calculate by scaling all values with the basin wide VKT. 6-5
Table 6-4. Annual average basin-wide emissions based on fuel consumption and fuel-based emission factors. 6-6
Table 6-5. Basin wide VKT, road dust PM_{10} emission factors, and total road dust PM emissions. 6-6
Table 6-6. Wood burning parameter inconsistencies between this study and Fitz and Lents (2004). 6-7
Table 6-7. Emissions for the Tahoe basin from wintertime residential wood combustion and summertime campfires. 6-9
Table 6-8. CARB Stationary Source Emission Inventory for CARB Tahoe Air Basin (i.e. portions of El Dorado and Placer counties). The base year of the inventory is 2003. All emission units are in Mg/yr. 6-10
Table 6-9. . CARB Area Source Emission Inventory for CARB Tahoe Air Basin (i.e. portions of El Dorado and Placer counties). The base year of the inventory is 2003. All emission units are in Mg/yr. 6-11
Table 6-10. CARB Mobile Source Emission Inventory for CARB Tahoe Air Basin (i.e. portions of El Dorado and Placer counties). The base year of the inventory is 2003. All emission units are in Mg/yr. 6-12
Table 6-11. CARB Natural Source Emission Inventory for CARB Tahoe Air Basin (i.e. portions of El Dorado and Placer counties). The base year of the inventory is 2003. All emission units are in Mg/yr. 6-13
Table 6-12. Comparison of annual emissions estimated from this study with scaled emissions from the CARB Tahoe Air Basin. 6-13
Table 6-13. Emission Inventory for Tahoe Basin. Emissions are estimated by scaling the CARB Tahoe Air Basin emissions with a multiplier based on land area, population, or VKT. Sources marked with an asterisk (*) were measured as part of this study. All emissions are presented with units of Mg/yr. 6-15

TABLE OF FIGURES

Figure 2-1. Schematic of In-Plume Sampling System..... 2-2
Figure 2-2. Upper panel shows the raw CO2 concentration with the moving 100 sec window percentile baselines. The time series shows that the CO2 baseline decrease by ~20 ppm over the period and that the 15th percentile baseline best fits the non-plume points. The lower panel shows the CO2 concentration with the 15th percentile value subtracted (line with marker points). The blue line is 3 times the analytical uncertainty of the CO2 measurement. 2-12
Figure 2-3. Distribution of the number of vehicle plumes attributed to individual CO2 peaks. The average traffic volumes at Lakeshore and Southwood were 183 and 153 vehicles per hour, respectively. Lower volume roads result in fewer peaks with coincident vehicles. 2-13
Figure 2-4. Concentration time series of CO2, CO, NO, NO2, N2O, NH3, H2O, and PM measured by ELPI and DustTraks. The shaded areas are periods when the measured plume is linked to the passage of one or more vehicles. The dashed black line represents the analytical uncertainty of the gaseous measurements. 2-14
Figure 2-5. ELPI size distributions of exhaust samples measured using elevated and ground level inlets. 2-17
Figure 2-6. Particle densities inferred from ELPI and PM2.5 filter-based measurements. The black columns are samples corresponding exclusively to diesel exhaust and ~10% road dust. The gray columns are samples from a mixed fleet of both gasoline and diesel vehicles collected at road level and composed of 41% road dust. 2-18
Figure 2-7. Comparison of DustTrak PM with filter-based PM. Data represents five sampling periods from a mixed fleet of vehicles operating in Lake Tahoe. The road level inlet was used to collect the samples. The dotted line has a slope of 1 for reference.... 2-19
Figure 2-8. Road side sampling equipment deployed ~300 m south of entrance to Sand Harbor on Highway 28. 2-21
Figure 2-9. Vertical profile of PM concentration 1 m away from the side of paved road (upper panel). Time series of PM10 flux perpendicular to road calculated from DustTraks and wind vane. The shaded band represents the range of wind directions that are within 45 degrees of perpendicular to the road. 2-23
Figure 2-10. TRAKER influence monitors measure the concentration of particles behind the tires. A background monitor is used to establish a baseline. 2-24
Figure 2-11. TRAKER vehicle and instrumentation: a) Location of inlets (right side and background shown); b) Generator and pumps mounted on a platform on the back of the van; c) Two sampling plenums (bottom), a suite of DustTrak particle monitors (top right), and three rotameters used for ensuring proper flows through plena; and d) a dashboard-mounted computer screen used to view the data stream and a GPS to log the TRAKER's position every 1 s. 2-26
Figure 2-12. TRAKER Control Panel. Real-time figures show the magnitude of the response of DustTraks. The 10 lights at the top left of the screen serve as indicators of the health of onboard instruments (green = OK; red = not functioning)..... 2-28
Figure 2-13. TRAKER coefficient of variation expressed as a percentage for left and right PM10 DustTrak signals as a function of speed. The data represent left and right PM10 DustTrak signals averaged over a 1-mile stretch of road near Boise, Idaho

(Etyemezian et al., 2003). The coefficient of variation provides an estimate of the precision and is equal to the standard deviation of a measurement divided by the average. 2-29
Figure 2-14. Relationship between differential DustTrak measurements and vehicle speed for tests conducted on a common road section in a) Fort Bliss, near El Paso, TX, and b) a suburb of Boise, ID. 2-31
Figure 2-15. Regression of measured PM emission factors with TRAKER measurements. The line through points was drawn by holding the exponent of the regression equation at 1/3. 2-33
Figure 3-1. Pair comparison of chemical abundances of fireplace emissions between hardwoods (top) and softwoods (bottom). 3-8
Figure 3-2. Pair comparison of chemical abundances of woodstove emissions between hardwoods (top) and softwoods (bottom). 3-9
Figure 3-3. Comparisons of composite chemical abundance profiles for wood fuels type of fireplace (top) and woodstove (bottom). 3-10
Figure 3-4. Species comparison of abundances in fireplaces and woodstoves burning hardwood and softwood. Lower panel shows an expanded y-axis of the data in the upper panel. 3-14
Figure 3-5. Residential wood combustion profiles. 3-16
Figure 3-6. Average size distributions of total aerosol and source component measured by the ELPI for all wood burning source profiles. 3-17
Figure 4-1. Map showing sampling locations of motor vehicle exhaust source monitoring in Incline Village, NV, on the northwest shore of Lake Tahoe. 4-1
Figure 4-2. Images of In-plume gas monitoring module (FTIR) (upper panel left) and real-time particle monitoring module (upper panel right) and filter sampling module (lower panel). 4-2
Figure 4-3. Images of in-plume sampling equipment set-up and vehicle passing over inlet at Southwood and Mays on 7/23/03. 4-3
Figure 4-4. Image of in-plume sampling configuration at Lakeshore and Village in Incline Village on 7/26/03. 4-4
Figure 4-5. Fleet distribution at two sites in Incline Village where source samples were collected. 4-6
Figure 4-6. Column chart of individual profiles from motor vehicle sampling locations in Incline Village, NV. 4-11
Figure 4-7. Column chart of composited source profiles from Southwood-Mays and Lakeshore-Village 4-12
Figure 4-8. Intercomparison of Southwood-Mays and NFRAQS motor vehicle emission profiles. 4-13
Figure 4-9. Average size distributions of total aerosol and source component measured by the ELPI for all motor vehicle in-plume measurement source profiles. 4-14
Figure 4-10. Comparison of fraction of road dust measured on filters using CMB with the fraction of PM measured on the DustTraks associated with the vehicle plumes. .. 4-15
Figure 5-1. Map showing location of flux tower ~300 m south of main entrance to Sand Harbor State Park. 5-1
Figure 5-2. Grouping of TRAKER Measurements by region. The different color segments represent different roadway jurisdictions and usage classifications. 5-8

Figure 5-3. TRAKER PM_{10} emission factors over the study period for all measurement dates with more than 500 valid data points. The dashed line represents a best-linear-fit to the data (R^2=0.58). 5-9
Figure 5-4. Comparison of TRAKER PM_{10} road dust emission factors for the California and Nevada portions of the Lake Tahoe TRAKER loop over the study period. 5-9
Figure 5-5. Comparison of TRAKER PM_{10} emission factors for local roads (off the main Tahoe loop), Incline Village, and South Lake Tahoe over the study period. 5-10
Figure 5-6. TRAKER PM_{10} emission factors for the Mt. Rose Pass over the study period. The figure also shows emission factors measured on California Rt. 267 on 6/4/2003. 5-10
Figure 5-7. Comparison of TRAKER PM_{10} emission factors between spring (3/31/03 – 5/16/03) and summer (5/17/03 – 7/17/03) portions of the study by road group. The vertical bars correspond to standard deviations of PM_{10} emission factors among the different times when each road group was measured. The numbers at the bottom indicate the number of different measurement periods used to obtain the average emission factor for each road group. 5-11
Figure 5-8. Comparison of TRAKER PM_{10} emission factors over study period with SNOTEL data from Mt. Rose. 5-11
Figure 5-9. Comparison of TRAKER PM_{10} emission factors over study period for California and Nevada portions of Lake Tahoe loop with SNOTEL data from Heavenly Valley, Rubicon, and Marlette Lake. 5-12
Figure 5-10. Composite source profiles of grab samples collected in Incline Village between 7/26/03 and 7/29/03. 5-18
Figure 5-11. Coarse PM source profiles of roadside samples collected in near Sand Harbor State Park, NV, between 3/12/03 and 4/10/03. 5-18
Figure 6-1. Map of Carb Tahoe Air Basin. 6-4
Figure 6-2. Distribution of estimated PM10 emission sources in the Lake Tahoe Basin. The asterisk (*) denotes that the emissions from this source were measured in this study. 6-16
Figure 6-3. Distribution of estimated NO_x emission sources in the Lake Tahoe Basin. The asterisk (*) denotes that the emissions from this source were measured in this study. 6-16
Figure 6-4. Distribution of estimated CO emission sources in the Lake Tahoe Basin. The asterisk (*) denotes that the emissions from this source were measured in this study. 6-17
Figure 6-5. Distribution of estimated TOG emission sources in the Lake Tahoe Basin. The asterisk (*) denotes that the emissions from this source were measured in this study. 6-17

1. INTRODUCTION

Lake Tahoe, situated along the border of California and Nevada, is a world-renowned scenic basin with diverse natural, cultural, and recreational attributes. This basin is bounded by the Sierra Nevada mountain range (with peaks at 3000 m above mean sea level [MSL]) to the west and the Carson Range to the east. The surface of Lake Tahoe is at an elevation of 1897 m, and the lake is up to ~500 m deep. Snow, rain, and streams feed the lake, which covers an area approximately 35 km long by 19 km wide. Four distinctive seasons characterize the Lake Tahoe Basin climate, which attracts tourists year-round.

The Lahontan Regional Water Quality Control Board and the Tahoe Regional Planning Agency (TRPA) wish to develop cost-effective control strategies for improving water clarity in Lake Tahoe. Lake Tahoe's water clarity has declined from ~30 m to ~20 m since 1970. It is estimated that 40% of the precipitation that falls into the basin lands directly on the lake, with the remaining precipitation draining through granite-based soils (http://tahoe.usgs.gov/facts.html). To improve water clarity, a comprehensive knowledge of the pollutants entering the lake through dry deposition, wet deposition, runoff, etc. is needed. This report addresses the local emissions of air pollutants in the Lake Tahoe Basin from sources that are likely to be the largest contributors to dry deposition in the lake.

Both meteorology and emissions drive the process of dry deposition. In general, during winter months, ground-level inversions hold airborne emissions within a shallow mixing depth close to the lake. In summer, atmospheric mixing is more turbulent and emissions are mixed higher and may be transported out of the basin more frequently than in winter.

Based on particulate matter (PM) inventories elsewhere, the major local sources of PM in the basin are assumed to include residential wood combustion (RWC), wild fires, prescribed fires, on-road motor vehicle exhaust, road dust, and wind blown dust from disturbed soils. Source contributions vary by season. RWC activity occurs during colder months (November–April) for home heating, whereas prescribed fires are usually set during the spring and fall, and wild fires frequently occur in late summer. Emissions from vehicle exhaust are a year-round source tied to vehicle activity, which is 37 to 42% lower during winter than in summer (Fitz, 2003). Resuspended road dust is associated with traction control material applied to the streets during winter. Wind blown dust occurs primarily in late summer during high-wind events when soil moisture is at a minimum.

The composition of these types of sources are also generally well known (Chow et al., 2004; Watson et al., 2002; Chow et al., 2000). Wood combustion produces PM that is enriched with organic carbon (OC) and elemental carbon (EC). The relative OC/EC ratio varies by the type of fire and fuel. A hot wildfire achieves nearly complete combustion, emitting predominantly ash, whereas a smoldering fireplace may emit larger amounts of OC with respect to EC (Turn et al., 1997; Houck et al., 1998). An abundance of OC and EC in vehicle exhaust is also apparent. Motor vehicle PM emissions from well-tuned gasoline vehicles are quite small when compared to emissions from malfunctioning and older vehicles. The cause and severity of the malfunction can result in a broad range of OC to EC ratios (Gillies and Gertler, 2000).

Road dust is a combination of traction control material, brake and tire wear, vegetative debris, deposited exhaust, and track-out soil from unpaved roads. Chemical analysis of this road surface material from other locations indicates that most of the PM is composed of crustal

species (e.g., oxides of Al, Si, Ca, Fe, and Ti). The carbonaceous content of road surface PM_{10} can range from 0 to 35% (Watson et al., 1998; Chow et al., 2004).

1.1. Objectives

The specific objectives of the project are to:

- Chemically characterize PM mass emissions from RWC, motor vehicle exhaust, and road dust.
- Develop PM emission factors for RWC, motor vehicle exhaust, and road dust, and estimate basin-wide emissions for these sources.
- Document methods and present results.

1.2. Guide to Report

The report is divided into nine sections. Section 1 is the introduction, which states the background and objectives of the project. Section 2 describes the various technologies used to collect the measurements. Sections 3 to 5 present the results of the wood burning, exhaust, and road dust experiments, respectively. Section 6 compares source activity measurements and summarizes emissions for the entire basin. Section 7 presents the conclusions of the report. Section 8 makes recommendations for future research to improve quantification of these emission sources. Section 9 contains the references, and section 10 contains the appendices.

2. MEASUREMENT METHODS

This section describes the instrumental setups used for this project. The In-Plume Sampling System was used to develop emission factors for RWC and roadside motor vehicle exhausts, and the TRAKER (Testing Re-entrained Aerosol Kinetic Emissions from Roads) vehicle and Flux Tower were used for road dust.

2.1 In-Plume Sampling System

The In-Plume Sampling System was developed at Desert Research Institute (DRI) to measure concentrations of gaseous and PM emissions from combustion sources. Using a carbon mass balance approach, fuel-based emission factors (in grams of pollutant per kg fuel burned) can be calculated from the simultaneous measurements of gases and particles provided by the system (Pokharel et al., 2002; Moosmüller et al., 2003). The sampling inlet is placed near a source plume cooled and diluted with ambient air. Since emissions of pollutants are referenced to the total carbon emitted (i.e., CO_2 + CO + HC), it is not necessary to capture the entire plume to obtain an emission factor. The In-Plume Sampling System has the following advantages: (1) the emission factors at specific conditions can be estimated in a short time if real-time measurements of pollutants are available in the system, and (2) emission factors for sources in the real world can be estimated with parameters that can affect source emissions. For example, emission factors for motor vehicle exhaust in the fleet can be estimated by deploying the system roadside to collect partial plumes from passing vehicles, which vary by year, make, model, type, and speed.

Figure 2-1 shows a schematic of the In-Plume Sampling System and Table 2-1 describes the instrumentation used. Gaseous emissions are measured with a Fourier Transform Infrared (FTIR) spectrometer equipped with a ducted gas cell to permit fast response times (1.5 s) over a 10 m optical path. Particles are measured using a combination of real-time and integrated techniques including TSI DustTraks, an Electronic Low Pressure Impactor (ELPI), and filter-based methods. The sampling system is field transportable. Instruments are mounted on two hand carts for easy offloading and positioning near the plume. The In-Plume System uses a time-integrated filter-based PM sampling system for chemical sampling speciation. Teflon-coated Bendix 240 cyclones are used to remove particles greater than a specified aerodynamic diameter from the sample flow prior to PM sample collection. PM_{10} and $PM_{2.5}$ 50% cutpoints for the Bendix 240 cyclone were achieved by running the sample flows at 45 lpm and 113 lpm, respectively. Sample flows, temperature, and gauge pressure behind each filter pack are monitored by TSI Series 4102 mass flow meters. These data are logged on a field computer. The operator can adjust the flow control valves over the sampling period to maintain the appropriate particle size cut for each filter.

The real-time gas and particle sampling instruments using the FTIR and ELPI were deployed during initial tests on 3/12/03 and 3/31/03 along Highway 28 near Sand Harbor. The initial setup used a 1 m tall by 10 cm wide funnel oriented vertically next to the traffic lane. Emissions from passing vehicles entered the funnel and were drawn into the gas and particle sampling instruments. Vehicles passed the equipment at 60 to 90 km/hr. During the sampling, winds were approximately 3–5 m/sec. Initial tests found that the roadside plume was too dilute to resolve exhaust emissions. Increased particle concentrations in the fine and coarse size ranges, measured with DustTraks and the ELPI, were detected downwind.

The sampling system was reconfigured to collect gas and particle measurements closer to exhaust pipes. A cable protector designed to prevent vehicles from damaging extension cords across roads was fitted with a sampling line, and a 2.54 cm inlet hole was drilled in the middle of the cable protector to draw air into the sampling system from the center of the traffic lane. The inlet line was then connected to a plenum and redirected to numerous sampling instruments. Tests with this configuration indicated that CO_2 could be measured above background (>600 part per million (ppm)) for vehicles traveling at speeds of less than 50 km/hr. Optimal sampling occurred when the plume was not dispersed over a long distance (i.e., slow vehicle speed).

Figure 2-1. Schematic of In-Plume Sampling System.

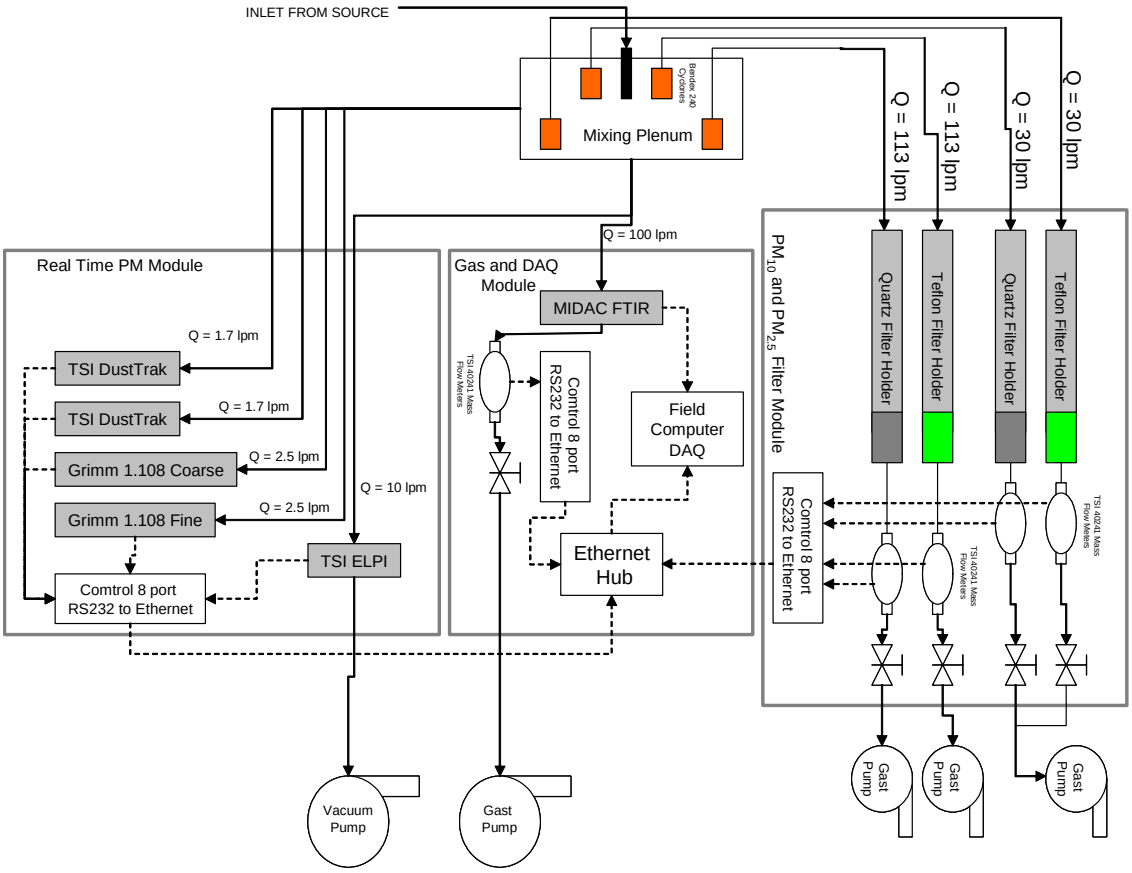

Table 2-1. Instrumentation of In-Plume Sampling System.

Instrument	Measurement	Method	Response Time (s)
Midac I-Series FTIR	Molecular gas species concentration	Dispersive IR	1.5
Dekati Electronic Low Pressure Impactor (10 lpm)	Aerodynamic number size distribution of particles	Current dissipation arising from deposition of charged particles to impactor substrates	5
TSI DustTrak	Particle mass	780 nm laser light scattering of particle stream at 90 degrees	1
Nuclepore filter sampler	Mass and chemical composition of particles and gases	Collection and analysis of exposed filters	>1000
TSI 4043 Mass Flow Meters	Mass flow through filter	Hot wire anemometer	<1
Timemark Delta III Traffic Counter	Vehicle speed, direction, axle spacing, acceleration, and classification	Timing intervals of wheel strikes on road tubes across lane	1
Video	Vehicle type	CCD	<1

2.1.1 Instrument Descriptions

2.1.1.1 FTIR

A Midac FTIR spectrometer was used to measure infrared exhaust absorption spectra at a frequency of one scan per 1.5 s. The instrument uses a Michelson interferometer with a mercury-cadmium-tellurium (MCT) liquid nitrogen cooled detector. Measured species, wave number regions, calibration ranges, and typical concentrations are listed for 10 gases in Table 2-2. Calibration spectra were created using EPA-certified gases diluted with ultra-pure nitrogen using an Environics gas dilution system. A custom ducted gas cell with a 10 m folded optical path length was designed to facilitate rapid air changes in the 2 liter analytical volume. Typical flow rates through the gas cell are 100 lpm. The FTIR is referenced with ambient air in the field. As a result, gas concentrations are measured as the difference from the ambient air. For example, a typical vehicle pass over the road level inlet at 20 km/hr results in a 7 sec CO_2 peak with an average concentration of 150 ppm above ambient air.

Table 2-2. Gases analyzed using classical least squares analysis of infrared spectra from FTIR.

Species	Reference Region (cm^{-1})		Average In-Plume Concentration (ppm)	Uncertainty Standard Error (ppm)	Calibration Range (ppm)		Typical Ambient Concentration (ppm)
	Lower υ_1	Lower υ_2					
CO_2	723.00	750.00	150	17	100	4730	400
CO	2133.31	2142.20	1.93	0.05	1.0	1005	1
NH_3	955.55	976.14	0.04	0.01	1.0	110	0.01
NO	1873.00 1880.60 1898.60 1926.00 1934.60	1878.50 1883.80 1901.30 1932.00 1939.90	0.12	0.13	0.2	20	0.05
H_2O	1200.00	1300.00	93	27	5.0	5294	5000
C_4H_{10}	3041.30	2825.64	0.04	0.05	1.0	100	0.2
C_6H_{14}	3029.79	2817.96	0.06	0.04	0.2	200	0.01
C_2H_4	957.97	936.57	0.00	0.08	0.5	20	0.02
NO_2	1584.00 1597.50 1604.30 1610.60	1588.70 1600.20 1605.90 1613.80	0.00	0.11	0.2	20	0.05
SO_2	1112.50 1123.40 1138.60 1153.60 1166.60 1176.60 1188.00 1199.90 1226.90	1120.30 1134.00 1148.10 1164.00 1172.50 1185.10 1197.20 1209.00 1235.70	0.00	0.14	1.0	100	0.0005

2.1.1.2 ELPI

The ELPI (Dekati Instruments, Finland) uses a unipolar corona charger to impart a positive charge on the measured aerosol. The particles then travel through a cascade impactor and are deposited on 1 of 12 substrates (0.030 µm to 9.6 µm) based on their aerodynamic diameter. The substrates are electrically isolated with Teflon supports and the accumulating charge on each of the substrates is measured by an array of electrometers. The measured current on each of the stages is proportional to the number of particles depositing on the stage. The ELPI measures the number concentration of particles based on their aerodynamic size at a frequency of 1 Hz.

Van Gulijk et al. (2001) investigated the performance of the ELPI through controlled tests on a diesel soot aerosol. Scanning electron microscopy (SEM) analysis of the impactor stages indicated that the fractal structure of the aerosol quickly formed mounds on the impactor substrates, resulting in a dynamic shift in the impactor cut sizes. Subsequent analyses (van Gulijk et al., 2003) found that the use of oiled sintered stages on the impactor extended the

sampling capacity of the ELPI by more than a factor of 50 by wicking particles away from the impact area. For this study, the ELPI was operated using oiled sintered substrates followed by a filter stage.

The mass of particles collected on the filter stage is negligible (<0.01%) with respect to the larger stages. However, the abundance of these nanoparticles in the sample stream can cause a bias in the measurement of coarse particles. The corona charger imparts a positive charge on all particles passing through the impactor. While most particles deposit onto the substrates due to inertial forces, a fraction of the smallest particles diffuse to all impactor surfaces and deposit their charge. The charge deposited to the upper stages of the impactor by nanoparticles is substantially larger than the charge deposited by coarse aerosol particles. Marjamäki et al. (2002) developed an algorithm to use the number concentration of particles collected on the filter stage to estimate the diffusion of particles to the upper stages of the impactor. This algorithm was applied to all ELPI measurements to reduce the coarse particle artifact in the dataset.

Measurements of diesel exhaust size distributions (assuming unit density particles) indicate that the coarse particle correction algorithm may not be entirely correct for nanoparticles that deposit a charge on the upper stages while passing through the filter stage. Experiments were performed by measuring a mixed fleet of vehicles passing over the cable protector inlet and by using the probe to sample exhaust from elevated diesel stacks. Chemical analysis of filters sampled using these two methods indicated that the soil (the sum of the oxide forms of aluminum [Al], silica [Si], calcium [Ca], iron [Fe], and titanium [Ti]) accounted, on average, for 41% of the $PM_{2.5}$ mass for samples collected at road level using the cable protector inlet and 8% of the $PM_{2.5}$ mass using the probe on elevated exhaust stacks. Previous studies of tailpipe exhaust show that more than 90% of exhaust particles are less than 1 µm in size (Brown et al., 2000; Kleeman et al., 2000). In contrast, road dust emissions are predominantly associated with particles larger than 1 µm (Kuhns et al., 2001). The results of the elevated and road level measurements both showed very large coarse particles modes accounting for more than 95% of the mass above 1 um. This is inconsistent with the chemical speciation data that less than half of the total particle mass should be in the coarse mode. Based on these contradictory results, the coarse stages of the ELPI are considered invalid when measuring fresh exhaust particles.

2.1.1.3 DustTrak

The TSI DustTrak nephelometer measures particle scattering at a wavelength of 780 nm in a cone of scattering angles near 90 degrees. PM_{10} and $PM_{2.5}$ aerodynamic size cut inlets may be installed upstream of the analytical chamber to limit the size of measured aerosol particles. The DustTrak has a flow rate of 1.7 lpm and is calibrated using National Institute of Standards and Technology (NIST) Arizona Road Dust. The calibration material is lightly absorbing with a median diameter of approximately 2 µm. The instrument is most sensitive to non-absorbing particles with diameters on the same length scale as the light source (0.78 µm). The sensitivity is reduced for particles of other sizes. Exhaust particles have a DustTrak mass scattering efficiency similar to the calibration aerosol despite their difference in size and index of refraction (Arnott W.P.(DRI), personal communication). As a result, the DustTrak provides reasonable (within a factor of 3) measurements of aerosol mass for both exhaust and dust particles. In an evaluation of the DustTrak and other real-time instruments, Moosmüller et al. (2001) determined that the DustTrak provided a useful fast response measurement of particle concentration. Accurate real-time measurements of PM mass are possible if the DustTrak is calibrated with filter-based measurements (Yanosky et al., 2004). A scaling factor that accounts for the proportionality

between the DustTrak measurement and the filtered mass can be used to correct the DustTrak data.

2.1.1.4 Filter Media and Filter Pack Configuration

Lippman (1989), Lee and Ramamurthi (1993), Watson and Chow (1993, 1994), and Chow (1995) evaluated substrates for different sampling and analyses. The configurations of filter sampling used in the In-Plume Sampling System include: 1) polyolefin-ringed Teflon membranes (Gelman [Ann Arbor, MI], 2.0 µm pore size [#R2PJ047] for mass and elemental analysis) followed by a pre-fired quartz-fiber filter (Pallflex [#2500QAOT-UP]) to quantify volatilized carbon; 2) a pre-fired quartz-fiber filter for soluble ions (chloride [Cl^-], nitrate [NO_3], sulfate [$SO_4^=$], and ammonium [NH_4^+]) and carbon analyses followed by a cellulose-fiber filter (Whatman 31ET) impregnated with citric acid to collect gaseous ammonia (NH_3).

Teflon-membrane filters are individually light-checked for the absence of holes and flaws. Teflon-membrane filters are placed in Petri dishes for equilibration in a controlled environment (temperature 21.5 ± 1.5 °C and relative humidity 35 ± 5%) for at least three weeks before gravimetric determination. Quartz-fiber filters are prefired at 900 °C for six hours and stored under refrigeration. Whatman cellulose-fiber filters are impregnated with citric acid and stored under refrigeration. Two filters out of each batch of 100 are analyzed to determine that elemental background levels are within 2 times the detection limits. If the limits are exceeded, the batch is rejected. Blank quartz-fiber filters are heated for at least three hours at 900 °C to remove organic artifacts. Two filters from each batch of 100 are acceptance tested for Cl^-, NO_3^-, $SO_4^=$, NH_4^+, OC, and EC, and NH_3. Levels cannot exceed 1 µg/filter or the batch is rejected. After acceptance testing, the filters are refrigerated in sealed bags until sampling.

2.1.1.5 Resuspension of Bulk Samples

The DRI resuspension laboratory is designed to suspend bulk material—including but not limited to soil samples, road dust, and process materials such as baghouse dust—as a uniform aerosol onto Teflon-membrane and quartz-fiber filters for gravimetric and chemical analyses. The resuspension process is intended to duplicate the natural wind-blown processes of bulk soils and the resuspension of road dust by motor vehicles, and simply to provide a uniform deposit of other types of material on a filter for analysis.

Bulk materials collected from each roadside sampling location were sieved to <38 µm diameter (400 mesh screen), resuspended in small quantities using a high velocity air stream, blown into a large chamber for dispersion and mixing, and collected onto filters using a modified Parallel Impactor Sampling Device (PISD, OMNI Environmental, 1985). The PISD includes dust caps and impactor plates, both of which serve as size fractionation devices. The filters were periodically weighed during the resuspension process to monitor loading, then analyzed gravimetrically. Chemical analyses include X-ray fluorescence (XRF) for elemental composition, ion chromatography (IC) for water soluble anions, atomic absorption (AA) for water soluble metals, automated colorimetry (AC) for ammonium ion, pH measurements for acidity, and thermal/optical reflectance analysis (TOR) for carbon species.

2.1.1.6 Road Tube Counter

Traffic activity in the test area was monitored using a road tube counter and a video camera. Pressure transducers within the traffic counter measured the wheel strikes of passing vehicles on

two tubes spaced at ~5 m and perpendicular to the flow of traffic. The timing of the wheel strikes was processed to determine vehicle classification, direction, speed, acceleration, and axle spacing. A video camera recorded each vehicle. For measurements conducted in Lake Tahoe, a technician, subsequently, logged the passage of each vehicle and recorded the vehicle type (i.e., light duty car, pickup truck, sport utility vehicle, or heavy duty vehicle) for association with individual exhaust plumes.

2.1.1.7 PM_{10} and $PM_{2.5}$ Filter Samplers and Flowmeters

The exhaust sample stream was split after air was sampled through the inlet. One stream went to the real-time instrumentation (FTIR, ELPI, and TSI DustTraks) and the other entered a filter sampling plenum. Air was drawn from the plenum through a parallel array of Bendix 240 cyclones. The sample air then passed through Nuclepore filter holders with 47 mm quartz-fiber and Teflon filters. The cyclones were operated at 113 lpm and 45 lpm to achieve 2.5 µm and 10 µm size cuts, respectively. Each filter was monitored at 1 Hz with a digital mass flow meter to facilitate accurate volume determination.

2.1.1.8 Data Acquisition System

Data from the flow meters, FTIR, DustTraks, and ELPI were logged in real time through serial ports into Ethernet hubs on each cart. The hubs were each linked to an Ethernet switch and data was logged and displayed in real time using a portable computer. When operating multiple instruments, the use of real-time displays increases data recovery because the user can monitor the status of all instruments from a single location. The data acquisition system assigns a common time stamp to all measurements to ensure that 1 Hz data are synchronized.

2.1.2 Laboratory Sample Analysis

2.1.2.1 Mass

$PM_{2.5}$ mass was measured gravimetrically as the difference between pre- and post-sampling masses measured on a 47-mm diameter Teflon-membrane filter. Weighing was performed on an MT5 (Mettler, Placerville, CA) electromicrobalance with ± 1 µg sensitivity.

2.1.2.2 Elements

After gravimetric analysis, samples collected on the Teflon-membrane filters were also analyzed by energy dispersive X-ray fluorescence (ED-XRF, Epsilon 5, PanAnalytical, the Netherlands) for the following 40 elements: sodium (Na), magnesium (Mg), aluminum (Al), silicon (Si), phosphorus (P), sulfur (S), chlorine (Cl), potassium (K), calcium (Ca), titanium (Ti), vanadium (V), chromium (Cr), manganese (Mn), iron (Fe), cobalt (Co), nickel (Ni), copper (Cu), zinc (Zn), gallium (Ga), arsenic (As), selenium (Se), bromine (Br), rubidium (Rb), strontium (Sr), yttrium (Y), zirconium (Zr), molybdenum (Mo), palladium (Pd), silver (Ag), cadmium (Cd), indium (In), tin (Sn), antimony (Sb), barium (Ba), gold (Au), mercury (Hg), thallium (Tl), lead (Pb), lanthanum (La), and uranium (U).

2.1.2.3 Inorganic Ions (Chloride, Nitrate, Sulfate, and Ammonium)

Water-soluble anions (Cl^-, NO_3^-, $SO_4^=$) and a cation (NH_4^+) were determined from the deposit on a quartz-fiber filter collected in parallel with a Teflon-membrane filter. Each quartz-fiber filter was cut in half, and one filter half was placed in a polystyrene extraction vial with 15

ml of doulble de-ionized water. The extraction vials were capped and sonicated for 60 minutes, shaken for 60 minutes, then aged overnight to assure complete extraction of the deposited material. After extraction, these solutions were stored under refrigeration prior to analysis. Cl^-, NO_3^-, and $SO_4^=$ were measured by IC with a Dionex 500x (Dionex, Sunnyvale, CA). Approximately 2 ml of the filter extract was injected into the IC system.

An Astoria 2 AC system (Astoria–Pacific, Clackamas, OR) was used to measure NH_4^+ concentration by the indolphenol method. Each sample was mixed with reagents and subjected to appropriate reaction periods before submission to the colorimeter. Beer's Law relates the liquid's absorbency to the amount of the ion in the sample. A photomultiplier tube measured this absorbency through an interference filter, which is specific to NH_4^+. Two ml of extract in a sample vial were placed in a computer-controlled autosampler.

2.1.2.4 Organic and Elemental Carbon

Owing to differences in carbon analysis methods, both transmittance and reflectance were measured following the IMPROVE protocol to determine OC and EC on portions of the quartz-fiber filters by using a DRI thermal/optical carbon analyzer. These thermal evolution methods are based on the principle that different types of carbon-containing particles are converted to gases under different temperature and oxidation conditions. The carbon analyzer consists of a thermal system and an optical system. Reflected light is continuously monitored throughout the analysis cycle. The negative change in reflectance or transmittance is proportional to the degree of pyrolytic conversion of carbon that takes place during OC analysis. After oxygen is introduced, the reflectance increases rapidly as the light-absorbing carbon burns off the filter. The carbon that is measured after the reflectance attains the value it had at the beginning of the analysis cycle is defined as EC.

2.1.2.5 Gaseous Ammonia

A citric acid impregnated cellulose-fiber filter was used to collect ammonia NH_3 downstream of the dilution sampling system. These filters were extracted in citrate and then analyzed for NH_4^+ using the AC method.

2.1.3 Data Processing

The real time data must be processed to calculate fuel based emission factors (i.e. grams of pollutant per kg of fuel burned). By quantifying the concentration of CO_2, CO, HC, and the pollutant above the ambient background, the fuel based emission factor were calculated. The data processing steps to achieve this result are listed below.

After sampling, all data were downloaded from the field computer to a data server. The ELPI, DustTrak, traffic counter, and flow meter data were imported into a relational database and constant time offsets were added to each dataset to synchronize the occurrence of concentration peaks.

The FTIR spectra were processed using the Autoquant Pro version 4 package. Concentrations were calculated using a classical least squares fit of the data. These data were then processed using linear interpolation to fit the 0.66 Hz dataset to coincide with the other 1 Hz datasets. The FTIR 1 Hz dataset was imported into the relational database and joined to the other data based on time. The master table of all measurements was then exported and processed to identify peaks in the CO_2 signal.

Fuel-based emission factors were calculated from the background subtracted average peak concentrations. Using the carbon mass balance technique described by Moosmüller et al. (2003) and Fraser et al. (1998), the fuel-based emission factors were calculated as:

Error! Objects cannot be created from editing field codes. (2-1)

where EF_P is the emission factor of pollutant P in g pollutant per g fuel, CMF_{fuel} is the carbon mass fraction of the fuel (typically 85% to 88% for gasoline and diesel, and 45% to 50% for wood fuel), C_P is the mass concentration of pollutant P in grams per cubic meter, and M_i is the molecular (or atomic) weight of species *i* in grams per mole.

The start and stop points of the CO_2 peaks were used to integrate the pollutant concentrations. To ensure a high signal to noise ratio, peaks with integrated CO_2 concentrations of less than 1000 ppm sec were discarded. A CO_2 peak exists when CO_2 is above the background by more than 3 standard errors of the CO_2 measurement. The background is defined as the 15th percentile value of the CO_2 over a 100 sec window centered on the measurement. This process provides an unambiguous peak definition while compensating for low frequency drift in the background CO_2 measurement.

Background concentrations, which are defined as the pollutant concentrations corresponding to the 15th percentile CO_2 value of the 100 sec window, were subtracted from the average peak pollutant concentrations. The exhaust concentrations of each species were calculated as the instantaneous signal measured during each peak minus the average of the points in the 100 sec window that are not associated with CO_2 peaks.

2.1.3.1 Example of the calculation of fuel-based emission factors: Motor Vehicle Exhaust

In order to determine fuel-based emission factors, the exhaust portion of each ambient measurement must be extracted from the background concentration. A simple peak finding algorithm is applied to determine when a peak is present. Since CO_2 is the dominant species in the vehicle exhaust, the peak finding algorithm is applied to CO_2 to determine the beginning and ending points of each peak.

The simplest form of peak finder compares a measurement with a threshold value to determine if the point is significantly above background. For roadside measurements of CO_2, the background concentration can vary by 50 ppm or more over the course of a day. These variations may be associated with atmospheric mixing of combustion emissions close to the ground and vegetative respiration that consumes CO_2. To account for the low frequency changes in background concentration, the CO_2 data are filtered by subtracting the 15th percentile value from a moving 100 sec window (i.e., 50 sec ahead and 50 sec behind) surrounding each data point. The choice of the percentile value and the size of the window are arbitrary and should be based on how frequently the inlet is sampling a plume. If no plumes are present, the background would be defined at the 50th percentile or median concentration. In dense traffic areas, this percentile is likely to reflect CO_2 concentrations impacted by vehicle exhaust and a lower percentile value should be used. The size of the moving window should be sufficiently larger than the duration of the individual peaks so that the 15th percentile value will be representative of a point that is not influenced by exhaust plumes.

Figure 2-2 shows the time series of the mid-road CO_2 measurements between 14:35 and 14:40 PDT on 7/26/03 at the southeast corner of the intersection of Country Club and Lakeshore.

The CO_2 gas concentrations are referenced to ambient concentrations at the beginning of the sampling period. For periods where there is no apparent exhaust peak (i.e., 14:37:25 PDT to 14:37:45 PDT and 14:38:40 PDT to 14:39:00 PDT), the moving 15th percentile background appears to pass through the middle of these background data points.

The choice of the percentile value and the size of the moving window are arbitrary and should be based on how frequently the inlet is sampling a plume. If no plumes are present, the background would be defined at the 50th percentile or median concentration. In very dense traffic areas, the 50th percentile is likely to reflect CO_2 concentrations impacted by vehicle exhaust and a lower percentile value should be used. The size of the moving window should be sufficiently larger than the duration of the individual peaks so that the 15th percentile value will be representative of a point that is not influenced by exhaust plumes.

The lower panel of Figure 2-2 shows the background (i.e., moving 15th percentile value of 100 sec window) subtracted from the raw CO_2 signal. This signal is then compared with the analytical uncertainty (i.e., standard error) of the CO_2 measurement. If the background subtracted signal is more than 3 times the uncertainty, then the data point is defined as part of a peak. If the next data point is also greater than 3 times, then the uncertainty is associated with the same peak. To ensure that the peak is sufficiently large to calculate a meaningful fuel- based emission factor, the time integrated CO_2 peak must be more than 1000 ppm sec. In many instances, plumes from passing vehicles are insufficient to meet this criteria and these results are not included in average emission factor calculations.

The sensitivity of CO_2 peak integral to the choice of the percentile background value can be assessed with the data in Figure 2-2. The peak that begins at 14:36:12 PDT and ends at 14:36:19 PDT is 7 sec long and has an integral of 1366 ppm sec using the 15th percentile 100 sec window as background. If the 5th percentile or 25th percentile background had been used, the integrated values of the peak would have been 1282 ppm sec (-9%) or 1422 ppm sec (+4%), respectively. Thus, the choice of background percentile may introduce <10% uncertainty into the emission factor calculations.

Fleet average fuel-based emission factors were calculated for each filter sampling interval. The following criteria are applied to the in-plume data set. Only peaks with integrated CO_2 greater than 1000 ppm sec are included in the analysis. This restriction eliminated 33% of the 962 detected peaks from 7/23/03, 07/26/03, and 7/29/03. To exclude anomalous data points from the final dataset, all data points with CO_2 standard errors greater than 40 ppm were flagged as invalid. This accounted for less than 2% of all identified vehicle exhaust peaks. A final criterion on the completeness of data required that at least 80% of the 1 sec data points be present and complete for a peak to be valid. This eliminated 17% of all identified peaks. After applying these criteria, a total of 541 out of 962 peaks were validated from the three days of field measurements. Each identified CO_2 peak represents the passage of one or more vehicles. Video camera images and traffic counter results were analyzed to determine the distribution of vehicle numbers for each identified peak (Figure 2-3). Southwood and Mays had lower vehicle volumes than did Lakeshore and Village. Consequently, the relative number of peaks representing the emissions from more than one vehicle is higher at the higher volume site.

Figure 2-4 shows a time series of concentration data measured by the sampling system. With a traffic density of ~200 vehicles per hour per lane, many of the identified plumes represent the emissions of more than one vehicle traveling close together. The lower panel of Figure 2-4 is the

CO_2 time series. The segments identified as single peaks using the algorithm described above are shaded black. The vehicles passing over the inlet that were identified by video are labeled in Table 2-3. The periods of the species time series affected by exhaust plumes are shaded black. The analytical uncertainties of the measurements are shown by the dotted line in each figure, with the exception of the particle data from the DustTraks and ELPI, since these instruments do not report an uncertainty.

The resolution of the video camera images was insufficient to determine individual license plate numbers. It is therefore difficult to conclude that all of the vehicles in this example were powered by spark-ignition gasoline engines.

The times series show very different chemical profiles for each of the plumes. Plume 355 not only has the lowest integrated CO_2 concentration, but also has the highest CO concentration, indicating a higher fuel-based CO emission factor than the other plumes in Figure 2-4. Plume 359 shows features that indicate mixing of two or more exhaust plumes. The first 10 sec of the plume show elevated levels of NO and NO_2, and these levels decrease in the latter 20 sec of the plume, although CO_2 and CO remain above background. This composition of plume 359 is very different from plume 358, which shows elevated N_2O and NH_3 concentrations. These species likely represent the emissions from a vehicle with a three-way catalytic converter that is reducing thermal NO_x beyond N_2 and O_2 to create NH_3.

Particle emissions show similar variability between vehicles. The mass of particles (assuming spheres) with aerodynamic diameter below 0.1 μm are shown in the upper panel of Figure 2-3. During this experiment, ELPI was operated with the electrometers set to their largest detectable range (400,000 fA). This resulted in a very sensitive measurement. However, the time scales of the measurements were on the order of 20 s. As a result, the ELPI was able to detect fresh ultrafine emissions from the vehicles, but the time response was too slow to link these concentrations to individual plumes. In later experiments, the ELPI was operated at a range of 10,000 fA, and plumes from individual vehicles were distinguishable. The TSI DustTrak has a fast 1 Hz time response. The time series of the DustTraks operating with 2.5 μm and 10 μm inlets are shown below the ELPI time series in Figure 2-3. A PM_{10} and $PM_{2.5}$ peak was observed during the middle of plume 359. This peak does not appear to be associated with the same vehicle that created the NO peak. The first peak in the DustTrak time series appears to precede the CO_2 peak. These elevated levels may be due to exhaust or road dust from a vehicle passing in the opposite direction.

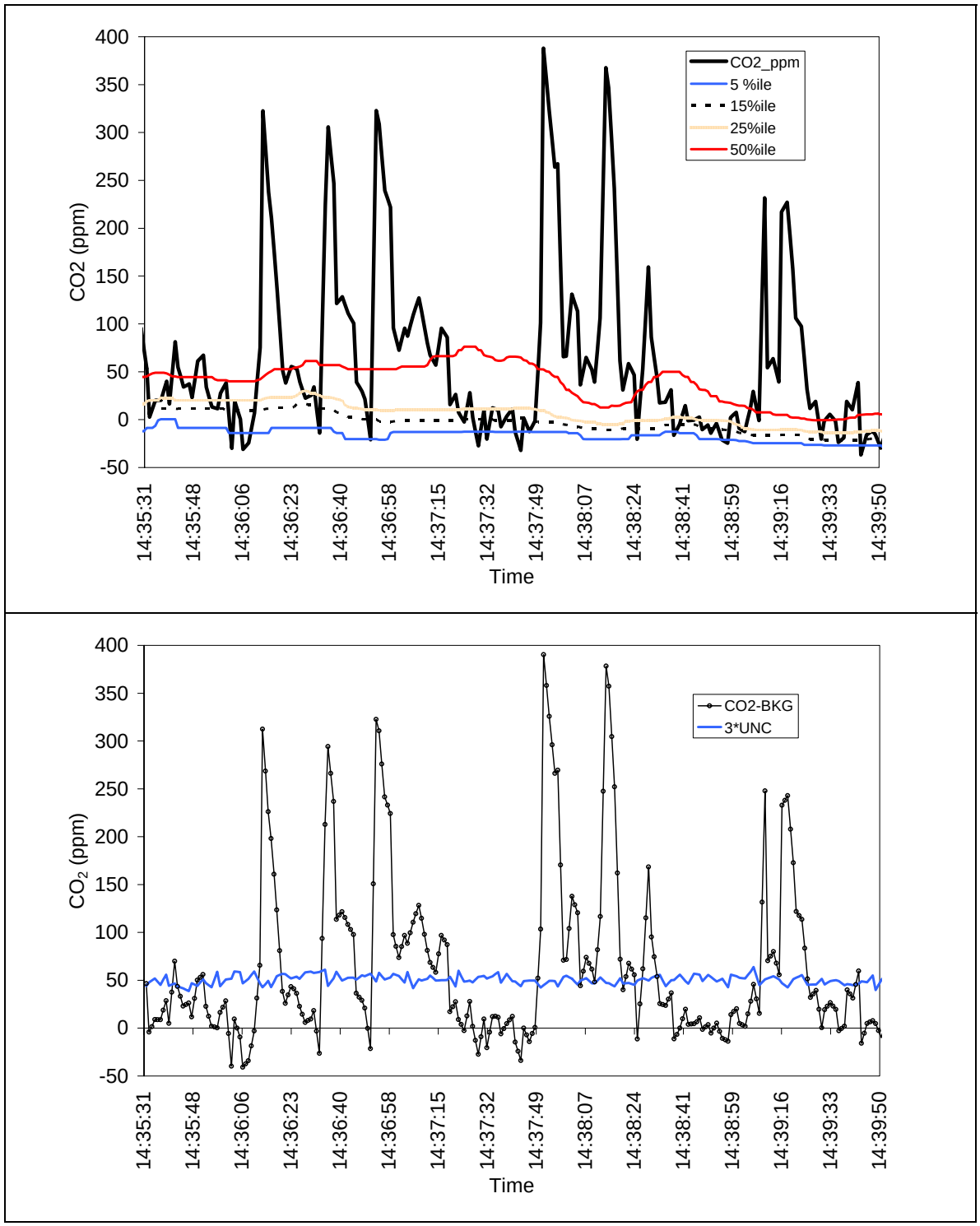

Figure 2-2. Upper panel shows the raw CO2 concentration with the moving 100 sec window percentile baselines. The time series shows that the CO2 baseline decrease by ~20 ppm over the period and that the 15th percentile baseline best fits the non-plume points. The lower panel shows the CO2 concentration with the 15th percentile value subtracted (line with marker points). The blue line is 3 times the analytical uncertainty of the CO2 measurement.

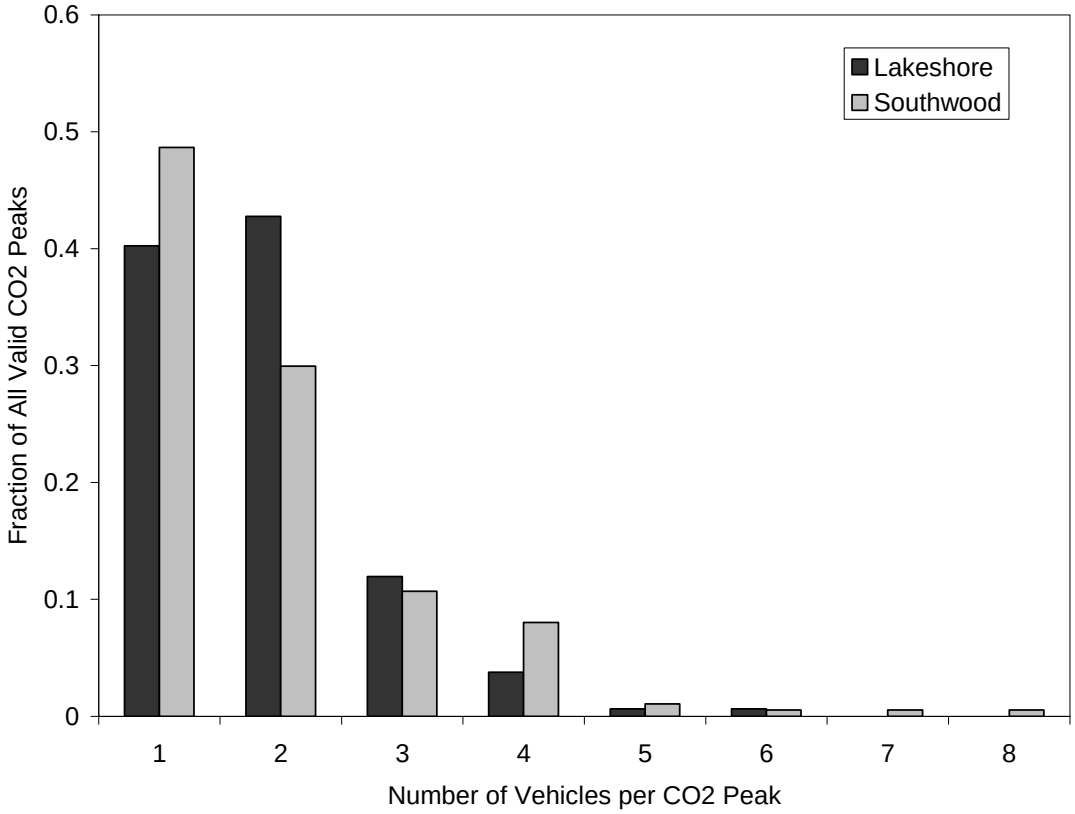

Figure 2-3. Distribution of the number of vehicle plumes attributed to individual CO2 peaks. The average traffic volumes at Lakeshore and Southwood were 183 and 153 vehicles per hour, respectively. Lower volume roads result in fewer peaks with coincident vehicles.

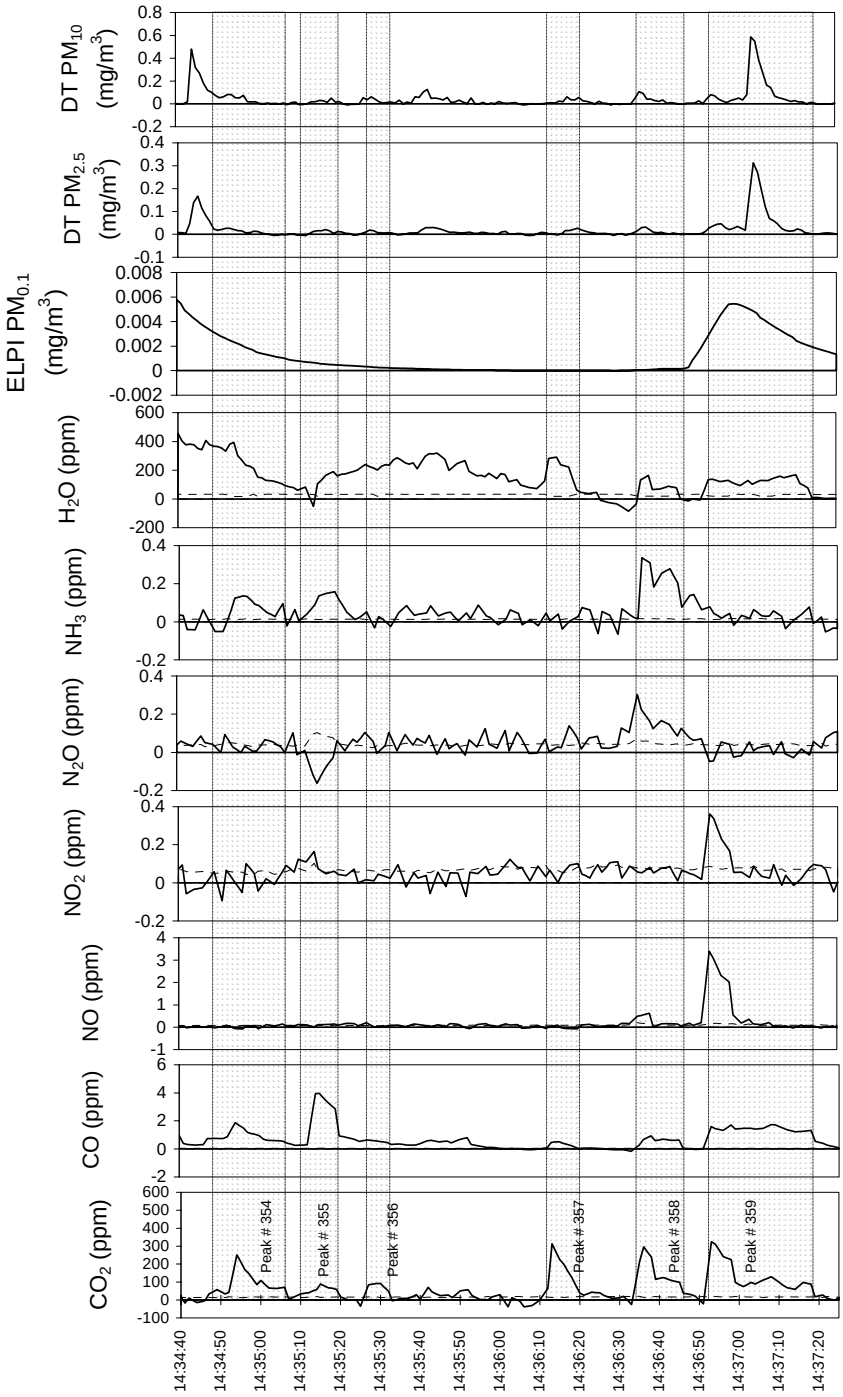

Figure 2-4. Concentration time series of CO2, CO, NO, NO2, N2O, NH3, H2O, and PM measured by ELPI and DustTraks. The shaded areas are periods when the measured plume is linked to the passage of one or more vehicles. The dashed black line represents the analytical uncertainty of the gaseous measurements.

Emission factors for all species measured and their propagated uncertainties are shown in Table 2-3. To ensure sufficient plume densities for each peak, valid CO_2 peaks were required to have integrated plume values of more than 1000 ppm s. Peaks 355 and 356 had integrated values of ~500 ppm s, resulting in larger emission factor uncertainties. The detection limit of the In-Plume Sampling System is affected by both the variability of the ambient background and the detection sensitivity of instruments used. The measurement of water appears to be influenced by the background concentrations. Figure 2-4 shows that variations in background water concentrations are generally larger than the variations introduced by vehicle exhaust. Although the FTIR can measure propane hexane, ethylene, formaldehyde, sulfur dioxide (SO_2), and other species found in exhaust, the levels typically observed in the exhaust are lower then can be detected.

Table 2-3. Emission factor results for vehicles associated with individual plumes.

Peak Number	354	357	358	359
Vehicles	Volkswagen Car Dodge Car	Lincoln Car	GMC PU Toyota Car	GMC PU Ford PU Ford SUV
CO_2 * Plume Duration (ppm s)	1645	1366	1771	3257
Species	**Emission Factors (g/kg fuel)**	**Emission Factors (g/kg fuel)**	**Emission Factors (g/kg fuel)**	**Emission Factors (g/kg fuel)**
CO	15.8 ± 3.0	0.3 ± 0.4	4.2 ± 0.8	19.0 ± 2.8
NO	-1.1 ± 1.9	-1.3 ± 2.1	3.0 ± 2.0	12.0 ± 2.7
NO_2	-1.1 ± 2.0	0.4 ± 1.5	0.5 ± 1.9	1.4 ± 2.0
N_2O	-0.7 ± 1.5	0.1 ± 0.8	2.6 ± 1.2	-1.2 ± 1.1
H_2O	2703 ± 925	917 ± 1217	-1493 ± 502	-542 ± 551
Formaldehyde	-1.5 ± 2.5	-0.3 ± 1.5	0.0 ± 1.6	0.2 ± 1.8
Hexane	-2.9 ± 2.4	-1.9 ± 3.0	-5.5 ± 2.9	-1.0 ± 2.3
Propane	-0.9 ± 2.2	-0.4 ± 1.5	-0.4 ± 1.7	0.0 ± 1.8
NH_3	0.4 ± 0.2	-0.1 ± 0.2	1.6 ± 0.3	0.0 ± 0.2
Ethylene	-0.5 ± 0.5	0.0 ± 0.3	-0.1 ± 0.4	0.3 ± 0.4
SO_2	-0.8 ± 8.0	4.3 ± 7.2	-4.5 ± 5.1	1.2 ± 5.7
$PM_{2.5}$ (DustTrak)	0.03	-0.02	-0.02	0.73
PM_{10} (DustTrak)	0.29	-0.07	0.06	1.13

Figure 2-5 shows the measured volume size distributions normalized to the total volume of particles collected on stages 1 through 10 (particles less than 2.3 µm aerodynamic diameter) for samples collected with the elevated and road-level inlets. Both size distributions show a large increase in particle volume on Stages 9 and 10 (0.9 µm to 2.3 µm) accounting for more than 40% of the total particle volume. For experiments using the road-level inlet, some enhancement in particle concentrations on the upper stages of the impactor is to be expected because road dust was sampled along with the exhaust. This is not the case with the elevated inlet, where vehicles (i.e., buses) are stopped or traveling at speeds of less than 10 km/hr and soil concentrations are less than 10% of the $PM_{2.5}$ mass. The increase in particle concentrations on Stages 9 and higher appears to be an artifact of sampling fresh exhaust with large number concentrations of nucleating particles and not an indication of coarse particles.

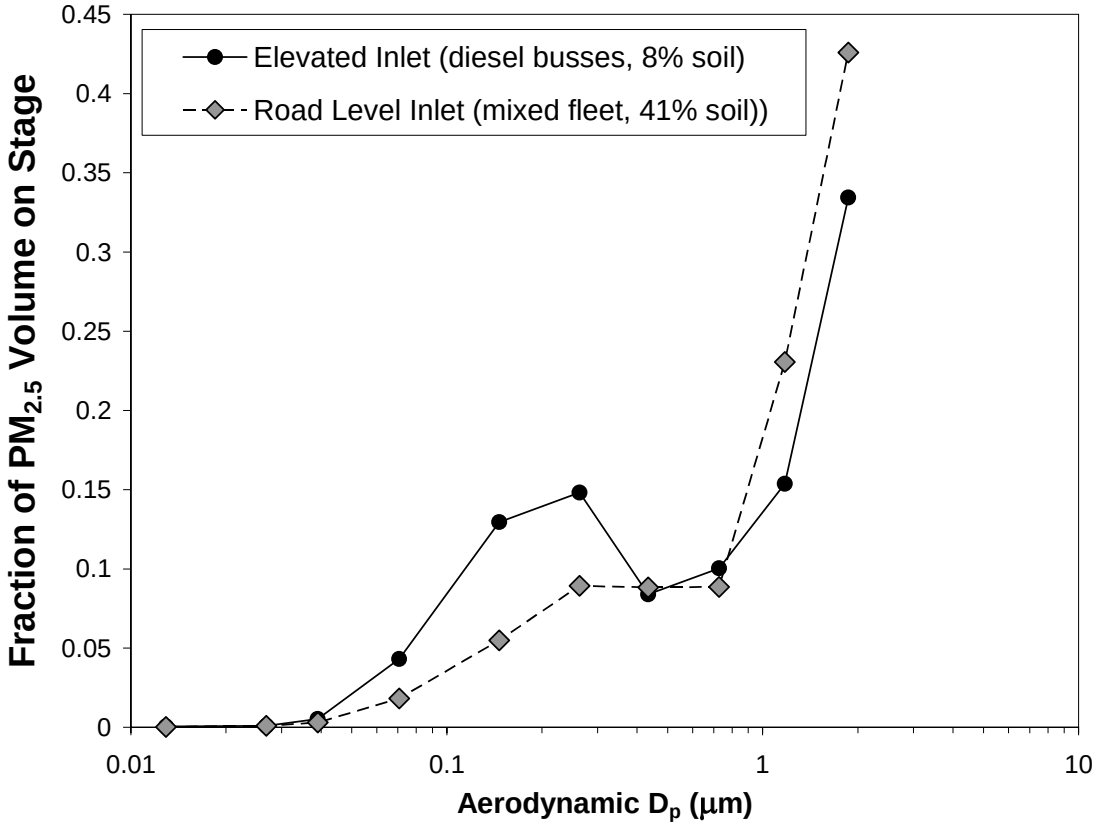

Figure 2-5. ELPI size distributions of exhaust samples measured using elevated and ground level inlets.

For this study, the bulk density of particles was calculated by dividing the particle volume on stages 10 and below (assuming spherical particles) by the mass of $PM_{2.5}$ measured using a filter sampler. The calculated particle densities are shown in Figure 2-6. Densities range from 0.5 to 1.5 g/cm^3. The inter-sample variability is larger than the density differences between diesel exhaust (black columns) and exhaust from the mixed fleet (gray columns).

DustTraks were operated in parallel with the ELPI and after the sample stream passed through the optical path of the FTIR on the In-Plume Sampling System. Figure 2-7 compares DustTrak PM concentrations with filter-based PM concentrations for PM_{10} and $PM_{2.5}$. The correlation coefficient for the relationship between the DustTrak signal and $PM_{2.5}$ ($r^2 = 0.85$) is much stronger than the PM_{10} correlation ($r^2 = 0.31$).

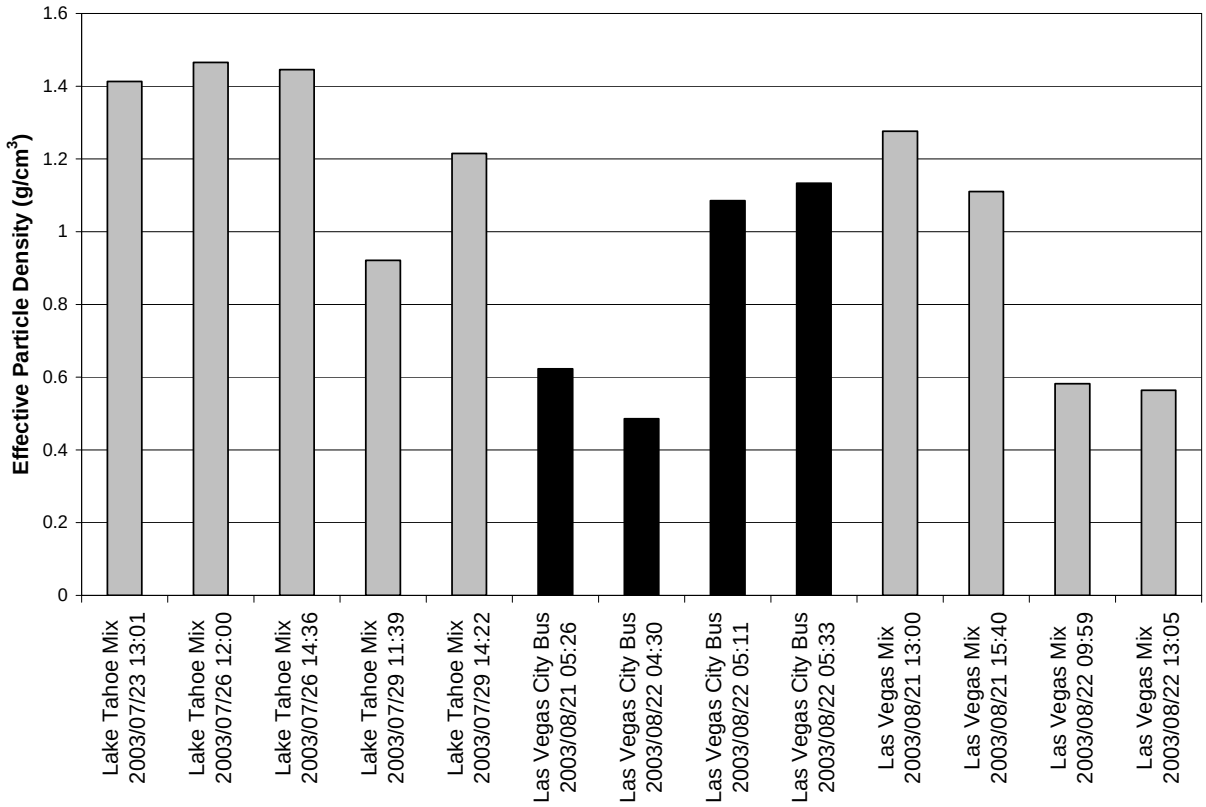

Figure 2-6. Particle densities inferred from ELPI and PM2.5 filter-based measurements. The black columns are samples corresponding exclusively to diesel exhaust and ~10% road dust. The gray columns are samples from a mixed fleet of both gasoline and diesel vehicles collected at road level and composed of 41% road dust.

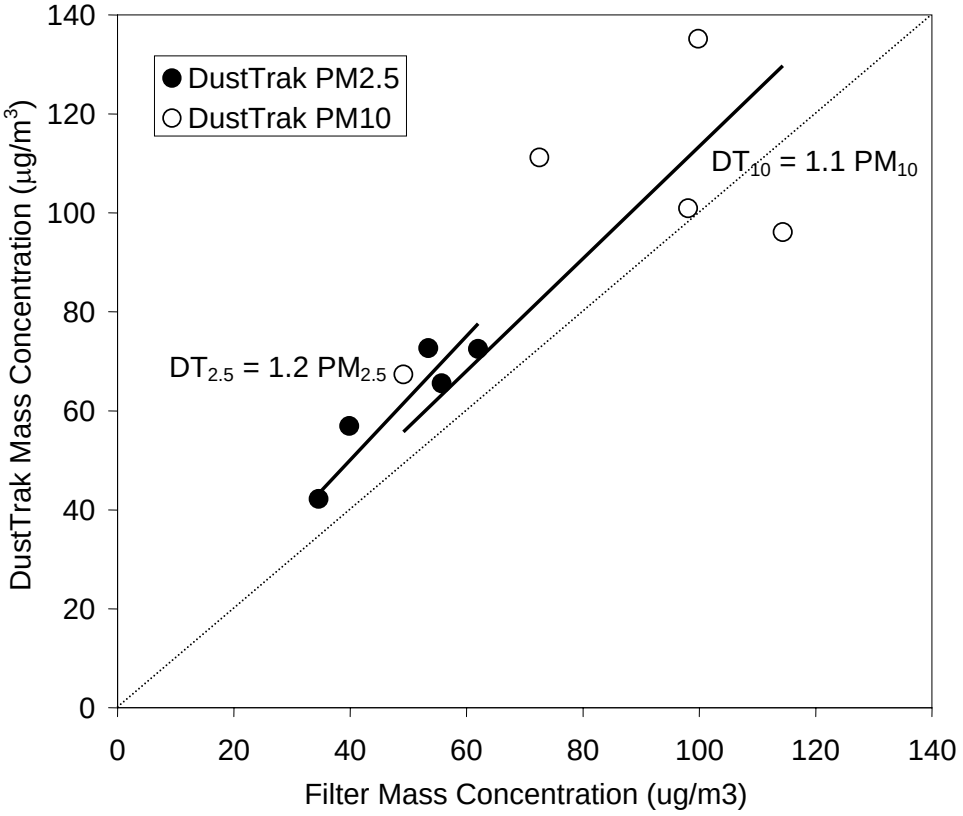

Figure 2-7. Comparison of DustTrak PM with filter-based PM. Data represents five sampling periods from a mixed fleet of vehicles operating in Lake Tahoe. The road level inlet was used to collect the samples. The dotted line has a slope of 1 for reference.

2.2 Flux Towers and Ambient Monitors

The flux tower measurements conducted at Lake Tahoe were based on an upwind/downwind technique that has been used by other investigators (e.g., Gillies et al., 1999). In this case, one tower was set up ~1.5 m away from the lane edge on a section of Highway 28 (Figure 2-8). Historical meteorological data indicated that winds would be predominantly from the west to southwest with speeds increasing in the afternoon.

The downwind tower was instrumented with eight TSI DustTraks (four with PM_{10} inlets and four with $PM_{2.5}$ inlets) mounted at 0.5 m, 1 m, 2 m, and 3 m above the level of the travel lane. The DustTraks measured particle concentrations at intervals of 1 s. One combined wind vane/anemometer was mounted ~2 m from the tower to record wind speed and direction at 2 m above the level of the lane. The meteorological data were stored on a datalogger (Campbell Scientific, Model # 10X) at 1 sec intervals. A road tube counter was installed across the road to record gross vehicle type (based on axle spacing), speed, and direction.

At the beginning of each day, the zero baselines were set for each DustTrak on the flux tower with a high-efficiency particle arresting (HEPA) filter. Analysis of the DustTrak data indicated that baseline drift over the course of a day did not affect all instruments equally. The range of this drift was less than 5 $\mu g/m^3$. To isolate the high frequency PM flux associated with vehicle-generated road dust and exhaust plumes, a low frequency filter similar to that used with the In-Plume System was applied to the DustTrak dataset. The minimum value of a 100 sec window was subtracted from each DustTrak signal. This ensured that the resulting concentrations were due only to road dust emissions generated by passing vehicles.

Background PM concentrations between PM peaks were less than 7 $\mu g/m^3$ on all days.

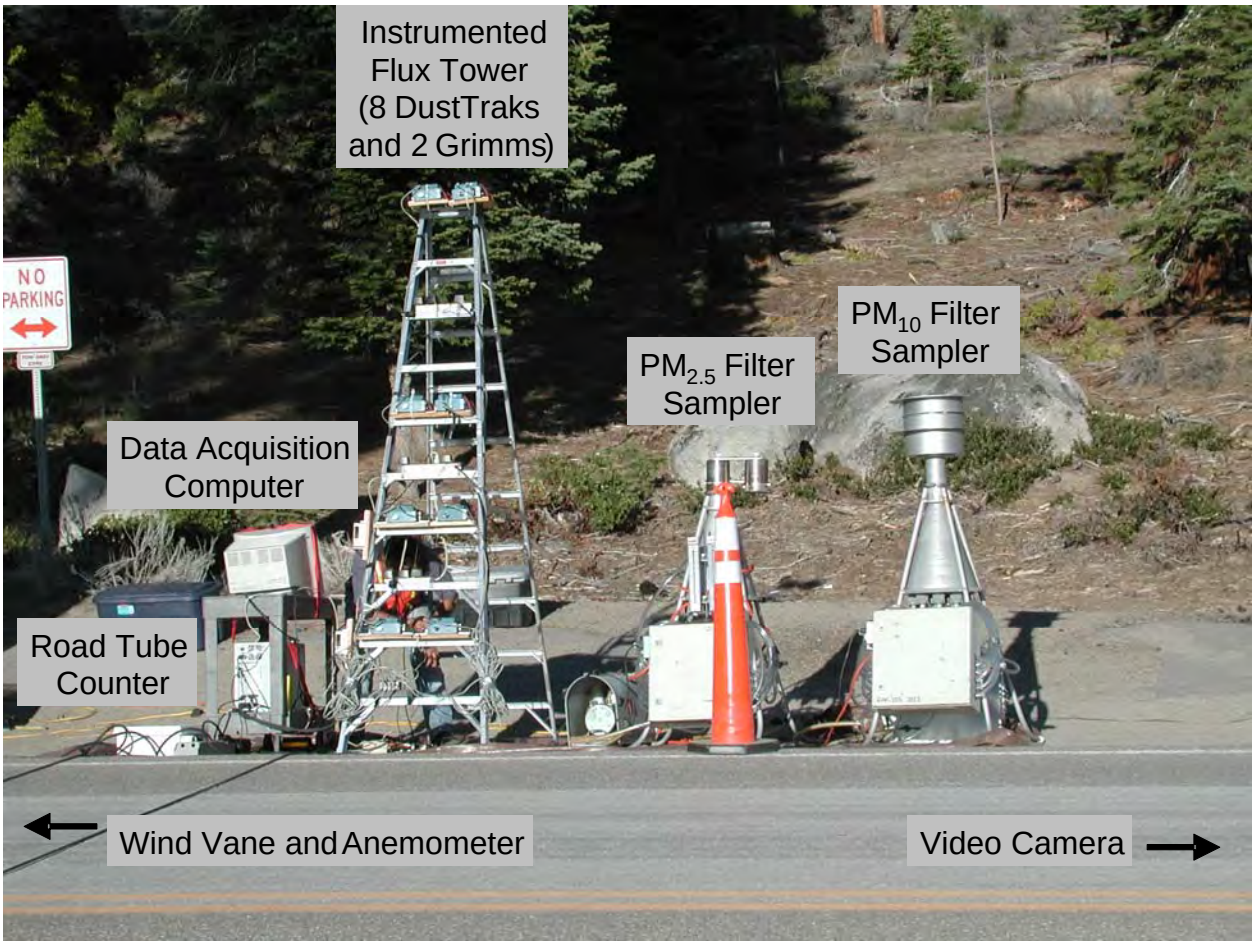

Figure 2-8. Road side sampling equipment deployed ~300 m south of entrance to Sand Harbor on Highway 28.

The flux of PM perpendicular to the roadway was calculated using the equation:

$$Flux(mg/m) = u(\tfrac{m}{s})\cos(\theta)\sum_{i=1}^{4} C_i(\tfrac{mg}{m^3})\Delta z_i(m)\Delta t(s) \qquad \textbf{(2-2)}$$

where *Flux* is the total flux of PM in mg per m perpendicular to the road, θ is the angle between the wind direction and a line perpendicular to the road, i is one of the four positions of the monitors on the tower, u is the measured wind speed in m/sec, C_i is the PM concentration in mg/m^3 as measured by the ith monitor over the period Δt, Δz in m is the vertical interval represented by the ith monitor, and Δt in sec is the duration that the plume impacts the tower. The upper panel of Figure 2-9 shows the average PM concentration over the sampling interval from 12:06 to 16:36 on 3/31/03. The marker points represent the location of each DustTrak sampler measuring C_i. The error bars represent the vertical layer represented by each DustTrak (Δz_i). In this example, the concentration of PM_{10} at the 3 m DustTrak is less than half the concentration measured at the 0.5 m and 1 m levels.

Previous deployments of the flux tower on low volume (<50 vehicles per hour) unpaved roads permitted the calculation of emission factors for individual vehicle passes (Etyemezian et

al., 2003). The intensity of traffic (~400 vehicles/hr) on Highway 28 precluded the isolation of individual vehicle plumes based on the PM dataset. An example time series of the 1 sec PM flux perpendicular to the highway is shown in the lower panel of Figure 2-9. Flux measurements were validated only when winds were blowing within 45 degrees of perpendicular to the road. (The regular cycle of 0 degree wind direction readings is associated with a timeout error in the wind vane data acquisition program. Measurements collected during these periods were not included in the fleet average emission factor calculation.) The time series shows large variability in the flux rates associated with sporadic traffic flows and the occasional passage of heavy duty tractor trailers that suspended large amounts of sand in their wake. Aggregate emission factors for all vehicles were calculated by dividing the total flux of PM perpendicular to the road (Eq. 2-2) by the number of vehicles passing the tower:

$$EF(g/vkt) = \frac{Flux(\frac{mg}{m})}{Traffic\ Volume\ (vehicles)}\left(\frac{1g}{1000mg}\right)\left(\frac{1000m}{1km}\right) \qquad \textbf{(2-3)}$$

In addition to the real-time instrumentation deployed on the flux tower, filter-based PM_{10} and $PM_{2.5}$ samplers were also operated. The samples collected with these medium-volume samplers were used to calculate source profiles related to road sanding and brine application.

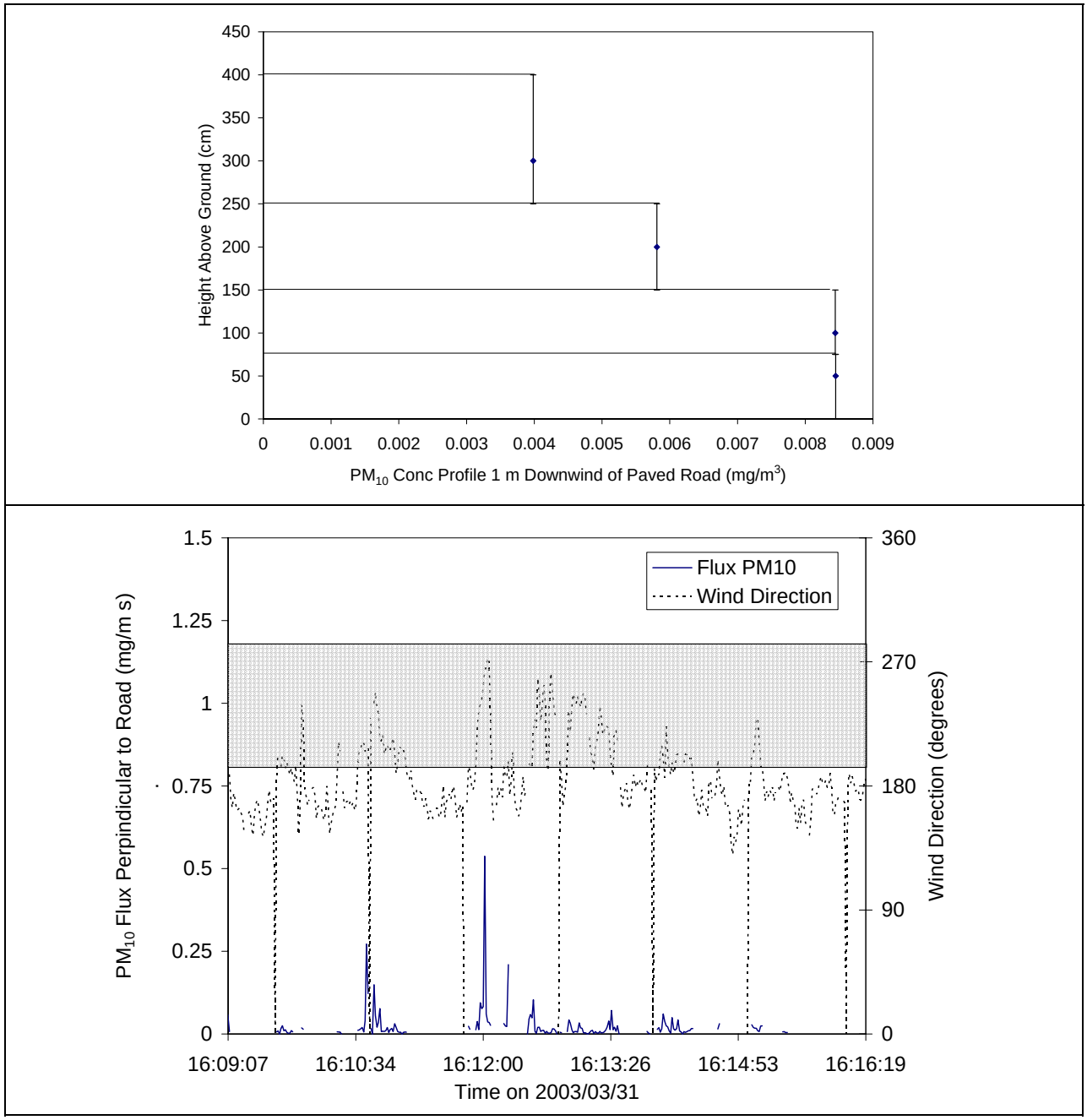

Figure 2-9. Vertical profile of PM concentration 1 m away from the side of paved road (upper panel). Time series of PM10 flux perpendicular to road calculated from DustTraks and wind vane. The shaded band represents the range of wind directions that are within 45 degrees of perpendicular to the road.

2.3 TRAKER Vehicle

The TRAKER system was first used in Las Vegas to survey road dust on over 100 miles of paved roads (Kuhns et al., 1999). The principle behind the TRAKER is illustrated in Figure 2-10. The concentration of airborne particles is monitored through inlets that are mounted near

the front tires of a vehicle. These particle sensors are influenced by the road dust generated from the spinning of a tire. A background measurement of particle concentrations is obtained simultaneously at a location on the vehicle farther away from the tires. The difference in the signals between the influence monitors and the background monitor is related to the amount of road dust generated:

$$T = T_T - T_b \qquad \textbf{(2-4)}$$

where T is the raw TRAKER signal, T_T is the particle concentration measured behind the tire, and T_B is the background concentration.

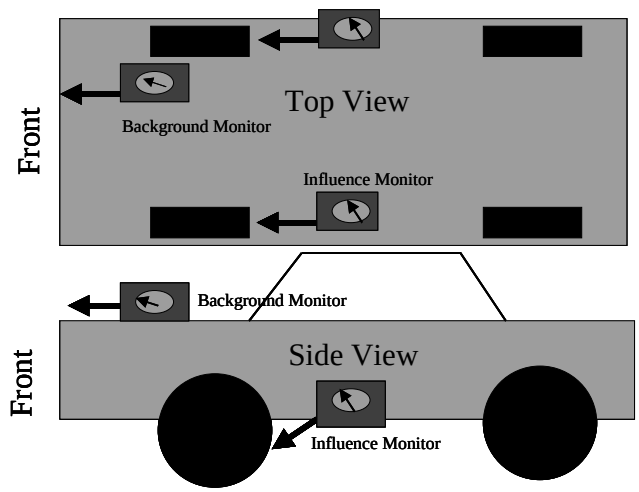

Figure 2-10. TRAKER influence monitors measure the concentration of particles behind the tires. A background monitor is used to establish a baseline.

The TRAKER is composed of a van that has been equipped with three exterior steel pipes acting as inlets for the onboard instruments (Figure 2-11a). Two of the pipes are located behind the left and right front tires and are used to measure emissions from the tires. The third pipe runs along the centerline of the van underneath the body and extends through the front bumper. This pipe is the inlet for background air. Dust and exhaust emissions from other vehicles on the road can cause fluctuations in the particle concentration above the road surface. The background measurement is used to correct the measurements behind the tires for those fluctuations.

The three exterior pipes enter the cargo compartment of the van through the underbody. Each pipe then goes into a plenum/manifold; the plenum can be used to distribute the sample air to up to five instruments (Figure 2-11c). For the present study, two TSI DustTraks with 10 μm inlets were operated in parallel at each of the three inlet lines.

A central computer collected all the data generated by the onboard instruments (Figure 2-11d). Data from TRAKER measurements were imported into a Microsoft Access database for subsequent data processing and analysis.

2.3.1 Inlets

Unlike gases, particles have inertia; as a result, the sampling of particles through an inlet results in some particle losses to inlet surfaces. These losses could be due to the diffusion of

particles toward inlet walls or the impaction/settling of particles upon inlet walls. Diffusion is a phenomenon that governs the motion of very small particles (less than 0.1 μm). Since road dust is composed primarily of larger particles (greater than 0.3 μm), diffusion is not an important consideration for TRAKER. Impaction and gravitational settling, however, are important processes for sampling particles with aerodynamic diameters greater than 1 μm. Gravitational settling can be minimized by reducing the amount of time a particle spends in the inlet lines (e.g., by increasing the speed of the flow). On the other hand, particle impaction can be minimized by reducing the speed of the flow at turns within the inlet lines.

The inlet lines, visible in Figure 2-11a, are 19 mm (3/4") in diameter and 2.3 m (7.5') long for the tire lines and 3.7 m (12') long for the background line. The influence inlets on the right and left are in slightly different positions with respect to the tires. On the right, the inlet is 165 mm (6.5") above the ground, 50 mm (2") behind the tire, and 63 mm (2.5") in (toward the center of the vehicle) from the outside edge of the tire. On the left, the inlet is 165 mm (6.5") above the ground, 63 mm (2.5") behind the tire, and 63 mm (2.5") in from the outside edge of the tire. Because of the vehicle's configuration, it is not possible to avoid bends in the inlet lines. However, the bends have been kept as shallow as possible in order to minimize losses of particles to the inlet walls. Each of the inlet lines feeds into a 600 mm (20") long torpedo-shaped plenum (Figure 2-11c). All particle sampling instruments are connected through the plenum via short Tygon tubes that are in turn attached to 200 mm (8") long steel tubes that extend into the body of the plenum. Flowrates through the inlets are 75 liters per minute (lpm), corresponding to an inlet face velocity of 4 meters per sec (m/sec) and 0.3 m/sec in the plena.

a.

b.

c.

d.

Figure 2-11. TRAKER vehicle and instrumentation: a) Location of inlets (right side and background shown); b) Generator and pumps mounted on a platform on the back of the van; c) Two sampling plenums (bottom), a suite of DustTrak particle monitors (top right), and three rotameters used for ensuring proper flows through plena; and d) a dashboard-mounted computer screen used to view the data stream and a GPS to log the TRAKER's position every 1 s.

2.3.2 Instruments Used Onboard TRAKER

2.3.2.1 TSI DustTraks

The TSI DustTrak is a rugged portable monitor that uses particle light scattering to infer PM concentrations. In this study, six DustTraks were used onboard the TRAKER. Each of the three plena (left, right, and background) was equipped with two DustTraks using the manufacturer-provided 10 μm inlet.

2.3.2.2 Ashtech Promark GPS

The TRAKER uses an onboard GPS (Ashtech, Promark) to relate road dust emission measurements to a specific position on the road network. The accuracy of the GPS signal varies between 3 m and 15 m depending on the access. All data obtained from the mobile GPS used in this study were logged to a central TRAKER computer every 1 sec.

2.3.3 Data Acquisition and Measurement Documentation

The TRAKER may utilize up to 10 instruments (six DustTraks, three Grimm particle size analyzers, and one GPS), with each generating data at a rate of up to 60 readings per minute. A central onboard computer is used to capture the data in real time. Data from individual instruments are transferred via RS-232 serial interfaces to a multiplexing unit that is in turn connected to the computer. Specialized software has been written to capture the data, use the computer clock to provide a common time stamp, write to a database in real time, and provide the operator(s) with feedback regarding the status of instruments. An example of the TRAKER display panel is shown in Figure 2-12.

2.3.4 TRAKER Data Processing

The DustTrak instrumentation onboard the TRAKER vehicle has a resolution of 1 $\mu g/m^3$. Thus, the smallest measurable difference in concentration between the tire and the background monitors is 1 $\mu g/m^3$. This corresponds approximately to a single-point minimum detection limit equivalent to an emission factor of 0.9 g/VKT for unpaved roads (or 0.04 g/VKT for paved roads), meaning that any 1 sec measurement can be resolved to within this value only. Substantially smaller emission factors can be measured with the TRAKER if multiple data points are used to calculate an average. At the other end of the measurement range, DustTrak readings above 150 mg/m^3 are not reliable. This corresponds to an emission factor for PM_{10} of approximately 50 g/VKT.

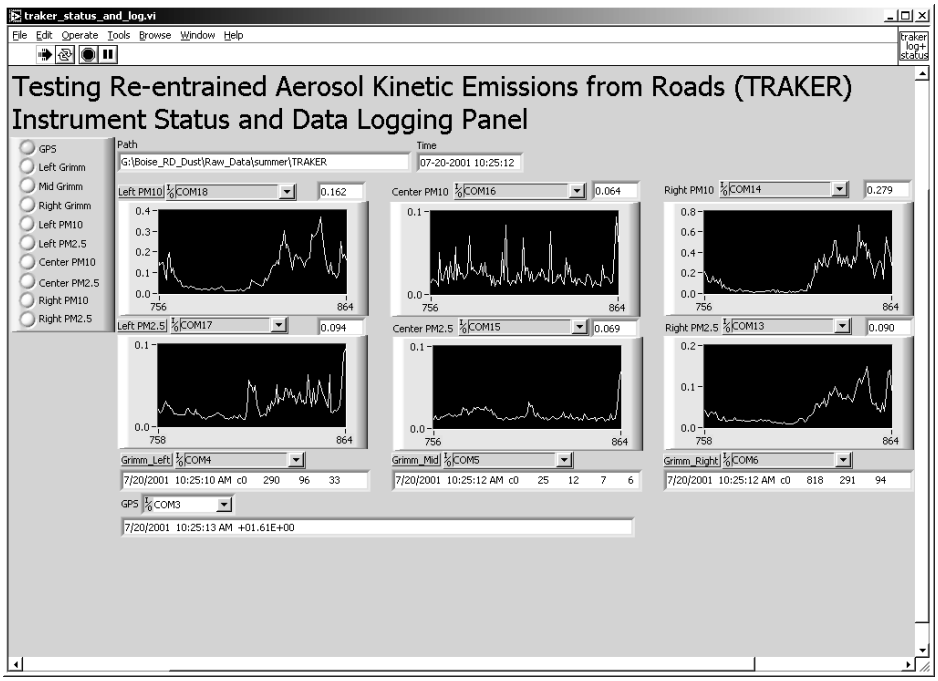

Figure 2-12. TRAKER Control Panel. Real-time figures show the magnitude of the response of DustTraks. The 10 lights at the top left of the screen serve as indicators of the health of onboard instruments (green = OK; red = not functioning).

Figure 2-13 shows the TRAKER coefficient of variation calculated from the left and right PM_{10} DustTrak signals as a function of vehicle speed. The coefficient of variation is a measure of the relative precision and is equal to the standard deviation of the measurement divided by the average of the measurement. In the figure, the measurement corresponds to multiple passes on the same 1-mile stretch of road (Etyemezian et al., 2003). The figure shows that the precision of the measurement improves with increasing vehicle speed. The precision is 84% at 5 m/sec, 30% at 9 m/sec, and approximately 10% above 14 m/sec. Note that most TRAKER measurements occur at speeds greater than 9 m/sec (approximately 20 mph). The poor precision at low speeds is probably due to the influence of fluctuating ambient winds on the flow regime behind the front tires. As the vehicle speed increases, such fluctuations become less important compared to the speed of the vehicle.

A TRAKER data point is considered valid only if it meets all of the criteria outlined in Table 2-4. Criteria are applied to the speed, acceleration, deceleration, and the wheel angle of the TRAKER vehicle. If a data point does not meet any of the criteria, then that data point is flagged as “Invalid” and is not used in any subsequent data processing activities. The TRAKER measurement uses the difference between the particle concentration measured behind the front tire and the concentration measured through the front bumper. Under certain conditions, the concentration at the front bumper may be higher than it is behind the front tire, resulting in a negative measurement. Negative values are not considered invalid and are retained in the database. It is important to retain negative values so that a systematic bias is not introduced into the dataset.

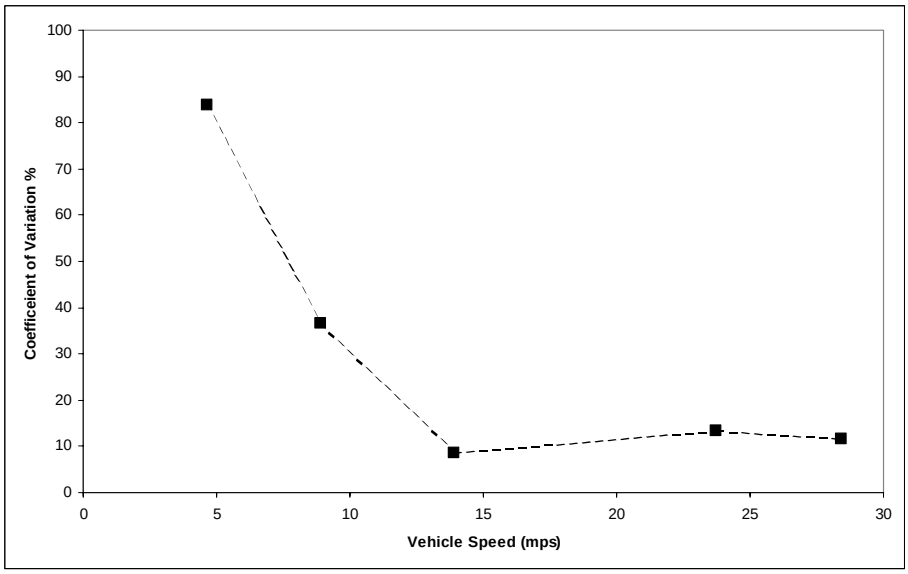

Figure 2-13. TRAKER coefficient of variation expressed as a percentage for left and right PM10 DustTrak signals as a function of speed. The data represent left and right PM10 DustTrak signals averaged over a 1-mile stretch of road near Boise, Idaho (Etyemezian et al., 2003). The coefficient of variation provides an estimate of the precision and is equal to the standard deviation of a measurement divided by the average.

Table 2-4. Validity criteria applied to each 1 sec TRAKER data point.

Parameter	Criterion	Threshold	Description
Speed	>	5 m/sec – paved roads (~11 miles/hr)	Minimize disturbances due to ambient winds.
Acceleration	<	0.5 m/sec^2 (~1.1 miles/hr/sec)	Lateral shear during acceleration and transient airflow around the TRAKER inlets render TRAKER measurements during times of high acceleration unreliable.
Deceleration	<	0.5 m/sec^2 (~1.1 miles/hr/sec)	Applying the brakes releases dust particles and may result in false high road dust readings.
Wheel Angle	<	3 degrees with respect to the vehicle body	Turns cause the front wheels to form an angle with the vehicle body. This in turn changes the orientation of the TRAKER inlets with respect to the front tires. Data associated with sharp turns are not valid.

The vehicle speed can become important in moderate to high winds. If the TRAKER is not moving fast enough, crosswinds and fluctuations in the ambient winds can lead to unsteady flow conditions between the front tire and the inlet. To avoid this possibility, a minimum speed of 5 m/sec is required to consider a data point valid. Acceleration/deceleration criteria (<0.5 m/sec^2) are also applied to the TRAKER measurement. During periods of high acceleration, the flow regime around the inlets may be transient; during periods of deceleration, dust from the brakes may influence the particle concentrations behind the front tire. In addition, the wheel angle must

be less than 3 degrees with respect to the vehicle body. This is to ensure that the orientation of the inlets with respect to the front tires is not changing over the course of the measurements. The criteria shown in Table 2-4 are based on empirical observations and statistical analyses of the TRAKER measurement under a variety of driving regimes. They are conservative and intended to ensure that the measurements used in this study are valid.

2.3.5 Relationship of TRAKER measurement to vehicle speed

Experiments were conducted to determine the variation of the TRAKER signal with vehicle speed. Tests were conducted on paved roads at the Fort Bliss Military Base near El Paso, TX, and on South Cloverdale Lane in Boise, ID (Etyemezian et al., 2003).

At Fort Bliss, a 1200 m section of road was traveled in the northbound direction. Three passes were run at speeds of 5, 9, 14, 19, 24, and 29 m/sec (equivalently, 10, 20, 30, 40, 50, and 60 mph) for a total of 18 passes. The differential between the tire and the background monitors was averaged over each pass based on the start and stop times of the run. The measurements of PM_{10} and $PM_{2.5}$ by DustTrak and particle counts per size bin were averaged for the left and right inlets.

For the Boise, ID, tests, a 440 m section of road was selected for testing. Passes were run over the same range of speeds as in Fort Bliss tests. The same lane of travel was surveyed with the vehicle traveling in both northbound and southbound directions. Using this approach, both the left and right inlets sampled the same tracks on the road. Values were averaged over each pass.

The resulting values from both sets of tests were regressed against the vehicle speed using a power function:

$$T_T - T_B = T^* s^b \qquad \textbf{(2-5)}$$

where T_T is the aerosol concentration at the vehicle tire, T_B is the background aerosol concentration at the bumper inlet, and *s* is the speed of the vehicle. The parameters T^* and b were iteratively calculated by minimizing the least squares error between the observed and predicted values. Figure 2-14 shows the example of the regression for DustTrak PM_{10} measurements from the Fort Bliss and Boise speed tests, where the regressions of TRAKER signal versus speed give exponents, *b*, of 2.8 (R^2=0.92) and 3.0 (R^2=0.97), respectively. Since all factors except for the speed of the TRAKER were held constant during these two tests, the strong regressions shown in Figure 2-13(a) and (b) indicate that T^* is a measure of the road segment's inherent potential for dust emission (See Section 5 for a discussion of the emission potential as a measure of road dust available for emission.)

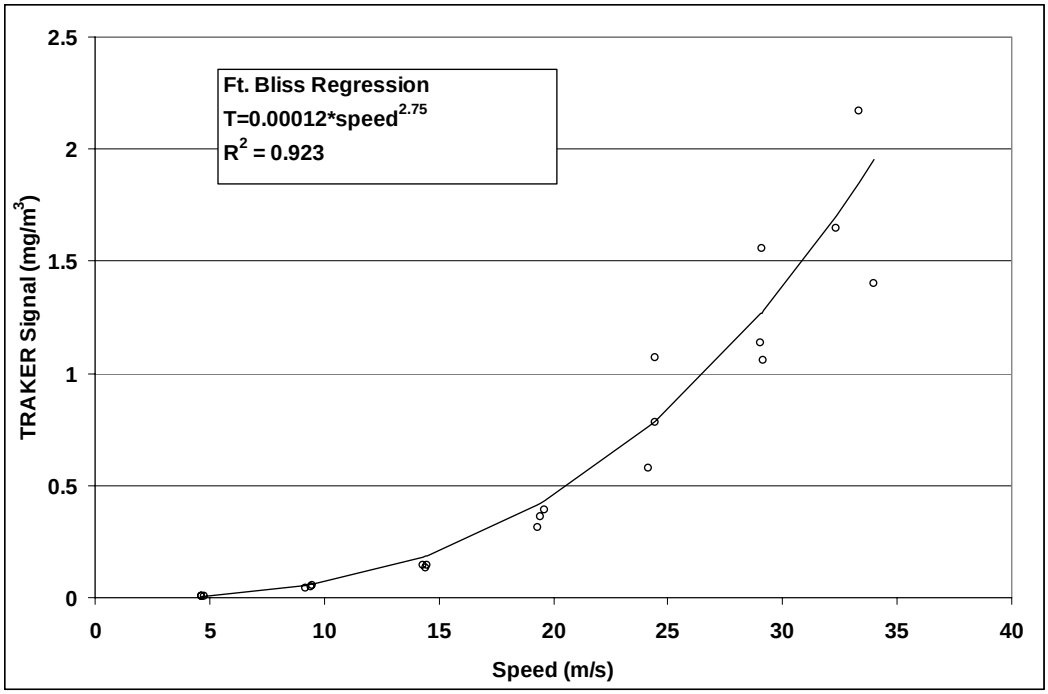

a.

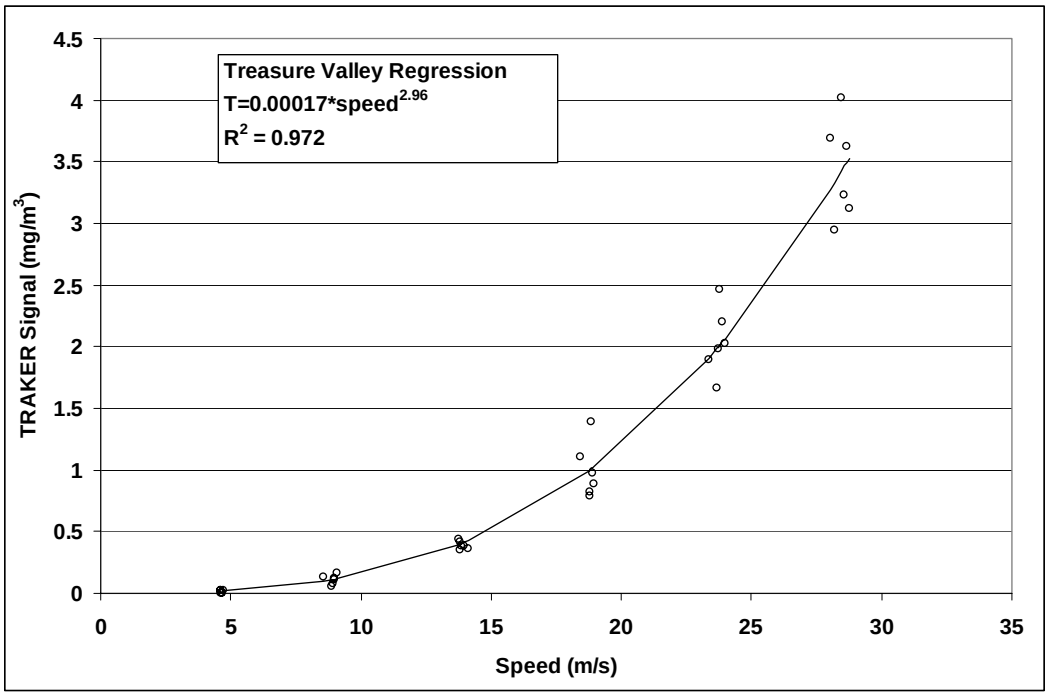

b.

Figure 2-14. Relationship between differential DustTrak measurements and vehicle speed for tests conducted on a common road section in a) Fort Bliss, near El Paso, TX, and b) a suburb of Boise, ID.

2.4 Comparison of TRAKER with Flux Towers

On 03/31/03, the TRAKER was operated in conjunction with the horizontal flux tower. The TRAKER signal was compared with the flux of particles measured downwind of a road. The flux of particles past the tower was calculated only when the winds were blowing within 45 degrees of perpendicular of the road. Between 12:10 and 16:40, this criterion eliminated 10,300 of the 16,141 1 sec measurements on the tower. The resultant winds for the period were from the southwest (222 degrees) at 1.6 m/sec.

Over the same interval, the TRAKER vehicle made 45 (23 southbound and 22 northbound) passes in front of the instrumented tower. The average and standard deviation of the TRAKER vehicle speed over the 150 m before and after the tower was 20.1 m/sec ± 0.1 m/sec. For comparison, the average speed of all vehicles as measured by the road tube counter collocated with the flux tower was 21.1 m/sec ± 0.3 m/sec. The average and standard deviation of the TRAKER signal over the 45 passes was 0.748 mg/m^3 ± 0.415 mg/m^3.

The flux of PM_{10} normal to the road was calculated when winds were within the 45 degree criterion. The flux was then multiplied by the total number of seconds between 12:10 and 16:40 and divided by the number of valid one second measurements (i.e. 16,141/5841). This scaling factor was used to estimate the total flux over the time interval from the subset of valid flux measurements when the winds were within 45 degrees of perpendicular to the road. The total flux in units of mg/m over the period was divided by the total number of vehicles (1683) passing the tower to calculate the fleet average PM_{10} emission factor of 0.305 g/vkt.

Prior to these measurements, the TRAKER vehicle had not been compared with directly measured paved road particulate matter (PM) emissions. Figure 2-15 below shows the average measured TRAKER signal versus the fleet average emission factors from 03/31/03. The points on the upper right of the figure were calculated from unpaved road experiments (Etyemezian et al., 2003; Kuhns et al., 2004). The paved road emission factor is lower than the unpaved road trend line by approximately a factor of 25.

The reason for this discrepancy is unknown. Hypotheses include:

- The traffic counter identified the fleet passing the flux tower as 98% light duty and 2% heavy duty vehicles. Recent field studies indicated that unpaved road dust emission factors increase linearly with both vehicle weight and vehicle speed (Gillies et al., 2004). Typical light duty vehicles have a mass of ~1.5 Mg (1 Mg = 1 metric ton) and heavy duty trucks have a mass of ~9 Mg. Based on these assumptions, the average mass of a vehicle passing the flux tower was ~1.6 Mg per vehicle, whereas TRAKER has a mass of ~3.1 Mg. If the relationship between emission factors (in g PM/vkt) and vehicle mass exists for paved roads as well as unpaved roads, then the fleet average emission factors should be lower than the TRAKER emission factor by a factor of 2 (i.e. 1.6 Mg/3.1 Mg). This would bring the LT emission factors more in line with the unpaved road measurements.
- Material suspended from unpaved roads may be entrained by the wake of the vehicle. If this is not occurring on paved roads, the flux of particles downwind of the roadway may be less.

The Lake Tahoe emission factor is the only comparison of the TRAKER signal with a paved road emission factor. In this study, TRAKER exclusively surveyed paved roads. Based only on

the one calibration point collected at Sand Harbor, the revised equation relating the fleet average emission factors with the TRAKER signal is:

$$EF\left(\frac{g}{vkt}\right) = 0.33\left(T\left(\frac{mg}{m^3}\right)\right)^{0.33} \qquad \textbf{(2-6)}$$

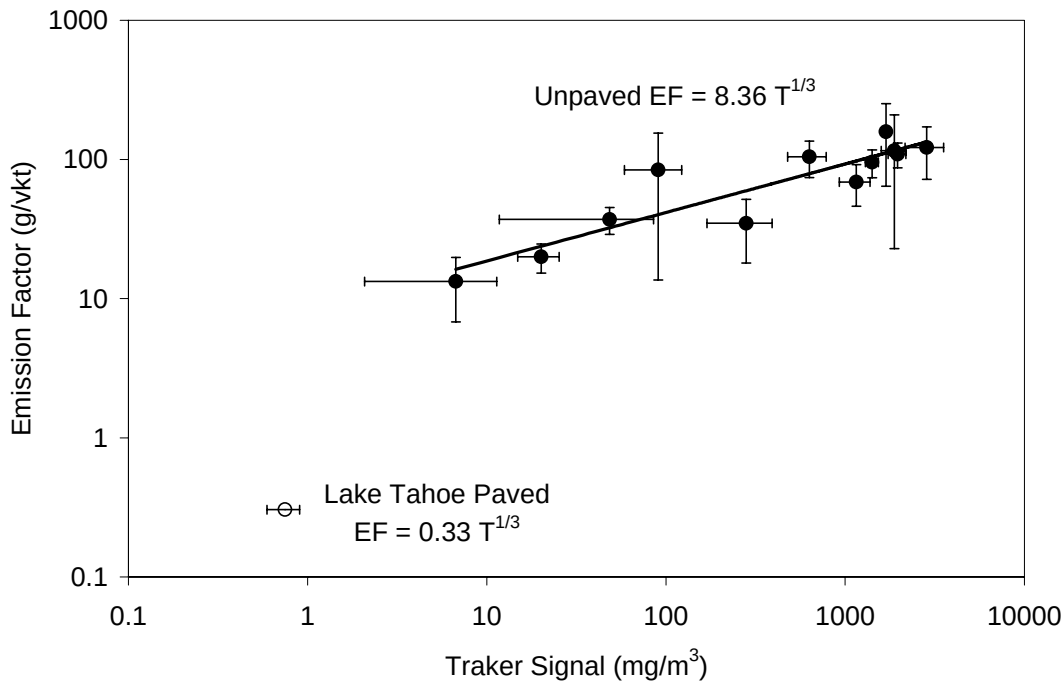

Figure 2-15. Regression of measured PM emission factors with TRAKER measurements. The line through points was drawn by holding the exponent of the regression equation at 1/3.

3. RESIDENTIAL WOOD COMBUSTION (RWC)

Source profiles and emission factors for RWC were directly measured by using emissions from residential chimneys in the Lake Tahoe Basin during November and December 2003. The ambient temperatures during the study period were less than 3 ºC and typical of conditions associated with the use of residential wood burning in the Lake Tahoe region. The in-plume emission test stand, which incorporated the FTIR and ELPI, along with the filter samplers, was deployed to measure gaseous and fine particle emissions from the chimneys. Flexable conductive tubing was attached to an 8 m piece of rigid PVC pipe support to bring the sampling inlet into the plume of a wood burning appliance from outside a house.

3.1. Summary of wood burning appliances and wood fuels in the Lake Tahoe region

A survey of wood burning practices in the Tahoe Basin provided the basis that was used to collect representative wood burning profiles (Fitz and Lentz, 2003). As of 4/24/03, 131 surveys were returned and tabulated into a database. The survey found that 16% of respondents used some type of wood device as their primary mode of heating, and 90% of yearly wood burning occurred in the winter season. The distribution of appliances was 59% woodstove, 25% fireplace without insert, 10% fireplace with insert, and 6% pellet stove. Nearly twice as many respondents claimed to burn softwood versus hardwood, but half of them either did not know the types of wood burned or claimed to burn both hard and soft woods. About 74% of the time, the wood burning appliance was used in the evening and the wood fuel was left to smolder overnight. It was estimated that the average camper burns a two-hour fire every evening, using an average of four logs. The average residence burns 7.4 logs over six hours a day during the winter months. The wood burned is a combination of hard and soft wood.

3.2. Source testing for RWC

Based on the survey results, the selection of wood burning appliances for this study focused on woodstoves (both U.S. EPA-certified and non-certified) and fireplaces with and without inserts. Lake Tahoe residents were recruited as volunteers for the study. A pre-visit was made to each residential site to coordinate the source characterization testing. It was found that a majority of the volunteers' appliances were either certified woodstoves or fireplaces with inserts. Since the main purpose of the appliances was to generate heat, residents had used high thermal heating efficiency as a criterion for selecting the appliances. Emissions from residence wood burning were conducted for conditions specified in Table 3-1.

Supplemental information on commercially available wood fuel types in the Lake Tahoe region is presented in Table 3-2.

Table 3-1. Wood burning tests conducted at Lake Tahoe residences during November and December 2003.

Type of furnace	Model	Type of Wood	Filter ID	Sampling Date	Sampling Period	Location	Ambient Temperature During Testing	Ratio of Source Signal to Total DustTrak PM2.5
Certified Woodstove[a]	Country Striker S160	Juniper/Cedar	LZST048 LZST054	Nov. 5, 2003 Nov. 4, 2003	45 minutes 55 minutes	Sierra College, NV	33ºF 33ºF	0.81 0.98
Conventional Woodstove[b]	Trailblaizer Classic 1000	Almond (hardwood)	LZST040 LZST044 LZST046	Nov.. 19, 2003 Nov. 18, 2003 Nov. 19, 2003	104 minutes 57 minutes 120 minutes	Camp Richardson, CA	37ºF 37ºF 37ºF	0.50 0.69 0.47
		Pine (softwood)	LZST034 LZST042	Nov. 19, 2003 Nov. 19, 2003	150 minutes 105 minutes		37ºF 37ºF	0.44 0.44
Fireplace	NA[c]	Oak (hardwood)	LZST024 LZST032	Dec. 18, 2003* Dec. 18, 2003	105 minutes 105 minutes	Incline Village, NV.	31ºF 31ºF 31ºF	0.48 0.89
		Juniper (softwood)	LZST022 LZST038 LZST062	Dec. 19, 2003* Dec. 19, 2003 Dec. 19, 2003	55 minutes 104 minutes 80 minutes		31ºF 31ºF	0.61 0.77 0.77

- *a. Country Striker Model S16, made in 1999*
- *b. The wood stove was manufactured by Heating Energy Systems, Inc., PO Box 503, Clackamas, OR 97015. The serial number is 03300. Model: Trailblazer Classic 1000. Tested to UL 737, 1482. Test date: May 1991, Report No. 91-021. Trailblazer Classic 1000 is identical structure to Trailblazer Classic 1300. Model 1300 is listed as EPA certified woodstove, yet Model 1000 was not on the list.*
- *c. not available*

**. Snow precipitation 2 days prior to sampling.*

Table 3-2. Availability of wood fuel at commercial stores in Lake Tahoe region.

Location	Company/Store	Product Name	Type of Wood	Cost	Quantity
Kings Beach	Ace Hardware	(no label on wood)	Hardwood	$4.99	not given
Kings Beach	Safeway	Cal-Sierra Kindling	Cedar, Fir, Pine, Spruce	$5.09	0.75 cu ft
Kings Beach	Safeway	Cal Oak Firewood www.hotwood.com	Seasoned Hardwood - Oak	11.19	2 cu ft
	Safeway	Duraflame Fire Log www.duraflame.com	Compressed Sawdust/Wax		
Kings Beach	Rockwood Inc.		Soft wood - Pine, Fir Mix	$185	cord
Kings Beach	Rockwood Inc.		Hardwood - Almond	$300	cord
Incline Village	Raley's	California Hot Wood	Hardwood: Almond, Madrone, Walnut, Tan Oak, Black Oak	$6.99	0.8 cu ft
Incline Village	Raley's	Lignetics of West Virginia wwwlignetics.com	Wood Pellet Fuel (sawdust)	$4.50	40 lb
Incline Village	Incline Firewood		Soft Wood - Tamarack	$270	cord
Incline Village	Incline Firewood		Hardwood - Almond	$290	cord
Incline Village	Incline Woodstove Distributors		Wood Pellet Fuel - Fir		
Round Hill	Safeway	Cal Oak Firewood www.hotwood.com	Seasoned Hardwood - Oak	11.19	2 cu ft
South Lake Tahoe	Meek's The Builders Choice	Lodge Warmer- Hager's Quality Firewood	Mixture of Hard & Soft Wood	$3.99	0.75 cu ft
South Lake Tahoe	Meek's The Builders Choice	Lignetics of West Virginia www.lignetics.com	Wood Pellet Fuel (Sawdust)	$4.49	40 lbs
South Lake Tahoe	Albertson's	California Hot Wood			
South Lake Tahoe	Albertson's	Fireside Wood Pak	Soft Wood - (Harvested & Recycled Pine, Fir & Walnut)		0.90 cu ft
South Lake Tahoe	Albertson's	Firelogs: Firelog, Pine Mountain, Duraflame			
South Lake Tahoe	Safeway	Cal Oak Firewood www.hotwood.com	Seasoned Hardwood - Oak	11.19	2 cu ft
South Lake Tahoe	Safeway	Fireside Wood Pak	Soft Wood - (Harvested & Recycled Pine, Fir & Walnut)	$4.59	1 cu ft
Truckee	Fletchers Firewood		Soft Wood - Pine, Fir Mix	$200	cord
	Northshore Wood Service		Soft Wood - Pine Fir Mix	$270	cord
	Northshore Wood Service		Hard Wood - Almond	$290	cord

- *Source: MacLaren, 2003.*

Homeowners were informed of sampling procedures, and any obstacles that would impede the sampling were identified. Wood burning exhaust was sampled approximately 2–3.5 m away from each chimney, where the exhaust was cooled and mixed with ambient air. Multiple samples for each RWC type were used to determine the variability in the emission. The emission sample collections were conducted from ~8:30 p.m. to 6:00 a.m. to minimize interferences from cooking and vehicle exhaust. The ambient temperature during sampling was low (<3 ºC) with low to calm winds (<2 m/sec). Each sampling session included kindling and steady burning, following the guidelines in U.S. EPA Method 28 (U.S. EPA, 1997). One log (3–4 kg) was used to initiate the fire and the wood combustion appliance was recharged with a log every 15–20 minutes to

maintain steady wood burning. The wood fuel burn rate used in the study is considered as the maximum burn rate, based on Method 28. The sampling period was determined by projecting mass loading on the filters from DustTrak readings. The wood fuel fed to the appliance was weighed on scales, and unburned wood fuel was extracted from the wood heating appliance and weighed hot. Data were recorded on a field data sheet modified from EPA Method 28 for this study.

3.3. Summary of Wood Burning Profiles

A total of 12 individual RWC emission samples were obtained from the following sources: a non-EPA certified woodstove burning juniper (also known as cedar) (two samples: LZST034, LZST042) and almond (three samples: LZST040, LZST044, LZST046) at Camp Richardson, CA; an EPA-certified wood-burning stove (LZST048 for kindling and LZST054 for steady wood burning) at Sierra Nevada College, NV; and a fireplace burning oak (two samples: LZST024, LZST032) and juniper (three samples: LZST022, LZST038, LZST062) at Incline Village, NV. The chemical compositions from these RWC emission exhausts are compared in Table 3-3, Table 3-4, Figure 3-1, and Figure 3-2.

Table 3-3. Summary of residential wood combustion profiles. All values are in percent of total mass.

Sample ID	lzst054	lzst024	lzst032	lzst022	lzst038	lzst062
Sample Start Time	11/4/2003 23:06	12/18/2003 21:10	12/18/2003 1:10	12/19/2003 2:10	12/19/2003 3:20	12/19/2003 12:30
Sample End Time	11/4/2003 23:59	12/18/2003 22:14	12/18/2003 2:14	12/19/2003 3:04	12/19/2003 4:24	12/19/2003 1:49
Location	Sierra College	Incline	Incline	Incline	Incline	Incline
Facility	Wood Stove	Fire place	Fire place	Fire place	Fire place	Fire place
Fuel		Oak	Oak	Juniper	Juniper	Juniper
Size (um)	2.5	2.5	2.5	2.5	2.5	2.5
Ammonia (NH3)	16.3266 ± 2.3432	0.7552 ± 0.2841	1.5918 ± 0.8295	0.7953 ± 0.2185	0.6472 ± 0.1654	1.3110 ± 0.2594
Chloride (Cl–)	0.8551 ± 0.6324	0.0000 ± 0.0784	0.3146 ± 0.2297	0.0779 ± 0.0660	0.0387 ± 0.0484	0.0111 ± 0.0725
Nitrate (NO3–)	2.4810 ± 0.3510	0.3206 ± 0.0383	0.1547 ± 0.0648	0.1054 ± 0.0246	0.0715 ± 0.0185	0.1226 ± 0.0292
Sulfate (SO4=)	2.3253 ± 0.2557	0.4614 ± 0.0376	0.6415 ± 0.0890	0.0646 ± 0.0236	0.0527 ± 0.0179	0.0566 ± 0.0279
Ammonium (NH4+)	0.9675 ± 0.2453	0.2885 ± 0.0350	0.1992 ± 0.0896	0.2281 ± 0.0271	0.0964 ± 0.0186	0.1284 ± 0.0288
Soluble Sodium (Na+)	0.0754 ± 0.1329	0.0215 ± 0.0059	0.2795 ± 0.0194	0.0080 ± 0.0040	0.0000 ± 0.0030	0.0010 ± 0.0047
Soluble Potassium (K+)	4.0398 ± 0.5267	0.7022 ± 0.1259	0.3338 ± 0.0878	0.1124 ± 0.0770	0.0726 ± 0.0750	0.0882 ± 0.0780
O1TC	16.7651 ± 3.6038	31.5899 ± 6.1079	8.0278 ± 2.7993	25.6856 ± 4.9656	33.0933 ± 6.3904	21.9533 ± 4.2486
O2TC	8.1990 ± 0.8361	13.2217 ± 2.5540	11.0623 ± 1.1236	6.8332 ± 1.3252	8.4774 ± 1.6360	5.6531 ± 1.1022
O3TC	11.3789 ± 3.3165	15.4918 ± 2.9943	30.9151 ± 2.4941	8.3255 ± 1.6202	8.3540 ± 1.6167	6.2172 ± 1.2280
O4TC	9.8720 ± 0.5376	9.3356 ± 2.6828	10.8553 ± 1.6798	4.2296 ± 1.2158	4.8111 ± 1.3827	3.1895 ± 0.9179
OPTC	0.0450 ± 1.4844	1.1542 ± 0.3272	5.2969 ± 1.4534	1.2906 ± 0.2394	1.8636 ± 0.3072	0.7885 ± 0.1822
OC (IMPROVE)	46.1332 ± 3.9772	70.7766 ± 3.8998	66.1164 ± 1.7439	46.3527 ± 2.5591	56.5895 ± 3.1122	37.7879 ± 2.0989
E1TC	75.2353 ± 13.1952	5.7148 ± 0.2377	5.6881 ± 1.3070	3.8304 ± 0.1597	5.5046 ± 0.2279	7.3844 ± 0.3059
E2TC	1.9827 ± 0.5717	1.1629 ± 0.3575	4.3975 ± 1.4477	1.0941 ± 0.3357	0.8034 ± 0.2464	2.2740 ± 0.6959
E3TC	0.5986 ± 2.4597	0.2495 ± 0.0819	0.2465 ± 0.1397	0.1289 ± 0.0426	0.1139 ± 0.0375	0.2296 ± 0.0790
EC (IMPROVE)	77.7855 ± 13.0149	5.9716 ± 0.4477	5.0314 ± 1.1238	3.7641 ± 0.2613	4.5573 ± 0.2895	9.0998 ± 0.5347
TCTC (IMPROVE)	123.9187 ± 5.4866	76.7525 ± 3.5125	71.1478 ± 5.2759	50.1168 ± 2.2978	61.1494 ± 2.7914	46.8878 ± 2.1575
Sodium (Na)	1.1290 ± 1.1347	0.0000 ± 0.2397	0.0946 ± 0.4104	0.0000 ± 0.1552	0.0269 ± 0.0846	0.0283 ± 0.1980
Magnesium (Mg)	0.0000 ± 0.2368	0.0000 ± 0.0304	0.0000 ± 0.0853	0.0000 ± 0.0345	0.0090 ± 0.0170	0.0000 ± 0.0418
Aluminum (Al)	0.0812 ± 0.2436	0.0319 ± 0.0278	0.0000 ± 0.0950	0.0306 ± 0.0213	0.0035 ± 0.0178	0.0252 ± 0.0253
Silicon (Si)	0.3354 ± 0.0943	0.0147 ± 0.0118	0.2341 ± 0.0348	0.0239 ± 0.0090	0.0127 ± 0.0068	0.0270 ± 0.0107
Phosphorus (P)	0.0000 ± 0.0506	0.0038 ± 0.0071	0.0000 ± 0.0158	0.0033 ± 0.0033	0.0000 ± 0.0035	0.0000 ± 0.0053
Sulfur (S)	0.6272 ± 0.0396	0.1292 ± 0.0041	0.1213 ± 0.0100	0.0335 ± 0.0026	0.0293 ± 0.0021	0.0503 ± 0.0033
Chlorine (Cl)	0.8588 ± 0.1286	0.0359 ± 0.0067	0.1081 ± 0.0180	0.1314 ± 0.0055	0.1194 ± 0.0044	0.1616 ± 0.0066
Potassium (K)	3.7453 ± 0.0531	0.5813 ± 0.0071	0.4473 ± 0.0143	0.1104 ± 0.0038	0.0944 ± 0.0029	0.1389 ± 0.0044
Calcium (Ca)	0.3270 ± 0.0392	0.2612 ± 0.0060	0.1863 ± 0.0128	0.0231 ± 0.0033	0.0092 ± 0.0024	0.0531 ± 0.0040
Titanium (Ti)	0.0060 ± 0.1915	0.0030 ± 0.0249	0.0218 ± 0.0732	0.0016 ± 0.0195	0.0000 ± 0.0154	0.0010 ± 0.0224
Vanadium (V)	0.0000 ± 0.0925	0.0001 ± 0.0119	0.0015 ± 0.0349	0.0005 ± 0.0093	0.0000 ± 0.0086	0.0000 ± 0.0107
Chromium (Cr)	0.0006 ± 0.0221	0.0000 ± 0.0028	0.0294 ± 0.0076	0.0000 ± 0.0022	0.0000 ± 0.0024	0.0002 ± 0.0026
Manganese (Mn)	0.0080 ± 0.0088	0.0091 ± 0.0011	0.0137 ± 0.0043	0.0005 ± 0.0010	0.0000 ± 0.0010	0.0011 ± 0.0010
Iron (Fe)	0.0525 ± 0.0187	0.0191 ± 0.0024	0.2646 ± 0.0074	0.0120 ± 0.0018	0.0010 ± 0.0014	0.0221 ± 0.0022
Cobalt (Co)	0.0000 ± 0.0058	0.0000 ± 0.0008	0.0039 ± 0.0050	0.0001 ± 0.0007	0.0000 ± 0.0005	0.0001 ± 0.0008
Nickel (Ni)	0.0015 ± 0.0051	0.0000 ± 0.0007	0.0065 ± 0.0015	0.0000 ± 0.0005	0.0000 ± 0.0004	0.0001 ± 0.0006
Copper (Cu)	0.0057 ± 0.0055	0.0013 ± 0.0006	0.0101 ± 0.0021	0.0000 ± 0.0007	0.0000 ± 0.0005	0.0012 ± 0.0006
Zinc (Zn)	0.0792 ± 0.0049	0.0106 ± 0.0006	0.1008 ± 0.0021	0.0038 ± 0.0005	0.0029 ± 0.0004	0.0075 ± 0.0006
Gallium (Ga)	0.0000 ± 0.0321	0.0000 ± 0.0042	0.0000 ± 0.0121	0.0000 ± 0.0032	0.0000 ± 0.0025	0.0000 ± 0.0038
Arsenic (As)	0.0000 ± 0.0169	0.0000 ± 0.0023	0.0010 ± 0.0064	0.0000 ± 0.0018	0.0000 ± 0.0014	0.0000 ± 0.0020
Selenium (Se)	0.0008 ± 0.0069	0.0000 ± 0.0010	0.0005 ± 0.0027	0.0000 ± 0.0007	0.0000 ± 0.0006	0.0000 ± 0.0008
Bromine (Br)	0.0047 ± 0.0043	0.0008 ± 0.0005	0.0009 ± 0.0022	0.0006 ± 0.0004	0.0004 ± 0.0003	0.0013 ± 0.0005
Rubidium (Rb)	0.0000 ± 0.0075	0.0008 ± 0.0007	0.0022 ± 0.0031	0.0001 ± 0.0008	0.0000 ± 0.0006	0.0000 ± 0.0009
Strontium (Sr)	0.0032 ± 0.0088	0.0018 ± 0.0009	0.0033 ± 0.0025	0.0000 ± 0.0009	0.0000 ± 0.0007	0.0000 ± 0.0011
Yttrium (Y)	0.0045 ± 0.0106	0.0000 ± 0.0014	0.0020 ± 0.0042	0.0000 ± 0.0011	0.0000 ± 0.0009	0.0000 ± 0.0013
Zerconium (Zr)	0.0000 ± 0.0124	0.0000 ± 0.0017	0.0023 ± 0.0050	0.0000 ± 0.0013	0.0000 ± 0.0010	0.0000 ± 0.0015
Molybdenum (Mo)	0.0125 ± 0.0219	0.0000 ± 0.0030	0.0000 ± 0.0087	0.0000 ± 0.0023	0.0000 ± 0.0018	0.0000 ± 0.0027
Palladium (Pd)	0.0041 ± 0.0232	0.0000 ± 0.0030	0.0000 ± 0.0091	0.0000 ± 0.0024	0.0000 ± 0.0018	0.0000 ± 0.0027
Silver (Ag)	0.0000 ± 0.0307	0.0000 ± 0.0042	0.0017 ± 0.0116	0.0000 ± 0.0032	0.0000 ± 0.0024	0.0000 ± 0.0037
Cadmium (Cd)	0.0201 ± 0.0290	0.0018 ± 0.0038	0.0066 ± 0.0104	0.0010 ± 0.0027	0.0015 ± 0.0022	0.0012 ± 0.0034
Indium (In)	0.0121 ± 0.0358	0.0000 ± 0.0047	0.0026 ± 0.0137	0.0012 ± 0.0037	0.0003 ± 0.0028	0.0000 ± 0.0043
Tin (Sn)	0.0000 ± 0.0573	0.0006 ± 0.0073	0.0051 ± 0.0215	0.0000 ± 0.0058	0.0000 ± 0.0043	0.0000 ± 0.0066
Antimony (Sb)	0.0000 ± 0.0606	0.0007 ± 0.0081	0.0059 ± 0.0240	0.0000 ± 0.0064	0.0000 ± 0.0048	0.0003 ± 0.0074
Barium (Ba)	0.0000 ± 0.3038	0.0081 ± 0.0396	0.0000 ± 0.1165	0.0000 ± 0.0309	0.0045 ± 0.0235	0.0000 ± 0.0357
Lanthanum (La)	0.0000 ± 0.3719	0.0000 ± 0.0488	0.0231 ± 0.1456	0.0000 ± 0.0385	0.0128 ± 0.0294	0.0086 ± 0.0446
Gold (Au)	0.0000 ± 0.0275	0.0000 ± 0.0037	0.0067 ± 0.0107	0.0000 ± 0.0028	0.0000 ± 0.0022	0.0000 ± 0.0033
Mercury (Hg)	0.0013 ± 0.0123	0.0000 ± 0.0017	0.0000 ± 0.0048	0.0000 ± 0.0013	0.0000 ± 0.0010	0.0000 ± 0.0015
Thallium (Tl)	0.0000 ± 0.0116	0.0000 ± 0.0015	0.0000 ± 0.0046	0.0002 ± 0.0012	0.0003 ± 0.0009	0.0002 ± 0.0014
Lead (Pb)	0.0189 ± 0.0180	0.0000 ± 0.0032	0.0019 ± 0.0093	0.0000 ± 0.0025	0.0000 ± 0.0019	0.0000 ± 0.0029
Uranium (U)	0.0000 ± 0.0992	0.0000 ± 0.0029	0.0000 ± 0.0136	0.0005 ± 0.0021	0.0001 ± 0.0016	0.0000 ± 0.0025
Sum of species	135.3474 ± 5.5808	78.7953 ± 3.5148	74.1231 ± 5.2880	50.8142 ± 2.2999	61.5522 ± 2.7924	47.4966 ± 2.1604

Table 3-4. Summary of residential wood combustion profiles. All values are in percent of total mass. The grey column denote an invalid source sample.

Sample ID	lzst034	lzst042	lzst040	lzst044	lzst046	lzst048
Sample Start Time	11/19/2003 23:25	11/19/2003 20:41	11/19/2003 3:43	11/18/2003 23:20	11/19/2003 0:57	11/5/2003 0:15
Sample End Time	11/20/2003 1:49	11/19/2003 22:39	11/19/2003 5:33	11/19/2003 0:17	11/19/2003 3:08	11/5/2003 0:59
Location	Camp Richardson	Camp Richardson	Camp Richardson	Camp Richardson	Camp Richardson	Sierra College
Facility	Wood Stove	Wood Stove	Wood Stove	Wood Stove	Wood Stove	Wood Stove
Fuel	Pine	Pine	Almond	Almond	Almond	
Size (um)	2.5	2.5	2.5	2.5	2.5	2.5
Ammonia (NH3)	3.0018 ± 0.5387	4.2970 ± 1.0961	4.2823 ± 0.1780	2.3140 ± 0.1315	7.3520 ± 0.2588	0.7616 ± 0.0869
Chloride (Cl–)	0.0000 ± 0.1432	0.0000 ± 0.2903	0.0000 ± 0.0472	0.3836 ± 0.0563	0.1814 ± 0.0742	0.4340 ± 0.0525
Nitrate (NO3–)	0.0000 ± 0.0576	0.0000 ± 0.1171	0.0000 ± 0.0190	0.1967 ± 0.0236	0.0000 ± 0.0275	0.1798 ± 0.0197
Sulfate (SO4=)	0.0000 ± 0.0576	0.0000 ± 0.1171	0.0000 ± 0.0190	0.4143 ± 0.0185	0.1098 ± 0.0277	0.3100 ± 0.0130
Ammonium (NH4+)	0.0823 ± 0.0576	0.1679 ± 0.1171	0.0194 ± 0.0190	0.0658 ± 0.0141	0.1335 ± 0.0276	0.1312 ± 0.0095
Soluble Sodium (Na+)	0.0055 ± 0.0098	0.0043 ± 0.0198	0.0021 ± 0.0032	0.0357 ± 0.0033	0.0130 ± 0.0048	0.0092 ± 0.0018
Soluble Potassium (K+)	0.1032 ± 0.0426	0.0381 ± 0.0143	0.0007 ± 0.0021	0.9136 ± 0.0352	0.2343 ± 0.0222	0.6142 ± 0.0747
O1TC	5.7281 ± 1.2043	0.3826 ± 0.3234	0.0000 ± 0.0476	18.6294 ± 3.7881	6.1978 ± 1.2755	62.6442 ± 12.7160
O2TC	2.2349 ± 0.1967	1.2657 ± 0.2727	0.0875 ± 0.0396	5.5027 ± 0.3542	5.4844 ± 0.3616	20.6834 ± 1.3176
O3TC	4.8840 ± 1.2670	5.6217 ± 1.6183	0.3081 ± 0.1430	3.8473 ± 0.9225	12.7845 ± 3.0291	6.2233 ± 1.4671
O4TC	1.6580 ± 0.1212	1.4868 ± 0.2368	0.0946 ± 0.0381	2.6479 ± 0.0667	4.0510 ± 0.1072	2.8996 ± 0.0726
OPTC	0.9381 ± 0.3665	1.1705 ± 0.4777	0.0000 ± 0.0277	3.5010 ± 1.2639	1.1767 ± 0.4386	20.3824 ± 7.3501
OC (IMPROVE)	15.4173 ± 0.9460	9.8717 ± 1.1276	0.4683 ± 0.1621	34.1221 ± 1.7354	29.6818 ± 1.5321	112.8280 ± 5.6980
E1TC	3.4943 ± 0.6156	1.0579 ± 0.2259	0.0000 ± 0.0206	12.5513 ± 2.2007	2.8318 ± 0.4975	46.1341 ± 8.0889
E2TC	1.2044 ± 0.2942	1.3742 ± 0.3601	0.0368 ± 0.0272	0.1437 ± 0.0389	0.6886 ± 0.1663	0.7430 ± 0.1752
E3TC	0.1246 ± 0.0852	0.0000 ± 0.0563	0.0000 ± 0.0086	0.1218 ± 0.0767	0.0938 ± 0.0593	0.1048 ± 0.0717
EC (IMPROVE)	3.8844 ± 0.6468	1.2583 ± 0.3322	0.0376 ± 0.0338	9.3164 ± 1.4886	2.4367 ± 0.4067	26.5992 ± 4.2454
TCTC (IMPROVE)	19.3017 ± 0.9457	11.1300 ± 1.1525	0.5059 ± 0.1694	43.4365 ± 1.7412	32.1185 ± 1.3158	139.4272 ± 5.5544
Sodium (Na)	0.0262 ± 0.3883	0.0000 ± 0.6964	0.0000 ± 0.1538	0.0290 ± 0.1623	0.0000 ± 0.2359	0.0000 ± 0.0648
Magnesium (Mg)	0.0000 ± 0.0920	0.0120 ± 0.1110	0.0039 ± 0.0190	0.0000 ± 0.0323	0.0000 ± 0.0276	0.0007 ± 0.0090
Aluminum (Al)	0.0100 ± 0.0597	0.0157 ± 0.1146	0.0292 ± 0.0173	0.0186 ± 0.0132	0.0137 ± 0.0286	0.0000 ± 0.0094
Silicon (Si)	0.0852 ± 0.0223	0.0984 ± 0.0446	0.0080 ± 0.0073	0.0036 ± 0.0073	0.0141 ± 0.0106	0.0034 ± 0.0036
Phosphorus (P)	0.0028 ± 0.0106	0.0214 ± 0.0163	0.0002 ± 0.0040	0.0000 ± 0.0042	0.0030 ± 0.0056	0.0008 ± 0.0018
Sulfur (S)	0.0934 ± 0.0066	0.0857 ± 0.0126	0.0568 ± 0.0025	0.2074 ± 0.0029	0.0960 ± 0.0042	0.0244 ± 0.0011
Chlorine (Cl)	0.2342 ± 0.0136	0.1632 ± 0.0236	0.2203 ± 0.0054	0.6007 ± 0.0073	0.6873 ± 0.0103	0.0553 ± 0.0023
Potassium (K)	0.6495 ± 0.0111	0.3614 ± 0.0176	0.3676 ± 0.0044	1.7312 ± 0.0070	0.7134 ± 0.0070	0.0690 ± 0.0016
Calcium (Ca)	0.0861 ± 0.0087	0.1431 ± 0.0161	0.0109 ± 0.0032	0.0083 ± 0.0266	0.0103 ± 0.0124	0.0041 ± 0.0013
Titanium (Ti)	0.0014 ± 0.0476	0.0045 ± 0.0926	0.0000 ± 0.0164	0.0000 ± 0.0123	0.0028 ± 0.0225	0.0000 ± 0.0079
Vanadium (V)	0.0000 ± 0.0262	0.0000 ± 0.0446	0.0000 ± 0.0091	0.0000 ± 0.0069	0.0000 ± 0.0107	0.0000 ± 0.0037
Chromium (Cr)	0.0000 ± 0.0071	0.0001 ± 0.0106	0.0000 ± 0.0025	0.0000 ± 0.0019	0.0000 ± 0.0025	0.0000 ± 0.0009
Manganese (Mn)	0.0009 ± 0.0030	0.0035 ± 0.0042	0.0004 ± 0.0010	0.0000 ± 0.0008	0.0000 ± 0.0012	0.0000 ± 0.0004
Iron (Fe)	0.0698 ± 0.0045	0.0358 ± 0.0090	0.0054 ± 0.0015	0.0014 ± 0.0011	0.0038 ± 0.0021	0.0023 ± 0.0007
Cobalt (Co)	0.0006 ± 0.0019	0.0007 ± 0.0029	0.0000 ± 0.0005	0.0000 ± 0.0004	0.0000 ± 0.0007	0.0000 ± 0.0003
Nickel (Ni)	0.0006 ± 0.0012	0.0014 ± 0.0025	0.0000 ± 0.0004	0.0000 ± 0.0003	0.0000 ± 0.0006	0.0000 ± 0.0002
Copper (Cu)	0.0020 ± 0.0013	0.0046 ± 0.0024	0.0003 ± 0.0006	0.0001 ± 0.0005	0.0003 ± 0.0008	0.0000 ± 0.0003
Zinc (Zn)	0.0589 ± 0.0013	0.0200 ± 0.0023	0.0110 ± 0.0004	0.0947 ± 0.0006	0.0169 ± 0.0006	0.0008 ± 0.0002
Gallium (Ga)	0.0029 ± 0.0077	0.0037 ± 0.0155	0.0000 ± 0.0026	0.0000 ± 0.0019	0.0000 ± 0.0037	0.0000 ± 0.0013
Arsenic (As)	0.0001 ± 0.0041	0.0021 ± 0.0080	0.0002 ± 0.0014	0.0007 ± 0.0011	0.0000 ± 0.0020	0.0000 ± 0.0008
Selenium (Se)	0.0004 ± 0.0016	0.0006 ± 0.0034	0.0000 ± 0.0006	0.0000 ± 0.0004	0.0000 ± 0.0008	0.0000 ± 0.0003
Bromine (Br)	0.0017 ± 0.0010	0.0025 ± 0.0021	0.0014 ± 0.0003	0.0037 ± 0.0003	0.0018 ± 0.0005	0.0002 ± 0.0002
Rubidium (Rb)	0.0010 ± 0.0019	0.0011 ± 0.0038	0.0002 ± 0.0007	0.0010 ± 0.0004	0.0000 ± 0.0010	0.0000 ± 0.0003
Strontium (Sr)	0.0015 ± 0.0022	0.0004 ± 0.0043	0.0000 ± 0.0008	0.0001 ± 0.0006	0.0000 ± 0.0011	0.0000 ± 0.0004
Yttrium (Y)	0.0004 ± 0.0026	0.0000 ± 0.0052	0.0000 ± 0.0009	0.0000 ± 0.0007	0.0000 ± 0.0013	0.0001 ± 0.0005
Zerconium (Zr)	0.0033 ± 0.0023	0.0000 ± 0.0061	0.0000 ± 0.0011	0.0000 ± 0.0008	0.0000 ± 0.0016	0.0000 ± 0.0006
Molybdenum (Mo)	0.0003 ± 0.0054	0.0024 ± 0.0108	0.0000 ± 0.0019	0.0000 ± 0.0015	0.0000 ± 0.0027	0.0000 ± 0.0010
Palladium (Pd)	0.0027 ± 0.0056	0.0023 ± 0.0112	0.0001 ± 0.0019	0.0000 ± 0.0015	0.0043 ± 0.0020	0.0004 ± 0.0009
Silver (Ag)	0.0000 ± 0.0072	0.0000 ± 0.0149	0.0002 ± 0.0025	0.0000 ± 0.0019	0.0000 ± 0.0036	0.0006 ± 0.0012
Cadmium (Cd)	0.0025 ± 0.0068	0.0061 ± 0.0141	0.0000 ± 0.0022	0.0000 ± 0.0018	0.0014 ± 0.0034	0.0000 ± 0.0012
Indium (In)	0.0021 ± 0.0089	0.0062 ± 0.0175	0.0000 ± 0.0030	0.0002 ± 0.0022	0.0009 ± 0.0042	0.0001 ± 0.0015
Tin (Sn)	0.0000 ± 0.0135	0.0000 ± 0.0263	0.0000 ± 0.0046	0.0000 ± 0.0036	0.0000 ± 0.0065	0.0015 ± 0.0023
Antimony (Sb)	0.0017 ± 0.0146	0.0000 ± 0.0299	0.0000 ± 0.0051	0.0000 ± 0.0039	0.0019 ± 0.0074	0.0000 ± 0.0025
Barium (Ba)	0.0000 ± 0.0727	0.0000 ± 0.1472	0.0003 ± 0.0250	0.0038 ± 0.0187	0.0016 ± 0.0359	0.0000 ± 0.0125
Lanthanum (La)	0.0269 ± 0.0890	0.0248 ± 0.1804	0.0119 ± 0.0311	0.0158 ± 0.0233	0.0007 ± 0.0447	0.0020 ± 0.0155
Gold (Au)	0.0000 ± 0.0068	0.0072 ± 0.0132	0.0000 ± 0.0023	0.0000 ± 0.0033	0.0000 ± 0.0033	0.0000 ± 0.0011
Mercury (Hg)	0.0000 ± 0.0029	0.0000 ± 0.0059	0.0000 ± 0.0010	0.0000 ± 0.0008	0.0000 ± 0.0015	0.0000 ± 0.0005
Thallium (Tl)	0.0001 ± 0.0028	0.0000 ± 0.0055	0.0003 ± 0.0010	0.0000 ± 0.0007	0.0000 ± 0.0013	0.0000 ± 0.0005
Lead (Pb)	0.0039 ± 0.0058	0.0002 ± 0.0115	0.0000 ± 0.0020	0.0009 ± 0.0016	0.0000 ± 0.0029	0.0000 ± 0.0010
Uranium (U)	0.0000 ± 0.0070	0.0000 ± 0.0240	0.0000 ± 0.0017	0.0000 ± 0.0013	0.0000 ± 0.0026	0.0000 ± 0.0008
Sum of species	20.4091 ± 0.9728	12.0723 ± 1.2406	0.9750 ± 0.1857	46.4165 ± 1.7430	33.3473 ± 1.3208	140.5766 ± 5.5548

Two performance measures were used to quantify similarities and differences among profile pairs: 1) the correlation coefficient (r) between the F_{ij} (fractional abundance of species "i" in source "j") quantifies the strength of association between profiles, and 2) the distribution of weighted differences:

$$[\text{residual}(R)/\text{uncertainty}(U)=(F_{i1}-F_{i2})/(\sigma_{i1}^{2}+\sigma_{i2}^{2})^{0.5}] \qquad (3\text{-}1)$$

Where: F_{i1}=Fraction of species "i" in profile "1"

F_{i2}=Fraction of species "i" in profile "2"

σ_{i1}=Uncertainity of species "i" in profile "1"

σ_{i1}=Uncertainity of species "i" in profile "2"

This shows how many of the chemical abundances differ by multiples of the uncertainty of the difference. The variance (r^2) and the R/U ratio are chemical mass balance (CMB) performance measures (Watson et al., 1998) that quantify the agreement between measured receptor concentrations and those produced by the source profiles and source contribution estimates. These pair comparisons are summarized in Table 3-5. Reasonable agreements are found within each RWC type ($r^2 > 0.85$) except LZST040, which is not associated ($r^2 < 0.1$) with the other two samples from the woodstove burning almond. LZST040 contains unreasonably low carbon and ionic fractions for this type of source (Table 3-3). A sampling artifact in the quartz-fiber filter is speculated. The two RWC samples from Sierra Nevada College shows significant variability ($r^2 \sim 0.67$), and their total carbon (TC) content are unreasonably high. These three samples are not included in further analysis. The remaining nine samples are composited into four source profiles representing a hardwood-burning fireplace (oak), softwood-burning fireplace (juniper), hardwood-burning woodstove (almond), and softwood-burning woodstove (pine), respectively (Table 3-6). These profiles are compared in Figure 3-3.

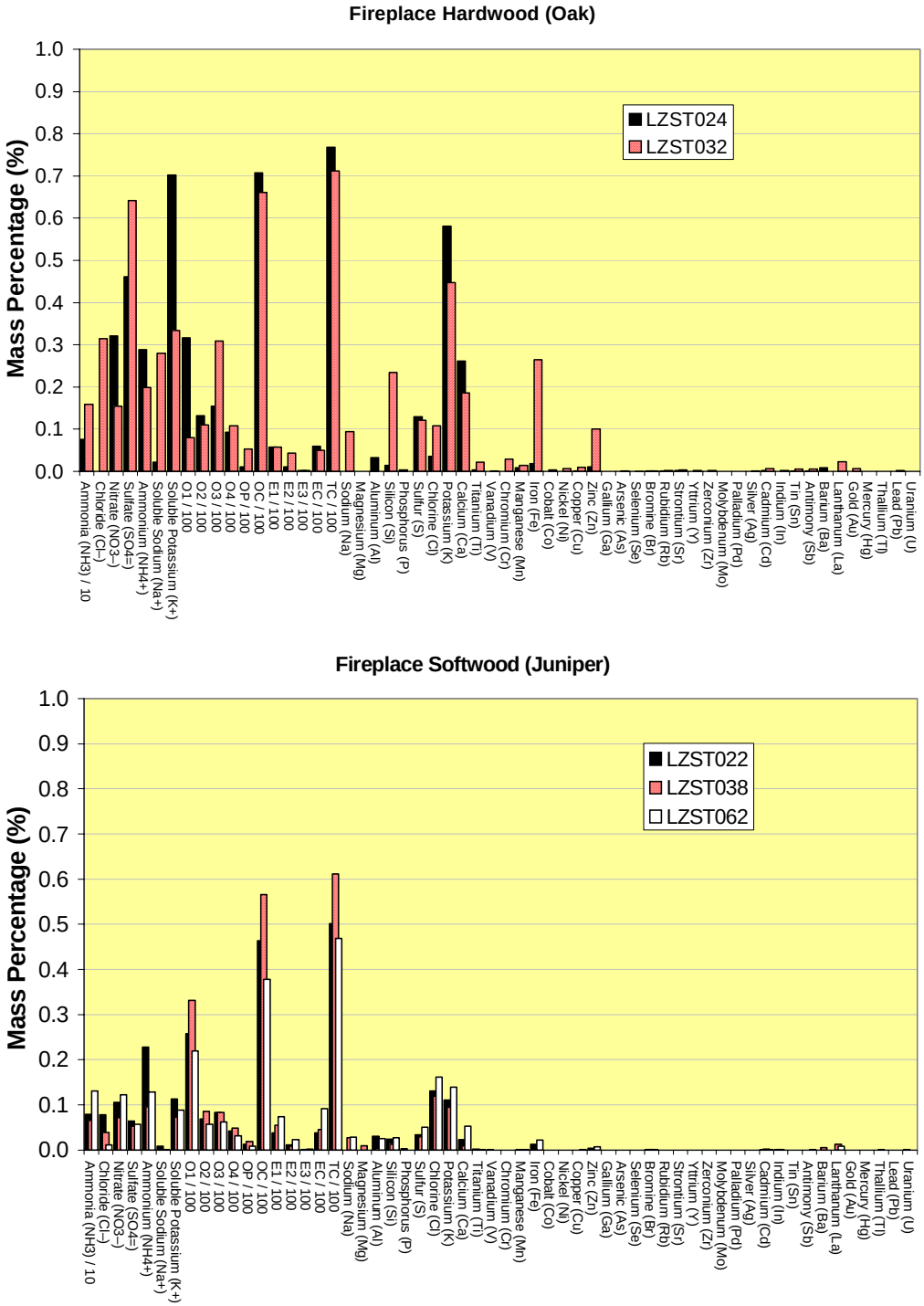

Figure 3-1. Pair comparison of chemical abundances of fireplace emissions between hardwoods (top) and softwoods (bottom).

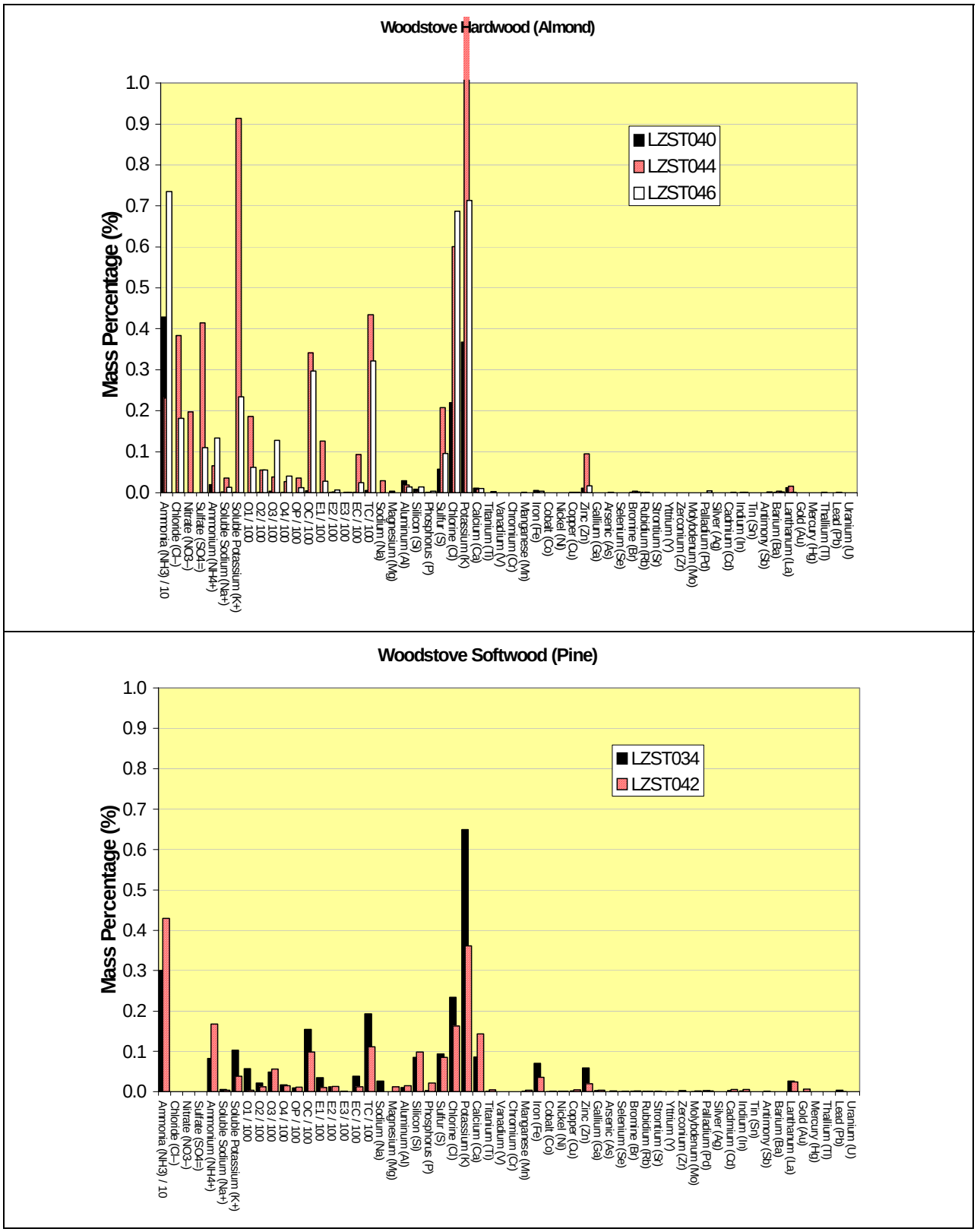

Figure 3-2. Pair comparison of chemical abundances of woodstove emissions between hardwoods (top) and softwoods (bottom).

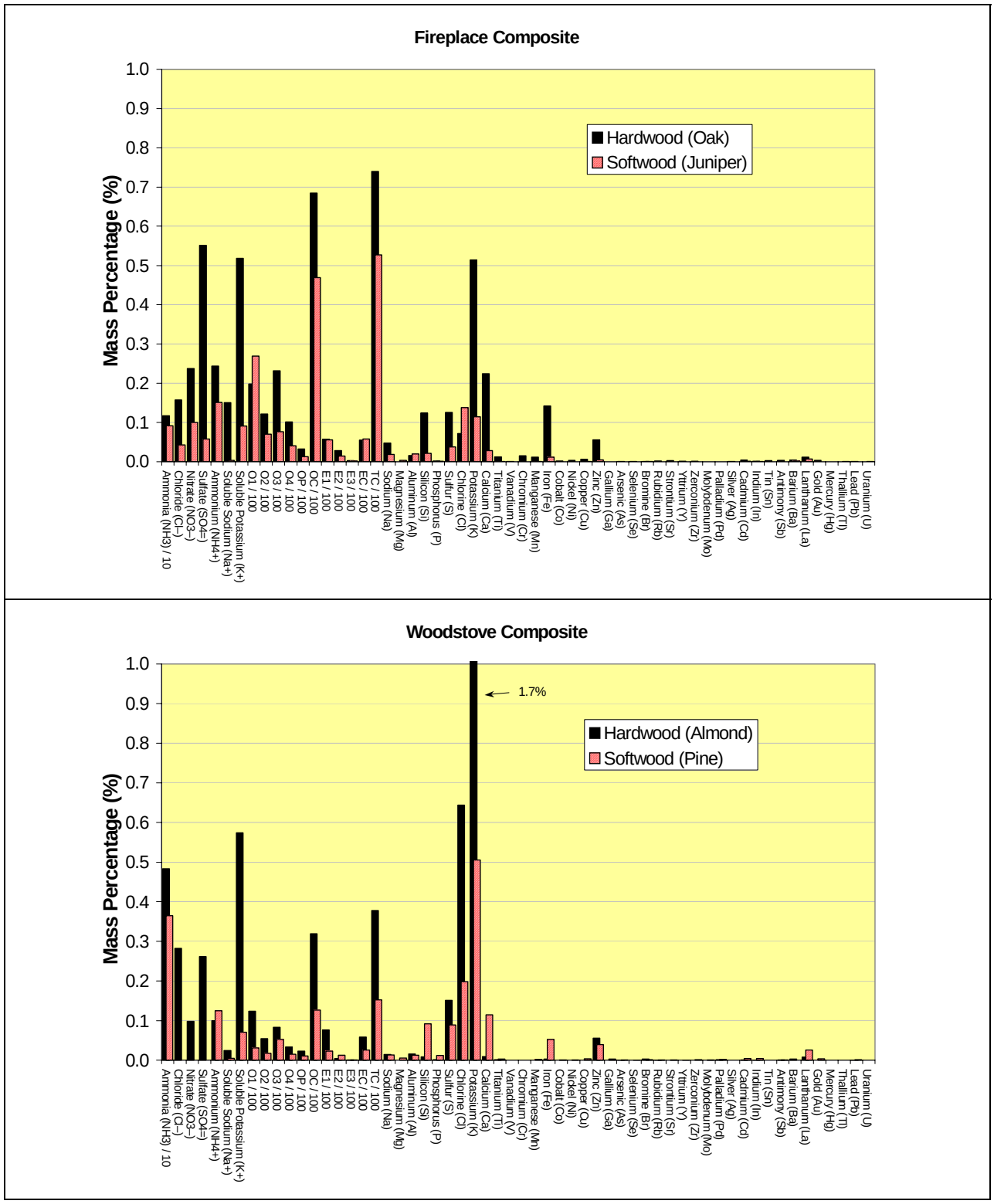

Figure 3-3. Comparisons of composite chemical abundance profiles for wood fuels type of fireplace (top) and woodstove (bottom).

Table 3-5. Intercomparisons among samples for each combination of wood fuel and residential wood combustion appliance.

Appliance	Profile x	Profile y	R/U Ratio				Correlation	Note
			<1	1-2	2-3	>3	r^2	
Fireplace	LZST024	LZST032	38	4	4	12	0.92	Burning Oak
Fireplace	LZST022	LZST038	43	7	2	6	0.99	Burning Juniper/Cedar
Fireplace	LZST022	LZST062	39	9	2	8	0.98	Burning Juniper/Cedar
Fireplace	LZST038	LZST062	37	9	1	11	0.98	Burning Juniper/Cedar
Woodstove	LZST034	LZST042	44	3	2	9	0.89	Burning Lodgepole Pine
Woodstove	LZST040	LZST044	33	3	3	19	0.01	Burning Almond
Woodstove	LZST040	LZST046	36	3	2	17	0.05	Burning Almond
Woodstove	LZST044	LZST046	35	4	3	16	0.85	Burning Almond
Woodstove	LZST048	LZST054	33	6	3	16	0.67	Burning Juniper

Table 3-6. Composite of emission composition profiles for each combination of wood fuel type and RWC appliance. All values are in percent of total mass.

Composite				
Sample ID	lzst024 & 032	lzst022 & 038 & 062	lzst034 & 042	lzst044 & 046
Location	Incline	Incline	Camp Richardson	Camp Richardson
Facility	Fire place	Fire place	Wood Stove	Wood Stove
Fuel	Hardwood (Oak)	Softwood (Juniper)	Softwood (Pine)	Hardwood (Almond)
Size (um)	2.5	2.5	2.5	2.5
Ammonia (NH3)	1.1735 ± 0.5916	0.9178 ± 0.3485	3.6494 ± 0.9159	4.8330 ± 3.5624
Chloride (Cl–)	0.1573 ± 0.2225	0.0425 ± 0.0364	0.0000 ± 0.1618	0.2825 ± 0.1429
Nitrate (NO3–)	0.2376 ± 0.1173	0.0998 ± 0.0260	0.0000 ± 0.0652	0.0984 ± 0.1391
Sulfate (SO4=)	0.5515 ± 0.1273	0.0580 ± 0.0136	0.0000 ± 0.0652	0.2621 ± 0.2154
Ammonium (NH4+)	0.2439 ± 0.0631	0.1510 ± 0.0687	0.1251 ± 0.0653	0.0996 ± 0.0479
Soluble Sodium (Na+)	0.1505 ± 0.1824	0.0030 ± 0.0044	0.0049 ± 0.0110	0.0244 ± 0.0160
Soluble Potassium (K+)	0.5180 ± 0.2605	0.0910 ± 0.0443	0.0707 ± 0.0461	0.5739 ± 0.4803
O1TC	19.8089 ± 16.6609	26.9107 ± 5.6702	3.0554 ± 3.7798	12.4136 ± 8.7905
O2TC	12.1420 ± 1.5269	6.9879 ± 1.4185	1.7503 ± 0.6853	5.4936 ± 0.1687
O3TC	23.2035 ± 10.9059	7.6322 ± 1.2256	5.2528 ± 1.0276	8.3159 ± 6.3196
O4TC	10.0955 ± 1.5826	4.0767 ± 0.8216	1.5724 ± 0.1330	3.3494 ± 0.9922
OPTC	3.2255 ± 2.9293	1.3142 ± 0.5379	1.0543 ± 0.3011	2.3389 ± 1.6435
OC (IMPROVE)	68.4465 ± 3.2953	46.9101 ± 9.4132	12.6445 ± 3.9214	31.9020 ± 3.1398
E1TC	5.7014 ± 0.6642	5.5731 ± 1.7780	2.2761 ± 1.7228	7.6916 ± 6.8727
E2TC	2.7802 ± 2.2872	1.3905 ± 0.7788	1.2893 ± 0.2325	0.4161 ± 0.3853
E3TC	0.2480 ± 0.0810	0.1574 ± 0.0629	0.0623 ± 0.0881	0.1078 ± 0.0323
EC (IMPROVE)	5.5015 ± 0.6648	5.8071 ± 2.8791	2.5713 ± 1.8569	5.8766 ± 4.8646
TCTC (IMPROVE)	73.9501 ± 3.9631	52.7180 ± 7.4782	15.2158 ± 5.7783	37.7775 ± 8.0030
Sodium (Na)	0.0473 ± 0.2377	0.0184 ± 0.0885	0.0131 ± 0.3987	0.0145 ± 0.0955
Magnesium (Mg)	0.0000 ± 0.0453	0.0030 ± 0.0189	0.0060 ± 0.0721	0.0000 ± 0.0142
Aluminum (Al)	0.0159 ± 0.0495	0.0198 ± 0.0144	0.0128 ± 0.0646	0.0162 ± 0.0105
Silicon (Si)	0.1244 ± 0.1552	0.0212 ± 0.0075	0.0918 ± 0.0249	0.0088 ± 0.0075
Phosphorus (P)	0.0019 ± 0.0086	0.0011 ± 0.0024	0.0121 ± 0.0132	0.0015 ± 0.0023
Sulfur (S)	0.1252 ± 0.0056	0.0377 ± 0.0111	0.0895 ± 0.0071	0.1517 ± 0.0787
Chlorine (Cl)	0.0720 ± 0.0510	0.1375 ± 0.0217	0.1987 ± 0.0502	0.6440 ± 0.0612
Potassium (K)	0.5143 ± 0.0948	0.1146 ± 0.0225	0.5054 ± 0.2037	1.2223 ± 0.7197
Calcium (Ca)	0.2237 ± 0.0529	0.0285 ± 0.0224	0.1146 ± 0.0403	0.0093 ± 0.0098
Titanium (Ti)	0.0124 ± 0.0387	0.0009 ± 0.0112	0.0029 ± 0.0521	0.0014 ± 0.0086
Vanadium (V)	0.0008 ± 0.0184	0.0002 ± 0.0055	0.0000 ± 0.0259	0.0000 ± 0.0043
Chromium (Cr)	0.0147 ± 0.0208	0.0001 ± 0.0014	0.0000 ± 0.0064	0.0000 ± 0.0011
Manganese (Mn)	0.0114 ± 0.0033	0.0005 ± 0.0006	0.0022 ± 0.0026	0.0000 ± 0.0005
Iron (Fe)	0.1418 ± 0.1736	0.0117 ± 0.0106	0.0528 ± 0.0241	0.0026 ± 0.0017
Cobalt (Co)	0.0020 ± 0.0028	0.0001 ± 0.0004	0.0006 ± 0.0017	0.0000 ± 0.0003
Nickel (Ni)	0.0033 ± 0.0046	0.0000 ± 0.0003	0.0010 ± 0.0014	0.0000 ± 0.0002
Copper (Cu)	0.0057 ± 0.0062	0.0004 ± 0.0007	0.0033 ± 0.0018	0.0002 ± 0.0003
Zinc (Zn)	0.0557 ± 0.0638	0.0047 ± 0.0024	0.0395 ± 0.0275	0.0558 ± 0.0550
Gallium (Ga)	0.0000 ± 0.0064	0.0000 ± 0.0019	0.0033 ± 0.0086	0.0000 ± 0.0014
Arsenic (As)	0.0005 ± 0.0034	0.0000 ± 0.0010	0.0011 ± 0.0045	0.0004 ± 0.0008
Selenium (Se)	0.0003 ± 0.0014	0.0000 ± 0.0004	0.0005 ± 0.0019	0.0000 ± 0.0003
Bromine (Br)	0.0008 ± 0.0011	0.0008 ± 0.0005	0.0021 ± 0.0011	0.0028 ± 0.0013
Rubidium (Rb)	0.0015 ± 0.0016	0.0001 ± 0.0005	0.0010 ± 0.0021	0.0005 ± 0.0007
Strontium (Sr)	0.0025 ± 0.0013	0.0000 ± 0.0005	0.0009 ± 0.0024	0.0000 ± 0.0004
Yttrium (Y)	0.0010 ± 0.0022	0.0000 ± 0.0006	0.0002 ± 0.0029	0.0000 ± 0.0005
Zerconium (Zr)	0.0012 ± 0.0026	0.0000 ± 0.0008	0.0016 ± 0.0033	0.0000 ± 0.0006
Molybdenum (Mo)	0.0000 ± 0.0046	0.0000 ± 0.0013	0.0013 ± 0.0060	0.0000 ± 0.0010
Palladium (Pd)	0.0000 ± 0.0048	0.0000 ± 0.0013	0.0025 ± 0.0063	0.0021 ± 0.0030
Silver (Ag)	0.0008 ± 0.0062	0.0000 ± 0.0018	0.0000 ± 0.0083	0.0000 ± 0.0014
Cadmium (Cd)	0.0042 ± 0.0055	0.0012 ± 0.0016	0.0043 ± 0.0078	0.0007 ± 0.0013
Indium (In)	0.0013 ± 0.0073	0.0005 ± 0.0021	0.0042 ± 0.0098	0.0006 ± 0.0016
Tin (Sn)	0.0029 ± 0.0114	0.0000 ± 0.0033	0.0000 ± 0.0148	0.0000 ± 0.0025
Antimony (Sb)	0.0033 ± 0.0127	0.0001 ± 0.0036	0.0008 ± 0.0167	0.0010 ± 0.0028
Barium (Ba)	0.0041 ± 0.0616	0.0015 ± 0.0176	0.0000 ± 0.0821	0.0027 ± 0.0135
Lanthanum (La)	0.0116 ± 0.0768	0.0071 ± 0.0220	0.0258 ± 0.1006	0.0083 ± 0.0168
Gold (Au)	0.0033 ± 0.0056	0.0000 ± 0.0016	0.0036 ± 0.0074	0.0000 ± 0.0015
Mercury (Hg)	0.0000 ± 0.0026	0.0000 ± 0.0008	0.0000 ± 0.0033	0.0000 ± 0.0006
Thallium (Tl)	0.0000 ± 0.0024	0.0002 ± 0.0007	0.0001 ± 0.0031	0.0000 ± 0.0005
Lead (Pb)	0.0010 ± 0.0049	0.0000 ± 0.0014	0.0021 ± 0.0064	0.0004 ± 0.0011
Uranium (U)	0.0000 ± 0.0069	0.0002 ± 0.0012	0.0000 ± 0.0125	0.0000 ± 0.0010
Sum of species	76.4592 ± 3.9885	53.2877 ± 7.4788	16.2407 ± 5.7878	39.8819 ± 8.0411

As shown in Figure 3-4, the major components in RWC are OC and EC. In the fireplace emission, TC accounts for 74 ± 4% and 53 ± 7% of the $PM_{2.5}$ mass when hardwood and softwood are burned, respectively. Hardwood combustion in woodstoves also emits more abundant carbon (38 ± 4%) than does softwood (15 ± 6%), but their TC mass fractions are significantly lower than those for fireplaces. This also indicates more unidentified mass in the woodstove emissions, especially when burning softwood. The sum of species (carbon, ions, and elements) accounts for 53–76% of $PM_{2.5}$ mass for the fireplace emission but only 16–40% for the woodstove emission (Table 3.3). The EC/TC ratio ranges from 5 to 17%, with the larger values appearing in the woodstove profiles. Higher EC in woodstove emissions is likely due to incomplete combustion. It is noted that the carbon fractions (OC1-4, OP, and EC1-3) generally show larger variations than OC, EC, and TC in these source profiles. The carbon fractions could be more sensitive to the combustion conditions during both sampling and carbon analysis.

Soluble potassium (K^+) is a useful marker for vegetative burning. For fireplaces or woodstoves in the present study, Figure 3-4 shows that hardwood combustion generates more abundant K^+ (0.5–0.6%) than softwood combustion does (0.07 – 0.09%). This is consistent with the results reported by Tung et al. (1997), and provides a mean to distinguish sources of wood smoke. The soluble to total potassium ratio K^+/K is 0.82 to 1.0 and 0.14 to 0.48 in the woodstove profiles for hardwood and softwood, respectively. The low K^+/K in Camp Richardson softwood profiles might be due to fly ash around the sampling location.

The woodstove in Camp Richardson also emitted substantial NH_3, close to ~5% of the $PM_{2.5}$ mass. Whether this can be extrapolated to all woodstove emissions warrants further investigation. Other abundant ions in the profiles include NH_4^+, SO_4^{2-}, NO_3^-, Cl^-, and Na^+. All of these are likely plant nutrients concentrated from minute amounts in the water used by the plant over its lifetime. Generally, more abundant ions are found in hardwood combustion emissions.

Other potential markers include Br, which is above the minimum detection limit (MDL) for woodstove combustion but below the MDL for fireplace burning. Crustal elements, such as Al, Si, Ca, and Fe are also found in all these samples but with substantial variabilities (>100%). These elements are likely captured from background air during sampling rather than being directly emitted from combustion.

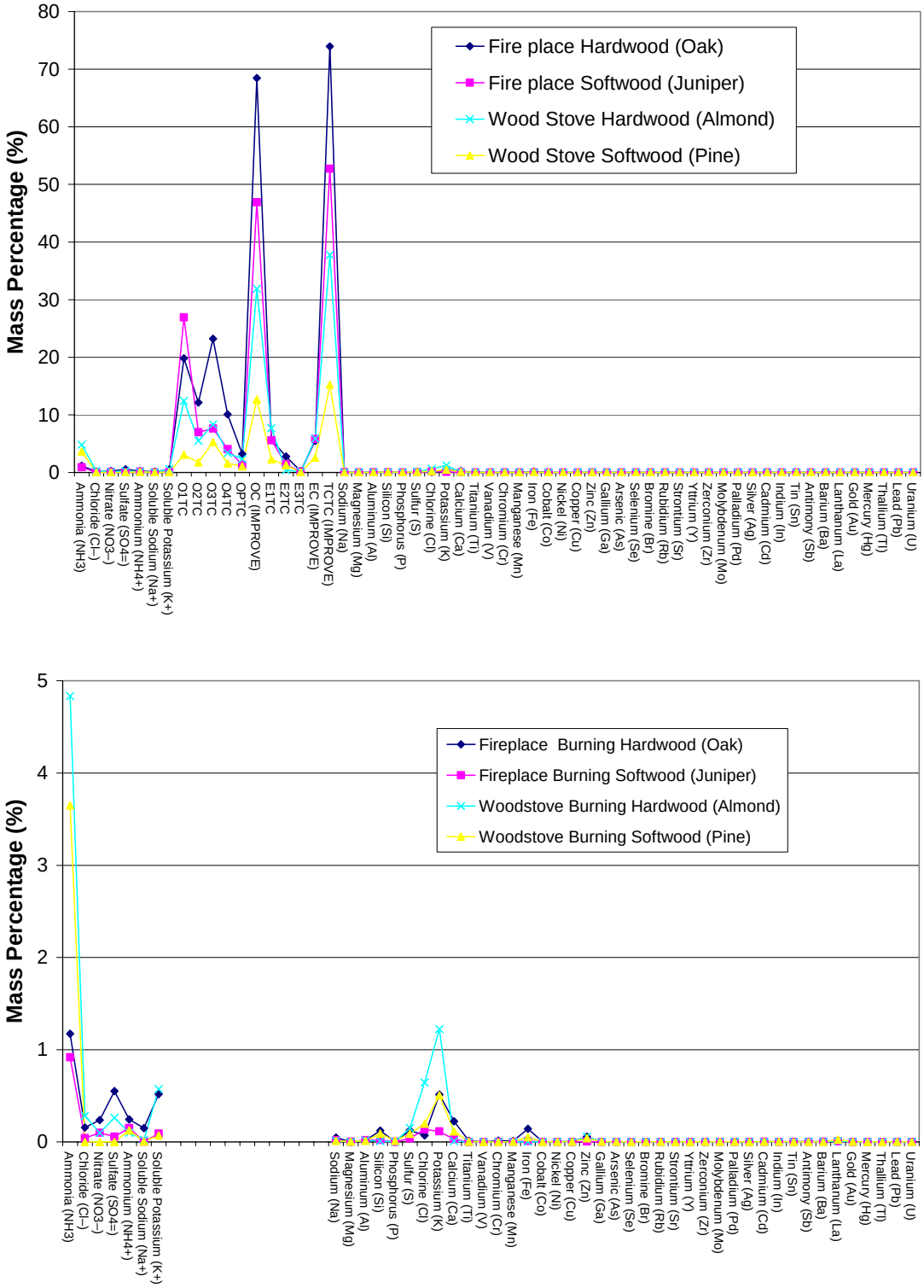

Figure 3-4. Species comparison of abundances in fireplaces and woodstoves burning hardwood and softwood. Lower panel shows an expanded y-axis of the data in the upper panel.

The RWC profiles acquired for this study are compared with those from the 1996-97 Northern Front Range Air Quality Study (NFRAQS), which was conducted in the Denver metropolitan area from 1/16/96 to 2/7/97 (Chow et al., 1998; Fujita et al., 1998; Watson et al., 1998; Zielinska et al., 1998). RWC profiles were collected using dilution tunnel sampling of emissions from fireplaces burning pine, pinion, apple/mesquite, bundled wood, hardwood, oak, and Duraflame, and woodstoves burning mixed hardwood and oak. Figure 3-5 (a) compares the composite for hardwood combustion in a fireplace (NWFHc) with the oak burning profile in the present study. Reasonable agreements are found in OC, EC, and TC, but not in seven carbon fractions (OC1– OC4, EC1–EC3). Negative ionic fractions (positive ions and NH_3 were not measured for the NFRAQS RWC profiles) including SO_4^{2-}, NO_3^-, and Cl^-, show excellent consistency between the two studies. The total K is much higher in the NFRAQS profile. Fireplaces burning softwood, however, exhibit a greater variation between the two studies (Figure 3-7[b]). The softwood burning profile (NWFSc) contains EC of ~33% in the NFRAQS study, but only ~6% in the present study. The NFRAQS profile also contains appreciably higher SO_4^{2-} and Cl^-. It is noted that the two studies used different types of softwood (Lake Tahoe used juniper, and NFRAQS used pine, pinion, and apple/mesquite), and this may explain the differences. Other parameters include the age of the furnace, combustion air supply rate, ambient air condition (temperature and relative humidity), moisture content in the wood fuel, wood fuel feeding rate, etc. The results from two studies suggest that burning hardwood in a fireplace generates richer OC, K, and ions than burning softwood. The woodstoves burning hardwood are compared in Figure 3-5(c). The NFRAQS profile shows appreciably higher carbon (OC, EC, and TC), SO_4^{2-}, and K fractions. The hardwood fuel in the NFRAQS profile is primarily oak but in the present study it is almond. These comparisons confirm a higher EC/TC ratio in woodstove burning than in fireplace burning.

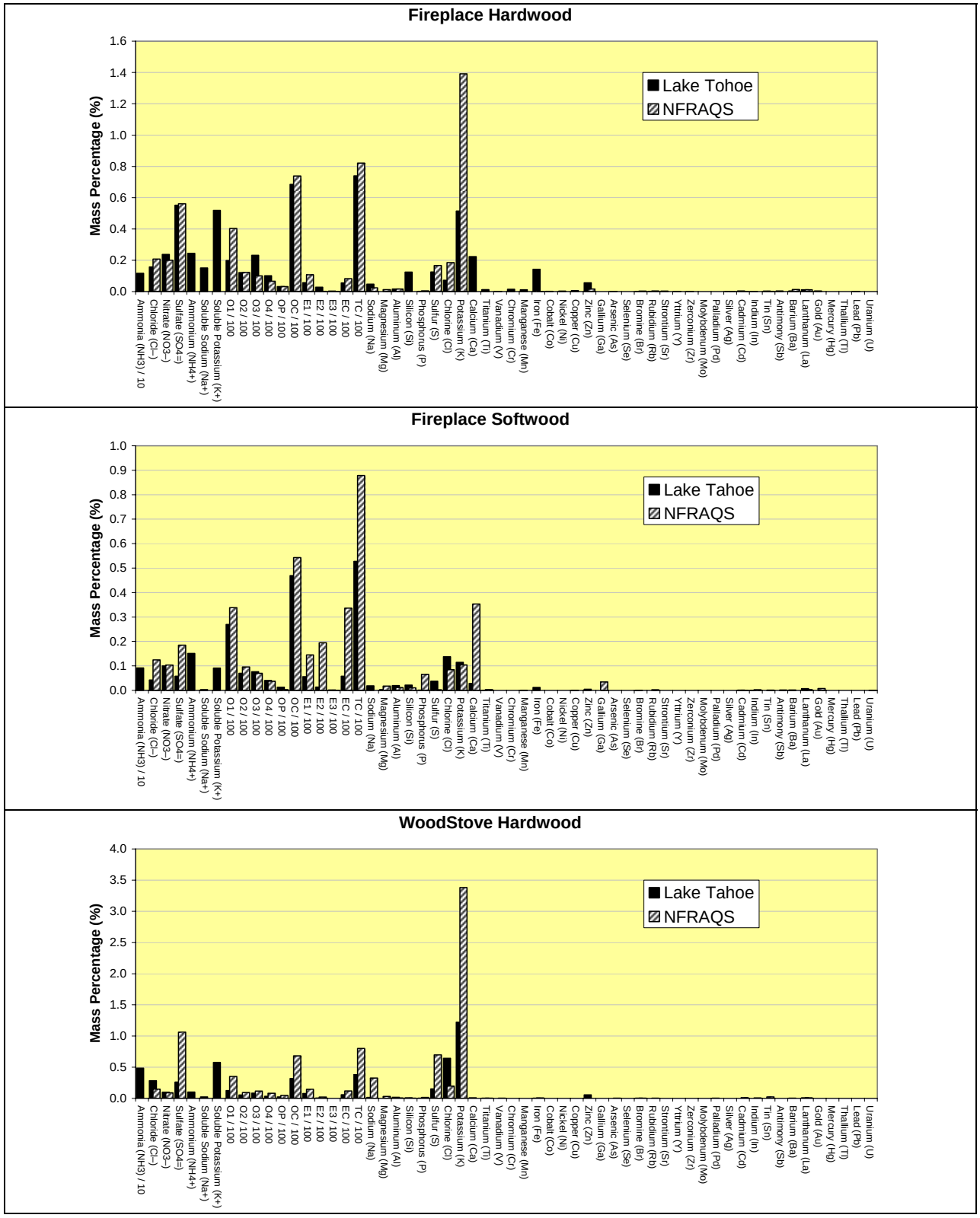

Figure 3-5. Residential wood combustion profiles.

3.4. Fraction of Background in RWC Source Profile

The real-time instrumentation deployed alongside the filter sampling train permitted an estimation of the fraction of mass on the filter that is composed of the wood burning source and the ambient background. Based on the assumption that the ambient background changes slowly over time and that influences of the local source were high frequency spikes superimposed on the background concentration, the relative attributions of each source were estimated by applying the same data filtering method described in Section 2. That is, the background component of the source was estimated as the 15th percentile value of a 100 s window surrounding each data point. The difference between the total concentration and the background value was assumed to be associated with the emissions from each chimney. Analyses of the $PM_{2.5}$ DustTrak data for each filter sample indicated that from 44% to 98% of the $PM_{2.5}$ DustTrak signal was associated with the source tested (Table 3-1). Factors affecting this ratio are the magnitude of the ambient background concentration, the intensity of the source, the location of the sampling probe, and the variability of the wind direction.

An identical analysis was also applied to the ELPI Dataset to determine the relative contribution of the source to the total measured size distribution (Figure 3-6). The background subtraction numerical filter was applied to concentration data from each impactor stage. The average source contribution for each particle stage was calculated for all wood-burning sampling periods shown in Table 3-1. The upper two stages corresponding to particle geometric mean aerosol diameters of 2.9 μm and 6.0 μm are not shown due the positive concentration bias introduced by charged nanoparticles diffusing to the upper electrometer stages (see Section 2).

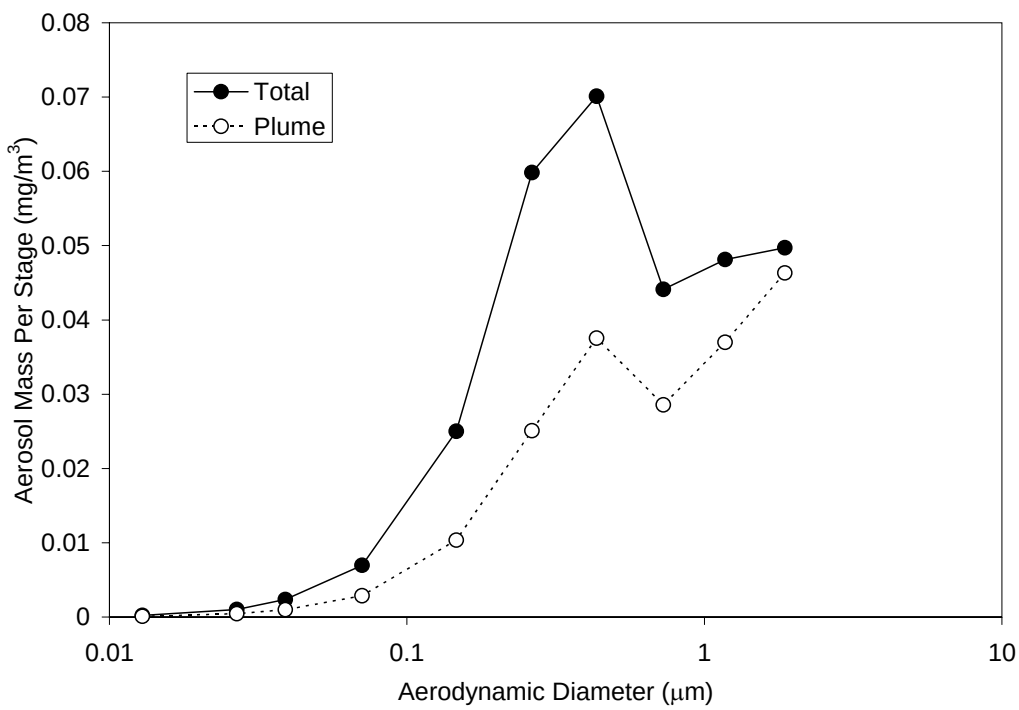

Figure 3-6. Average size distributions of total aerosol and source component measured by the ELPI for all wood burning source profiles.

The size distribution shows that both the background and the source aerosol have a mass concentration peak at 0.43 μm. Above this size, the relative fraction of the source aerosol mass appears to dominate over the background aerosol. This data indicates that although the chemical speciation filter packs were exposed in a source dominated environment, a fraction of the aerosol mass on the filter is not from the source sampled.

3.5. Fuel-Based Emission Factor Calculation for RWC

Emission factors for gases and $PM_{2.5}$ obtained by the In-Plume Sampling System are compared to those by AP-42 in Table 3-7. Emission factors for CO_2 and CO show good agreement between the in-plume method and AP 42. The total of NO, NO_2, and N_2O emission factors calculated from the In-Plume Method is 3–4 times higher than NO_x from AP 42; and SO_2 in the In-Plume Method is 10 times higher than SO_x in AP 42. Significantly high levels of NH_3, ethylene, hexane, and formaldehyde—in addition to SO_x, NO_x, CO, and CO_2—were shown in these results. PM emission factors in AP 42 are based on either Method 5G (dilution method) (U.S. EPA, 1997) or Method 5H (direct flue gas measurement), (U.S. EPA, 1997). The results show that the AP 42 PM_{10} emission factor is similar to in-plume method $PM_{2.5}$ emission factor for fireplaces, but is approximately 5 times higher than for woodstove emission factors. Emission factors in AP 42 are developed from new appliances in the laboratory and should be viewed only as a licensing process (Houck and Tiegs, 1998). The actual emission factors depend on owners' habits and preferences, maintenance, cleaning, age, frequency of use of the wood heater, and cleaning of the chimney; and generally are higher than those in AP 42.

The AP 42 emission factors represent the average from multiple appliances operated under a stringent test cycle whereas the emission factors from this study represent the emissions from a smaller number of sources under real operating conditions.

Table 3-7. Comparison of emission factors estimated from In-Plume Sampling System and AP-42 for RWC* study.

	Emission factors for gases and PM2.5 estimated based on In-Plume Sampling System (kg/Mg) (*)										AP 42 in kg/Mg	
Species	Incline Village Fireplace Oak		Incline Village Fireplace Cedar		Camp Richardon Woodstove Almond		Camp Richardson Woodstove Pine		Sierra College Woodstove Juniper		Residential Fireplace	Noncatalyst Woodstove
NH3	1.859 ±	0.532	2.058 ±	0.099	0.644 ±	0.189	1.097 ±	0.035	0.232 ±	0.068		
CO2	1683.451 ±	57.815	1638.852 ±	48.917	1662.763 ±	10.431	1667.400 ±	80.793	1650.525 ±	42.985	1700	1700
CO	95.379 ±	36.791	123.761 ±	31.129	108.545 ±	6.638	105.594 ±	51.414	116.333 ±	27.354	126	93
Ethylene	2.384 ±	0.383	2.594 ±	0.864	2.966 ±	0.518	2.725 ±	0.763	1.523 ±	1.293		
Formaldehyde	4.577 ±	0.990	6.056 ±	1.292	4.837 ±	1.624	6.409 ±	4.078	3.168 ±	3.162		
Hexane	1.859 ±	1.106	2.373 ±	0.631	2.003 ±	0.642	1.310 ±	1.073	1.405 ±	1.125		
Nitric Oxide	2.156 ±	0.104	2.330 ±	0.272	2.390 ±	0.563	1.385 ±	0.210	1.173 ±	0.325		
Nitrogen Dioxide	1.499 ±	0.202	1.764 ±	0.212	0.584 ±	0.170	0.672 ±	0.050	0.328 ±	0.176	1.3(1)	1.4(1)
Nitrous Oxide	1.647 ±	1.677	1.877 ±	0.681	0.894 ±	0.126	0.759 ±	0.001	0.361 ±	0.120		
Propane	0.960 ±	0.257	1.463 ±	0.284	2.332 ±	2.643	0.458 ±	0.005	0.290 ±	0.057		
SO2	3.013 ±	0.253	2.946 ±	0.186	2.082 ±	1.578	2.260 ±	0.209	0.447 ±	0.002	0.2(2)	0.2 (2)
Water	112.112 ±	135.106	70.524 ±	91.744	602.945 ±	406.893	655.274 ±	43.772	801.740 ±	108.480		
PM2.5 (**)	5.363 ±	0.352	23.570 ±	11.526	4.954 ±	7.413	0.794 ±	0.667	0.559 ±	0.651	17.3 (3)	15.55 (3)

* Assume 0.5g C/g wood fuel (Pedco Env., 1977; Barnet, 1991)

$$** \; PM_{2.5} = Filter_PM * \frac{ELPI_PM2.5(PeakFinder)}{ELPI_PM2.5(AccumulatedInSample)}$$

1. AP42 emission factor for NO_x
2. AP42 emission factor for SO_x
3. AP42 emission factor for PM_{10}

4. MOTOR VEHICLE EXHAUST

Source profiles for motor vehicle emissions used in the present study were constructed from ground-based roadside sampling at traffic intersections around Lake Tahoe where the sampled air was dominated by emissions from motor vehicle exhaust. Right-of-way permits were secured with the Nevada Department of Transportation prior to field sampling. At both locations, the sampling equipment was deployed ~50 m past an intersection controlled by a stop sign. Power for the equipment was supplied by two 5 kW generators located 25 m away from the sampling equipment. The In-Plume Sampling System was located on the sidewalk or shoulder within 2 m of the nearest traffic lane, with the sampling inlet placed beneath a rubber bumper on the road and across the lane. This way, the system directly sampled fresh emission plumes coming off tailpipes of motor vehicles driven over the bumper. Two sampling locations were selected for this study: Lakeshore-Village and Southwood-Mays (Figure 4-1).

Figure 4-1. Map showing sampling locations of motor vehicle exhaust source monitoring in Incline Village, NV, on the northwest shore of Lake Tahoe.

Figure 4-2 through Figure 4-4 show pictures of the equipment deployed at the Lakeshore site (07/26/03) and the Southwood site (07/23/03 and 07/29/03). The lower panel of Figure 4-4 shows a map of the two sampling locations at Incline Village. Weather conditions during the sampling periods were mild, with temperatures between 20 °C and 32 °C. On 07/23/03 at 16:00 PDT, a rainstorm ended the sampling day; total precipitation was less than 0.5 cm over a 2-hour period. This was the only recorded rainfall for the month of July. Winds during the sampling periods were less than 15 km/hr.

Figure 4-2. Images of In-plume gas monitoring module (FTIR) (upper panel left) and real-time particle monitoring module (upper panel right) and filter sampling module (lower panel).

Figure 4-3. Images of in-plume sampling equipment set-up and vehicle passing over inlet at Southwood and Mays on 7/23/03.

Figure 4-4. Image of in-plume sampling configuration at Lakeshore and Village in Incline Village on 7/26/03.

4.1. Exhaust source profiles with soil subtraction

The Lakeshore-Village site is close to the popular Incline Beach, where a slow and steady mix of local and tourist traffic was observed in the summer. The Southwood-Mays site is near the Incline Village Post Office and represents primarily local traffic. Two and three samples with durations ranging from 1 to 3 hours were obtained at Lakeshore-Village and Southwood-Mays, respectively between 7/23/2004 and 7/29/2004 (Table 4-1). The traffic was videotaped during the entire roadside sampling duration in order to count the numbers and types of vehicles passing by. Motor vehicle counts and relative percentages for the two sites are shown in Figure 4-5.

Table 4-1. Filter sampling data for vehicle exhaust filters collected in Incline Village, NV.

QID	TID	Start Time	End Time	Size	Location	Fratction of PM above background (based on DT measurements)	Fraction Road Dust by CMB	Number of Vehicles in Lane with Inlet	Average Speed (km/hr)	Average Acceleration (m/s^2)
LZSQCC012	LZST011	20030723 13:01:00	20030723 16:08:00	PM_{10}	Southwood -Mays	0.40	0.43 +/- 0.04	Traffic Counter not Operational		
LZSQ011	LZST012	20030723 13:01:00	20030723 16:08:00	$PM_{2.5}$	Southwood -Mays	0.30	0.32 +/- 0.02	Traffic Counter not Operational		
LZSQCC008	LZST007	20030726 12:00:00	20030726 14:33:00	PM_{10}	Lakeshore-Village	0.67	0.83 +/- 0.08	553	21 +/- 9	-0.2 +/- 0.7
LZSQ007	LZST008	20030726 12:00:00	20030726 14:33:00	$PM_{2.5}$	Lakeshore-Village	0.70	0.79 +/- 0.05	553	21 +/- 9	-0.2 +/- 0.7
LZSQCC020	LZST019	20030726 14:36:00	20030726 16:50:00	PM_{10}	Lakeshore-Village	0.79	0.76 +/- 0.07	333	21 +/- 9	-0.2 +/- 0.7
LZSQ019	LZST020	20030726 14:36:00	20030726 16:50:00	$PM_{2.5}$	Lakeshore-Village	0.73	0.80 +/- 0.05	333	21 +/- 9	-0.2 +/- 0.7
LZSQCC006	LZST006	20030729 11:39:00	20030729 14:16:00	PM_{10}	Southwood -Mays	0.56	0.71 +/- 0.07	385	25 +/- 9	0.3 +/- 0.6
LZSQ005	LZST005	20030729 11:39:00	20030729 14:16:00	$PM_{2.5}$	Southwood -Mays	0.57	0.62 +/- 0.04	385	25 +/- 9	0.3 +/- 0.6
LZSQCC010	LZST010	20030729 14:22:00	20030729 16:28:00	PM_{10}	Southwood -Mays	0.71	0.74 +/- 0.07	352	25 +/- 9	0.3 +/- 0.6
LZSQ009	LZST009	20030729 14:22:00	20030729 16:28:00	$PM_{2.5}$	Southwood -Mays	0.68	0.68 +/- 0.04	352	25 +/- 9	0.3 +/- 0.6

Video images collected during the source sampling campaign were reviewed to identify the types of vehicles operating in Incline Village. Vehicles were grouped into one of nine categories. Figure 4-5 shows the distribution of the fleet passing the In-Plume Sampling System and source sampling instrumentation inlets. The number of positively identified diesel vehicles is ~2% in both locations. Additional diesel vehicles may exist within the pickup (PU) truck and sport utility vehicle (SUV) groups since many late-model vehicle manufacturers have chosen diesel engines as a more fuel efficient power source for larger vehicles.

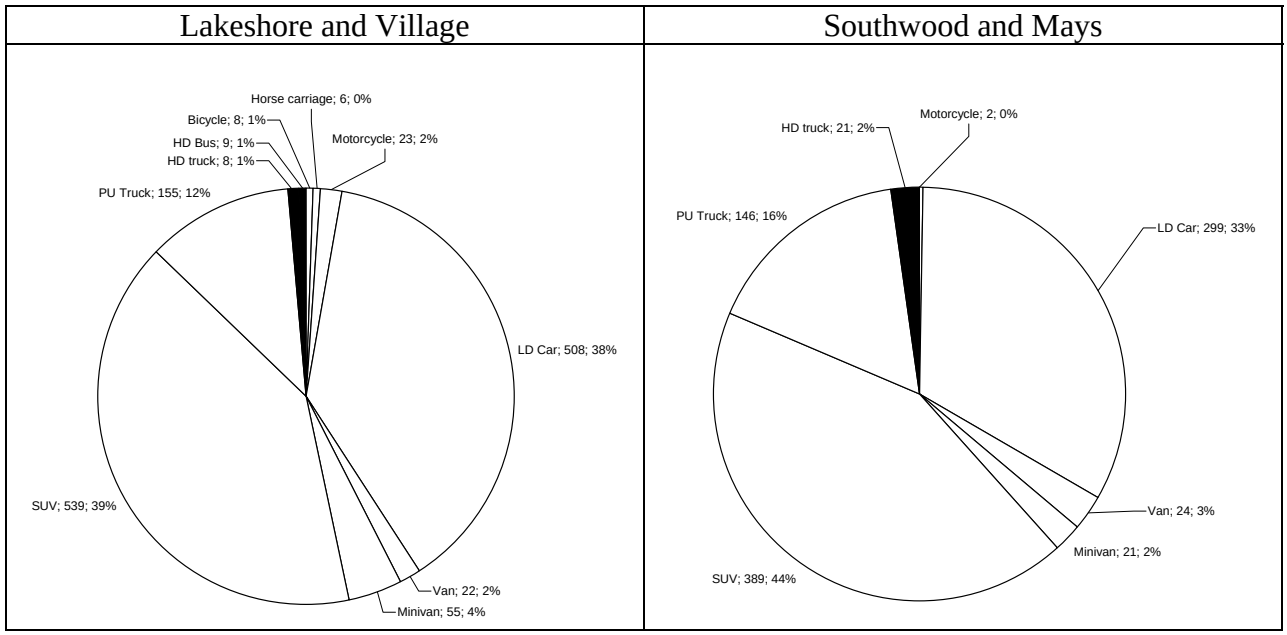

Figure 4-5. Fleet distribution at two sites in Incline Village where source samples were collected.

Because these samples were collected from the roadside, they are likely to be affected by vehicle-related resuspended road dust. The geological contribution was reduced by using a $PM_{2.5}$ inlet on the sampling system. The remaining geological components can be subtracted from each of the roadside sample profiles by using the CMB model to estimate the contributions from geological material to the concentrations of all chemical species (Chow et al. 1988). This was achieved using the geological source profiles determined from the roadside dust collected near the sampling sites (see Section 5). Only the crustal species (i.e., Al, Si, Ca, and Fe) were used as fitting species to estimate geological source contributions, since these species are not commonly present at significant levels in motor vehicle exhaust. The calculated concentrations of both the fitting and non-fitting species were then subtracted from the original roadside motor vehicle exhaust sample concentrations, and the remaining species concentrations were normalized to the reconstructed mass from the following species: (SO_4^{2-} + NO_3^- + NH_4^++ OC×1.4+EC, crustal material + trace elements). Crustal material is defined as the sum of the oxides of elements primarily associated with soil (Sisler et al. 1996; Cahill et al. 1981; Pitchford et al. 1981):

$$[\text{Crustal Material}] = 2.20[\text{Al}] + 2.49[\text{Si}] + 1.63[\text{Ca}] + 2.42[\text{Fe}] + 1.94[\text{Ti}] \quad (4\text{-}1)$$

As indicated in Table 4-1, the geological material contributes substantially to the raw roadside motor vehicle exhaust samples (32 – 80%). The five individual profiles are shown in Table 4-2 and compared in Figure 4-6.

The same pair-wise comparison of source profiles as described in Section 3 was applied to the motor vehicle exhaust source profiles. These pair comparisons are summarized in Table 4-4. Although Figure 4-6 shows appreciable variations between these profiles, under such performance tests good agreements are found for each sampling location (e.g., $r^2 > 0.95$). Therefore, all samples from the two locations are utilized and composited into two profiles representing Southwood-Mays and Lakeshore-Village on-road vehicle emissions (Table 4-3 and Figure 4-7).

Carbonaceous material (OC and EC) is the most abundant component in these profiles. The total carbon exceeds $PM_{2.5}$ gravimetric mass in four of the five samples, likely resulting from the discrepancy between quartz-fiber (carbon) and Teflon (mass) filter sampling of organic matter. Adsorption of volatile organic vapors onto quartz-fiber filters is a well-known artifact that inflates the abundance of particulate organic matter (Turpin et al. 1994; Mader and Pankow 2000). EC accounts for 14 ± 4% and 18 ± 2% of the reconstructed $PM_{2.5}$ mass at Lakeshore-Village and Southwood-Mays, respectively. The EC/TC ratio is slightly higher at Southwood-Mays (0.25) than at Lakeshore-Village (0.21), but they are both significantly higher than EC/TC ratios in RWC profiles (~0.1). This provides a criterion to distinguish motor vehicle and RWC emissions. At Southwood-Mays, most of EC is high-temperature EC (i.e., EC2 and EC3); this is also different from RWC profiles, which are dominated by EC1.

NH_4^+, $SO_4^=$, and NO_3 ions combined account for 3.4% and 3.3% of $PM_{2.5}$ at Southwood-Mays and Lakeshore-Village, respectively. Since sulfates are mostly secondary particles formed in the atmosphere, the ammonium sulfate may be from ambient air rather than automobile exhausts. Species of mass fraction higher than 0.1%, excluding the fitting crustal elements noted above, are K, Cu, Zn, and Ba. The K^+/K ratios in these profiles are <<1, and therefore K is mostly of crustal origin as well. Cu is abundant, accounting for 2.3 ± 0.2% of $PM_{2.5}$ mass at Lakeshore-Village. Ba is above the detection limit only at Southwood-Mays. The sum of species reaches 78% and 77% of $PM_{2.5}$ mass at Lakeshore-Village and Southwood-Mays, respectively.

The Southwood-Mays motor vehicle profile is compared with a composite profile of non-smoker gasoline vehicles obtained from NFRAQS in Figure 4-8, since the majority of Southwood-Mays traffic is non-diesel vehicles. Motor vehicle exhaust emission profiles from NFRAQS were derived from dynamometer tests on smoker and non-smoker gasoline vehicles, light-duty diesel, and heavy-duty diesel vehicles under summer and winter ambient conditions. The test procedure contains Federal Test Procedure (FTP) driving cycles. The NFRAQS test minimizes the influence of ambient air and on-road dust.

In general, EC—including EC fractions—shows better agreements between the NFRAQS and Southwood-Mays motor vehicle source profiles. This confirms the larger uncertainty in OC measurements. $SO_4^=$and NO_3 levels are substantially lower for the NFRAQS profile. These profiles were collected by sampling 100% vehicle exhaust diluted with HEPA filtered air. Cu and Ba are unique at Southwood-Mays, which warrants more investigation.

Table 4-2. Individual source profiles of the five motor vehicle exhausts collected in the Lake Tahoe Study. Values have units of percent of total mass measured on filter.

Sample ID	LZSQ005	LZSQ007	LZSQ009	LZSQ019	LZSQ011
Sample Date	'7/29/2003	7/29/2003	7/23/2003	7/26/2003	7/26/2003
Source Type	Motor Vehicle	Motor Vehicle	Motor Vehicle	Motor Vehicle	Motor Vehicle
Location	Southwood-Mays	Southwood-Mays	Southwood-Mays	Lakeshore-Village	Lakeshore-Village
Size	2.5	2.5	2.5	2.5	2.5
Ammonia (NH3)	151.1379 ± 15.3425	126.0386 ± 14.2062		114.9317 ± 12.2456	92.8519 ± 9.8969
Chloride (Cl–)	0.5245 ± 0.6904	0.2640 ± 0.6754	0.7600 ± 0.4060	0.5487 ± 0.6663	0.1208 ± 0.5957
Nitrate (NO3–)	0.4574 ± 0.3111	0.5156 ± 0.3328	0.3930 ± 0.1899	0.7277 ± 0.3458	0.5414 ± 0.3242
Sulfate (SO4=)	1.8631 ± 0.6248	1.9189 ± 0.6483	2.1238 ± 0.4045	2.2614 ± 0.6532	1.3448 ± 0.5771
Ammonium (NH4+)	0.9607 ± 0.2190	1.0041 ± 0.2491	1.0090 ± 0.1849	0.7477 ± 0.2464	1.0376 ± 0.2581
Soluble Potassium (K+)	0.0775 ± 0.1097	0.0366 ± 0.1354	0.2144 ± 0.0497	0.0000 ± 0.1538	0.0194 ± 0.1555
O1TC	2.2441 ± 1.0614	0.6291 ± 1.1278	6.6346 ± 1.1179	6.1594 ± 1.5712	7.6561 ± 1.7372
O2TC	16.5421 ± 1.9359	17.7854 ± 2.3079	16.4626 ± 1.2982	17.6868 ± 2.2265	17.7621 ± 2.2354
O3TC	30.2162 ± 3.8729	27.8150 ± 4.0341	13.2727 ± 1.4164	26.4028 ± 3.6824	21.4303 ± 3.2203
O4TC	6.4191 ± 1.4432	9.1422 ± 1.8898	6.1356 ± 0.8776	7.1350 ± 1.6687	7.1664 ± 1.6759
OPTC	0.0000 ± 1.9374	0.0000 ± 2.3810	14.2548 ± 2.1058	0.0000 ± 1.7859	0.0000 ± 1.7368
OC (IMPROVE)	52.3336 ± 6.8231	51.4162 ± 7.5931	56.5951 ± 4.0703	56.3252 ± 7.3826	52.2159 ± 6.9968
E1TC	1.4965 ± 1.0629	0.0000 ± 1.2600	9.5497 ± 0.9421	2.6078 ± 0.9393	11.3760 ± 1.5799
E2TC	14.2938 ± 1.6745	14.9027 ± 1.9071	18.2160 ± 1.5005	7.4909 ± 1.0250	4.1160 ± 0.7043
E3TC	0.0531 ± 0.3858	1.0455 ± 0.5440	1.3740 ± 0.3317	0.0274 ± 0.4798	0.0000 ± 0.4710
EC (IMPROVE)	18.7099 ± 3.2235	19.3905 ± 3.7675	14.8852 ± 2.5734	10.9646 ± 2.4570	16.7138 ± 2.9826
TCTC (IMPROVE)	71.0063 ± 8.9941	70.8067 ± 10.1050	71.4799 ± 5.2524	67.2898 ± 9.3077	68.9298 ± 9.4589
Sodium (Na)	0.0000 ± 2.8579	0.0000 ± 3.4656	0.0000 ± 1.5824	0.0000 ± 3.9284	0.0000 ± 3.8528
Magnesium (Mg)	0.7203 ± 0.5871	0.8469 ± 0.6960	0.0000 ± 0.4181	0.1508 ± 0.9964	0.7680 ± 0.8143
Aluminum (Al)	0.0000 ± 0.5741	0.0000 ± 0.7127	0.0000 ± 0.2209	0.0000 ± 0.7474	0.0000 ± 0.7669
Silicon (Si)	0.0000 ± 1.8741	0.0000 ± 2.3380	0.0000 ± 0.6943	0.0000 ± 2.3140	1.3882 ± 2.3834
Phosphorus (P)	0.0000 ± 0.0731	0.0000 ± 0.0822	0.0000 ± 0.0456	0.0000 ± 0.1280	0.0000 ± 0.1270
Sulfur (S)	1.5770 ± 0.1896	1.1962 ± 0.1742	1.1439 ± 0.0961	1.1769 ± 0.1828	1.2121 ± 0.1865
Chlorine (Cl)	0.0000 ± 0.0562	0.0000 ± 0.0634	0.0035 ± 0.0301	0.0000 ± 0.0617	0.0000 ± 0.0615
Potassium (K)	0.2353 ± 0.1926	0.1570 ± 0.2329	0.1543 ± 0.0768	0.1557 ± 0.2580	0.1926 ± 0.2620
Calcium (Ca)	0.1041 ± 0.4791	0.3946 ± 0.6000	0.0846 ± 0.1803	0.6980 ± 0.7053	0.0447 ± 0.6993
Titanium (Ti)	0.0219 ± 0.1996	0.0000 ± 0.2266	0.0000 ± 0.1130	0.1835 ± 0.2289	0.1856 ± 0.2290
Vanadium (V)	0.0000 ± 0.1172	0.0000 ± 0.1369	0.0000 ± 0.0692	0.0137 ± 0.1386	0.0203 ± 0.1375
Chromium (Cr)	0.0035 ± 0.0250	0.0000 ± 0.0316	0.0056 ± 0.0142	0.0069 ± 0.0277	0.0000 ± 0.0278
Manganese (Mn)	0.0059 ± 0.0158	0.0003 ± 0.0189	0.0027 ± 0.0076	0.0581 ± 0.0203	0.0238 ± 0.0190
Iron (Fe)	1.2410 ± 0.5622	1.0985 ± 0.6805	0.5921 ± 0.2122	1.1707 ± 0.7539	0.5471 ± 0.7366
Cobalt (Co)	0.0153 ± 0.1400	0.0129 ± 0.1689	0.0351 ± 0.0369	0.0493 ± 0.1883	0.0326 ± 0.1832
Nickel (Ni)	0.0000 ± 0.0063	0.0000 ± 0.0096	0.0000 ± 0.0048	0.0000 ± 0.0077	0.0000 ± 0.0079
Copper (Cu)	1.4498 ± 0.1477	1.8098 ± 0.2045	0.1396 ± 0.0113	2.2232 ± 0.2373	2.4364 ± 0.2596
Zinc (Zn)	0.2768 ± 0.0326	0.3066 ± 0.0397	0.0703 ± 0.0085	0.4171 ± 0.0504	0.2915 ± 0.0382
Gallium (Ga)	0.0000 ± 0.0455	0.0000 ± 0.0493	0.0000 ± 0.0294	0.0000 ± 0.0457	0.0041 ± 0.0452
Arsenic (As)	0.0040 ± 0.0228	0.0000 ± 0.0265	0.0000 ± 0.0134	0.0027 ± 0.0267	0.0000 ± 0.0271
Selenium (Se)	0.0024 ± 0.0096	0.0000 ± 0.0113	0.0000 ± 0.0054	0.0000 ± 0.0117	0.0027 ± 0.0119
Bromine (Br)	0.0113 ± 0.0074	0.0182 ± 0.0086	0.0156 ± 0.0039	0.0129 ± 0.0096	0.0138 ± 0.0098
Rubidium (Rb)	0.0026 ± 0.0080	0.0000 ± 0.0115	0.0000 ± 0.0063	0.0000 ± 0.0089	0.0000 ± 0.0090
Strontium (Sr)	0.0000 ± 0.0114	0.0000 ± 0.0131	0.0000 ± 0.0060	0.0000 ± 0.1062	0.0000 ± 0.1073
Yttrium (Y)	0.0000 ± 0.0143	0.0000 ± 0.0171	0.0000 ± 0.0088	0.0011 ± 0.0179	0.0088 ± 0.0162
Zerconium (Zr)	0.0017 ± 0.0134	0.0056 ± 0.0151	0.0080 ± 0.0080	0.0000 ± 0.0228	0.0000 ± 0.0229
Molybdenum (Mo)	0.0000 ± 0.0289	0.0000 ± 0.0343	0.0000 ± 0.0182	0.0000 ± 0.0349	0.0138 ± 0.0342
Palladium (Pd)	0.0000 ± 0.0466	0.0000 ± 0.0563	0.0000 ± 0.0223	0.0107 ± 0.0611	0.0037 ± 0.0618
Silver (Ag)	0.0040 ± 0.0578	0.0000 ± 0.0687	0.0000 ± 0.0278	0.0023 ± 0.0744	0.0000 ± 0.0751
Cadmium (Cd)	0.0139 ± 0.0576	0.0068 ± 0.0706	0.0008 ± 0.0281	0.0000 ± 0.0778	0.0071 ± 0.0778
Indium (In)	0.0022 ± 0.0686	0.0068 ± 0.0822	0.0140 ± 0.0343	0.0072 ± 0.0898	0.0209 ± 0.0901
Tin (Sn)	0.0112 ± 0.0981	0.0120 ± 0.1155	0.0000 ± 0.0502	0.0000 ± 0.1249	0.0240 ± 0.1246
Antimony (Sb)	0.0659 ± 0.0990	0.0229 ± 0.1308	0.0004 ± 0.0564	0.0117 ± 0.1413	0.0054 ± 0.1404
Barium (Ba)	0.1586 ± 0.4515	0.4378 ± 0.4691	0.1355 ± 0.2489	0.0000 ± 0.4602	0.0000 ± 0.5032
Lanthanum (La)	0.0000 ± 0.5663	0.0000 ± 0.6712	0.0479 ± 0.3071	0.0815 ± 0.7178	0.0000 ± 0.7167
Gold (Au)	0.0058 ± 0.0327	0.0000 ± 0.0371	0.0000 ± 0.0181	0.0000 ± 0.0401	0.0101 ± 0.0378
Mercury (Hg)	0.0000 ± 0.0175	0.0000 ± 0.0209	0.0000 ± 0.0102	0.0011 ± 0.0235	0.0041 ± 0.0236
Thallium (Tl)	0.0049 ± 0.0170	0.0011 ± 0.0202	0.0011 ± 0.0093	0.0000 ± 0.0214	0.0000 ± 0.0216
Lead (Pb)	0.0000 ± 0.0298	0.0000 ± 0.0346	0.0000 ± 0.0188	0.0000 ± 0.0386	0.0223 ± 0.0348
Uranium (U)	0.0000 ± 0.0246	0.0032 ± 0.0295	0.0000 ± 0.0152	0.0046 ± 0.0311	0.0000 ± 0.0305
Sum of mass	78.4913 ± 9.3273	78.8033 ± 10.5306	77.0735 ± 5.3657	76.6873 ± 9.7837	77.2780 ± 9.9366

Table 4-3. Composite source profiles of motor vehicle exhausts at Lake Tahoe.

Composite	LZSQ 005 & 007 & 009	LZSQ 019 & 011
Sample ID	'7/29/2003	7/26/2003
Source Type	Motor Vehicle	Motor Vehicle
Location	Southwood-Mays	Lakeshore-Village
Size	2.5	2.5
Ammonia (NH3)	138.5883 ± 17.7479	103.8918 ± 15.6128
Chloride (Cl–)	0.5161 ± 0.3492	0.3348 ± 0.4469
Nitrate (NO3–)	0.4553 ± 0.1645	0.6345 ± 0.2370
Sulfate (SO4=)	1.9686 ± 0.3290	1.8031 ± 0.6481
Ammonium (NH4+)	0.9913 ± 0.1266	0.8926 ± 0.2050
Soluble Potassium (K+)	0.1095 ± 0.0931	0.0097 ± 0.1093
O1TC	3.1693 ± 3.1078	6.9077 ± 1.1712
O2TC	16.9301 ± 1.0934	17.7245 ± 1.5775
O3TC	23.7680 ± 9.1681	23.9165 ± 3.5161
O4TC	7.2323 ± 1.6601	7.1507 ± 1.1825
OPTC	4.7516 ± 8.2300	0.0000 ± 1.2456
OC (IMPROVE)	53.4483 ± 3.6633	54.2705 ± 5.0857
E1TC	3.6820 ± 5.1363	6.9919 ± 6.2000
E2TC	15.8041 ± 2.1108	5.8034 ± 2.3864
E3TC	0.8242 ± 0.6877	0.0137 ± 0.3362
EC (IMPROVE)	17.6619 ± 2.4286	13.8392 ± 4.0653
TCTC (IMPROVE)	71.0976 ± 4.8373	68.1098 ± 6.6352
Sodium (Na)	0.0000 ± 1.5875	0.0000 ± 2.7512
Magnesium (Mg)	0.5224 ± 0.4568	0.4594 ± 0.6434
Aluminum (Al)	0.0000 ± 0.3138	0.0000 ± 0.5354
Silicon (Si)	0.0000 ± 1.0253	0.6941 ± 1.6610
Phosphorus (P)	0.0000 ± 0.0397	0.0000 ± 0.0902
Sulfur (S)	1.3057 ± 0.2364	1.1945 ± 0.1306
Chlorine (Cl)	0.0012 ± 0.0300	0.0000 ± 0.0435
Potassium (K)	0.1822 ± 0.1039	0.1741 ± 0.1839
Calcium (Ca)	0.1944 ± 0.2629	0.3714 ± 0.4966
Titanium (Ti)	0.0073 ± 0.1075	0.1845 ± 0.1619
Vanadium (V)	0.0000 ± 0.0643	0.0170 ± 0.0976
Chromium (Cr)	0.0030 ± 0.0143	0.0035 ± 0.0196
Manganese (Mn)	0.0030 ± 0.0086	0.0410 ± 0.0243
Iron (Fe)	0.9772 ± 0.3410	0.8589 ± 0.5270
Cobalt (Co)	0.0211 ± 0.0741	0.0410 ± 0.1314
Nickel (Ni)	0.0000 ± 0.0042	0.0000 ± 0.0055
Copper (Cu)	1.1331 ± 0.8790	2.3298 ± 0.1759
Zinc (Zn)	0.2179 ± 0.1287	0.3543 ± 0.0888
Gallium (Ga)	0.0000 ± 0.0244	0.0020 ± 0.0321
Arsenic (As)	0.0013 ± 0.0125	0.0013 ± 0.0190
Selenium (Se)	0.0008 ± 0.0053	0.0014 ± 0.0084
Bromine (Br)	0.0150 ± 0.0040	0.0134 ± 0.0069
Rubidium (Rb)	0.0009 ± 0.0051	0.0000 ± 0.0063
Strontium (Sr)	0.0000 ± 0.0061	0.0000 ± 0.0755
Yttrium (Y)	0.0000 ± 0.0080	0.0050 ± 0.0121
Zerconium (Zr)	0.0051 ± 0.0072	0.0000 ± 0.0162
Molybdenum (Mo)	0.0000 ± 0.0161	0.0069 ± 0.0244
Palladium (Pd)	0.0000 ± 0.0255	0.0072 ± 0.0434
Silver (Ag)	0.0013 ± 0.0313	0.0011 ± 0.0528
Cadmium (Cd)	0.0071 ± 0.0318	0.0035 ± 0.0550
Indium (In)	0.0077 ± 0.0375	0.0141 ± 0.0636
Tin (Sn)	0.0077 ± 0.0532	0.0120 ± 0.0882
Antimony (Sb)	0.0297 ± 0.0578	0.0086 ± 0.0996
Barium (Ba)	0.2440 ± 0.2323	0.0000 ± 0.3410
Lanthanum (La)	0.0160 ± 0.3101	0.0407 ± 0.5072
Gold (Au)	0.0019 ± 0.0175	0.0051 ± 0.0276
Mercury (Hg)	0.0000 ± 0.0097	0.0026 ± 0.0166
Thallium (Tl)	0.0024 ± 0.0093	0.0000 ± 0.0152
Lead (Pb)	0.0000 ± 0.0165	0.0112 ± 0.0260
Uranium (U)	0.0011 ± 0.0138	0.0023 ± 0.0218
Sum of species	78.1227 ± 5.0186	76.9827 ± 6.9724

Table 4-4. Pair comparisons between motor vehicle profiles in the Lake Tahoe study.

Profile x	Profile y	R/U Ratio				Correlation
		<1	1-2	2-3	>3	r^2
LZSQ005	LZSQ007	51	5	0	0	0.979
LZST005	LZST009	55	1	0	0	0.998
LZST007	LZST009	50	5	1	0	0.974
LZST019	LZST011	40	12	3	1	0.960

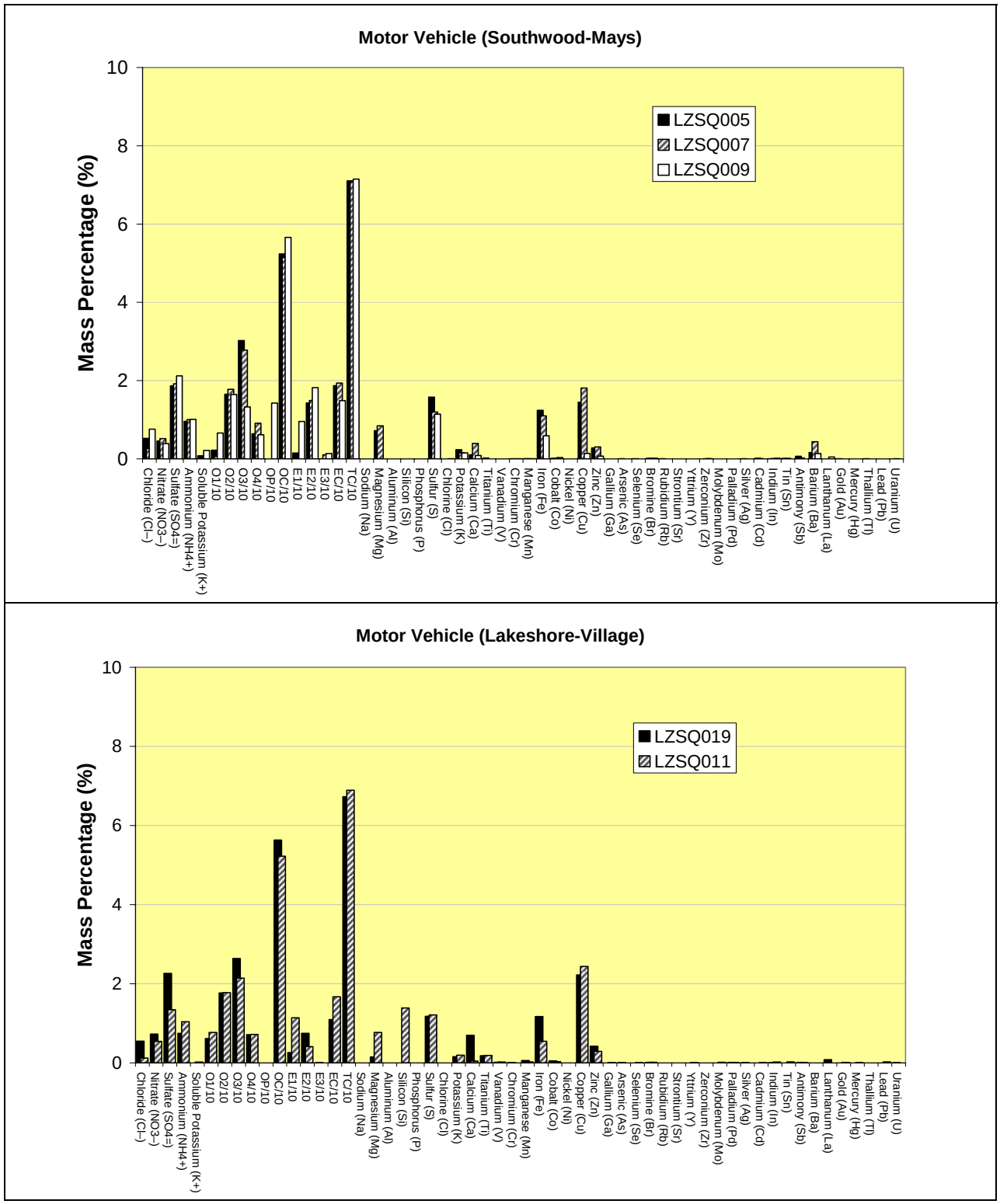

Figure 4-6. Column chart of individual profiles from motor vehicle sampling locations in Incline Village, NV.

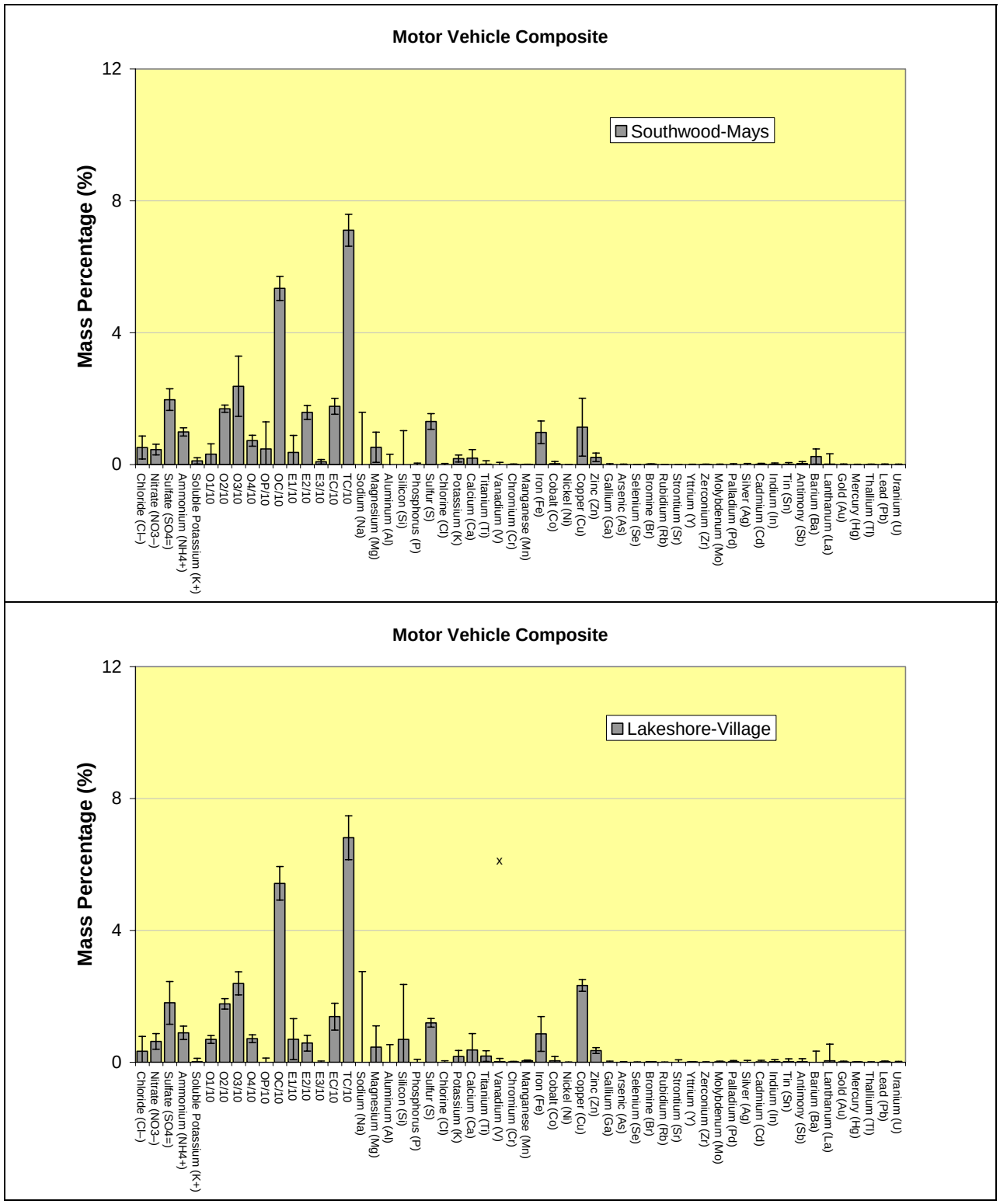

Figure 4-7. Column chart of composited source profiles from Southwood-Mays and Lakeshore-Village.

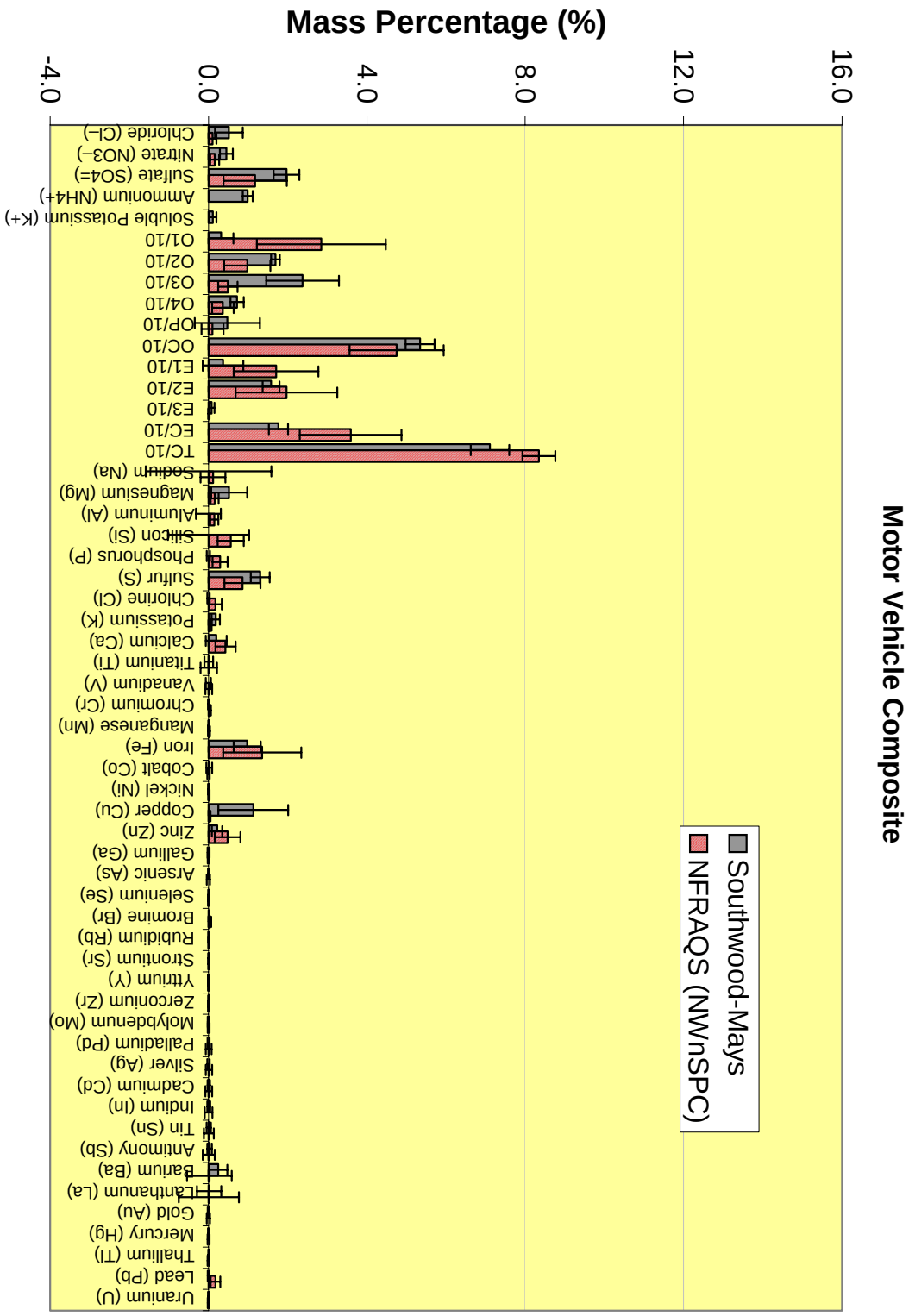

Figure 4-8. Intercomparison of Southwood-Mays and NFRAQS motor vehicle emission profiles.

4.2. Fraction of Background in Motor Vehicle Exhaust Source Profile

Using the same approach as described in Section 3, the relative contribution of the source peaks to the total PM was estimated using DustTraks instrumented with both PM_{10} and $PM_{2.5}$ inlets. For each of the filter sampling periods, the relative fraction of PM associated with the passing vehicles ranged from 30% to 73% for $PM_{2.5}$ and 40% to 79% for PM_{10}. The source contribution to the measured particle size distribution is shown in Figure 4-9.

The size distribution shows that the source dominates the background aerosol mass for particles <150 nm and particles >600 nm. Moreover, particles greater than 1 μm dominate both the total and plume-integrated $PM_{2.5}$ mass. Pure motor vehicle exhaust has a mass median diameter of < 200 nm (Allen et al. 2001), whereas road dust emitted from the vehicle's tire in contact with roads has a mass median diameter of ~5 μm or greater (Kuhns et al. 2001). These ELPI results are consistent with the high relative loading of road dust material on the PM_{10} and $PM_{2.5}$ filters.

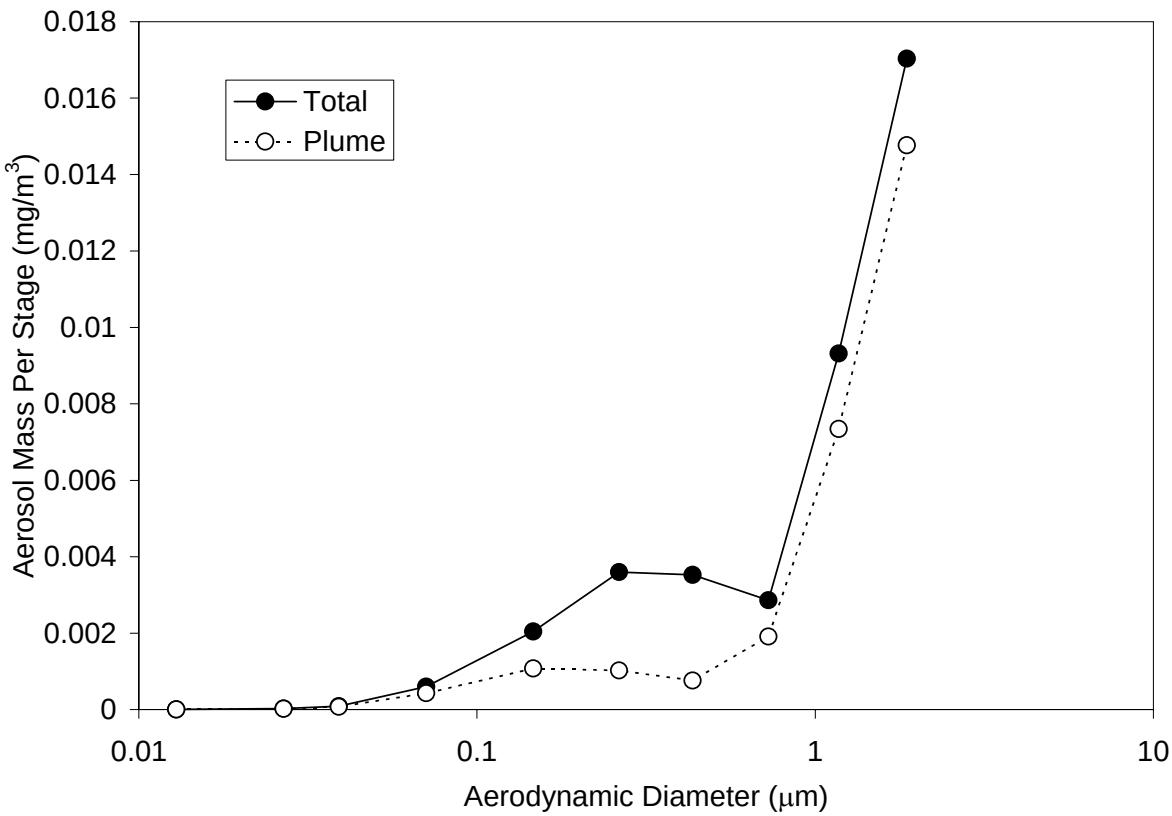

Figure 4-9. Average size distributions of total aerosol and source component measured by the ELPI for all motor vehicle in-plume measurement source profiles.

The fractions of road dust measured on both the PM_{10} and $PM_{2.5}$ filters are compared with the fraction of DustTrak-measured PM_{10} and $PM_{2.5}$ associated with vehicle plumes (i.e., high frequency peaks) in Figure 4-10. High time-resolution aerosol composition data would permit the segregation of road dust and vehicle exhaust for each vehicle pass; however technologies to measure these properties are still in their infancy. The high degree of correlation seen in the

figure indicates that the majority of the mass measured with the DustTraks appears to be associated with road dust rather than with engine exhaust.

Because the ELPI measures aerodynamically size-segregated particle concentrations, a fleet average exhaust emission factor was calculated for the particle size range of less than 0.59 μm (Stages 1 through 7). These particles are dominated by exhaust and have negligible levels of road dust particles. In addition, the bias introduced by charged nanoparticles diffusing to the upper stages of the impactor does not affect the measurements on these lower stages. Using the equation for fuel-based emission factors as described in Section 2 and assuming a particle density of 1 g/cm^3, the fuel-based exhaust emission factor for particles less than 0.59 μm was calculated to be 0.083 g PM/kg fuel. These results are in good agreement with PM emission factors measured by remote sensing (0.06 g PM/kg fuel) and in tunnels (0.11 g PM/kg fuel) (Table 4-5).

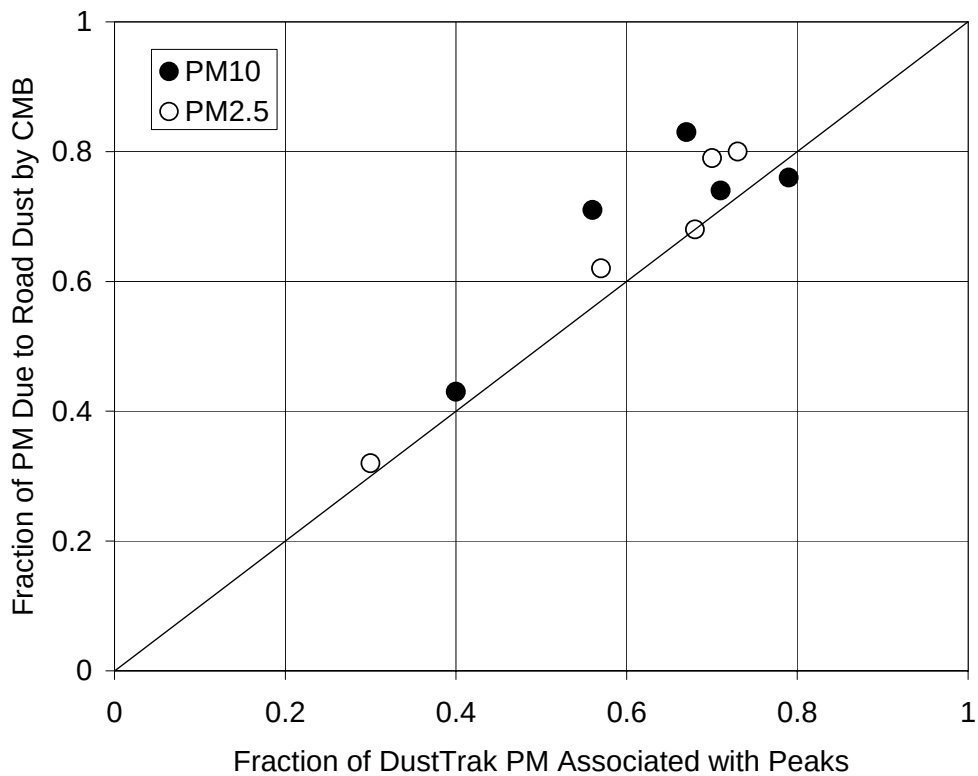

Figure 4-10. Comparison of fraction of road dust measured on filters using CMB with the fraction of PM measured on the DustTraks associated with the vehicle plumes.

4.3. Fuel Based Emission Factors for Motor Vehicle Exhaust

4.3.1. CO Emission Factors

CO has the highest signal-to-noise ratio in vehicle exhaust of all species measured with the FTIR. The emission factor measurements at Incline Village are less than half of the values measured with remote sensing by 2004) in Las Vegas, NV (average vehicle model age of 1994) and about one-eighth of the values measured in a Los Angeles roadway tunnel in 1993 by Fraser

et al. 1998) (average vehicle model age of 1986). Remote sensing analyses have shown that CO emission factors increase with vehicle age. These results from Las Vegas and Los Angeles are consistent with the age versus CO emission factor relationship shown by 2004). The lower emission factors observed in Incline Village, NV, may be associated with a much newer and/or better maintained vehicle fleet than the prior studies. NO and ethylene emission factors are also markedly lower than those measured by Kirchstetter et al. 1999) (average model year 1991) and Fraser et al. 1998), respectively. The resolution of the video camera was unable to capture individual license plates, precluding the estimation of vehicle age based on registration information.

4.3.2. NH_3 Emission Factors

Mobile sources of NH_3 can be a large fraction urban NH_3 emission inventories. NH_3 is of interest with regard to air quality regulation because it is a precursor to both ammonium sulfate ammonium nitrate secondary aerosol. Although ammonium nitrate is a relatively small fraction (~6.5%) of the total fine aerosol mass in the Sierras (Malm et al. 2000), the analysis of mobile NH_3 emissions on an in-use fleet provides a valuable check on the overall quality of the in-plume measurements. NH_3 emissions from vehicles are a reaction product generated in the three-way catalytic converter (Baum et al. 2001). The catalytic converter is designed to reduce CO and NO simultaneously via the chemical reaction:

$$2NO + 2CO \rightarrow N_2 + 2CO_2 \qquad (4\text{-}2)$$

When hydrocarbons are present in the exhaust, hydrogen may be produced in the catalytic converter via the reaction:

$$C_nH_{(2n+2)} + 2nH_2O \rightarrow (3n+1)H_2 + nCO_2 \qquad (4\text{-}3)$$

In turn, the hydrogen is then available initiate a competing reaction with equation 4-2 as:

$$NO + CO + 1.5H_2 \rightarrow NH_3 + CO_2 \qquad (4\text{-}4)$$

Unlike NO, CO, and HC, studies have shown that high NH_3 emissions may originate from late-model and properly maintained vehicles Huai et al. 2003. The fleet average NH_3 emission factors measured in Incline Village are in excellent agreement (<15% difference) with published results from Baum et al. 2001 using remote sensing and Allen et al. 2001) based on tunnel studies, but are about half of those reported by Fraser and Cass 1998 from another study.

Table 4-5. Measured emission factors for on road vehicles in Incline Village compared with published values from in-use vehicles. Negative value emission factors for NO_2, N_2O, Formaldehyde, and SO_2 are an artifact of the low signal to noise ratio for the measurement of these species with the FTIR. These values should be interpreted at below the detectable limits of the system and its configuration in the field.

Species	Lake Tahoe In-Plume Average Emission Factor and Standard Error (g pollutant/kg fuel) for 541 CO_2 peaks	Remotely Sensed Emission Factors (g pollutant/kg fuel)		Tunnel Studies (g pollutant/kg fuel)		Other Source (g pollutant/ kg fuel)
CO	22.6 ± 1.8	49 103	Kuhns et al. 2004 Baum et al. 2001	176	Fraser et al. 1998	
NH_3	0.35 ± 0.02	0.39	Baum et al. 2001	0.76 0.29 ± 0.06	Fraser and Cass 1998[1] Allen et al. 2001	
DustTrak $PM_{2.5}$ (Road Dust)	0.76 ± 0.06					
DustTrak PM_{10} (Road Dust)	1.29 ± 0.09					
ELPI $PM_{0.59}$ (Exhaust)	0.083[2]	0.06	Kuhns et al. 2004[3]	0.11 0.70	Kirchstetter et al. 1999 Fraser et al. 1998[4]	
NO	1.6 ± 0.2	8.8 10	Kuhns et al. 2004 Baum et al. 2001[5]	5.9	Kirchstetter et al. 1999	
Ethylene	0.19 ± 0.02			0.86	Fraser et al. 1998	
Hexane	2.62 ± 0.46	2.8	Kuhns et al. 2004[6]	0.18	Fraser et al. 1998	
Propane	0.43 ± 0.39			0.06	Fraser et al. 1998	
H_2O	740 ± 138					1300[7]
NO_2	-0.10 ± 0.08	<0.18	Baum et al. 2000			
N_2O	-1.5 ± 0.2	<4	Jimenez et al. 2000			
Formaldehyde	-0.01 ± 0.06			0.17	Fraser et al. 1998	
SO_2	-1.07 ± 0.50					0.0001[8]

[1] Assuming 7.1 km/L fuel and fuel density of 0.67 kg/L
[2] Calculated from total integrated ELPI (stages 1 through 7), CO_2, CO, hexane, and propane above background since ELPI settings resulted in lower response times than other instruments.
[3] Exhaust only measured by Lidar backscattering
[4] $PM_{1.6}$ includes geologic material as well as exhaust
[5] Assuming fuel density of 0.67 kg/L
[6] Total HC as measure by remote sensor
[7] Assuming fuel composition of n CH_2 and stoiciometric combustion to produce CO_2 and H_2O.
[8] Assuming 50 ppm Sulfur fuel

4.3.3. PM Emission Factors

Particulate matter emission factors measured with the In-Plume System need to be considered within the context of the sampling system. Unlike dynamometer testing, where sampling probes are connected directly to the exhaust pipe of a vehicle, the location of the In-Plume sampling inlet in the middle of the road results in the simultaneous sampling of road dust, brake/tire wear material, and engine exhaust. Chemical analysis of aerosol filter samples collected with the In-Plume System indicate that as much as 75% of the PM_{10} and $PM_{2.5}$ is composed of geologic material (i.e., oxides of Fe, Al, Si, Ca, and Ti). Analysis of exhaust emissions from dynamometer studies in Denver, CO, indicated that ~88% of exhaust PM_{10} is composed of a combination of OC and EC (Cadle et al. 1999).

A limitation of the In-Plume System is that for vehicles with bumper-level exhaust pipes, plumes of exhaust are immediately mixed with road dust suspended by the vehicle's tires. Consequently, elevated levels of combustion products (i.e., CO_2, CO, and NO) are accompanied by increased levels of both road dust and exhaust PM. Using the results from the CMB resuspended road dust subtraction (Section 4.4), the fraction of road dust PM sampled by the In-Plume System was estimated (Table 4-1). Road dust PM accounted for between 32 ± 2% and 80 ± 5% of the $PM_{2.5}$ collected on the filters and between 43 ± 4% and 83 ± 8% of the filtered PM_{10}. The relative fraction of road dust is smallest (~45% of PM_{10}) on 07/23/03 prior to the rain event. On subsequent sampling days (7/26 and 7/29), the road dust component of the emissions accounts for 73% and 84% of the PM_{10}. These results are consistent with the TRAKER findings that indicate larger emissions of road dust following periods of precipitation. It is likely that soil and detritus either washed or was tracked out onto the road after the rain event. The relative amounts of coarse exhaust (i.e., the non-road dust component of the PM associated with the CO_2 peaks) vary from 1% to 23% and the fine fraction of exhaust varies from 11% to 33%.

4.3.4. Emission Factors of NO

NO is a thermal product of combustion formed when free oxygen and free nitrogen combine. Characteristically, compression ignition (i.e., diesel) vehicles have significantly higher NO emissions associated with their high engine compression ratios than do spark ignition (i.e., gasoline) vehicles. As described above, both NO and CO should be converted to N_2 and CO_2 in the catalytic converter. Older vehicles tend to have higher emission of NO and CO due to lack of maintenance and/or a decreased efficiency of the catalytic converter. NO is an important precursor to the formation of ammonium nitrate aerosol. NO emission factors in Incline Village calculated from the In-Plume System are about one-third or less of those measured in tunnels and by remote sensing (Table 4-5). These discrepancies may be due to a newer and better maintained fleet in the area or to the lack of diesel vehicles sampled by the In-Plume System.

4.3.5. Emissions from Other Species

The remaining emission factors measured by the In-Plume System were either in agreement with or lower than results from comparable studies. The measurements of SO_2, NO_2, and N_2O by IR spectrometry is plagued with weak absorbance bands that are difficult to resolve through a high water vapor background. The fleet average emission factors for these species are most likely below the limits of detection of the instrumentation.

The FTIR is very selective for the measurement of ethylene, whereas the instrument is not as selective for alkanes, such as hexane and propane. Consequently, the sum of hexane and propane emission factors should be interpreted as a gross approximation of all alkane emissions. The sum of propane and hexane are in good agreement with the average light duty gasoline vehicle emission factor measured by remote sensing (Table 4-5). The fleet average water vapor emissions were ~40% lower than would be expected by stoichiometry assuming fuel with the form of nCH_2. Ambient water vapor measurements were generally too high during the study to detect the relatively small increment of water due to combusted fuel.

5. ROAD DUST

Resources for the road dust component of this project were leveraged with another DRI project to expand the original scope of work with the California Air Resources Board (ARB). Dr. Alan Gertler and Dr. Jack Gillies of DRI were funded by National Cooperative Highway Research Program (NCHRP) to investigate the effect of sweeping and sanding on road dust emissions. The scope of the NCHRP program was to erect a flux tower downwind of paved roadways to measure the horizontal flux of PM in real time as vehicles pass. We have coordinated these two studies to collocate the TRAKER measurements with the horizontal flux measurements and thus achieve a paved road calibration data point for the TRAKER system. The TRAKER provides a large-scale perspective of the road dust emission potential that is not obtainable with the limited point measurements from the flux tower.

5.1. Flux Tower Location and Dates

The instrumented flux tower was deployed on six days between 03/06/02 and 04/10/03 on State Highway 28 approximately 100 m south of the main entrance to Sand Harbor State Park (Figure 5-1). Quartz-fiber and Teflon filter samples of both PM_{10} and $PM_{2.5}$ were collected on six days adjacent to the flux tower. These samples provided source profile information of the road dust associated with clean roads, road sanding, and road deicing with a brine solution.

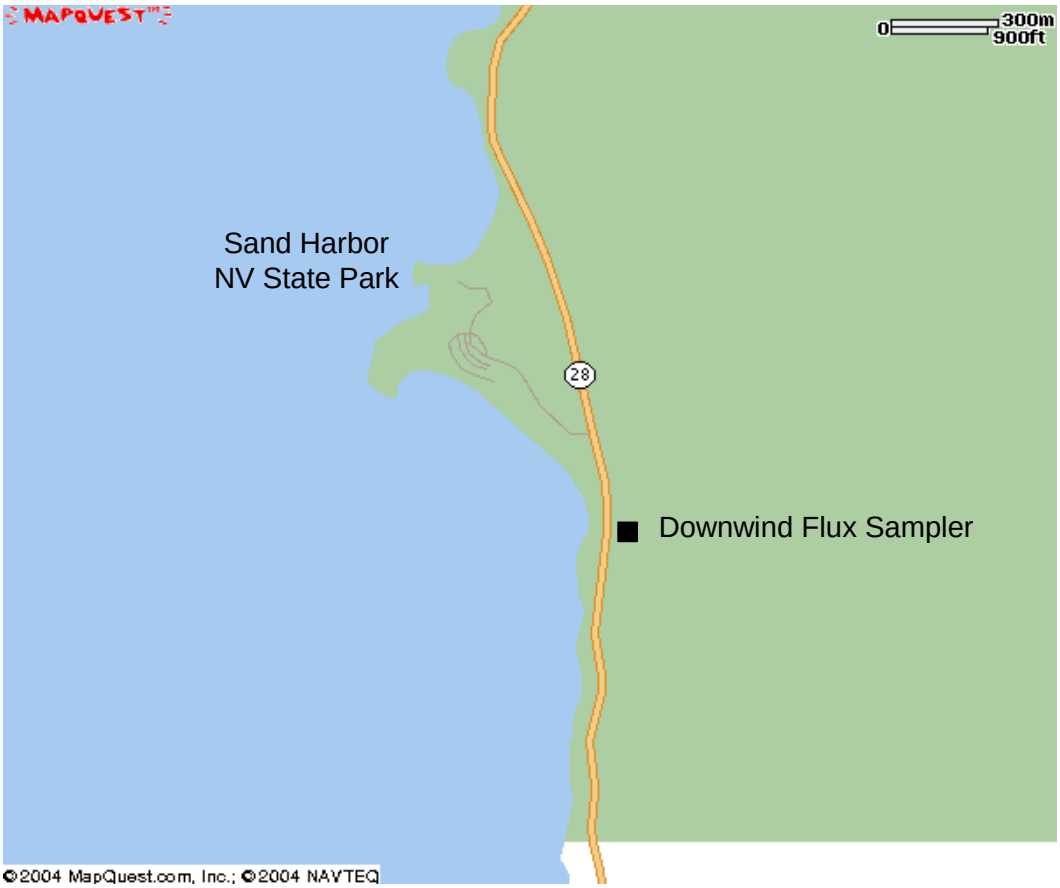

Figure 5-1. Map showing location of flux tower ~300 m south of main entrance to Sand Harbor State Park.

5.1.1. Calculated Emission Factors

Paved road emission factors were calculated using the algorithm described in Section 2. The remaining calculations for each of the filter sampling periods are summarized in Table 5-1. Road tube counters were used to classify vehicles as either heavy duty or light duty based on axle spacing. The table also shows the ambient concentrations of PM_{10} and $PM_{2.5}$ measured by filter samplers and DustTraks. Neither road tube counters nor $PM_{2.5}$ filter samplers were operational on 03/06/03 and 03/12/03. The average ratio of DustTrak PM concentration to filter-based PM concentration was 2.2 for $PM_{2.5}$ and 0.97 for PM_{10}. Consequently, PM_{10} emission factors calculated from the DustTrak-instrumented tower are likely to be representative of filter measurements, whereas $PM_{2.5}$ emission factors may be biased high by a factor of 2 or more. The table shows that DustTrak PM_{10} and $PM_{2.5}$ emission factors ranged from 296 mg/vkt and 35 mg/vkt, respectively, on 03/12/03 to 735 mg/vkt and 211 mg/vkt, respectively, on 04/10/03. National Resources Conservation Service SNOwpack TELemetry (SNOTEL) precipitation data from the Marlette Lake site ~5 km to the east indicated measurable precipitation on ~75% of the days between sampling periods.

The plume apportioning method to distinguish background PM from the source-generated PM (see Sections 3 and 4) was also applied to the roadside PM concentrations. Background concentrations at the Sand Harbor site were generally very low: ~3 ug/m3 $PM_{2.5}$ and ~7 ug/m3 PM_{10}. Between 36% and 81% percent of the $PM_{2.5}$ and between 59 and 89% of PM_{10} measured by the DustTraks at the 50 cm or 100 cm levels were associated with emissions from the roads.

The road in front of the flux tower was treated with a brine solution at about noon on 03/31/03. The application resulted in ~25% increase in the paved road emission factor for both PM_{10} and $PM_{2.5}$. A prolonged snow storm depositing 2.5 cm of snow at Marlette Lake occurred between 04/01/03 and 04/06/03. The emission factors measured directly after the storm showed a doubling of the PM_{10} emission factors from 310 mg/vkt on 03/31/03 to 612 mg/vkt on 04/07/03. Emissions remained elevated on the next day (04/08/03) and after the area was swept by a street sweeper on 04/10/03. These results are consistent with a recent study by Kuhns et al. (2003), where the authors did not find a detectable reduction in road dust emission potential immediately after street sweeping. It is unclear if routine street sweeping reduces emissions of PM from a paved road over longer periods of time.

Table 5-1. Samples collected and emission factors measured downwind of paved road on Highway 28 near Sand Harbor State Park.

QID	TID	Start Time (yyyymmdd hh:mm:ss)	End Time (yyyymmdd hh:mm:ss)	Size	Fleet (Light Duty /Heavy Duty)	Downwind Filter Concentration (ug/m^3)	Average DustTrak Concentration (ug/m^3)	Fraction of DustTrak Signal Associated with Highway	Emission Factor from DustTraks (mg/vkt)	Comments
-	-	20030306 13:46:45	20030306 15:47:42	$PM_{2.5}$	N/A	N/A	4	0.81	108**	Baseline
TMTQ001	TMTT001	20030306 *	20030306 *	PM_{10}	N/A	20.0 +/- 1.5	21	0.75	715**	Baseline
TMFQ002	TMFT002	20030312 10:29:00	20030312 16:40:00	$PM_{2.5}$	N/A	3.6 +/- 0.6	11	0.36	35**	Baseline
TMTQ002	TMTT002	20030312 11:07:00	20030312 16:42:00	PM_{10}	N/A	16.1+/- 1.0	22	0.67	296**	Baseline
-	-	20030331 10:44:42	20030331 12:04:30	$PM_{2.5}$	168/6	N/A	4	0.58	76	Before Brining
-	-	20030331 10:44:42	20030331 12:04:30	PM_{10}	168/6	N/A	12	0.53	229	Before Brining
TMFQ003	TMFT003	20030331 12:05:00	20030331 17:01:00	$PM_{2.5}$	591/8	2.7 +/- 0.7	6	0.47	99	After Salting
TMTQ003	TMTT003	20030331 12:05:00	20030331 17:05:00	PM_{10}	591/8	13.8 +/- 1.0	15	0.58	310	After Salting
TMFQ004	TMFT004	20030407 10:48:00	20030407 17:04:27	$PM_{2.5}$	951/18	2.3 +/- 0.6	5	0.82	112	1st Dry Day After Storm
TMTQ004	TMTT004	20030407 10:53:00	20030407 16:59:00	PM_{10}	951/18	28.1 +/- 1.5	19	0.89	612	1st Dry Day After Storm
TMFQ005	TMFT005	20030408 10:25:00	20030408 16:54:00	$PM_{2.5}$	839/14	5.1 +/- 0.6	8	0.65	133	2nd Dry Day After Storm
TMTQ005	TMTT005	20030408 10:25:00	20030408 17:02:00	PM_{10}	839/14	27.7 +/- 1.5	23	0.79	660	2nd Dry Day After Storm
TMFQ006	TMFT006	20030410 10:15:00	20030410 16:00:00	$PM_{2.5}$	928/35	6.3 +/- 0.7	14	0.38	211	After Sweeping
TMTQ006	TMTT006	20030410 10:15:00	20030410 16:00:00	PM_{10}	928/35	24.1 +/- 1.4	26	0.59	735	After Sweeping

*Unknown absolute start and end time. Duration of 195.2 minutes measured by clock on sampler flow controller.
**Traffic counters not operational. Estimates based on average traffic flow on other days (i.e., 350 vehicles per hour).

5.2. TRAKER Survey Routes and Dates

Undergraduate students from Sierra Nevada College were trained in the operation of the TRAKER vehicle. The students resided in Incline Village at the base of the Mt. Rose pass (NV State Route 431) and were able to deploy the TRAKER vehicle with a minimal setup time.

For this study, 13 passes over Mt. Rose under a variety of snow, sand, and brine conditions were completed. In addition, the students conducted nine circuits around Lake Tahoe (~100 km). Table 5-2 shows the dates of the surveyed routes by TRAKER through 8/17/03. The lake circuits incorporated several sections of residential roads. Daily maps of the routes and the resulting emission potentials (i.e., emission factor divided by vehicle speed) are shown in the appendix of the report. The emission potential is a measure of the dirtiness of the road and does not factor the velocity of the vehicle, whereas the emission factor is the amount of PM that is suspended from a road for a vehicle traveling at a certain speed.

TRAKER was also operated upwind of an instrumented 3.5 m tower to directly compare the measured onboard signal with the horizontal PM emission flux from the paved road. Prior to

Table 5-2. Schedule of TRAKER measurements conducted in the vicinity of Lake Tahoe.

Date	Mt. Rose Pass	Lake Loop
4/7/2003		COMPLETE
4/8/2003		COMPLETE
4/11/2003	COMPLETE	COMPLETE
4/22/2003	COMPLETE	
4/23/2003	COMPLETE	
4/27/2003	Incline Village Only	COMPLETE
4/30/2003		NV Side Only
5/5/2003	COMPLETE	
5/11/2003	COMPLETE	COMPLETE
5/13/2003	COMPLETE	
5/16/2003	COMPLETE	
6/3/2003		NV Side Only
6/4/2003		COMPLETE
6/12/2003	COMPLETE	
6/17/2003	COMPLETE	
6/18/2003	COMPLETE	
7/2/2003	COMPLETE	COMPLETE
7/3/2003	COMPLETE	COMPLETE
7/9/2003	COMPLETE	
7/15/2003		NV Side, and North Lake
7/17/2003		COMPLETE
Total COMPLETE	**13**	**9**

these tests, the TRAKER calibration had been limited to experiments on unpaved roads (Etyemezian et al., 2003; Kuhns et al., 2004). A road tube counter was deployed near the flux tower to measure the speed and vehicle type (based on axle number and spacing) of passing vehicles. Road dust emission factors for light duty and heavy duty vehicles were calculated by integrating the vehicle classification data with the horizontal flux results.

5.2.1. Summary of TRAKER measurements

Data from the TRAKER portion of the study have been analyzed for both spatial and temporal trends. The spatial analysis includes a comparison among groups of roads as well as between Nevada and California roads.

All data were imported into a GIS-format database. Using the Lake Tahoe GIS coverage shown in Figure 5-2 and a built-in software utility for joining spatial data, each TRAKER measurement was associated with a road segment. When attributing road dust emission potentials or emission factors to an individual link, all 1 s valid TRAKER data obtained on the same day for that link were averaged. If there were fewer than 10 valid TRAKER measurements for a link, the link was not considered to have a valid measurement.

Road segments (links) were grouped, based on location, for the purpose of spatial analyses. Figure 5-2 shows the eight groups of road segments. The mutually exclusive groups correspond to roads in Incline Village, NV ("Inc_Vill"), South Lake Tahoe, CA ("South_Lake_Tahoe"), highways adjacent to the lake on the Nevada side ("NV_Loop") and the California side ("CA_Loop"), residential roads that are not directly on the Tahoe loop in Nevada ("NV_Local") and in California ("CA_Local"), Mt Rose Pass to the Northeast of the Lake ("MT_Rose"), and Rt. 267 to the Northwest of the Lake ("RT_267").

Figure 5-3 shows a time series of all TRAKER data obtained during the Lake Tahoe study on measurement days when at least 500 valid data points were obtained. Emission factors over the study period ranged from 0.08 g/vkt (6/18/03) to 0.56 g/vkt (4/8/03) with an overall average of 0.23 g/vkt. The dashed line in the figure represents a best linear fit to the data (R^2 = 0.58). There is no reason to believe that the change in emission factors over time should follow a linear trend. However, the line in the figure serves to illustrate that a temporal pattern associated with the data exists. Overall, emission factors tend to decrease significantly from late spring to early summer by as much as a factor of 3.8 based on the linear regression. This observation applies not only to the study area as a whole, but also to individual groups of roads as is illustrated in Figure 5-4, Figure 5-5, and Figure 5-6.

This type of seasonal difference in emission factors between winter/early spring and summer is not unique to the Lake Tahoe area. Kuhns et al. (2003) noted that in Treasure Valley, ID, emission factors for PM_{10} paved road dust decreased between February and July 2001. Figure 5-7 compares the average emission factors during early to mid-spring (3/31/03–5/16/03) and late spring through mid-summer (5/17/03–7/17/03). The 5/16/03 date was chosen as a cutoff because data from SNOTEL monitors indicate that snowfall in the area had curbed significantly after that date (see Figure 5-8 and Figure 5-9). The measurements indicate that emission factors decrease for several groups of roads between late spring and early summer by more than a factor of 2.

There are several reasons why such seasonal differences may appear. First, during winter, road sanding and de-icing materials may contribute to the loading of dust that is available for suspension by tires. Figure 5-8 shows data from a SNOTEL monitor located near Mt Rose and

emission factors for the Mt Rose Pass. The figure shows that the end of the major snowfall season (nominally 5/16/03) coincides with an overall reduction in emission factors. A similar pattern is also observed with SNOTEL data from monitors in the Lake Tahoe Basin and from emission factors from groups of roads within the basin (Figure 5-9). While a correlation exists between PM_{10} road dust emission factors and periods when snowfall occurs frequently (i.e., late spring), it is difficult to discern from the data if there is a direct correlation between the magnitude of individual snow events and the emission factors for PM_{10} road dust measured shortly after those events. Sufficient data does not exist to determine if a) the most recent snow event has the greatest influence on the emission factors, or b) increased emission factors are the cumulative effect of long-term snowfall. A second reason for the differences between late spring and summer is that precipitation during winter may result in the movement of sediment from hillsides, unpaved road shoulders, and from sources of mud (such as construction sites) onto the road surface, thereby causing an increase in the potential for PM_{10} road dust emissions. Third, during the winter, vertical mixing close to the ground occurs to a lesser degree than during warmer periods. This results in a decrease in the dispersion and movement of air pollutants emitted close to the ground. Thus, in winter, it is possible that a larger fraction of the PM_{10} dust that is emitted from vehicle travel on roads deposits back onto the road. In contrast, when atmospheric mixing occurs to a greater degree, pollutants that are emitted close to the ground may be dispersed vertically and carried further downwind of the source prior to depositing. It is unclear which of these factors most influences the apparent seasonal dependence of road dust emissions. Future work should aim to provide additional insight into the relative contribution of these three factors.

Over the winter of 2002-2003, Washoe County, NV, sweepers collected 1052 cubic yards of debris, but applied only 532 cubic yards of sand to roadways (Washoe County MEP). Similarly, South Lake Tahoe collected 2444 tons of material, but applied only 650 tons of cinders in the same period (South Lake Tahoe MEP). These results indicate that either traction control material applied in other areas or erosion material is migrating throughout the basin on the roadway network.

Because of differences in street sweeping practices and relative locations of the roadways, it is useful to compare emission factors from roads in California with those from comparable roads in Nevada. Figure 5-4 shows a time series of the emission factors from the California and Nevada portions of the Lake Tahoe loop. Both groups of roads exhibit emission factors that are higher in spring than in summer. However, emission factors from the Nevada portion of the Lake Tahoe loop are generally lower than those from California. On days when measurements are available for both groups of roads, PM_{10} emission factors are lower in Nevada in every case. In Figure 5-5, a similar figure is shown for lower-speed roads in the two states. From the data available, it appears that emission factors for PM_{10} road dust are comparable between Incline Village, NV, and South Lake Tahoe, CA. However, in the spring, emission factors on California local roads are higher than Nevada local roads.

Hypotheses regarding why differences are observed between California and Nevada road dust emissions include:

- ***Roadway age and composition of paving material***. The two states pave roads according to their own maintenance cycles. Age and roadway composition may influence the road dust emission potential.

- ***Variations in routine sweeping practices*.** For the period of study (3/31/03 to 3/07/17), California highways were swept with Elgin Eagle sweepers using a water sprayer. Tenant Centurion sweepers were used on Nevada highways. Differences in sweeper types and sweeping frequency may affect road dust emissions (Mark Kinter, Eagle Sweeper).
- ***Proximity to unswept areas***. A common feature of the TRAKER results from the highways surrounding the lake is the increase in emission potential in the vicinity of cities and entrances to neighborhoods (see maps in appendix). Suspendable fine PM is being tracked onto highways from these areas. The local road managers must remove snow and add traction material for safety purposes, but regulations regarding sweeping practices are the jurisdiction of either the TRPA, the county, or the municipality.

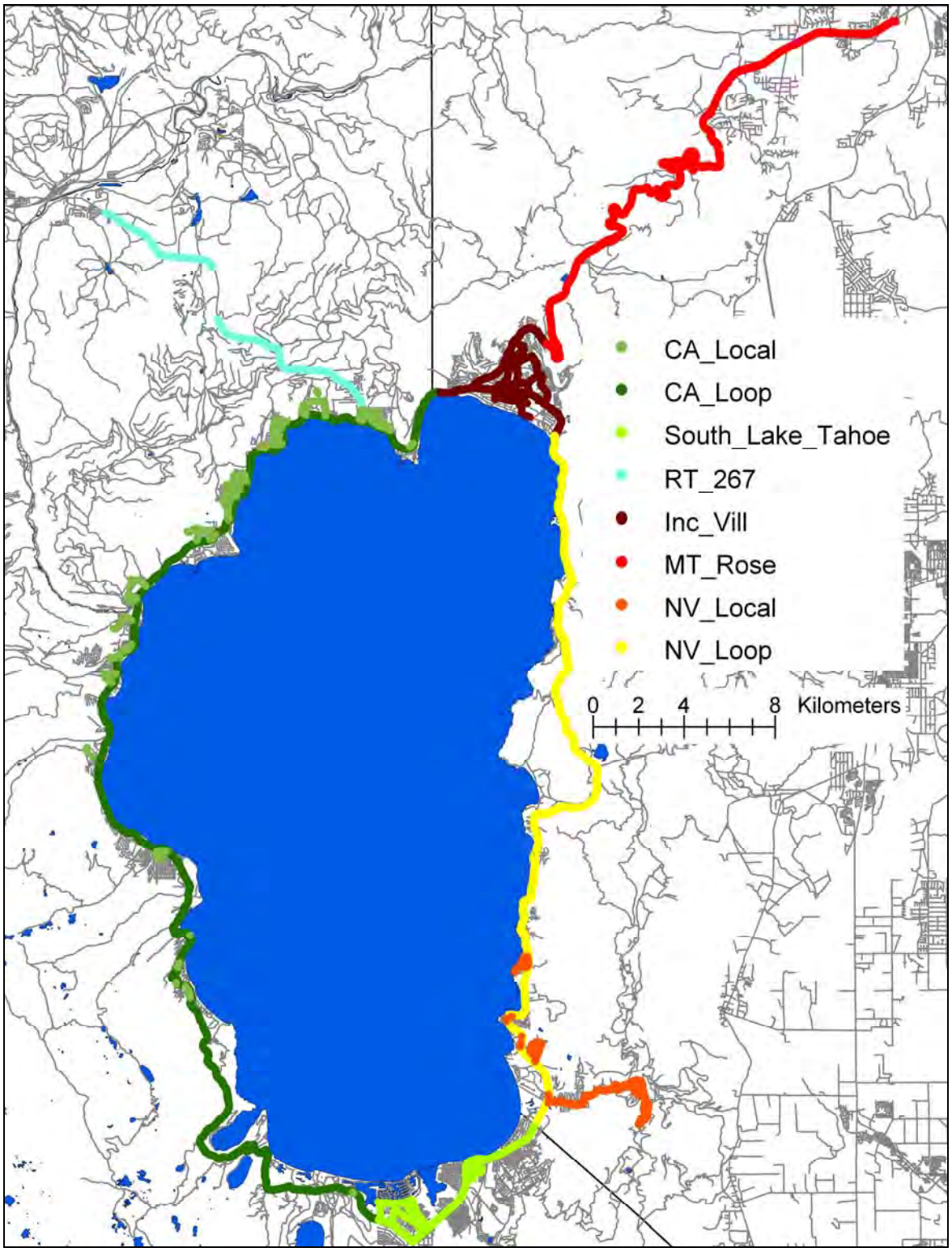

Figure 5-2. Grouping of TRAKER Measurements by region. The different color segments represent different roadway jurisdictions and usage classifications.

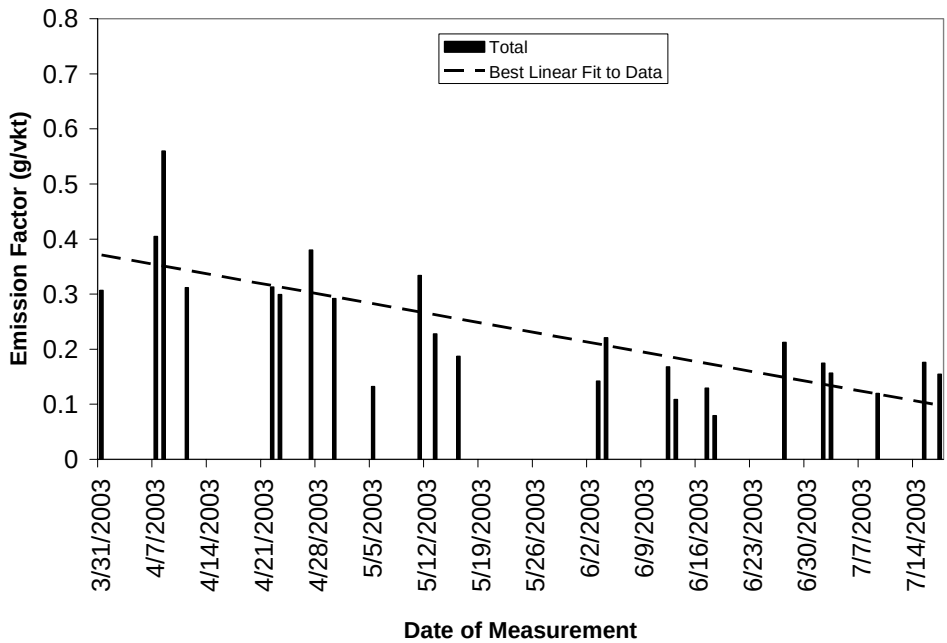

Figure 5-3. TRAKER PM_{10} emission factors over the study period for all measurement dates with more than 500 valid data points. The dashed line represents a best-linear-fit to the data (R^2=0.58).

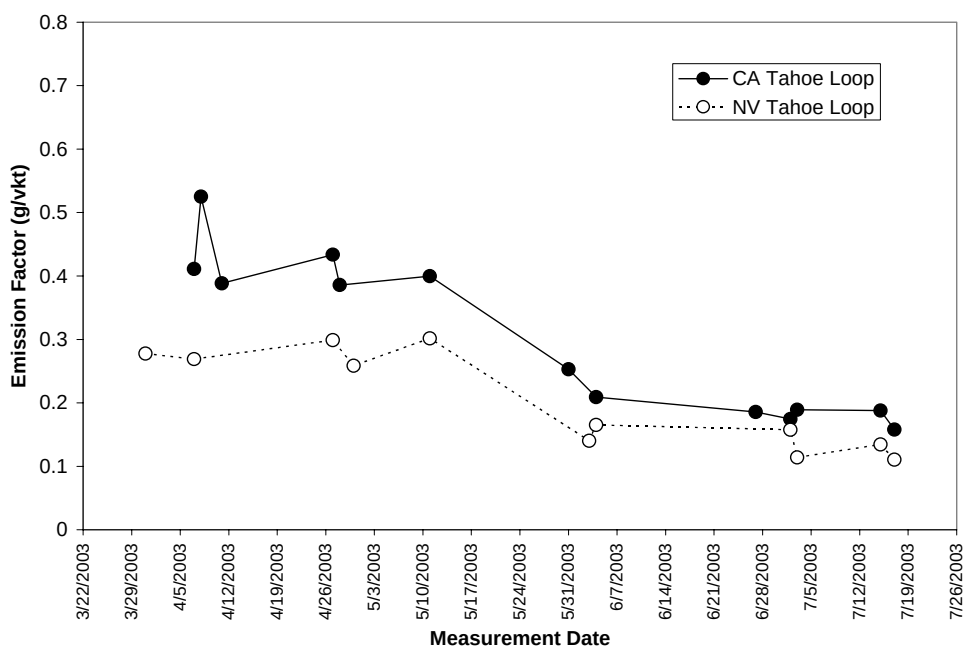

Figure 5-4. Comparison of TRAKER PM_{10} road dust emission factors for the California and Nevada portions of the Lake Tahoe TRAKER loop over the study period.

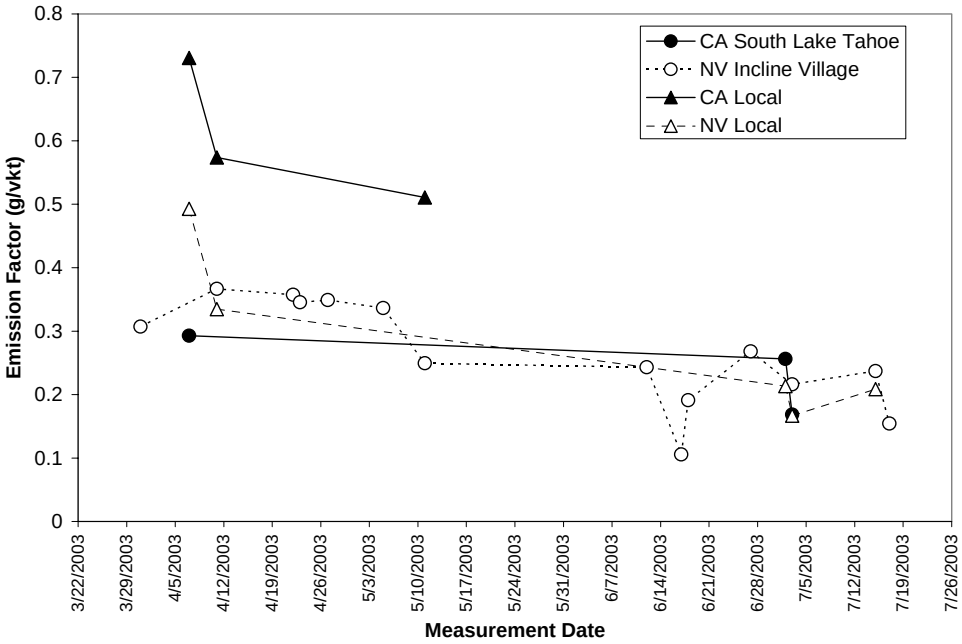

Figure 5-5. Comparison of TRAKER PM_{10} emission factors for local roads (off the main Tahoe loop), Incline Village, and South Lake Tahoe over the study period.

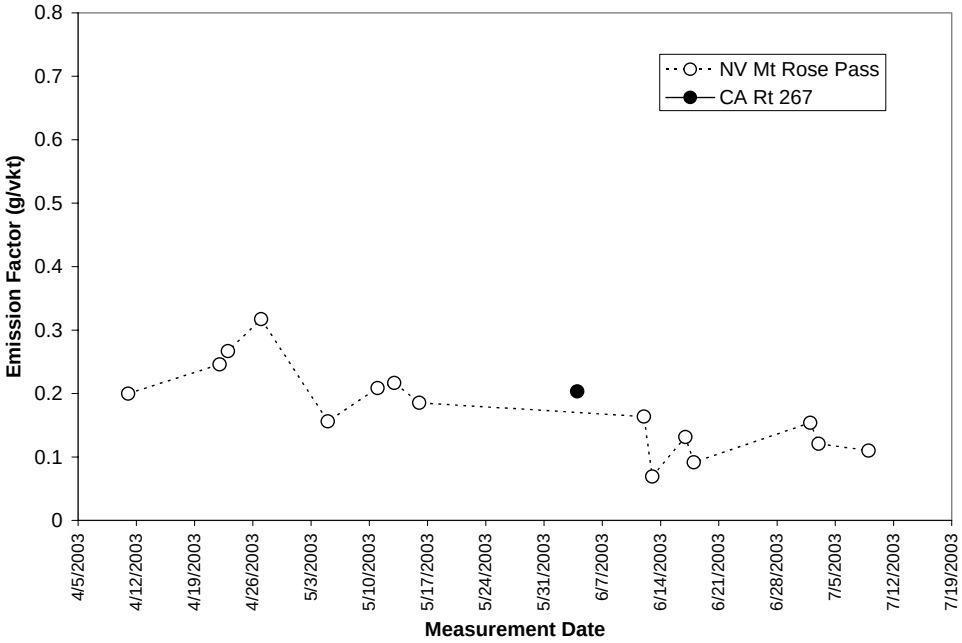

Figure 5-6. TRAKER PM_{10} emission factors for the Mt. Rose Pass over the study period. The figure also shows emission factors measured on California Rt. 267 on 6/4/2003.

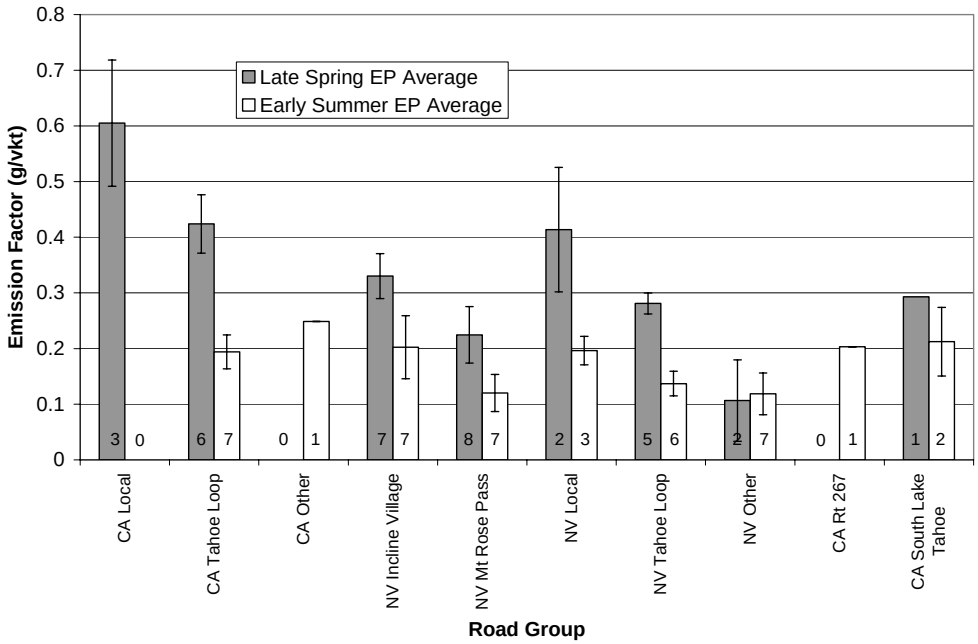

Figure 5-7. Comparison of TRAKER PM_{10} emission factors between spring (3/31/03 – 5/16/03) and summer (5/17/03 – 7/17/03) portions of the study by road group. The vertical bars correspond to standard deviations of PM_{10} emission factors among the different times when each road group was measured. The numbers at the bottom indicate the number of different measurement periods used to obtain the average emission factor for each road group.

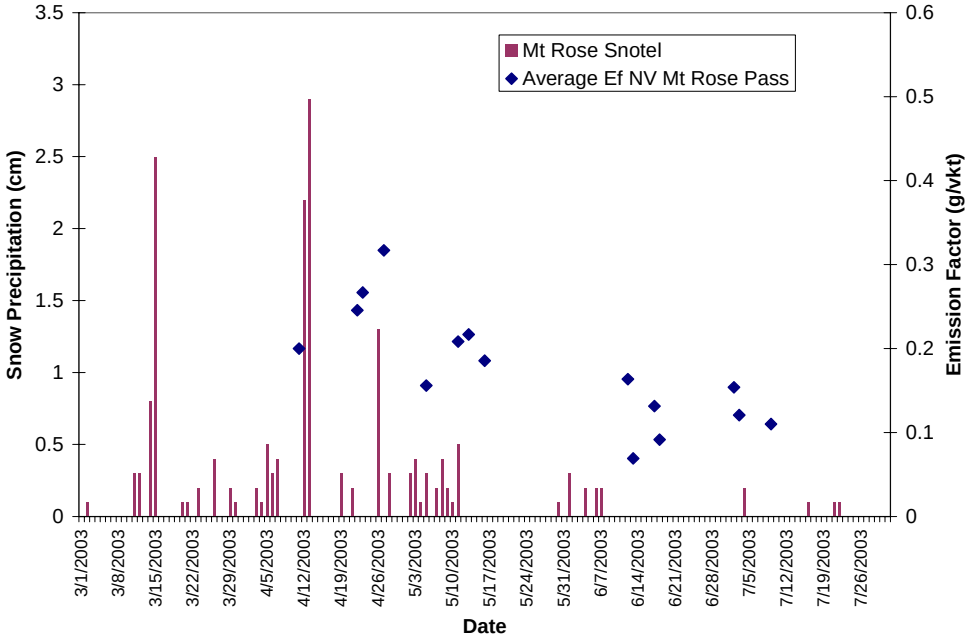

Figure 5-8. Comparison of TRAKER PM_{10} emission factors over study period with SNOTEL data from Mt. Rose.

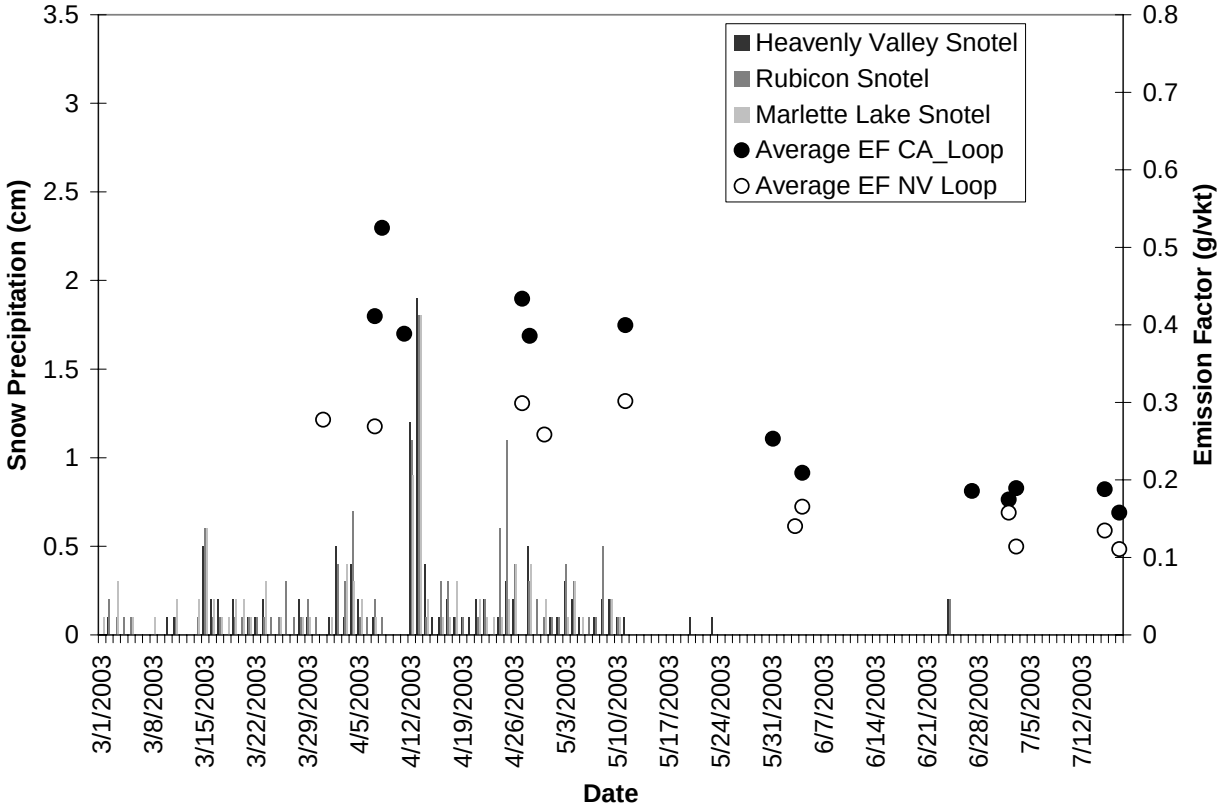

Figure 5-9. Comparison of TRAKER PM_{10} emission factors over study period for California and Nevada portions of Lake Tahoe loop with SNOTEL data from Heavenly Valley, Rubicon, and Marlette Lake.

5.3. Geological source profiles

Two geological samples were collected using grab sampling techniques near the two locations where roadside sampling for motor vehicle exhausts took place (Village-Lakeshore and Southwood-Mays). These profiles are representative of summertime road dust composition. An additional six samples were collected alongside the flux tower deployed on Highway 28 near Sand Harbor State Park. These samples represent what would be emitted from the road in winter when treated with traction control material and a deicing brine solution.

The grab samples were collected by vacuuming a section of the roadway and gutter to fill a high-efficiency filter vacuum bag. The two collected samples were dried at 40 °C and 20% relative humidity and sieved through a Tyler 400 mesh screen (<38 μm geometric diameter) prior to resuspension in the laboratory chamber following the procedures described by Chow et al. (1994). Filter samples were drawn through PM_{10} and $PM_{2.5}$ inlets. Chemical analysis was performed and similar compositions were found for the PM_{10} and $PM_{2.5}$ geological profiles (Chow et al., 1994). Identification numbers of RS686 and RS687 were assigned to the resuspension sample from Village-Lakeshore and Southwood-Mays, respectively.

The chemical abundances (in percentage mass) in these profiles are shown in Figure 5-10 and compared in Table 5-3. Si was the dominant component for both PM_{10} and $PM_{2.5}$ profiles in the present study, accounting for 29–31% of PM_{10} and 15–20% of $PM_{2.5}$. Similar distributions were

also observed for common crustal material, such as Al, Ca, K, and Fe. This confirms that PM_{10} is richer in crustal material than $PM_{2.5}$. Elements of mass percentage higher than 0.1% include Ti, Na (as Na^+), Cl, Sr, Ba, and S. S is found in both $PM_{2.5}$ and PM_{10} at both sites. The molar abundance of S is much higher than for SO_4^{2-}, suggesting that there could be substantial insoluble S in these dust samples. Sr is significant (~1% mass) only at Village-Lakeshore.

NO_3^- is below the detection limit but substantial NH_4^+ is present in the fine-mode particles. The road surface material was likely influenced by motor vehicle exhaust emissions. However, the NH_4^+ could result from biogenic origins as well. The abundance of total K was approximately 10 times the abundance of soluble potassium (K^+) in all $PM_{2.5}$ profiles, and 15 to 30 times in PM_{10} profiles. This is an important distinction, since K^+ is one of the key markers for vegetative burning. In vegetative burning profiles, the K^+/K ratio is usually close to unity.

OC was the second most abundant species in these profiles after Si and accounted for 9–18% of the particulate mass of both PM_{10} and $PM_{2.5}$. EC was less abundant, accounting for 1–2% of the particulate mass. The OC/TC ratios were therefore very high (~0.9). The differences between samples acquired at these two locations are limited except for Sr. The sum of species explains measured PM_{10} (73–65%) better than $PM_{2.5}$ (44–55%). The unidentified mass mostly resides in the fine fraction of particles. When accounting for oxygen associated with crustal elements, the mass closure improves to 85–90% for PM_{10} and 60–70% for $PM_{2.5}$.

The samples collected at Sand Harbor were used to create additional source profiles associated with wintertime sanding and brining operations around Lake Tahoe. The majority of road dust PM is composed of particles in the coarse size mode between 2.5 µm and 10 µm. Road dust source profiles were obtained by subtracting the ambient $PM_{2.5}$ source profile concentrations from the ambient PM_{10} source profiles collected beside the highway. The roadside source profiles are presented in Table 5-4 through Table 5-6. Figure 5-11 shows the coarse PM source profiles from each of these measurements.

As with the grab samples, Si was the dominant component of the coarse mode profiles, accounting for 19–28% of the aerosol mass. Similar distributions were also observed for common crustal material, such as Al, Ca, K, and Fe. Soluble chloride (Cl^-) is the dominant species for the period after the brine solution was applied (4/07/03), comprising 22% of the aerosol mass. Levels of soluble and insoluble sodium and elemental chlorine were also elevated on the same sample.

Both NO_3^- and NH_4^+ accounted for less than 3% and 2%, respectively, of the coarse aerosol mass. As with the grab samples, the abundance of total K was approximately 10 times the abundance or more of K^+ in all roadside profiles.

OC was either the second or third most abundant species in these profiles after Si and A, accounting for between 4% and 24% of the coarse mass. With the exception of the brining sample, abundances of OC decreased from the first sample to the last. The abundances of organic carbonaceous material appeared to be offset by Si during this period, indicating a change in source of suspendable road dust material (i.e. the traction control sand). EC was less abundant, accounting for less than 2.5% of the particulate mass.

Table 5-3. Chemical source profiles of grab samples collected in Incline Village, NV, between 7/26/03 and 7/29/03. Values shown are percentage of total aerosol mass collected on the filter.

Sample ID	RS686			RS686			RS687			RS687		
Sample Date	7/26/2003			7/26/2003			7/29/2003			7/29/2003		
Location	Village Lakeshore			Village Lakeshore			Mays/Southwood			Mays/Southwood		
Size	10			2.5			10			2.5		
Chloride (Cl–)	0.1061	±	7.0939	0.1444	±	7.5029	0.0661	±	7.1072	0.1915	±	7.5934
Nitrate (NO3–)	0.0000	±	0.0458	0.0000	±	0.1176	0.0000	±	0.0238	0.0000	±	0.1259
Sulfate (SO4=)	0.8099	±	0.0441	0.4636	±	0.1158	0.2005	±	0.0226	0.2925	±	0.1233
Ammonium (NH4+)	0.0981	±	0.0735	0.1680	±	0.1208	0.0684	±	0.0269	0.2083	±	0.1253
Soluble Sodium (Na+)	0.1365	±	0.0447	0.1454	±	0.1164	0.0943	±	0.0231	0.1743	±	0.1243
Soluble Magnesium (Mg++)	0.0479	±	0.0359	0.0413	±	0.0912	0.0371	±	0.0190	0.0565	±	0.0974
Soluble Potassium (K+)	0.1426	±	0.0038	0.1527	±	0.0045	0.0684	±	0.0028	0.1570	±	0.0056
Soluble Calcium (Ca++)	1.2932	±	0.0363	0.8791	±	0.0916	0.9790	±	0.0185	1.2476	±	0.0975
O1TC	0.2090	±	0.0997	0.0000	±	0.1183	0.1973	±	0.0724	0.4448	±	0.1400
O2TC	1.1168	±	0.2469	0.5550	±	0.6270	1.2081	±	0.1329	1.2926	±	0.6832
O3TC	6.7684	±	0.2892	4.1566	±	0.6471	5.9019	±	0.2023	6.4664	±	0.7110
O4TC	3.2987	±	0.6406	2.7487	±	0.8411	2.4463	±	0.5175	4.2668	±	0.9866
OPTC	3.9570	±	0.4793	2.1904	±	0.7310	3.8891	±	0.3303	4.5511	±	0.8721
OC (IMPROVE)	15.3499	±	1.3249	9.6506	±	0.9602	13.6427	±	1.2863	17.0217	±	1.6455
E1TC	4.2215	±	1.7169	2.5457	±	1.7759	4.1928	±	1.5540	4.8389	±	2.4517
E2TC	1.1855	±	0.7318	0.9217	±	0.4744	0.8514	±	0.7249	1.3449	±	0.8599
E3TC	0.2858	±	0.1149	0.4469	±	0.1993	0.2244	±	0.0744	0.5477	±	0.2239
EC (IMPROVE)	1.7358	±	0.1537	1.7239	±	0.2703	1.3795	±	0.1157	2.1805	±	0.3182
TCTC (IMPROVE)	17.0857	±	1.4991	11.3745	±	1.1106	15.0222	±	1.4557	19.2022	±	1.8652
Carbonate (CO3=)	0.1685	±	1.6608	0.0655	±	2.7514	0.0543	±	1.2744	0.0523	±	3.1647
Sodium (Na)	0.1405	±	0.0721	0.3397	±	0.1554	0.1535	±	0.0331	1.2631	±	0.1609
Magnesium (Mg)	0.0000	±	0.8569	0.0000	±	1.8806	0.0378	±	0.5159	0.1509	±	1.7299
Aluminum (Al)	10.3117	±	0.1971	5.0129	±	0.4377	8.8902	±	0.1213	5.6027	±	0.4193
Silicon (Si)	30.3652	±	3.1140	15.6035	±	0.3848	29.1966	±	2.6821	19.5749	±	0.4316
Phosphorus (P)	0.0000	±	9.7504	0.0409	±	1.1454	0.0495	±	9.3667	0.0948	±	1.4454
Sulfur (S)	0.5918	±	0.0848	0.6464	±	0.0607	0.3697	±	0.0243	0.5860	±	0.0193
Chlorine (Cl)	0.2180	±	0.0427	0.1433	±	0.0501	0.2232	±	0.0267	0.2493	±	0.0464
Potassium (K)	2.2641	±	0.0654	1.6615	±	0.0276	2.0265	±	0.0662	1.7946	±	0.0333
Calcium (Ca)	3.9649	±	0.4651	2.3930	±	0.1240	3.3148	±	0.4161	2.3072	±	0.1350
Titanium (Ti)	0.4380	±	0.7294	0.3313	±	0.3960	0.3983	±	0.5977	0.4620	±	0.4147
Vanadium (V)	0.0062	±	0.0436	0.0000	±	0.1022	0.0089	±	0.0327	0.0329	±	0.1086
Chromium (Cr)	0.0117	±	0.0244	0.0123	±	0.0602	0.0112	±	0.0174	0.0167	±	0.0581
Manganese (Mn)	0.0834	±	0.0040	0.0757	±	0.0121	0.0857	±	0.0026	0.0989	±	0.0128
Iron (Fe)	4.8580	±	0.0065	4.8181	±	0.0086	4.7570	±	0.0064	5.2215	±	0.0101
Cobalt (Co)	0.0229	±	0.3438	0.0129	±	0.3518	0.0197	±	0.3379	0.0210	±	0.3846
Nickel (Ni)	0.0136	±	0.0751	0.0155	±	0.0762	0.0132	±	0.0733	0.0135	±	0.0826
Copper (Cu)	0.0213	±	0.0015	0.0195	±	0.0039	0.0164	±	0.0012	0.0222	±	0.0040
Zinc (Zn)	0.0951	±	0.0020	0.0888	±	0.0042	0.0676	±	0.0014	0.0824	±	0.0045
Gallium (Ga)	0.0000	±	0.0069	0.0000	±	0.0075	0.0010	±	0.0049	0.0000	±	0.0073
Arsenic (As)	0.0000	±	0.0034	0.0000	±	0.0119	0.0002	±	0.0018	0.0000	±	0.0108
Selenium (Se)	0.0000	±	0.0045	0.0000	±	0.0119	0.0001	±	0.0023	0.0007	±	0.0117
Bromine (Br)	0.0000	±	0.0017	0.0000	±	0.0057	0.0004	±	0.0008	0.0007	±	0.0053
Rubidium (Rb)	0.0075	±	0.0016	0.0076	±	0.0049	0.0084	±	0.0008	0.0082	±	0.0045
Strontium (Sr)	1.0520	±	0.0013	0.8667	±	0.0039	0.0809	±	0.0009	0.0695	±	0.0040
Yttrium (Y)	0.0009	±	0.0745	0.0000	±	0.0635	0.0023	±	0.0058	0.0040	±	0.0069
Zerconium (Zr)	0.0345	±	0.0024	0.0333	±	0.0081	0.0190	±	0.0008	0.0200	±	0.0069
Molybdenum (Mo)	0.0000	±	0.0365	0.0000	±	0.0121	0.0015	±	0.0019	0.0040	±	0.0066
Palladium (Pd)	0.0000	±	0.0061	0.0000	±	0.0150	0.0000	±	0.0022	0.0053	±	0.0130
Silver (Ag)	0.0000	±	0.0100	0.0000	±	0.0337	0.0000	±	0.0051	0.0000	±	0.0353
Cadmium (Cd)	0.0000	±	0.0121	0.0000	±	0.0410	0.0000	±	0.0063	0.0000	±	0.0429
Indium (In)	0.0000	±	0.0129	0.0000	±	0.0435	0.0000	±	0.0066	0.0000	±	0.0450
Tin (Sn)	0.0000	±	0.0143	0.0070	±	0.0490	0.0011	±	0.0075	0.0000	±	0.0508
Antimony (Sb)	0.0000	±	0.0190	0.0094	±	0.0653	0.0000	±	0.0099	0.0000	±	0.0672
Barium (Ba)	0.1633	±	0.0215	0.2682	±	0.0740	0.1162	±	0.0111	0.0000	±	0.0753
Lanthanum (La)	0.0000	±	0.0717	0.0000	±	0.2388	0.0000	±	0.0373	0.0000	±	0.2803
Gold (Au)	0.0000	±	0.1055	0.0000	±	0.3675	0.0000	±	0.0548	0.0000	±	0.3692
Mercury (Hg)	0.0000	±	0.0055	0.0000	±	0.0159	0.0007	±	0.0034	0.0000	±	0.0150
Thallium (Tl)	0.0000	±	0.0034	0.0000	±	0.0116	0.0013	±	0.0017	0.0000	±	0.0097
Lead (Pb)	0.0134	±	0.0033	0.0062	±	0.0107	0.0078	±	0.0014	0.0269	±	0.0104
Uranium (U)	0.0000	±	0.0037	0.0000	±	0.0174	0.0000	±	0.0019	0.0012	±	0.0125
Sum of species	72.2923	±	10.5301	43.6205	±	2.5362	64.7420	±	10.0063	55.6688	±	3.5238

Table 5-4. Chemical source profiles of roadside source samples collected in near Sand Harbor State Park, NV between 3/06/03 and 3/12/03. Values shown are percentage of total aerosol mass collected on the filter.

Sample ID	TMFQ001			TMFQ002			TMFQ002			TMFQ002		
Sample Location	Sand Harbor			Sand Harbor			Sand Harbor			Sand Harbor		
Date	3/6/03			3/12/03			3/12/03			3/12/03		
Size	10			2.5			10			C		
Chloride (Cl–)	1.5786	±	0.2987	2.4115	±	0.4651	3.5996	±	0.5586	4.4732	±	1.1262
Nitrate (NO3–)	0.5005	±	0.1766	1.3755	±	0.3707	0.8115	±	0.1841	0.3968	±	0.3996
Sulfate (SO4=)	0.6929	±	0.1819	0.9167	±	0.3420	0.5646	±	0.1599	0.3057	±	0.3644
Ammonium (NH4+)	0.9915	±	0.1990	2.1941	±	0.3786	1.1930	±	0.1934	0.4568	±	0.3857
Soluble Sodium (Na+)	1.0531	±	0.1251	0.6680	±	0.0588	3.2010	±	0.3353	5.0636	±	0.8885
Soluble Potassium (K+)	0.0866	±	0.0199	0.1432	±	0.0361	0.1069	±	0.0197	0.0803	±	0.0414
Soluble Calcium (Ca++)	0.4977	±	0.0996	0.6534	±	0.1750	0.8321	±	0.1141	0.9636	±	0.2509
O1TC	9.8726	±	1.3610	13.1212	±	1.4370	12.1694	±	1.5318	11.4695	±	2.7693
O2TC	7.5431	±	1.0121	12.9413	±	1.3743	7.8932	±	0.9560	4.1810	±	1.5134
O3TC	11.7334	±	1.7671	22.3819	±	2.8614	13.2897	±	1.7797	6.6035	±	3.0880
O4TC	4.8899	±	0.6948	8.5964	±	1.0403	4.2995	±	0.5680	1.1397	±	0.9764
OPTC	0.2246	±	0.2422	1.7004	±	0.6139	1.2470	±	0.3572	0.9137	±	0.7516
OC (IMPROVE)	34.2669	±	4.4464	58.7283	±	5.9353	38.9077	±	4.4951	24.3324	±	7.0652
E1TC	1.3507	±	0.2602	2.1986	±	0.4441	1.5791	±	0.2639	1.1235	±	0.5262
E2TC	1.2191	±	0.3028	3.3613	±	0.6709	1.5321	±	0.3168	0.1869	±	0.6790
E3TC	0.0000	±	0.0737	0.1789	±	0.1537	0.0000	±	0.0677	0.0000	±	0.1642
EC (IMPROVE)	2.3423	±	0.6118	4.0523	±	1.0505	1.8529	±	0.4817	0.2355	±	1.0827
TCTC (IMPROVE)	36.6091	±	4.8777	62.7815	±	6.6432	40.7606	±	4.8542	24.5672	±	7.7641
Sodium (Na)	2.2715	±	0.5457	2.9493	±	0.7349	3.1695	±	0.6149	3.3315	±	1.2096
Magnesium (Mg)	0.0000	±	0.3827	0.2735	±	0.5509	0.5319	±	0.1258	0.7220	±	0.4678
Aluminum (Al)	4.6633	±	1.4861	0.5561	±	0.0936	3.0886	±	0.9761	4.9510	±	1.8194
Silicon (Si)	14.3644	±	4.8025	1.7618	±	0.1566	11.9695	±	3.9470	19.4759	±	7.3341
Phosphorus (P)	0.0000	±	0.0698	0.0009	±	0.0569	0.0000	±	0.0622	0.0000	±	0.1158
Sulfur (S)	0.4023	±	0.0503	0.6084	±	0.0566	0.3795	±	0.0426	0.2112	±	0.0626
Chlorine (Cl)	1.4586	±	0.4536	0.3294	±	0.0433	5.4812	±	1.6696	9.2696	±	3.1643
Potassium (K)	1.0385	±	0.2362	0.1413	±	0.0256	0.8870	±	0.1958	1.4353	±	0.3910
Calcium (Ca)	1.5239	±	0.3050	0.2349	±	0.0291	1.7615	±	0.3386	2.8841	±	0.7051
Titanium (Ti)	0.1450	±	0.1460	0.0000	±	0.2771	0.0960	±	0.1224	0.1667	±	0.2953
Vanadium (V)	0.0000	±	0.0824	0.0000	±	0.1569	0.0000	±	0.0494	0.0000	±	0.1437
Chromium (Cr)	0.0000	±	0.0230	0.0000	±	0.0431	0.0000	±	0.0086	0.0000	±	0.0350
Manganese (Mn)	0.0302	±	0.0051	0.0028	±	0.0184	0.0261	±	0.0036	0.0432	±	0.0160
Iron (Fe)	1.8430	±	0.2183	0.4478	±	0.0383	1.5849	±	0.1661	2.4212	±	0.4266
Cobalt (Co)	0.0240	±	0.0293	0.0128	±	0.0038	0.0241	±	0.0254	0.0324	±	0.0443
Nickel (Ni)	0.0000	±	0.0040	0.0000	±	0.0073	0.0004	±	0.0035	0.0007	±	0.0081
Copper (Cu)	0.0027	±	0.0052	0.0284	±	0.0041	0.0132	±	0.0023	0.0020	±	0.0043
Zinc (Zn)	0.0294	±	0.0040	0.0808	±	0.0076	0.0362	±	0.0043	0.0034	±	0.0062
Gallium (Ga)	0.0000	±	0.0148	0.0000	±	0.0275	0.0051	±	0.0136	0.0088	±	0.0311
Arsenic (As)	0.0035	±	0.0121	0.0000	±	0.0239	0.0000	±	0.0109	0.0000	±	0.0258
Selenium (Se)	0.0020	±	0.0052	0.0055	±	0.0101	0.0023	±	0.0047	0.0000	±	0.0110
Bromine (Br)	0.0035	±	0.0057	0.0000	±	0.0101	0.0019	±	0.0051	0.0034	±	0.0115
Rubidium (Rb)	0.0020	±	0.0062	0.0000	±	0.0110	0.0000	±	0.0054	0.0000	±	0.0124
Strontium (Sr)	0.0289	±	0.0043	0.0000	±	0.0119	0.0241	±	0.0035	0.0418	±	0.0122
Yttrium (Y)	0.0040	±	0.0087	0.0000	±	0.0147	0.0012	±	0.0078	0.0020	±	0.0173
Zerconium (Zr)	0.0131	±	0.0037	0.0073	±	0.0174	0.0101	±	0.0032	0.0121	±	0.0141
Molybdenum (Mo)	0.0059	±	0.0173	0.0101	±	0.0303	0.0054	±	0.0156	0.0020	±	0.0350
Palladium (Pd)	0.0074	±	0.0163	0.0055	±	0.0266	0.0000	±	0.0163	0.0000	±	0.0344
Silver (Ag)	0.0000	±	0.0195	0.0000	±	0.0395	0.0105	±	0.0195	0.0182	±	0.0446
Cadmium (Cd)	0.0042	±	0.0186	0.0000	±	0.0385	0.0051	±	0.0183	0.0088	±	0.0426
Indium (In)	0.0000	±	0.0252	0.0000	±	0.0459	0.0000	±	0.0214	0.0000	±	0.0502
Tin (Sn)	0.0000	±	0.0406	0.0450	±	0.0762	0.0179	±	0.0358	0.0000	±	0.0836
Antimony (Sb)	0.0040	±	0.0468	0.0606	±	0.0882	0.0000	±	0.0416	0.0000	±	0.0973
Barium (Ba)	0.1306	±	0.2162	0.3955	±	0.4101	0.1489	±	0.1972	0.0000	±	0.4552
Lanthanum (La)	0.1054	±	0.2756	0.1734	±	0.5204	0.0000	±	0.2489	0.0000	±	0.5774
Gold (Au)	0.0047	±	0.0158	0.0229	±	0.0294	0.0000	±	0.0144	0.0000	±	0.0331
Mercury (Hg)	0.0092	±	0.0095	0.0128	±	0.0165	0.0074	±	0.0086	0.0034	±	0.0192
Thallium (Tl)	0.0000	±	0.0084	0.0000	±	0.0156	0.0000	±	0.0082	0.0000	±	0.0182
Lead (Pb)	0.0000	±	0.0176	0.0340	±	0.0112	0.0000	±	0.0159	0.0000	±	0.0291
Uranium (U)	0.0000	±	0.0143	0.0000	±	0.0257	0.0000	±	0.0128	0.0000	±	0.0292
Sum of species	65.4186	±	7.0451	74.3877	±	6.7348	69.8577	±	6.3974	66.7795	±	11.0186

Table 5-5. Chemical source profiles of roadside source samples collected in near Sand Harbor State Park, NV, between 3/31/03 and 4/07/03. Values shown are percentage of total aerosol mass collected on the filter.

Sample ID	TMFQ003			TMFQ003			TMFQ003			TMFQ004			TMFQ004			TMFQ004		
Sample Location	Sand Harbor			Sand Harbor			Sand Harbor			Sand Harbor			Sand Harbor			Sand Harbor		
Date	3/31/03			3/31/03			3/31/03			4/7/03			4/7/03			4/7/03		
Size	2.5			10			C			2.5			10			C		
Chloride (Cl–)	2.1446	±	0.3878	7.7882	±	1.1122	21.5040	±	7.3638	4.6015	±	0.7509	1.5557	±	0.3097	0.7672	±	0.3468
Nitrate (NO3–)	0.5906	±	0.2686	0.7148	±	0.1995	1.0169	±	0.9733	1.3753	±	0.4490	0.2881	±	0.1091	0.0066	±	0.1701
Sulfate (SO4=)	1.4764	±	0.2906	1.1523	±	0.2112	0.3646	±	0.9444	0.9754	±	0.4267	0.4091	±	0.1163	0.2625	±	0.1731
Ammonium (NH4+)	1.8338	±	0.2994	1.5436	±	0.2279	0.8382	±	0.9800	3.0211	±	0.4880	0.5248	±	0.1263	0.0000	±	0.1718
Soluble Sodium (Na+)	0.4274	±	0.0379	6.4237	±	0.5891	20.9970	±	6.5049	1.5073	±	0.1279	0.9726	±	0.1520	0.8342	±	0.1690
Soluble Potassium (K+)	0.0825	±	0.0274	0.1292	±	0.0226	0.2426	±	0.1209	0.1525	±	0.0447	0.0514	±	0.0130	0.0252	±	0.0180
Soluble Calcium (Ca++)	0.4955	±	0.1358	0.7212	±	0.1109	1.2696	±	0.6017	0.9177	±	0.2226	0.5140	±	0.0935	0.4095	±	0.1168
O1TC	26.5766	±	2.8429	15.9960	±	1.8431	0.0000	±	7.8636	16.0448	±	1.7732	3.3781	±	0.5824	0.0989	±	0.5267
O2TC	11.5869	±	1.1995	7.7810	±	0.8710	0.0000	±	3.1954	11.9689	±	1.3534	3.9216	±	0.6645	1.8383	±	0.6047
O3TC	17.6675	±	2.2378	11.3268	±	1.5471	0.0000	±	6.5515	16.3614	±	2.7306	9.5311	±	1.6730	7.7629	±	1.9533
O4TC	5.5523	±	0.7301	5.3307	±	0.6458	4.7924	±	2.7368	5.8345	±	1.0011	3.6411	±	0.6197	3.0733	±	0.7325
OPTC	1.5744	±	0.5132	0.6581	±	0.3011	0.0000	±	1.6621	0.8665	±	0.6460	0.5166	±	0.1941	0.4261	±	0.2908
OC (IMPROVE)	62.9839	±	6.0322	41.0744	±	4.3220	0.0000	±	15.3786	51.0954	±	5.6696	20.9905	±	3.4593	13.1970	±	3.3426
E1TC	0.8129	±	0.3027	0.9355	±	0.2268	1.2333	±	1.1008	1.0664	±	0.4757	1.0256	±	0.2078	1.0150	±	0.2877
E2TC	1.8649	±	0.4459	0.5797	±	0.2613	0.0000	±	1.5729	1.8419	±	0.6361	1.3540	±	0.2975	1.2277	±	0.3943
E3TC	0.0000	±	0.1189	0.0000	±	0.0817	0.0000	±	0.4027	0.0000	±	0.1923	0.0000	±	0.0443	0.0000	±	0.0747
EC (IMPROVE)	1.0879	±	0.5252	0.8533	±	0.3642	0.2833	±	1.7660	2.0841	±	0.8509	1.8627	±	0.4970	1.8054	±	0.6576
TCTC (IMPROVE)	64.0712	±	6.4248	41.9633	±	4.5956	0.0000	±	16.8753	53.0949	±	6.2473	22.8533	±	3.8245	15.0243	±	3.8421
Sodium (Na)	0.8793	±	1.7104	2.0009	±	0.6613	4.7270	±	4.9206	3.1121	±	3.3901	1.0438	±	1.0783	0.5083	±	1.6067
Magnesium (Mg)	0.2600	±	0.4396	0.6729	±	0.1332	1.6764	±	1.2567	1.4599	±	0.2646	0.4136	±	0.1146	0.1427	±	0.1403
Aluminum (Al)	0.4411	±	0.0743	3.7313	±	1.1560	11.7275	±	5.2541	0.4255	±	0.4764	6.5020	±	2.1642	8.0751	±	2.8725
Silicon (Si)	0.9324	±	0.0878	8.8172	±	2.8743	27.9801	±	12.8378	5.0975	±	0.4393	20.8611	±	7.2881	24.9420	±	9.5308
Phosphorus (P)	0.0000	±	0.0520	0.0000	±	0.0745	0.0000	±	0.2852	0.0000	±	0.0743	0.0000	±	0.0506	0.0000	±	0.0666
Sulfur (S)	0.8099	±	0.0708	0.7724	±	0.0738	0.6813	±	0.2827	0.4050	±	0.0459	0.2412	±	0.0391	0.1988	±	0.0434
Chlorine (Cl)	0.2857	±	0.0371	10.8741	±	3.2648	36.6075	±	15.5602	0.5319	±	0.0644	1.7391	±	0.5674	2.0516	±	0.7434
Potassium (K)	0.0974	±	0.0218	0.6390	±	0.1381	1.9553	±	0.7451	0.4986	±	0.0537	1.3704	±	0.3402	1.5960	±	0.4555
Calcium (Ca)	0.2469	±	0.0272	1.1688	±	0.2171	3.4094	±	1.2435	0.9241	±	0.0843	2.3335	±	0.5229	2.6983	±	0.7065
Titanium (Ti)	0.0000	±	0.2307	0.0000	±	0.1304	0.0000	±	0.7174	0.0103	±	0.3256	0.0593	±	0.1047	0.0720	±	0.1567
Vanadium (V)	0.0000	±	0.1345	0.0000	±	0.0529	0.0000	±	0.3739	0.0000	±	0.1320	0.0000	±	0.0540	0.0000	±	0.0761
Chromium (Cr)	0.0000	±	0.0383	0.0000	±	0.0085	0.0000	±	0.0974	0.0000	±	0.0218	0.0000	±	0.0142	0.0000	±	0.0188
Manganese (Mn)	0.0012	±	0.0161	0.0178	±	0.0029	0.0581	±	0.0439	0.0359	±	0.0068	0.0345	±	0.0060	0.0342	±	0.0077
Iron (Fe)	0.6683	±	0.0553	1.2751	±	0.1173	2.7499	±	0.8725	1.5278	±	0.1290	2.5306	±	0.3950	2.7902	±	0.5457
Cobalt (Co)	0.0191	±	0.0049	0.0136	±	0.0208	0.0000	±	0.0721	0.0115	±	0.0282	0.0245	±	0.0389	0.0279	±	0.0496
Nickel (Ni)	0.0036	±	0.0066	0.0025	±	0.0034	0.0000	±	0.0198	0.0038	±	0.0090	0.0008	±	0.0026	0.0000	±	0.0041
Copper (Cu)	0.0072	±	0.0084	0.0165	±	0.0021	0.0392	±	0.0243	0.0244	±	0.0054	0.0090	±	0.0017	0.0050	±	0.0021
Zinc (Zn)	0.1249	±	0.0107	0.0305	±	0.0035	0.0000	±	0.0638	0.0679	±	0.0078	0.0443	±	0.0071	0.0382	±	0.0080
Gallium (Ga)	0.0000	±	0.0239	0.0000	±	0.0136	0.0000	±	0.0744	0.0308	±	0.0359	0.0000	±	0.0087	0.0000	±	0.0144
Arsenic (As)	0.0000	±	0.0191	0.0000	±	0.0114	0.0000	±	0.0608	0.0000	±	0.0308	0.0008	±	0.0071	0.0010	±	0.0120
Selenium (Se)	0.0036	±	0.0084	0.0000	±	0.0047	0.0000	±	0.0260	0.0064	±	0.0128	0.0018	±	0.0032	0.0007	±	0.0052
Bromine (Br)	0.0072	±	0.0090	0.0072	±	0.0018	0.0073	±	0.0227	0.0051	±	0.0128	0.0026	±	0.0032	0.0020	±	0.0052
Rubidium (Rb)	0.0036	±	0.0096	0.0000	±	0.0051	0.0000	±	0.0292	0.0000	±	0.0141	0.0021	±	0.0037	0.0027	±	0.0059
Strontium (Sr)	0.0173	±	0.0038	0.0191	±	0.0026	0.0232	±	0.0134	0.0244	±	0.0054	0.0424	±	0.0068	0.0471	±	0.0095
Yttrium (Y)	0.0000	±	0.0131	0.0008	±	0.0068	0.0029	±	0.0395	0.0000	±	0.0205	0.0026	±	0.0048	0.0033	±	0.0080
Zerconium (Zr)	0.0066	±	0.0155	0.0064	±	0.0081	0.0058	±	0.0468	0.0192	±	0.0244	0.0105	±	0.0026	0.0083	±	0.0070
Molybdenum (Mo)	0.0173	±	0.0269	0.0123	±	0.0140	0.0000	±	0.0811	0.0000	±	0.0410	0.0050	±	0.0098	0.0063	±	0.0163
Palladium (Pd)	0.0000	±	0.0263	0.0000	±	0.0140	0.0000	±	0.0799	0.0192	±	0.0398	0.0000	±	0.0092	0.0000	±	0.0155
Silver (Ag)	0.0263	±	0.0341	0.0000	±	0.0191	0.0000	±	0.1073	0.0936	±	0.0190	0.0058	±	0.0111	0.0000	±	0.0150
Cadmium (Cd)	0.0000	±	0.0335	0.0000	±	0.0178	0.0000	±	0.1017	0.0449	±	0.0462	0.0074	±	0.0114	0.0000	±	0.0186
Indium (In)	0.0000	±	0.0400	0.0000	±	0.0212	0.0000	±	0.1214	0.0192	±	0.0564	0.0121	±	0.0149	0.0103	±	0.0237
Tin (Sn)	0.0030	±	0.0652	0.0152	±	0.0390	0.0450	±	0.2077	0.0000	±	0.0987	0.0000	±	0.0240	0.0000	±	0.0396
Antimony (Sb)	0.0000	±	0.0759	0.0000	±	0.0423	0.0000	±	0.2348	0.0000	±	0.1154	0.0021	±	0.0261	0.0027	±	0.0444
Barium (Ba)	0.1883	±	0.3445	0.2549	±	0.0717	0.4169	±	0.8789	0.2320	±	0.5386	0.3456	±	0.0681	0.3750	±	0.1660
Lanthanum (La)	0.0000	±	0.4435	0.0000	±	0.2545	0.0000	±	1.3871	0.0000	±	0.6742	0.1547	±	0.1582	0.1948	±	0.2658
Gold (Au)	0.0131	±	0.0263	0.0000	±	0.0148	0.0000	±	0.0823	0.0051	±	0.0372	0.0045	±	0.0092	0.0043	±	0.0151
Mercury (Hg)	0.0060	±	0.0144	0.0055	±	0.0081	0.0044	±	0.0445	0.0154	±	0.0218	0.0018	±	0.0050	0.0000	±	0.0085
Thallium (Tl)	0.0000	±	0.0143	0.0000	±	0.0076	0.0000	±	0.0436	0.0000	±	0.0218	0.0000	±	0.0050	0.0000	±	0.0085
Lead (Pb)	0.0102	±	0.0281	0.0216	±	0.0053	0.0494	±	0.0721	0.0487	±	0.0157	0.0047	±	0.0100	0.0000	±	0.0133
Uranium (U)	0.0030	±	0.0227	0.0000	±	0.0114	0.0000	±	0.0678	0.0013	±	0.0346	0.0061	±	0.0085	0.0073	±	0.0140
Sum of species	73.3915	±	6.4888	75.6413	±	5.7113	93.1952	±	24.1460	73.7681	±	6.4491	60.9863	±	8.5547	57.8393	±	10.7347

Table 5-6. Chemical source profiles of roadside source samples collected in near Sand Harbor State Park, NV, between 4/08/03 and 4/10/03. Values shown are percentage of total aerosol mass collected on the filter.

Sample ID	TMFQ005			TMFQ005			TMFQ005			TMFQ006			TMFQ006			TMFQ006		
Sample Location	Sand Harbor			Sand Harbor			Sand Harbor			Sand Harbor			Sand Harbor			Sand Harbor		
Date	4/8/03			4/8/03			4/8/03			4/10/03			4/10/03			4/10/03		
Size	2.5			10			C			2.5			10			C		
Chloride (Cl–)	2.4331	±	0.4333	1.4099	±	0.2808	0.8978	±	0.4054	1.8712	±	0.3357	0.9680	±	0.1974	0.3224	±	0.3556
Nitrate (NO3–)	0.8816	±	0.3107	0.3766	±	0.1163	0.1239	±	0.2191	2.5365	±	0.3715	2.1372	±	0.3644	1.8517	±	0.6331
Sulfate (SO4=)	1.4993	±	0.3197	0.6335	±	0.1381	0.2002	±	0.2227	3.2572	±	0.3541	1.6622	±	0.2585	0.5221	±	0.3514
Ammonium (NH4+)	2.2326	±	0.3392	0.7415	±	0.1488	0.0000	±	0.2204	3.9283	±	0.3729	1.9454	±	0.2884	0.5281	±	0.3490
Soluble Sodium (Na+)	0.6314	±	0.0505	1.1096	±	0.1708	1.3489	±	0.3089	0.4452	±	0.0358	0.5320	±	0.0738	0.5940	±	0.1426
Soluble Potassium (K+)	0.1713	±	0.0339	0.1483	±	0.0263	0.1368	±	0.0411	0.1136	±	0.0253	0.1006	±	0.0183	0.0913	±	0.0349
Soluble Calcium (Ca++)	0.7368	±	0.1572	0.6084	±	0.1050	0.5441	±	0.1652	0.5491	±	0.1224	0.7208	±	0.1119	0.8435	±	0.2334
O1TC	9.4102	±	0.9945	6.1648	±	1.0430	4.5406	±	1.3477	16.2584	±	1.6573	4.8545	±	0.7555	0.0000	±	1.4431
O2TC	11.0619	±	1.1210	3.9348	±	0.6579	0.3679	±	0.6805	9.4761	±	0.9361	4.7227	±	0.7186	1.3250	±	0.9118
O3TC	19.5083	±	2.4217	7.6450	±	1.3563	1.7078	±	1.6347	16.1519	±	1.9524	8.5016	±	1.3880	3.0333	±	2.0388
O4TC	7.1236	±	0.8532	3.6531	±	0.6135	1.9161	±	0.7299	7.2120	±	0.7712	4.5481	±	0.6881	2.6441	±	0.9800
OPTC	1.2988	±	0.5149	1.0844	±	0.3095	0.9772	±	0.5205	2.5552	±	0.6517	1.3375	±	0.3614	0.4672	±	0.7175
OC (IMPROVE)	48.4328	±	4.6771	22.4898	±	3.6463	9.5061	±	3.7256	51.6535	±	4.6807	23.9684	±	3.5366	4.1799	±	4.1004
E1TC	2.7800	±	0.4454	1.0447	±	0.2087	0.1762	±	0.3021	2.4300	±	0.3658	1.4145	±	0.2516	0.6886	±	0.4146
E2TC	3.8321	±	0.6759	1.0504	±	0.2424	0.0000	±	0.4340	3.6360	±	0.6034	2.1065	±	0.4097	1.0133	±	0.7034
E3TC	0.9287	±	0.2005	0.0000	±	0.0437	0.0000	±	0.1554	0.2820	±	0.1171	0.2617	±	0.0690	0.2472	±	0.1437
EC (IMPROVE)	6.2300	±	1.3756	1.0084	±	0.2918	0.0000	±	0.8433	3.7883	±	0.8773	2.4556	±	0.6105	1.5031	±	1.1344
TCTC (IMPROVE)	54.6637	±	5.4902	23.4982	±	3.8695	7.9008	±	3.9579	55.4424	±	5.2673	26.4038	±	3.9619	5.6479	±	4.8274
Sodium (Na)	2.3594	±	0.7393	0.9378	±	1.1650	0.2264	±	1.7745	0.0000	±	1.8222	0.0000	±	1.1614	0.0000	±	2.3796
Magnesium (Mg)	0.2827	±	0.5511	0.0997	±	0.2793	0.0081	±	0.5011	0.2033	±	0.4241	0.1810	±	0.2957	0.1651	±	0.5905
Aluminum (Al)	1.5541	±	0.1553	5.6396	±	1.8726	7.6843	±	3.0399	0.8782	±	0.0998	5.5037	±	1.7891	8.8099	±	3.4413
Silicon (Si)	5.1043	±	0.3945	20.6324	±	7.1867	28.4038	±	11.6215	3.5127	±	0.2685	18.0655	±	6.1748	28.4673	±	11.7036
Phosphorus (P)	0.0103	±	0.0617	0.0200	±	0.0507	0.0249	±	0.0821	0.0000	±	0.0561	0.0000	±	0.0713	0.0000	±	0.1286
Sulfur (S)	0.9724	±	0.0785	0.4112	±	0.0643	0.1303	±	0.0537	2.1480	±	0.1620	1.0570	±	0.1470	0.2772	±	0.1393
Chlorine (Cl)	0.5157	±	0.0524	1.4873	±	0.4839	1.9736	±	0.7815	0.0503	±	0.0697	0.4231	±	0.1364	0.6895	±	0.2691
Potassium (K)	0.5235	±	0.0478	1.5345	±	0.3785	2.0405	±	0.6420	0.4465	±	0.0398	1.2493	±	0.2968	1.8231	±	0.5921
Calcium (Ca)	0.9227	±	0.0748	2.5200	±	0.5606	3.3195	±	0.9690	0.6369	±	0.0513	2.1848	±	0.4633	3.2912	±	0.9715
Titanium (Ti)	0.0000	±	0.2639	0.1257	±	0.0384	0.1887	±	0.1474	0.0000	±	0.1955	0.1342	±	0.0364	0.2301	±	0.1588
Vanadium (V)	0.0000	±	0.1474	0.0000	±	0.0531	0.0000	±	0.1086	0.0000	±	0.1116	0.0000	±	0.0516	0.0000	±	0.1192
Chromium (Cr)	0.0000	±	0.0403	0.0000	±	0.0143	0.0000	±	0.0294	0.0000	±	0.0316	0.0000	±	0.0143	0.0000	±	0.0333
Manganese (Mn)	0.0163	±	0.0180	0.0369	±	0.0062	0.0472	±	0.0145	0.0071	±	0.0136	0.0385	±	0.0059	0.0609	±	0.0176
Iron (Fe)	1.5224	±	0.1156	2.6915	±	0.4139	3.2766	±	0.7495	1.0995	±	0.0818	2.2905	±	0.3168	3.1417	±	0.7330
Cobalt (Co)	0.0094	±	0.0257	0.0337	±	0.0414	0.0459	±	0.0639	0.0194	±	0.0065	0.0309	±	0.0355	0.0392	±	0.0612
Nickel (Ni)	0.0060	±	0.0069	0.0020	±	0.0029	0.0000	±	0.0055	0.0039	±	0.0052	0.0022	±	0.0027	0.0009	±	0.0059
Copper (Cu)	0.0257	±	0.0037	0.0097	±	0.0018	0.0017	±	0.0025	0.0168	±	0.0027	0.0110	±	0.0020	0.0069	±	0.0033
Zinc (Zn)	0.0557	±	0.0053	0.0377	±	0.0059	0.0287	±	0.0075	0.0361	±	0.0038	0.0320	±	0.0047	0.0291	±	0.0078
Gallium (Ga)	0.0206	±	0.0257	0.0009	±	0.0089	0.0000	±	0.0186	0.0000	±	0.0194	0.0000	±	0.0091	0.0000	±	0.0209
Arsenic (As)	0.0017	±	0.0214	0.0029	±	0.0072	0.0034	±	0.0152	0.0013	±	0.0161	0.0040	±	0.0073	0.0060	±	0.0170
Selenium (Se)	0.0000	±	0.0086	0.0009	±	0.0031	0.0013	±	0.0064	0.0039	±	0.0065	0.0003	±	0.0030	0.0000	±	0.0069
Bromine (Br)	0.0154	±	0.0027	0.0014	±	0.0034	0.0000	±	0.0054	0.0110	±	0.0026	0.0075	±	0.0017	0.0051	±	0.0032
Rubidium (Rb)	0.0000	±	0.0103	0.0049	±	0.0016	0.0073	±	0.0058	0.0000	±	0.0077	0.0024	±	0.0038	0.0042	±	0.0086
Strontium (Sr)	0.0180	±	0.0044	0.0417	±	0.0066	0.0536	±	0.0126	0.0148	±	0.0033	0.0358	±	0.0052	0.0507	±	0.0123
Yttrium (Y)	0.0043	±	0.0146	0.0000	±	0.0051	0.0000	±	0.0106	0.0000	±	0.0103	0.0046	±	0.0051	0.0078	±	0.0116
Zerconium (Zr)	0.0154	±	0.0172	0.0086	±	0.0024	0.0051	±	0.0092	0.0097	±	0.0123	0.0132	±	0.0027	0.0157	±	0.0101
Molybdenum (Mo)	0.0206	±	0.0292	0.0043	±	0.0103	0.0000	±	0.0212	0.0219	±	0.0072	0.0013	±	0.0100	0.0000	±	0.0181
Palladium (Pd)	0.0034	±	0.0300	0.0046	±	0.0100	0.0051	±	0.0213	0.0000	±	0.0226	0.0003	±	0.0100	0.0005	±	0.0235
Silver (Ag)	0.0308	±	0.0377	0.0000	±	0.0114	0.0000	±	0.0257	0.0245	±	0.0284	0.0000	±	0.0132	0.0000	±	0.0306
Cadmium (Cd)	0.0000	±	0.0343	0.0000	±	0.0114	0.0000	±	0.0243	0.0000	±	0.0284	0.0000	±	0.0121	0.0000	±	0.0290
Indium (In)	0.0000	±	0.0437	0.0000	±	0.0146	0.0000	±	0.0309	0.0000	±	0.0316	0.0000	±	0.0153	0.0000	±	0.0347
Tin (Sn)	0.0000	±	0.0703	0.0077	±	0.0229	0.0116	±	0.0492	0.0194	±	0.0542	0.0000	±	0.0242	0.0000	±	0.0569
Antimony (Sb)	0.0129	±	0.0814	0.0043	±	0.0263	0.0000	±	0.0567	0.0032	±	0.0619	0.0089	±	0.0275	0.0129	±	0.0647
Barium (Ba)	0.4960	±	0.1315	0.1409	±	0.0475	0.0000	±	0.0913	0.0000	±	0.2820	0.1982	±	0.0512	0.3399	±	0.2285
Lanthanum (La)	0.2724	±	0.4800	0.1269	±	0.1625	0.0540	±	0.3413	0.0000	±	0.3588	0.0949	±	0.1661	0.1628	±	0.3845
Gold (Au)	0.0094	±	0.0266	0.0000	±	0.0094	0.0000	±	0.0194	0.0000	±	0.0206	0.0000	±	0.0097	0.0000	±	0.0222
Mercury (Hg)	0.0017	±	0.0154	0.0051	±	0.0055	0.0069	±	0.0113	0.0065	±	0.0116	0.0056	±	0.0020	0.0051	±	0.0090
Thallium (Tl)	0.0000	±	0.0154	0.0000	±	0.0051	0.0000	±	0.0109	0.0000	±	0.0116	0.0000	±	0.0054	0.0000	±	0.0124
Lead (Pb)	0.0188	±	0.0309	0.0000	±	0.0106	0.0000	±	0.0222	0.0168	±	0.0226	0.0046	±	0.0105	0.0000	±	0.0242
Uranium (U)	0.0000	±	0.0240	0.0000	±	0.0086	0.0000	±	0.0176	0.0000	±	0.0174	0.0000	±	0.0083	0.0000	±	0.0190
Sum of species	73.0334	±	5.5871	61.4081	±	8.4238	55.6817	±	12.7462	74.2708	±	5.3507	63.5727	±	7.6026	55.9772	±	13.2295

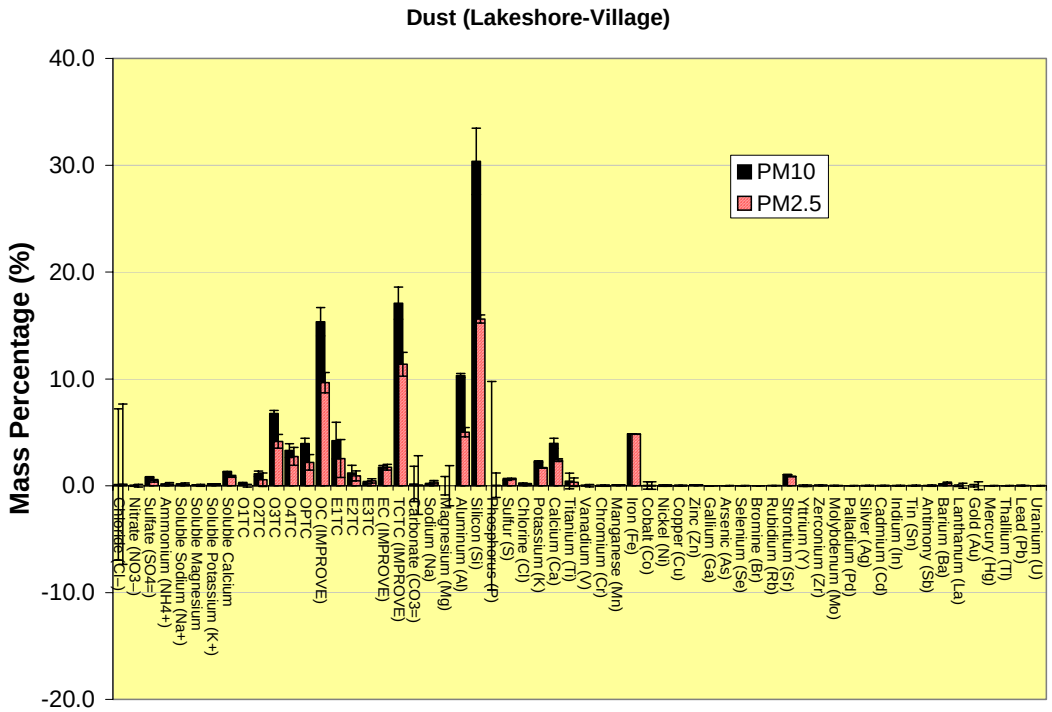

Figure 5-10. Composite source profiles of grab samples collected in Incline Village between 7/26/03 and 7/29/03.

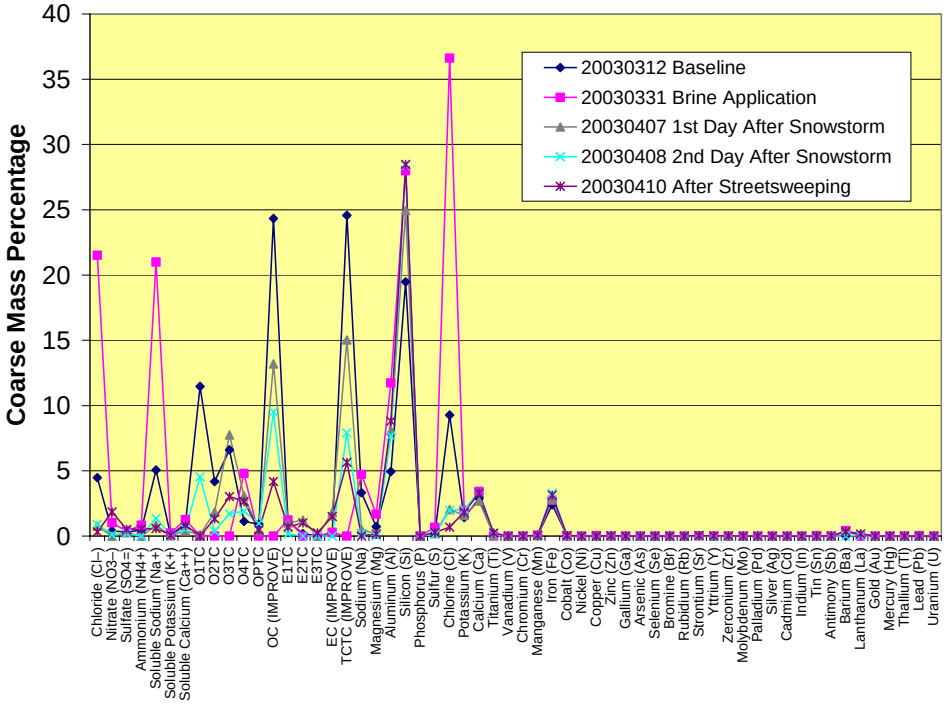

Figure 5-11. Coarse PM source profiles of roadside samples collected in near Sand Harbor State Park, NV, between 3/12/03 and 4/10/03.

6. BASIN WIDE EMISSIONS CALCULATIONS

Emission factors from the previous chapters are combined with activity data to determine air pollutant emissions for the Lake Tahoe Basin.

6.1. Motor Vehicle Exhaust

6.1.1 Vehicle kilometers traveled in the basin

Traffic models such as TRANPLAN and TRANSCAD simulate the movement of vehicle traffic on roadways between trip origins and destinations. These models incorporate census data and the locations of residences, schools, businesses, and local attractions to estimate the volume of traffic on the roadway network. The results are further calibrated and verified with traffic counters deployed throughout the area. A TRANPLAN model is currently maintained by the TRPA with the assistance of Parsons Brinkerhof (2004) and used to estimate basin wide VKT attributable to both residents and visitors (Lake Tahoe Basin Regional Transportation Plan, TRPA, 2004). For base year 2003, the basin wide VKT is 2,866,963 km/day.

6.1.2 Fuel sales and basin exhaust emissions

The MOBILE6 (U.S. EPA, 2002) and EMFAC (California Air Resources Board, 2001) mobile emission factor models use vehicle miles traveled as a principle activity factor to estimate emissions from mobile sources. Running these models requires an estimate of the vehicle kilometers traveled (VKT) within an air shed. The primary method for estimating VKT is to run a traffic demand and forecasting model to simulate the trips driven in an area. An alternative approach to estimate exhaust emissions is to base emissions on fuel sales, which can be measured with improved precision because fuel sales are taxed by the state. This approach has been applied in the San Francisco Bay Area and in Denver, and compares favorably with the distance-based emission estimation approach (Singer et al., 1999; Dreher and Harley, 1998; Pokharel et al., 2002).

Each mobile source estimation approach has a unique set of benefits and drawbacks. Both require that emission factors are applicable to the fleet being simulated. MOBILE6 and EMFAC require that estimates of VKT are accurate for the air shed. Fuel-based emission estimation assumes that fuel sales are known specifically within the area of interest and that the sales are representative of the fuel burned within the air shed. These assumptions and the potential biases may need special consideration in the Lake Tahoe Basin.

Lake Tahoe is a major tourist destination in both summer and winter. At any give time, the area is populated by a mix of full-time residents and visitors. Examples of activities that would result in fuel sales inaccurately representing fuel burned in the basin and the direction of these biases include:

- Residents leaving basin to refuel in Truckee, Reno, or Carson City at a lower cost: *Negative bias on fuel burned*
- Visitors driving to the basin and leaving without refueling: *Negative bias on fuel burned*

- Visitors driving more than approximately 200 km to get to the Tahoe Basin (e.g., from San Francisco Bay Area), refueling in the basin, and driving out of the basin: *Positive bias on fuel burned*

The relative size of these biases is unknown and could ultimately cause fuel sales estimates to either overestimate or underestimate the quantity of fuel actually burned in the basin.

As part of this study, efforts were made to acquire fuel sales data for the Tahoe Basin via a variety of methods. A "top down" approach was initially attempted by contacting representative from the California and Nevada taxation boards. Fuel sales data were available on a county level basis in both states. Data were not available for fuel sales only within the Tahoe Basin. Summation of the county level fuel sales would introduce a positive bias in Tahoe Basin fuel sales since this would include sales in Reno and parts of east Sacramento Area.

Alternatively, a "bottom-up" approach of contacting local gas station owners was attempted to learn how gas is distributed within the basin and how fuel sales records are kept. There are 20 gas stations within the Tahoe Basin (Table 6-1).

Table 6-1. Number of fuel pumps in the Lake Tahoe Basin.

County/State	***Station Name***	***Gas Pumps***	***Average Gas Sales (gal/month)***	***Summer Gas Sales (gal/month)***	***Winter Gas Sales (gal/month)***	Diesel Pumps
Washoe Co. (NV)	7-11 Incline Village	4				0
Washoe Co. (NV)	Chevron Incline Village	8				0
Douglas Co. (NV)	Lake Tahoe Oil Co.	8				0
Douglas Co. (NV)	Doug's Round Hill Shell	8				0
El Dorado Co. (CA)	American Gasoline	8				0
El Dorado Co. (CA)	Stop N Save	4				2
El Dorado Co. (CA)	Beacon Station	8				2
El Dorado Co. (CA)	Fox Gasoline	10				2
El Dorado Co. (CA)	Stateline 76	10	130,000			0
El Dorado Co. (CA)	Al's Chevron Way	12	135,000	210,000		0
El Dorado Co. (CA)	Swiss Mart Food & Gas	6	120,000			0
El Dorado Co. (CA)	Tahoe Tom's	8				0
Placer Co. (CA)	Tahoe City Chevron	8				0
Placer Co. (CA)	Tahoe City Shell	8	110,000			0
Placer Co. (CA)	Beacon Gas Station	4				0
Placer Co. (CA)	Rod's 76	8				0
Placer Co. (CA)	King's Beach Shell	8	100,000	140,000	90,000	0
	TOTAL	**130**				**6**

Responses from local station owners were mixed and inconsistent. Most of the stations did not respond to phone calls or visits; approximately one-third of owners who did respond indicated that they did not want to share the fuel sale information; and the 5 of the 17 owners supplied average fuel sales information.

Based on the five respondents, the annual average and standard error of fuel sales per pump was 13522 ± 2750 gal/month based on 44 out of 130 pumps in the basin. The annual average fuel sales in the basin were calculated as:

$$Annual\ Fuel\ Sales = (130\,pumps)\left(\frac{13522 \pm 414\ gallons}{month\ pump}\right)\left(\frac{3.79\,\text{liters}}{gallon}\right)\left(\frac{0.67kg}{liter}\right)\left(\frac{12months}{year}\right)\left(\frac{1Mg}{1000kg}\right)$$
$$= 53600 \pm 1600 Mg\ \ fuel / year$$

This result is used to estimate basin-wide emissions based on the measured in-plume emission factors described in the following sections.

6.1.3 Comparison of VKT with Fuel Sales

A comparison of the fuel sales and VKT data for the Tahoe basin along with the national fleet average fuel economy (http://www.eia.doe.gov/emeu/rtecs/nhts_survey/2001/appendix_k_energy_data.pdf) can provide a check of the validity of these two activity factors. The national fleet average fuel economy for on-road vehicles is 8.75 km/l (20.6 mpg). Thus, the annual quantity of fuel consumed in the basin can be estimated as:

$$Annual\ Fuel\ Consumption = \left(\frac{2{,}866{,}963\,\text{km}}{\text{day}}\right)\left(\frac{365\ day}{year}\right)\left(\frac{\text{liter}}{8.75\ km}\right)\left(\frac{0.67kg}{liter}\right)\left(\frac{1Mg}{1000kg}\right)$$
$$= 80127 Mg\ \ fuel / year$$

The estimated annual fuel consumption is 49% greater than the estimated mass of fuel sold in the Tahoe basin. This result appears to be reasonable since residents and visitors traveling outside the basin are likely to consume fuel purchased from outside of the basin.

These results may be further scrutinized by examining the classifications of vehicle trips from the TRANPLAN model output. All trips in the basin are assigned one of 10 purposes (Table 6-2). The purposes designate the vehicle operator (resident or visitor). The description also defines the origin/destination of the trip. Home based means that the trip begins or ends at the residence or visitor housing. External means the trip begins or ends outside of the basin. Through means that the trip begins and ends outside of the basin. Non home based means that the trip is an intermediate trip within the basin but not originating at a residence.

Table 6-2. Traffic demand and forecasting model attribution of trips and VKT by trip purpose for base year 2003.

Trip Purpose	Abbreviation	VKT	Trips
Resident Home-Based Work	RHBW	173,350	26,337
Resident Home-Based Other	RHBO	389,157	71,662
Resident Home-Based Recreational	RHBR	92,637	12,955
Resident Non Home-Based	RNHB	326,721	70,879
Visitor Home-Based Other	VHBO	198,321	24,621
Visitor Home-Based Recreational	VHBR	270,666	22,368
Visitor Non Home-Based	VNHB	237,039	38,707
In-Basin Trips		**1,687,891**	**267,529**
Resident External	REXT	137,905	10,676
Visitor External	VEXT	921,689	60,100
Through Trips	THRU	119,478	4,201
Out of Basin Trips		**1,179,071**	**74,977**
All Trips	**TOTAL**	**2,866,963**	**342,506**

Drivers of trips that begin and end in the basin are likely to fill up their vehicles in the basin, whereas drivers leaving or entering the basin may have fuel their vehicles elsewhere. If this is the case, then the in-basin fuel sales may be estimated from the VKT associated with *In-Basin Trips*:

$$In-Basin\ Fuel\ Sales = \left(\frac{1687891\,\text{km}}{\text{day}}\right)\left(\frac{365\ day}{year}\right)\left(\frac{\text{liter}}{8.75\ km}\right)\left(\frac{0.67 kg}{liter}\right)\left(\frac{1 Mg}{1000 kg}\right)$$
$$= 47200 Mg\ \ fuel / year$$

This estimate is within 12% of the estimated annual fuels sales from the gas station survey and suggests that VKT and fuel sales data are in reasonable agreement and are suitable for use as activity factor for emission inventory calculations.

6.1.4 Annual Average Tahoe Basin Vehicle Exhaust Emissions

Vehicle exhaust emissions are calculated here using two approaches: VKT based emissions and fuel based emissions. CARB estimates on-road mobile source emissions for the counties and air basins within California using the EMFAC2002 model (http://www.arb.ca.gov/msei/on-road/on-road.htm). Mobile source emissions are available for the portions of El Dorado and Placer counties within the CARB Tahoe Air Basin (Figure 6-1).

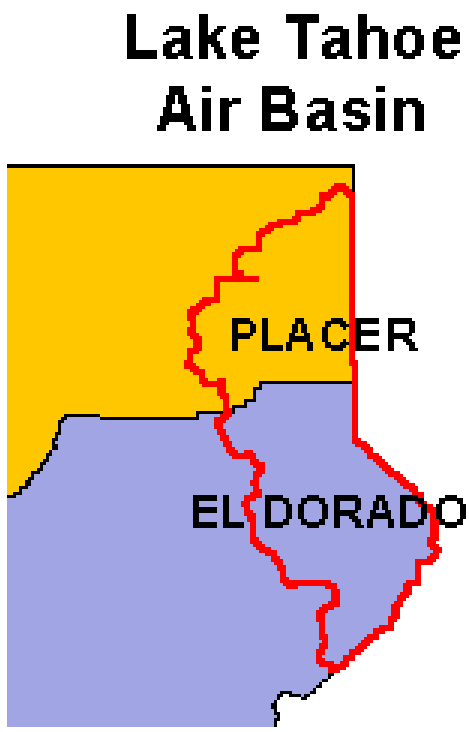

Figure 6-1. Map of Carb Tahoe Air Basin.

The EMFAC 2002 emissions for the CARB Tahoe Air Basin are presented in Table 6-3. Based on the census of registered vehicles, EMFAC also estimates the fuel consumption for both gasoline and diesel vehicles in the area. EMFAC's fleet average fuel economy (5.83 km/l [15.5 mpg]) is 25% lower than the DOE's national estimate (7.75 km/l [20.6 mpg]). The EMFAC data indicate that 21% of VKT in El Dorado is associated with medium duty vehicles (>8500 lbs and < 14000 lbs). For reference, Chevrolet Suburbans and Lincoln Navigators are classified as Light

Duty Trucks Tier 2 (LDT2), while AMC Hummers are classified as MDVs. Fitz and Lents (2003) also observed a large fraction MDV's in the Tahoe basin (22% in summer to 37% in winter). The shift of vehicle type by season is reasonable given that heavier duty 4 wheel drive vehicles are needed to navigate snowpacked roads in winter time. In comparison, the US Average fraction of VKT associated with MDV's is ~17% (EPA, 2003).

Basin wide emissions were estimated from the CARB EMFAC results by scaling the CARB Tahoe Air basin emissions with the VKT from the entire Tahoe Basin. These emissions assume that Nevada residents and visitors drive similar vehicles and trips as do the California residents and visitors to the lake. Distance based emission factors were calculated by dividing the total emissions from mobile sources by the VKT.

Table 6-3. Vehicle population, activity, and emissions for CARB Tahoe Air Basin and the entire Tahoe basin. Tahoe basin data are calculate by scaling all values with the basin wide VKT.

	CARB Tahoe Air Basin (CA only)	Tahoe Basin (CA + NV)	Emission Factor (g/km)
VKT per day	1887680	2866963	
Registered Vehicles	37036	56249*	
Trips per day	249979	379662*	
Gasoline Consumption (Mg/yr)	61620	93587*	
Diesel Consumption(Mg/yr)	6061	9205*	
Exhaust PM10 (Mg/Yr)	16	24*	0.023
Brake and Tire PM10 (Mg/Yr)	12	18*	0.017
NO (Mg/Yr)	1033	1568*	1.499
CO (Mg/Yr)	9649	14654*	14.004
TOG Exhaust (Mg/Yr)	616	935*	0.894
TOG Evap (Mg/Yr)	359	545*	0.521

*Extrapolated value based on basin wide VKT.

Alternatively, on-road vehicle exhaust emissions may be calculated by fuel consumption and emission factors measured in the basin as part of this study. The emission factors used in this calculation do not account for additional emissions related to vehicle cold starts. Cold start is defined as the period prior to the ignition of the catalytic converter (typically < 5 minutes). Remote sensing of vehicles in the Treasure Valley, Idaho indicated that wintertime cold start fuel based emission factors of CO, NO, HC, and PM may be 4 times or more higher than those during hot stabilized driving conditions (Kuhns et al., 2004). EMFAC exhaust modeling for the CARB Tahoe Air Basin attributed 26% of CO, 14% of NO, 43% of HC, and 0% of PM to cold start emissions.

Hot stabilized emission factors from Table 4-5 are shown for CO, NO, NH_3, HC, and PM0.59 in Table 6-4. Total annual emissions are estimated by multiplying these factors by the annual fuel consumption (80127 Mg/yr). Total emissions including cold start emissions are estimated by adding in the relative fraction of emissions associated with cold starts by the EMFAC model.

Table 6-4. Annual average basin-wide emissions based on fuel consumption and fuel-based emission factors.

Species	EF (g pollutant/kg fuel)	Emissions (Mg/yr)	Emissions with Cold Start (Mg/yr)
CO	23	1842	2489
NO	1.6	128	148
NH_3	0.35	28	28
HC (sum of propane and hexane)	3.0	240	421
$PM_{0.59} \approx PM_{2.5}$	0.083	6.7	6.7

6.2. Road Dust Emissions

Road dust emissions are estimated for summer and winter seasons using the TRAKER data. Emission factors are obtained from figures 5-4 and 5-5 for local, urban, and highway roads for both the winter and summer seasons. The distribution of VKT was estimated by Fitz and Lents (2003) as 15% residential/local, 55% arterial/urban, and 35% major arterial/highway. The authors also observed a 40% reduction in VKT during winter months with respect to summer months that are applied to the VKT. Annual emissions are calculated by assuming 182.5 days of summer and 182.5 days of winter. Seasonal VKT, PM_{10} emission factors, and basin wide emissions are presented in Table 6-5. Filter measurements downwind of the road at Sand Harbor indicate that ~15% to 30% of the PM_{10} road dust is $PM_{2.5}$.

Table 6-5. Basin wide VKT, road dust PM_{10} emission factors, and total road dust PM emissions.

Road Type	Winter VKT (1000 kms)	Summer VKT (1000 kms)	Winter PM_{10} EF (g/VKT)	Summer PM_{10} EF (g/VKT)	Winter PM_{10} Emissions (Mg/day)	Summer PM_{10} Emissions (Mg/day)	Annual PM_{10} Emissions (Mg/year)
Total	2150	3583	-	-	0.799	0.777	287
Local/ Residential	323	537	0.5	0.22	0.161	0.118	51
Arterial/Urban	1182	1970	0.33	0.22	0.390	0.433	150
Major Arterial/ Highway	752	1254	0.33	0.18	0.248	0.226	87

6.3. Wood Burning Emissions

Basin wide wood burning emissions were estimated by Fitz and Lents (2003) based on surveys of residents and campers and published PM emissions factors for residential wood combustion (Houck et al., 2001). Some inconsistencies were noted in the calculations by Fitz and Lents (2003). Some of these inconsistencies arose from the interpretation of incomplete surveys.

The survey data was revisited to calculate the number of days per week that respondents burned wood, the duration of wood burning, the number of logs burnt, and the number of cords stockpiled at the beginning of the season. The results of survey respondents that completed the activity survey and the values used by Fitz and Lents (2003) are reported in Table 6-6.

Table 6-6. Wood burning parameter inconsistencies between this study and Fitz and Lents (2004).

Term	Fitz and Lents (2003)	Proposed Value	Reference	Comment
Volume of a log	1 ft^3	0.27 ft^3		There is no standard definition of the volume of a log. The proposed value was calculated assuming a wood cylinder 2 ft long and 5 inches in diameter. A 1 ft^3 log would be 9.5 inches in diameter and 2 feet long.
Cord of wood	64 logs = 64 ft^3	80 ft^3 of solid wood	http://www.ca.uky.edu/agc/pubs/for/for35/for35.htm	A cord is defined as 4 ft x 4 ft x 8 ft = 128 ft^3. The solid wood content of a cord ranges from 100 ft^3 for a carefully stacked pile to 60 ft^3 for a loosely stacked pile.
Burns per week	7 days	3.8 days	CE-CERT Tahoe Wood Burning Survey	Most residents only burn wood on the weekend and evenings. This factor was not considered by Fitz and Lents (2003).
Hours per burn	5.9 hours	4.9 hours	CE-CERT Tahoe Wood Burning Survey	Using only data from respondents that completed the activity portion of survey. Fitz and Lents (2003) used all valid responses to this one question.
Logs per burn	7.4 logs	8.9 logs	CE-CERT Tahoe Wood Burning Survey	Using only data from respondents that completed the activity portion of survey.
Stockpiled Cords	1.7 cords per residence	1.7 cords per residence	CE-CERT Tahoe Wood Burning Survey	Using only data from respondents that answered stockpile question.
Wintertime burn rate based on logs per day	2556 Mg wood/day	450 Mg wood/day		Assuming wood density of 16.45 kg/ft^3, 21000 residences in basin.
Wintertime burn rate based on 1.7 cords burnt over 120 days.		391 Mg wood/day		Assuming wood density of 16.45 kg/ft^3, 21000 residences in basin, and all wood burned over 120 days in winter.

Term	Fitz and Lents (2003)	Proposed Value	Reference	Comment
Summertime burn rate	110 Mg wood/day	29 Mg wood/day		Assuming wood density of 17.13 kg/ft^3, 1567 campfires per day, and 4 logs per fire.

These basin wide emissions from campfires and residential wood combustion are calculated here along with the gas emissions of NO, NH_3, CO, and HC (total non methane organic carbon) using a combination of emission factors from this study and the published literature. For the purpose of calculating annual emissions, the winter burning season is assumed to last 4 months (December through March ~120 days) and the summer season is assumed to last 3 months (June through August ~90 days).

Table 6-7. Emissions for the Tahoe basin from wintertime residential wood combustion and summertime campfires.

Species	Emission Factor (g/kg)	Emission Factor Reference	Winter Residential Wood Combustion Emissions (Mg/day)	Summer Campfires Emissions (Mg/day)	Annual Emissions (Mg/Yr)
Wood Consumption			450	29	56000
PM_{10} Emissions	12	Houck (2001)	5.4	0.35	680
NO_x Emissions	2.9	This Study	1.3	0.084	187
CO Emissions	110	This Study	50	3.9	6400
Ammonia Emissions	1.2	This Study	0.54	0.035	68
Total Non Methane Organic Carbon	10	AP-42 (1.10-4)	4.5	0.29	570

6.4. Additional Sources

For reference, CARB estimates emissions from other sources in the CARB Lake Tahoe Basin (http://www.arb.ca.gov/ei/maps/basins/abltmap.htm). The methodologies and base data are describe in detail on the CARB webpage. The CARB emissions inventory is shown with units of Mg/yr in Table 6-8 through Table 6-11.

Table 6-8. CARB Stationary Source Emission Inventory for CARB Tahoe Air Basin (i.e. portions of El Dorado and Placer counties). The base year of the inventory is 2003. All emission units are in Mg/yr.

STATIONARY SOURCES	TOG	ROG	CO	NOX	SOX	PM	PM10	PM2.5
FUEL COMBUSTION								
MANUFACTURING AND INDUSTRIAL	0.0	0.0	0.0	9.9	0.0	0.0	0.0	0.0
SERVICE AND COMMERCIAL	3.3	0.0	6.6	29.6	0.0	3.3	3.3	3.3
OTHER (FUEL COMBUSTION)	0.0	0.0	3.3	6.6	-	0.0	0.0	0.0
*** TOTAL FUEL COMBUSTION**	3.3	3.3	9.9	49.3	0.0	3.3	3.3	3.3
WASTE DISPOSAL	0.0	0.0	0.0	0.0	0.0	0.0	0.0	0.0
SEWAGE TREATMENT	39.4	6.6	19.7	13.1	3.3	0.0	0.0	0.0
*** TOTAL WASTE DISPOSAL**	39.4	6.6	19.7	13.1	3.3	0.0	0.0	0.0
CLEANING AND SURFACE COATINGS								
LAUNDERING	3.3	0.0	-	-	-	-	-	-
DEGREASING	42.7	29.6	-	-	-	-	-	-
COATINGS AND RELATED PROCESS SOLVENTS	118.3	115.0	-	-	-	-	-	-
ADHESIVES AND SEALANTS	19.7	19.7	-	-	-	-	-	-
*** TOTAL CLEANING AND SURFACE COATINGS**	184.0	161.0	-	-	-	-	-	-
PETROLEUM PRODUCTION AND MARKETING	0.0	0.0	0.0	0.0	0.0	0.0	0.0	0.0
PETROLEUM MARKETING	88.7	26.3	-	-	-	-	-	-
*** TOTAL PETROLEUM PRODUCTION AND MARKETING**	88.7	26.3	-	-	-	-	-	-
INDUSTRIAL PROCESSES								
MINERAL PROCESSES	-	-	3.3	0.0	0.0	3.3	0.0	0.0
*** TOTAL INDUSTRIAL PROCESSES**	-	-	3.3	0.0	0.0	3.3	0.0	0.0
**** TOTAL STATIONARY SOURCES**	315.4	193.8	32.9	62.4	3.3	6.6	3.3	3.3

Table 6-9. . CARB Area Source Emission Inventory for CARB Tahoe Air Basin (i.e. portions of El Dorado and Placer counties). The base year of the inventory is 2003. All emission units are in Mg/yr.

AREA-WIDE SOURCES	TOG	ROG	CO	NOX	SOX	PM	PM10	PM2.5
SOLVENT EVAPORATION								
CONSUMER PRODUCTS	144.5	121.5	-	-	-	-	-	-
ARCHITECTURAL COATINGS AND RELATED PROCESS SOLVENTS	55.8	55.8	-	-	-	-	-	-
PESTICIDES/FERTILIZERS	3.3	3.3	-	-	-	-	-	-
ASPHALT PAVING / ROOFING	115.0	115.0	-	-	-	-	-	-
*** TOTAL SOLVENT EVAPORATION**	**321.9**	**295.7**	-	-	-	-	-	-
MISCELLANEOUS PROCESSES								
RESIDENTIAL FUEL COMBUSTION	896.8	394.2	3774.5	105.1	16.4	620.9	581.4	558.5
FARMING OPERATIONS	298.9	23.0	-	-	-	46.0	19.7	3.3
CONSTRUCTION AND DEMOLITION	-	-	-	-	-	279.2	134.7	29.6
PAVED ROAD DUST	-	-	-	-	-	689.9	315.4	52.6
UNPAVED ROAD DUST	-	-	-	-	-	749.0	446.8	95.3
FUGITIVE WINDBLOWN DUST	-	-	-	-	-	13.1	6.6	3.3
FIRES	0.0	0.0	3.3	-	-	0.0	0.0	0.0
WASTE BURNING AND DISPOSAL	154.4	69.0	887.0	23.0	3.3	101.8	98.6	92.0
COOKING	3.3	3.3	-	-	-	13.1	9.9	6.6
*** TOTAL MISCELLANEOUS PROCESSES**	**1356.7**	**492.8**	**4664.7**	**128.1**	**19.7**	**2509.7**	**1612.9**	**841.0**
**** TOTAL AREA-WIDE SOURCES**	**1678.6**	**788.4**	**4664.7**	**128.1**	**19.7**	**2509.7**	**1612.9**	**841.0**

Table 6-10. CARB Mobile Source Emission Inventory for CARB Tahoe Air Basin (i.e. portions of El Dorado and Placer counties). The base year of the inventory is 2003. All emission units are in Mg/yr.

MOBILE SOURCES	TOG	ROG	CO	NOX	SOX	PM	PM10	PM2.5
ON-ROAD MOTOR VEHICLES								
LIGHT DUTY PASSENGER (LDA)	230.0	216.8	1783.8	128.1	0.0	3.3	3.3	3.3
LIGHT DUTY TRUCKS - 1 (LDT1)	157.7	144.5	1747.6	115.0	0.0	3.3	3.3	0.0
LIGHT DUTY TRUCKS - 2 (LDT2)	111.7	101.8	1149.8	134.7	0.0	3.3	3.3	3.3
MEDIUM DUTY TRUCKS (MDV)	157.7	144.5	1609.7	190.5	0.0	3.3	3.3	3.3
LIGHT HEAVY DUTY GAS TRUCKS - 1 (LHDV1)	52.6	49.3	420.5	19.7	-	-	-	-
LIGHT HEAVY DUTY GAS TRUCKS - 2 (LHDV2)	6.6	6.6	52.6	3.3	-	-	-	-
MEDIUM HEAVY DUTY GAS TRUCKS (MHDV)	16.4	16.4	164.3	9.9	-	-	-	-
HEAVY HEAVY DUTY GAS TRUCKS (HHDV)	13.1	13.1	233.2	23.0	-	-	-	-
LIGHT HEAVY DUTY DIESEL TRUCKS - 1 (LHDV1)	0.0	0.0	3.3	16.4	-	-	-	-
LIGHT HEAVY DUTY DIESEL TRUCKS - 2 (LHDV2)	0.0	0.0	3.3	9.9	-	-	-	-
MEDIUM HEAVY DUTY DIESEL TRUCKS (MHDV)	3.3	0.0	9.9	52.6	0.0	0.0	0.0	0.0
HEAVY HEAVY DUTY DIESEL TRUCKS (HHDV)	6.6	6.6	23.0	115.0	0.0	3.3	3.3	3.3
MOTORCYCLES (MCY)	16.4	16.4	98.6	3.3	-	-	-	-
HEAVY DUTY DIESEL URBAN BUSES (UB)	0.0	0.0	3.3	19.7	-	0.0	0.0	0.0
HEAVY DUTY GAS URBAN BUSES (UB)	13.1	9.9	161.0	6.6	-	-	-	-
SCHOOL BUSES (SB)	0.0	0.0	6.6	6.6	-	0.0	0.0	0.0
MOTOR HOMES (MH)	9.9	6.6	325.2	9.9	-	-	-	-
*** TOTAL ON-ROAD MOTOR VEHICLES**	**798.3**	**732.6**	**7798.6**	**864.0**	**3.3**	**19.7**	**19.7**	**13.1**
OTHER MOBILE SOURCES								
AIRCRAFT	85.4	75.6	762.1	55.8	9.9	26.3	23.0	23.0
RECREATIONAL BOATS	262.8	243.1	1908.6	78.8	0.0	16.4	13.1	9.9
OFF-ROAD RECREATIONAL VEHICLES	417.2	384.3	1337.0	26.3	0.0	0.0	0.0	0.0
OFF-ROAD EQUIPMENT	184.0	167.5	1356.7	459.9	0.0	32.9	32.9	29.6
FARM EQUIPMENT	-	-	-	-	-	-	-	-
FUEL STORAGE AND HANDLING	42.7	42.7	-	-	-	-	-	-
*** TOTAL OTHER MOBILE SOURCES**	**988.8**	**913.2**	**5361.1**	**624.2**	**9.9**	**75.6**	**72.3**	**65.7**
**** TOTAL MOBILE SOURCES**	**1787.0**	**1645.8**	**13159.7**	**1488.1**	**16.4**	**92.0**	**88.7**	**75.6**

Table 6-11. CARB Natural Source Emission Inventory for CARB Tahoe Air Basin (i.e. portions of El Dorado and Placer counties). The base year of the inventory is 2003. All emission units are in Mg/yr.

NATURAL (NON-ANTHROPOGENIC) SOURCES	TOG	ROG	CO	NOX	SOX	PM	PM10	PM2.5
NATURAL SOURCES								
WILDFIRES	0.0	0.0	19.7	0.0	-	3.3	3.3	3.3
*** TOTAL NATURAL SOURCES**	**0.0**	**0.0**	**19.7**	**0.0**	-	**3.3**	**3.3**	**3.3**

6.5. Emissions Summary

Annualized basin wide emissions for on-road motor vehicle exhaust, paved road dust, residential wood combustion, and campfires are summarized in Table 6-12. The data are compared with the CARB emissions presented in Table 6-8 through Table 6-11. Mobile sources from the CARB Tahoe Air Basin EI were scaled to the entire Lake Tahoe Basin using the ratio of VKT tfor the entire basin o the California Tahoe VKT: 1.52 (Table 6-3). Residential wood combustion emissions from the CARB EI were scaled to the entire basin using the ratio of population in the entire basin in 2000 (61500 people) to the population of the CARB Tahoe Air Basin (46700 people): 1.31.

Table 6-12. Comparison of annual emissions estimated from this study with scaled emissions from the CARB Tahoe Air Basin.

Source Type	Data Source	PM10 (Mg/Yr)	NO (Mg/Yr)	CO (Mg/Yr)	Total Organic Gasses (TOG) (Mg/Yr)	NH3 (Mg/yr)
Exhaust including Cold Start	CARB (EMFAC)	24	1568	14654	935	
Exhaust including Cold Start	This Study	6.7	148	2489	421	28
Paved Road Dust	CARB (EMFAC)	479				
Paved Road Dust	This Study	287				
Residential Wood Combustion and Campfires	CARB	761	138	4944	1174	
Residential Wood Combustion and Campfires	This Study	680	187	6400	570	68

Motor vehicles emissions estimated by EMFAC 2002 are consistently larger than those directly measured from the vehicle fleet in Lake Tahoe. The source of this discrepancy may be attributable to several factors:

- The emission factors from EMFAC may represent an older vehicle fleet that is representative of the entire state of California whereas the fleet operating in Incline Village, NV may be newer and therefore have lower emissions.

- The default fleet used by EMFAC is composed of ~1/3 medium duty vehicles (MDVs). Diesel engines are the preferred power source for larger vehicles since they are less expensive to refuel. Based on visual observations on Tahoe roadways, the fraction of vehicles that are MDVs appears to be lower <5% when compared to the CARB fleet distribution.
- Because of their size, MDV's have a lower fuel economy than do LDVs. The EMFAC model assumes that more fuel is needed to operate LDV's and given the same fuel based emission factors, the EMFAC model will simulate higher emissions for the same VKT.

PM_{10} emissions from paved road dust are in reasonable agreement with the EMFAC results. The TRAKER/Tower measurement based emissions are ~40% less than those caclculated with EMFAC. Emissions from residential wood combustion are also in good agreement with the CARB estimates.

Using the emissions from this study combined with the emission inventory for the CARB Tahoe Air Basin, a basin wide emission inventory has been assembled. Emissions from Table 6-12 of on-road vehicle exhaust, paved road dust, residential wood combustion, and campfires were used directly. CARB Tahoe Air Basin emissions were scaled by a factor of 1.5 (ratio of basin land area to CARB Tahoe Air Basin area) for natural land based source, by 1.52 (ratio of VKT) for on-road mobile sources, and by 1.31 (ratio of population) for all other anthropogenic sources. The resulting inventory is shown in Table 6-13 and are summarized with pie charts in Figure 6-2 through Figure 6-5. Particulate matter emissions are dominated by residential wood combustion and unpaved road dust. Unpaved road emissions deserve additional scrutiny since they are likely to be negligible during wintertime. Nitrogen oxide emissions are dominated by off-road vehicles 68% and diesel construction and mining equipment in particular. This source also deserves additional investigation since Tahoe's construction is limited due to growth restrictions. The largest sources of carbon monoxide emissions are residential wood combustion, on road vehicles, and recreational boats. Total organic gases (TOG) are emitted primarily by on-road mobile sources, residential wood combustion, campfires, and off road recreational vehicles (i.e. snowmobiles and ATVs).

Table 6-13. Emission Inventory for Tahoe Basin. Emissions are estimated by scaling the CARB Tahoe Air Basin emissions with a multiplier based on land area, population, or VKT. Sources marked with an asterisk (*) were measured as part of this study. All emissions are presented with units of Mg/yr.

	Multiplier Basis	Multiplier	TOG	ROG	CO	NO_X	PM	PM_{10}	$PM_{2.5}$
NATURAL (NON-ANTHROPOGENIC) SOURCES	Approximate Land Area	1.5	0	0	30	0	5	5	5
ON ROAD MOBILE SOURCES*	***Measured***	1	1019	935	2489	148	7	7	4
AIRCRAFT	Population	1.31	112	99	998	73	34	30	30
RECREATIONAL BOATS	Population	1.31	344	318	2500	103	22	17	13
OFF-ROAD RECREATIONAL VEHICLES	Population	1.31	547	503	1751	34	0	0	0
OFF-ROAD EQUIPMENT	Population	1.31	241	219	1777	602	43	43	39
FUEL STORAGE AND HANDLING	Population	1.31	56	56					
RESIDENTIAL WOOD COMBUSTION AND CAMPFIRES*	***Measured***	1	570	251	6400	187	726	680	653
FARMING OPERATIONS	Population	1.31	392	30			60	26	4
CONSTRUCTION AND DEMOLITION	Population	1.31					366	176	39
PAVED ROAD DUST*	***Measured***	1					628	287	48
UNPAVED ROAD DUST	VKT	1.52					1138	679	145
FUGITIVE WINDBLOWN DUST	Population	1.31					17	9	4
WASTE BURNING AND DISPOSAL	Population	1.31	202	90	1162	30	133	129	120
COOKING	Population	1.31	4	4			17	13	9
SOLVENT EVAPORATION	Population	1.31	422	387					
STATIONARY SOURCES	Population	1.31	413	254	43	82	9	4	4
TOTAL			**4321**	**3148**	**17151**	**1260**	**3206**	**2105**	**1118**

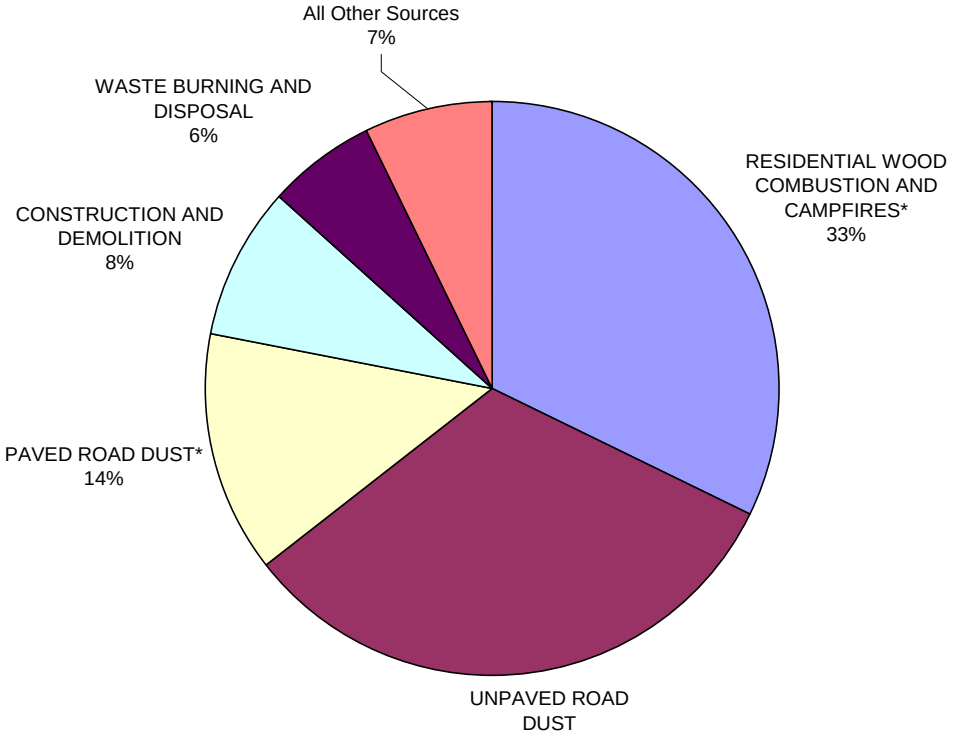

Figure 6-2. Distribution of estimated PM10 emission sources in the Lake Tahoe Basin. The asterisk (*) denotes that the emissions from this source were measured in this study.

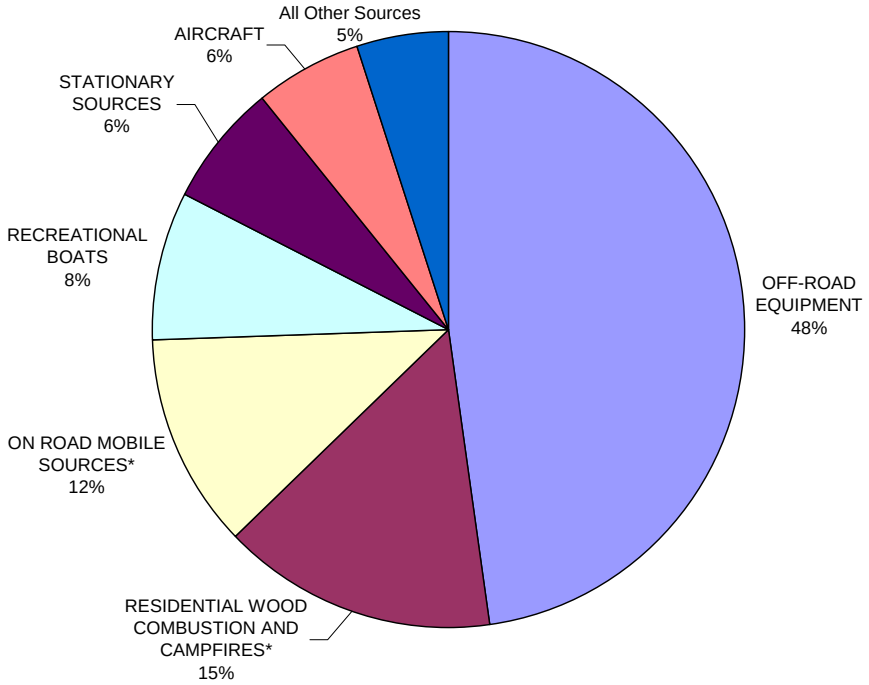

Figure 6-3. Distribution of estimated NO_x emission sources in the Lake Tahoe Basin. The asterisk (*) denotes that the emissions from this source were measured in this study.

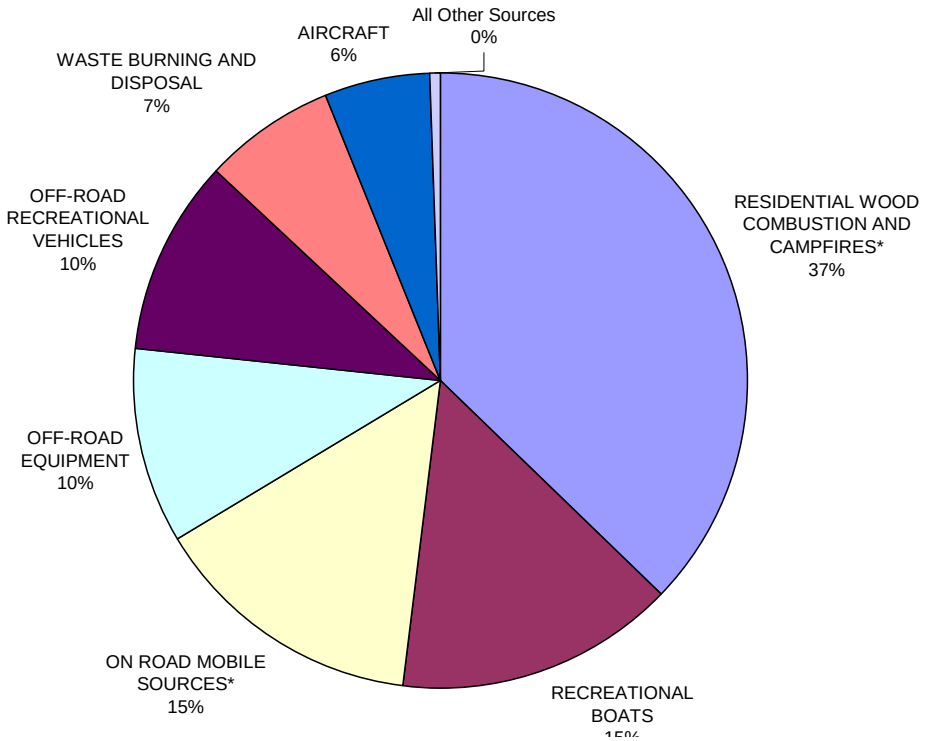

Figure 6-4. Distribution of estimated CO emission sources in the Lake Tahoe Basin. The asterisk (*) denotes that the emissions from this source were measured in this study.

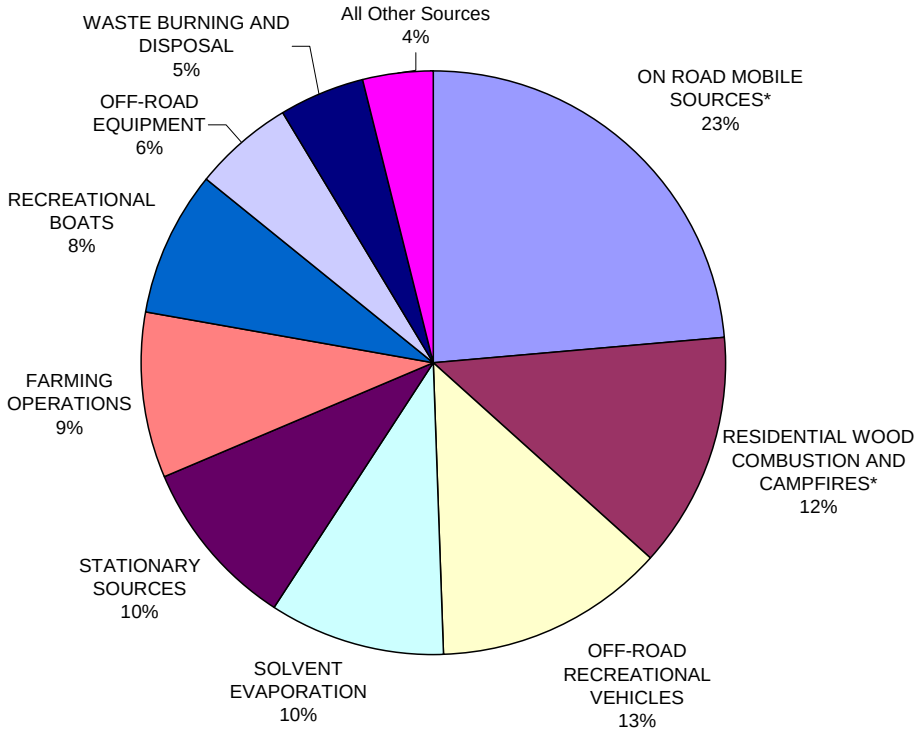

Figure 6-5. Distribution of estimated TOG emission sources in the Lake Tahoe Basin. The asterisk (*) denotes that the emissions from this source were measured in this study.

7. SUMMARY AND CONCLUSIONS

PM samples directly relevant to major PM sources in Lake Tahoe were collected and analyzed as part of this study. Sources sampled included RWC, motor vehicle exhaust, and entrainment of road dust, traction control material, and road deicing material.

In addition, several new emission measurement technologies were applied during this study. A portable emission test stand measured both gases and particles at 1 s resolution from RWC appliances and on-road motor vehicles. Measurements of plume concentrations were used to determine fuel-based emission factors based on the ratio of pollutant concentrations to CO_2, CO, and hydrocarbons. A background subtraction technique was applied to fast-response PM measurements to estimate the fraction of PM emitted by a source and collected on a filter.

A tower instrumented with fast-response PM monitors was erected downwind of a highway. The flux of particles past the tower was related to the number of vehicles traveling on the road to calculate a vehicle and distance-based emission factor for typical wintertime, post-storm, post-street sweeping, and post-deicing conditions.

An onboard road dust sampling system was operated on more than 2000 km of paved road in the Lake Tahoe Basin. The instrumented vehicle was operated on fixed routes around the lake and over Mt. Rose Pass to monitor the change in road dust emission factors between winter and summer. Onboard measurements were also related to the flux of PM downwind of the road to provide the first paved road calibration point for the mobile system. This data set permitted the extrapolation of fleet average emission factors to all areas surveyed by the mobile system.

The results of the study are summarized here in bullet form:

7.1. Source Profiles

- The major chemical components of wood-burning PM emissions are OC and EC. TC accounts for 15% to 74 % of $PM_{2.5}$ mass.
- TC emissions to $PM_{2.5}$ mass from hardwood are generally higher than from softwood, and higher from fireplaces than from woodstoves. These observations are consistent with NFRAQS (1996-1997).
- Crustal elements were found with high variability, probably contributed from ambient background during sample collection. NH_3 gas emission from residential wood combustion is substantial—close to 5% of $PM_{2.5}$ mass.
- Both in-plume sampling and roadside measurements of PM emitted by the passage of motor vehicles indicated that from 40% to 90% of PM mass emissions are composed of road dust.
- Road dust is predominantly composed of Si, Al, and Fe. The OC fraction of road dust decreased from 24% to 4% over a period of less than one month with moderate precipitation. Given the magnitude of road dust emissions with respect to motor vehicle exhaust, road dust may be the dominant source of coarse OC PM.
- The application of brine solution as a deicer on the roads produced downwind source profiles that were enriched with both sodium (21%) and chloride (22%).

- Motor vehicle exhaust was composed of OC (54%) and EC (15%), resulting in an EC to TC ratio of 0.23. This is approximately a factor of 2 higher than the ratio observed in wood smoke.
- Higher ratios of EC to TC from residential wood combustion range from 0.05 to 0.17, but are lower than from motor vehicle exhaust, which ranges from 0.21 to 0.25. EC/TC ratio can probably be used as marker to distinguish emissions from residential wood combustion and motor vehicle exhaust.
- In comparing the OC1-4 from residential wood combustion and motor vehicle exhaust, OC1 dominates in residential wood combustion and OC3 in motor vehicle exhaust. These distinguishing carbon fraction properties from wood fuel and motor fuels can be used for source apportionment study.

7.2. Emission Factors

- Emission factors of CO_2 and CO calculated from the In-Plume Sampling System in the field shows good agreement with those in AP 42 developed from the laboratory.
- Higher emission factors of NO_x and SO_x are observed from the In-Plume Sampling System, compared with AP 42; PM had wide ranges of emission factors.
- Emission factors for RWC are affected by burning rate, types of wood fuels and wood heaters, moisture content in wood fuels, owner practice, meteorological conditions when the plumes form, and maintenance of appliances.
- Measured motor vehicle exhaust fuel-based emission factors were compared with published values. Fleet average emissions of CO (23 g/kg fuel) and NO (1.6 g/kg fuel) were lower than recent remote sensing and tunnel studies by a factor of 3 or more.
- Diesel emissions in many urban areas can dominate the emissions of fine PM. Evaluation of video tapes and road tube counter data indicated that only ~1–3% of the fleet on local streets in Incline Village and on Highway 28 are heavy duty diesel vehicles (HDDV). In comparison, 4% of the VKT in Las Vegas is from HDDV.
- Both NH_3 (0.35 g/kg fuel) and $PM_{0.59}$ (0.083 g/kg fuel) emission factors were in good agreement with results from other studies.
- Around the lake, road dust emissions varied by a factor of 3, from 0.5 g/vkt in early April to 0.17 g/vkt in mid-July. These reductions were associated with a decrease in precipitation, as well as a reduction in mud track-out onto roads and/or a cessation of the application of traction control material.

7.3. Emission Inventory

- A business survey identified 17 gas stations in the basin selling at total of 53,600 Mg gasoline/year. The fuel sales were multiplied by the fuel-based emission factors to estimate annual of CO, NO, NH_3, and $PM_{0.59}$ as 1200 Mg/yr, 19 Mg/yr, 86 Mg/yr, and 4.4 Mg/yr, respectively. These estimates do not include contributions from cold starts, diesel vehicles, or fuel purchased outside of the basin.
- Measurements of road dust emission factors with the TRAKER vehicle consistently showed ~20%–30% higher PM emission factors in California than in Nevada. Road dust emission factors from South Lake Tahoe, CA, and Incline Village, NV, were nearly equivalent. The largest emission factors were observed at the entrance to subdivisions and neighborhoods. Differences in road maintenance practices based on jurisdiction may account for the variation in emission factors.
- Emission data from CARB's Lake Tahoe Air Basin was scale to the entire basin using VKT, population, and land area as surrogates. Measured emissions from motor vehicle exhaust, residential wood combustion, campfires, and paved road dust were substituted into the basinwide inventory. Motor vehicle exhaust based on the EMFAC model was between 2 and 10 times larger than the measured emission factors.
- Particulate matter emissions are dominated by residential wood combustion and unpaved road dust. Unpaved road dust was not measured as part of this study and may be considerably lower than these estimates since wintertime emissions should be negligible.
- Nitrogen oxide emissions are dominated by off-road vehicles and diesel construction and mining equipment in particular. This source also deserves additional investigation since Tahoe's construction is limited due to growth restrictions.
- The largest sources of carbon monoxide emissions are residential wood combustion, on road vehicles, and recreational boats.
- Total organic gases (TOG) are emitted primarily by on-road mobile sources, residential wood combustion, campfires, and off road recreational vehicles (i.e. snowmobiles and ATVs).

8. RECOMMENDATIONS

The recommendations derived from this project are as follows:

- Large spatial differences were observed in road dust emissions across roads of different management jurisdictions. A consistent road maintenance strategy is needed to contain traction control material at the place of application.
- Annual activity data currently exists for VKT, traction control material application (and collection for some districts), and hotel occupancy rates. A central repository is needed to monitor these activity indicators in order to evaluate annual trends and year-to-year variability.
- The activity data collected as part of CE-CERT and DRI emission projects need to be routinely updated to monitor emission trends in the basin. Annual updates should be collected for residential wood burning surveys, firewood sales from vendors, and fuel sales from gas stations.
- Fuel characteristics can greatly affect emissions from RWC. Future wood burning surveys should include a measurement of fuel moisture content and an updated summary of wood fuel species. Wood species should be compared for the types of burning appliances within the Tahoe Basin.
- Motor vehicle emission factors from the Tahoe Basin are generally lower than what is estimated with the EMFAC model. The affluence of the visitors and residents of the area likely means that they operate newer and better-maintained vehicles as compared with other areas. Accurate exhaust emission estimation with either EMFAC or MOBILE models will require fleet-specific data, including model year and vehicle classification. A study to read and cross-reference license plates with state DMVs would improve motor vehicle exhaust emission estimation.
- As newer and cleaner vehicles are introduced to the on-road fleet, a need exists to accurately estimate the in-use fleet average emissions. These data need to be reconciled with emission factor model output to ensure consistency. Fleet average emissions should be monitored on a five-year cycle.
- Road dust emissions appear to be highly variable, ranging over a factor of 3 over a four-month period. Improved measurements are needed to more accurately relate dust emissions to vehicle speed, traffic volume, precipitation, and control strategies such as installation of curbs and gutters, paved shoulders, and routine sweeping practices, as well as in different weather conditions and seasons.
- Potentially large emission sources that are not well estimated with local data include: *unpaved road dust, construction equipment, snowmobiles, recreational boats, wildland and prescribed fires, and lawn and garden equipment*. Locally collected activity data are needed to better estimate the relative contribution of these sources to lake clarity impairment.
- Emission inventories are useful indicators for monitoring trends that may affect lake clarity. They also serve as input to air quality models to simulate the behavior of pollution under various meteorological conditions. A critical mechanism that is not well-simulated by the models nor verified with measurements is the deposition of PM to vegetated canopies. Quantifying this process will be necessary to accurately simulate the deposition of airborne PM in the Tahoe Basin.

9. REFERENCES

Allen, J.O., P.R. Mayo, L.S. Hughes, L.G. Salmon, and G.R. Cass (2001). "Emissions of size-segregated aerosols from on-road vehicles in the Caldecott Tunnel." Environmental Science & Technology **35**(21): 4189-4197.

Barnett, S.G. (1991) "In-Home Evaluation of Emissions From Masonry Fireplaces and Heaters," OMNI Environmental Services, Inc., Beaverton, OR, September.

Baum, M.M., E.S. Kiyomiya, S. Kumar, A.M. Lappas, V.A. Kapinus and H.C. Lord, III (2001). "Multicomponent remote sensing of vehicle exhaust by dispersive absorption spectroscopy–2. Direct on-road ammonia measurements." Environmental Science & Technology **35**(18): 3735-3741.

Baum, M.M., E.S. Kiyomiya, S. Kumar, A.M. Lappas and H.C. Lord, III (2000). "Multicomponent remote sensing of vehicle exhaust by dispersive absorption spectroscopy–1. Effect of fuel type and catalyst performance." Environmental Science & Technology **34**(13): 2851-2858.

Board, C.A.R. (2001). Mobile Source Emission Inventory Program: EMFAC2000. Sacramento, CA, California Air Resources Board, Planning and Technical Support Division.

Brown, J.E., M.J. Clayton, D.B. Harris and F.G. King, Jr. (2000). "Comparison of particle size distribution of heavy duty diesel exhaust using a dilution tailpipe sampler and an in-plume sampler during on-road operations." Journal of the Air & Waste Management Association **50**(8): 1407-1416.

Cadle, S.H., P. Mulawa, E.C. Hunsanger, K. Nelson, R.A. Ragazzi, R. Barrett, G.L. Gallagher, D.R. Lawson, K.T. Knapp and R. Snow (1998). Light-duty motor vehicle exhaust particulate matter measurement in the Denver, Colorado area. Proceedings, $PM_{2.5}$: A Fine Particle Standard. J.C. Chow and P. Koutrakis. Pittsburgh, PA, Air & Waste Management Association**:** 539-558.

Cadle, S.H., P.A. Mulawa, E.C. Hunsanger, K. Nelson, R.A. Ragazzi, R. Barrett, G.L. Gallagher, D.R. Lawson, K.T. Knapp and R. Snow (1999). "Composition of light-duty motor vehicle exhaust particulate matter in the Denver, Colorado area." Environmental Science & Technology **33**(14): 2328-2339.

Cahill, T.A., L.L. Ashbaugh, R.A. Eldred, P.J. Feeney, B.H. Kusko and R.G. Flocchini (1981). Comparisons between size-segregated resuspended soil samples and ambient aerosols in the western United States Atmospheric Aerosol: Source/Air Quality Relationships. E.S. Macias and P.K. Hopke. Washington, DC, American Chemical Society**:** 269-285.

Chow, J.C., C.A. Frazier and J.G. Watson (1988). A survey of existing fugitive/area source characterization methods for receptor modeling. Proceedings, Particulate Matter/Fugitive

Dusts: Measurements and Control in Western Arid Regions G. F. Hoffnagle and M. Lebowitz. Pittsburgh, PA, Air Pollution Control Association**:** 176-189.

Chow, J.C., J.G. Watson, H.D. Kuhns, V. Etyemezian, D.H. Lowenthal, D.J. Crow, S.D. Kohl, J.P. Engelbrecht, and M.C. Green (2004). "Source profiles for industrial, mobile, and area sources in the Big Bend Regional Aerosol Visibility and Observational (BRAVO) Study." Chemosphere **54**(2): 185–208.

Chow, J.C., J.G. Watson, D. Crow, D.H. Lowenthal, and T. Merrifield (2001). Comparison of IMPROVE and NIOSH carbon measurement. Aerosol Science & Technology **34**: 23-34.

Chow J.C.; J.G. Watson, R.W. Wiener (2003). Method No. 508: $PM_{2.5}$ sampling and gravimetric analysis by Federal Reference Method. Air & Waste Management Association, accepted.

Chow, J.C., J.G. Watson, M.C. Green, D.H. Lowenthal, B.A. Bates, W. Oslund, G. Torres (2000). "Cross-border transport and spatial variability of suspended particles in Mexicali and California's Imperial Valley." Atmospheric Environment **34**(11): 1833–1843.

Chow, J.C.; J.G. Watson, L.C. Pritchett, W.R. Pierson, C.A. Frazier, and R.G. Purcell (1993). The DRI thermal/optical reflectance carbon analysis system: Description, evaluation, and application in U.S. air quality studies. Atmospheric Environment **27A:** 1185-1201.

Compilation of Air Pollutant Emission Factors, Fifth Edition. Volume I: Stationary Point and Area Sources, AP-42 Supplement B, GPO S/N 055-000-00565-6, November 1996. (Can be accessed through the web site http://www.epa.gov/ttn/chief/ap42etc.html).

Dreher, D. B. and R. A. Harley (1998). "A fuel-based inventory for heavy-duty diesel truck emissions." Journal of the Air & Waste Management Association **48**(4): 352-358.

Etyemezian, V., H. Kuhns, J. Gillies, M. Green, M. Pitchford and J. Watson (2003). "Vehicle-based road dust emission measurement: I - methods and calibration." Atmospheric Environment **37**(32): 4559-4571.

Fitz, Dennis and J. Lentz. Improvement of the PM Emission Inventory for the Lake Tahoe Region. September 2003 CE-CERT report to California Air Resource Board (0004-AP-ARB-01).

Fraser, M.P., G.R. Cass and B.R.T. Simoneit (1998). "Gas-phase and particle-phase organic compounds emitted from motor vehicle traffic in a Los Angeles roadway tunnel." Environmental Science & Technology **32**(14): 2051-2060.

Fraser, M. P. and G. R. Cass (1998). "Detection of excess ammonia emissions from in-use vehicles and the implications for fine particle control." Environmental Science & Technology **32**(8): 1053-1057.

Fujita, E.M., J.G. Watson, J.C. Chow, N.F. Robinson, L.W. Richards and N. Kumar (1998). Northern Front Range Air Quality Study. Volume C: Source apportionment and simulation methods and evaluation Reno, NV, Desert Research Institute.

Gillies, J.A. and A.W. Gertler, A.W. (2000). "Comparison and evaluation of chemically speciated mobile source $PM_{2.5}$ profiles." Journal of the Air & Waste Management Association **50**(8): 1459–1480.

Gillies, J.A., J.G. Watson, C.F. Rogers, D.W. DuBois, J.C. Chow, R. Langston and J. Sweet (1999). "Long term efficiencies of dust suppressants to reduce PM_{10} emissions from unpaved roads." Journal of the Air & Waste Management Association **49**(1): 3-16.

Houck J..J. Crouch, and R. Huntley (2001) Review of Wood Heater and Fireplace Emission Factors. http://www.epa.gov/ttn/chief/conference/ei10/pm/houck.pdf

Houck, J.E., Tiegs, P.E., Crouch, J., Keithly, C. (1998). "The PM_{10} reduction potential of new technology home heating appliances and fuels." In Proceedings, $PM_{2.5}$: A Fine Particle Standard; Chow, J.C. and Koutrakis, P., Eds.; Air & Waste Management Association: Pittsburgh, PA, pp. 1032–1043.

Houck, J.E. and Tiegs, P.E., Residential Wood Combustion Technology Review Volume 1. Technical Report, EPA-600/R-98-174a, December 1998.

Huai, T., T.D. Durbin, J.W. Miller, J.T. Pisano, C.G. Sauer, S.H. Rhee and J.M. Norbeck (2003). "Investigation of NH3 emissions from new technology vehicles as a function of vehicle operating conditions." Environmental Science & Technology **37**(21): 4841-4847.

Jimenez, J.L., J.B. McManus, J.H. Shorter, D.D. Nelson, M.S. Zahniser, M. Koplow, G.J. McRae and C.E. Kolb (2000). "Cross road and mobile tunable infrared laser measurements of nitrous oxide emissions from motor vehicles." Chemosphere—Global Change Science **2**(3-4): 397-412.

Kirchstetter, T.W., R.A. Harley, N.M. Kreisberg, M.R. Stolzenburg and S.V. Hering (1999). "On-road measurement of fine particle and nitrogen oxide emissions from light- and heavy-duty motor vehicles." Atmospheric Environment **33**(18): 2955-2968.

Kittelson, D.B., D.F. Dolan, R.B. Diver and E. Aufderheide (1978). "Diesel Exhaust Particle Size Distributions – Fuel and Additive Effects." Society of Automotive Engineers Paper No. 780787.

Kleeman, M.J., J.J. Schauer and G.R. Cass (2000). "Size and composition distribution of fine particulate matter emitted from motor vehicles." Environmental Science & Technology **34**(7): 1132-1142.

Kuhns, H.D., C. Mazzoleni, M.-C. Chang, J.C. Chow, G. Parthasarathy, V. Etyemezian, H. Moosmuller, P. Barber, N. Nussbaum, S.K. Nathagoundenpalayam, S. Kohl, D. Nikolic,

J. Watson (2004) Meridian School Bus Biodiesel Evaluation Study: Draft Final Report. Prepared for OMPASS, Meridian, ID by DRI, Reno, NV, July 1, 2004.

Kuhns, H.D., C. Mazzoleni, H. Moosmüller, D. Nikolic, R.E. Keislar, P.W. Barber, Z. Li, V. Etyemezian and J.G. Watson (2004). "Remote sensing of PM, NO, CO, and HC emission factors for on-road gasoline and diesel engine vehicles in Las Vegas, NV." Science of the Total Environment, in press.

Kuhns, H., V. Etyemezian, J. Gillies, D. DuBois, S. Ahonen, C. Durham and D. Nikolic (2004). "Spatial Variability of Unpaved Road Dust PM_{10} Emission Factors near El Paso, Texas." Journal of the Air & Waste Management Association, in press.

Kuhns, H., V. Etyemezian, M. Green, K. Hendrickson, M. McGown, K. Barton and M. Pitchford (2003). "Vehicle-based road dust emission measurement - Part II: Effect of precipitation, wintertime road sanding, and street sweepers on inferred PM_{10} emission potentials from paved and unpaved roads." Atmospheric Environment **37**(32): 4573-4582.

Kuhns, H., V. Etyemezian, D. Landwehr, C. MacDougall, M. Pitchford and M. Green (2001). "Testing Re-entrained Aerosol Kinetic Emissions from Roads (TRAKER): a new approach to infer silt loading on roadways." Atmospheric Environment **35**(16): 2815-2825.

Kuhns, H.D. and V. Etyemezian (1999). Testing re-entrained aerosol kinetic emissions from roads (TRAKER): A new approach to silt loadings on roads in Clark County, Nevada. Las Vegas, NV, Desert Research Institute.

MacLaren, M. (2003). Survey of wood fuel providers in the Lake Tahoe region.

Mader, B. T. and J.F. Pankow (2000). "Gas/solid partitioning of semivolatile organic compounds (SOCs) to air filters - 1. Partitioning of polychlorinated dibenzodioxins, polychlorinated dibenzofurans and polycyclic aromatic hydrocarbons to teflon membrane filters." Atmospheric Environment **34**(28): 4879-4887.

Malm, W.C., M.L. Pitchford, M. Scruggs, J.F. Sisler, R.G. Ames, S. Copeland, K.A. Gebhart and D.E. Day (2000). Spatial and seasonal patterns and temporal variability of haze and its constituents in the United States: IMPROVE Report III. Ft. Collins, CO, Cooperative Institute for Research in the Atmosphere, Colorado State University. **ISSN: 0737-5352-47.**

Marjamäki, M., L. Ntziachristos, A. Virtanen, J. Ristimäki, J. Keskinen, M. Moisio, M. Palonen and M. Lappi (2002). "Electrical Filter Stage for the ELPI." SAE Technical Paper Series **2002**(01): 0055.

Moosmuller, H., C. Mazzoleni, P.W. Barber, H.D. Kuhns, R.E. Keislar and J.G. Watson (2003). "On-road measurement of automotive particle emissions by ultraviolet lidar and transmissometer: Instrument." Environmental Science & Technology **37**(21): 4971-4978.

Moosmuller, H., W.P. Arnott, C.F. Rogers, J.L. Bowen, J.A. Gillies, W.R. Pierson, J.F. Collins, T.D. Durbin and J.M. Norbeck (2001). "Time resolved characterization of diesel particulate emissions–1. Instruments for particle mass measurements." Environmental Science & Technology **35**(4): 781-787.

Park, K., F. Cao, D.B. Kittelson and P.H. McMurry (2003). "Relationship between particle mass and mobility for diesel exhaust particles." Environmental Science & Technology 37: 577-583.

Pedco Environmental, Inc. (1977) "Source Testing For Fireplaces, Stoves, And Restaurant Grills In Vail, Colorado," EPA Contract No. 68-01-1999, , Cincinnati, OH, December.

Pitchford, M.L., R.G. Flocchini, R.G. Draftz, T.A. Cahill, L.L. Ashbaugh and R.A. Eldred (1981). "Silicon in submicron particles in the southwest." Atmospheric Environment **15**: 321-333.

Pokharel, S.S., G.A. Bishop and D.H. Stedman (2002). "An on-road motor vehicle emissions inventory for Denver: An efficient alternative to modeling." Atmospheric Environment **36**(33): 5177-5184.

Shi, J.P., D. Mark and R.M. Harrison (2000). "Characterization of particles from a current technology heavy-duty diesel engine." Environmental Science & Technology **34**(5): 748-755.

Singer, B.C., T.W. Kirchstetter, R.A. Harley, G.R. Kendall and J.M. Hesson (1999). "A fuel-based approach to estimating motor vehicle cold-start emissions." Journal of the Air & Waste Management Association **49**(2): 125-135.

Sisler, J.F., W.C. Malm and K.A. Gebhart (1996). Spatial and seasonal patterns and long-term variability of the haze in the United States: An analysis of data from the IMPROVE network. Ft. Collins, CO, Cooperative Institute for Research in the Atmosphere. **ISSN 0737-5352-32**.

Turn, S.Q., B.M. Jenkins, J.C. Chow, L.C. Pritchett, D.E. Campbell, T.A. Cahill and S.A. Whalen (1997). "Elemental characterization of particulate matter emitted from biomass burning: Wind tunnel derived source profiles for herbaceous and wood fuels." Journal of Geophysical Research **102**(D3): 3683-3699.

Turn, S.Q., Jenkins, B.M., Chow, J.C., Pritchett, L.C., Campbell, D.E., Cahill, T.A. and Whalen, S.A. (1997). “Elemental characterization of particulate matter emitted from biomass burning: Wind tunnel derived source profiles for herbaceous and wood fuels.” Journal of Geophysical Research **102**(D3): 3683–3699.

Turpin, B.J., J.J. Huntzicker and S.V. Hering (1994). "Investigation of organic aerosol sampling artifacts in the Los Angeles Basin." Atmospheric Environment **28**(19): 3061-3071.

U.S. EPA (2002). User's Guide to MOBILE6.0 Mobile Source Emission Factor Model. Ann Arbor, MI, U.S. Environmental Protection Agency, Office of Transportation and Air Quality, Assessment and Standards Division. **EPA420-4-02-001**.

U.S. EPA. Method 28, Certification and Auditing of Wood Heaters 40 CFR Part 60, Appendix A, pp.988-1069, July 1, 1997.

U.S. EPA. Method 5G Determination of particulate matter emissions from wood heaters (Dilution tunnel sampling location) 40 CFR Part 60, Appendix A, pp.662-671, July 1, 1997.

U.S. EPA. Method 5H Determination of particulate matter emissions from wood heaters (Dilution tunnel sampling location) 40 CFR Part 60, Appendix A, pp.672-684, July 1, 1997.

U.S. Geological Survey. Facts about Lake Tahoe. http://tahoe.usgs.gov/facts.html (accessed April 30, 2004).

van Gulijk, C., J.C.M. Marijnissen, M. Makkee and J.A. Moulijn (2003). "Oil-soaked sintered impactors for the ELPI in diesel particulate measurements." Journal of Aerosol Science **34**: 635-640.

van Gulijk, C., J. M. Schouten, J. C. M. Marijnissen, M. Makkee and J. A. Moulijn (2001). "Restriction for the ELPI in diesel particulate measurements." Journal of Aerosol Science **32**(9): 1117-1130.

Watson, J.G., Robinson, N.F., Lewis, C.W., Coulter, C.T., Chow, J.C., Fujita, E.M., Conner, T.L. and Pace, T.G. "CMB8 applications and validation protocol for PM2.5 and VOCs." 1808.2d1, prepared for U.S. Environmental Protection Agency, Research Triangle Park, NC, by Desert Research Institute: Reno, NV, 1998.

Watson, J.G., E.M. Fujita, J.C. Chow, B. Zielinska, L.W. Richards, W.D. Neff and D. Dietrich (1998). Northern Front Range Air Quality Study. Final report. Reno, NV, Desert Research Institute.

Watson, J.G., Chow, J.C., Lowenthal, D.H., Robinson, N.F., Cahill, C.F. and Blumenthal, D.L. (2002). "Simulating changes in source profiles from coal-fired power stations: Use in chemical mass balance of $PM_{2.5}$ in the Mt. Zirkel Wilderness." Energy & Fuels **16**(2): 311-324.

Watson, J.G., E.M. Fujita, J.C. Chow, B. Zielinska, L.W. Richards, W.D. Neff and D. Dietrich (1998). Northern Front Range Air Quality Study. Final report. Reno, NV, Desert Research Institute.

Yanosky, JD; Williams, PL; MacIntosh, DL. 2002. A comparison of two direct-reading aerosol monitors with the federal reference method for PM2.5 in indoor air. *Atmospheric Environment* 36 (1): 107-113.

Zielinska, B., J.D. McDonald, T. Hayes, J.C. Chow, E.M. Fujita and J.G. Watson (1998). Northern Front Range Air Quality Study, Volume B: Source measurements. Reno, NV, Desert Research Institute.

10. APPENDICES

10.1. Daily Maps of TRAKER Routes

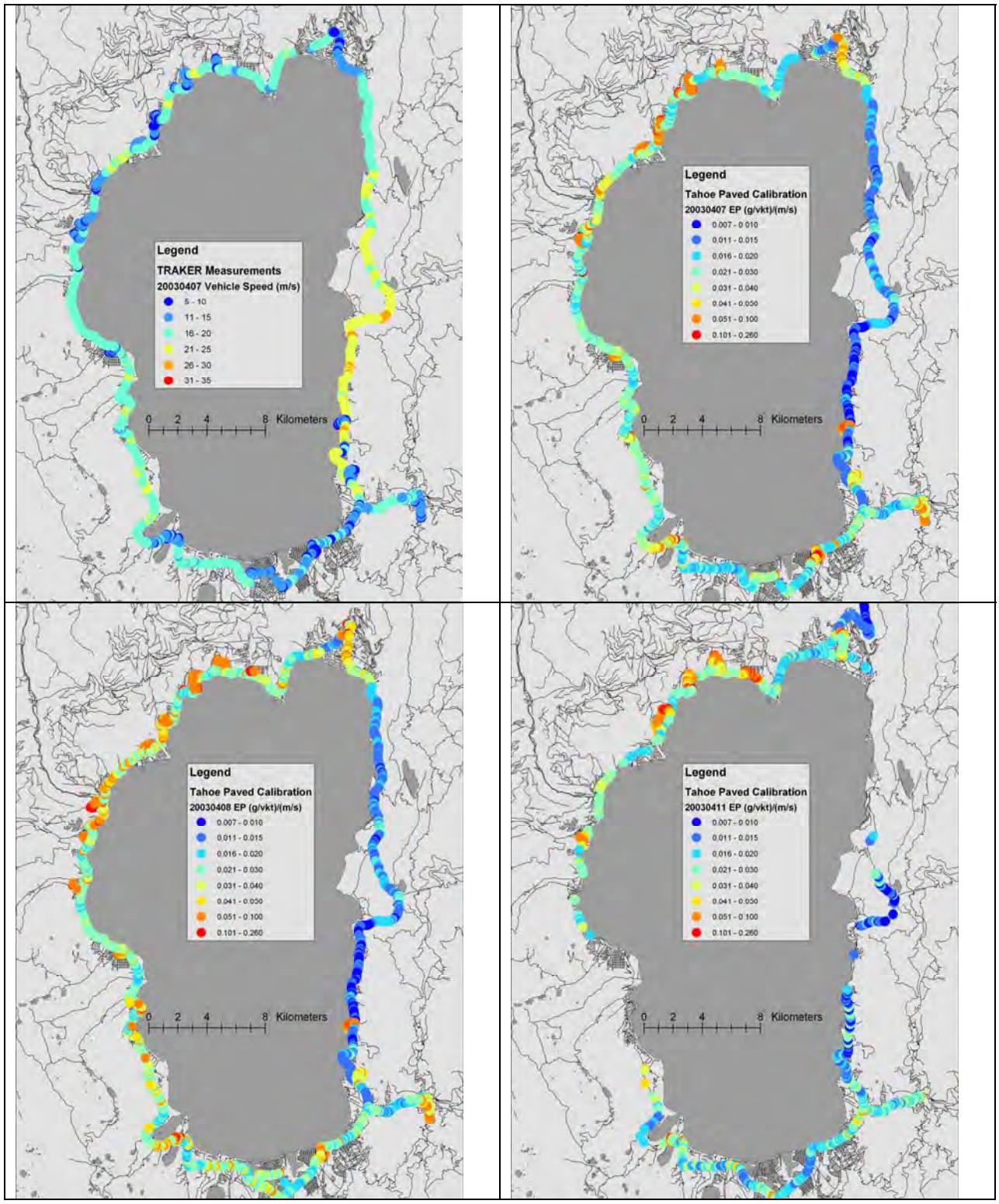
Legend
TRAKER Measurements
20030407 Vehicle Speed (m/s)
5 - 10
11 - 15
16 - 20
21 - 25
26 - 30
31 - 35
0 2 4 8 Kilometers
Legend
Tahoe Paved Calibration
20030407 EP (g/vkt)/(m/s)
0.007 - 0.010
0.011 - 0.015
0.016 - 0.020
0.021 - 0.030
0.031 - 0.040
0.041 - 0.050
0.051 - 0.100
0.101 - 0.260
0 2 4 8 Kilometers
Legend
Tahoe Paved Calibration
20030408 EP (g/vkt)/(m/s)
0.007 - 0.010
0.011 - 0.015
0.016 - 0.020
0.021 - 0.030
0.031 - 0.040
0.041 - 0.050
0.051 - 0.100
0.101 - 0.260
0 2 4 8 Kilometers
Legend
Tahoe Paved Calibration
20030411 EP (g/vkt)/(m/s)
0.007 - 0.010
0.011 - 0.015
0.016 - 0.020
0.021 - 0.030
0.031 - 0.040
0.041 - 0.050
0.051 - 0.100
0.101 - 0.260
0 2 4 8 Kilometers

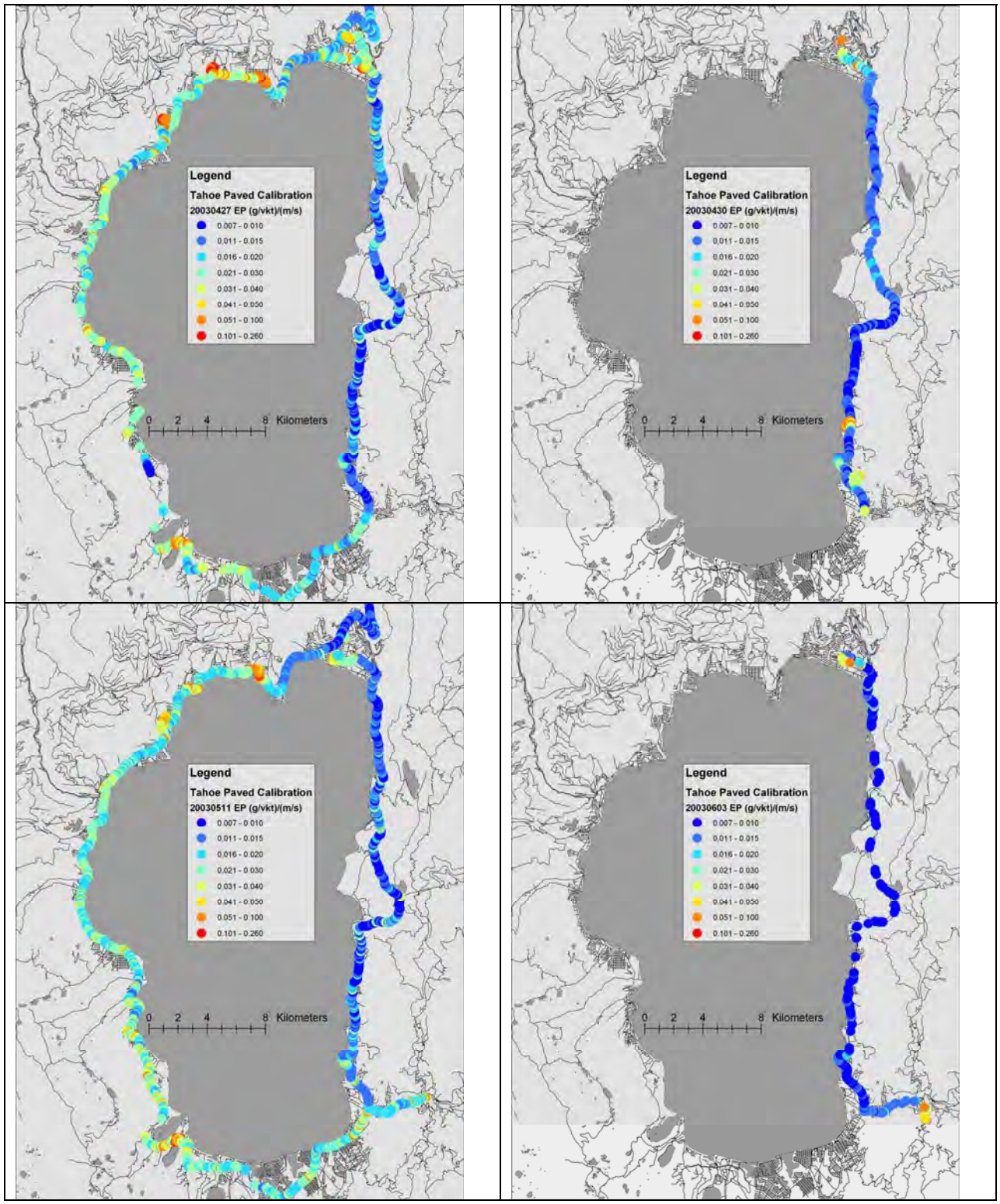
Legend
Tahoe Paved Calibration
20030427 EP (g/vkt)/(m/s)
0.007 - 0.010
0.011 - 0.015
0.016 - 0.020
0.021 - 0.030
0.031 - 0.040
0.041 - 0.050
0.051 - 0.100
0.101 - 0.260
0 2 4 8 Kilometers
Legend
Tahoe Paved Calibration
20030430 EP (g/vkt)/(m/s)
0.007 - 0.010
0.011 - 0.015
0.016 - 0.020
0.021 - 0.030
0.031 - 0.040
0.041 - 0.050
0.051 - 0.100
0.101 - 0.260
0 2 4 8 Kilometers
Legend
Tahoe Paved Calibration
20030511 EP (g/vkt)/(m/s)
0.007 - 0.010
0.011 - 0.015
0.016 - 0.020
0.021 - 0.030
0.031 - 0.040
0.041 - 0.050
0.051 - 0.100
0.101 - 0.260
0 2 4 8 Kilometers
Legend
Tahoe Paved Calibration
20030603 EP (g/vkt)/(m/s)
0.007 - 0.010
0.011 - 0.015
0.016 - 0.020
0.021 - 0.030
0.031 - 0.040
0.041 - 0.050
0.051 - 0.100
0.101 - 0.260
0 2 4 8 Kilometers

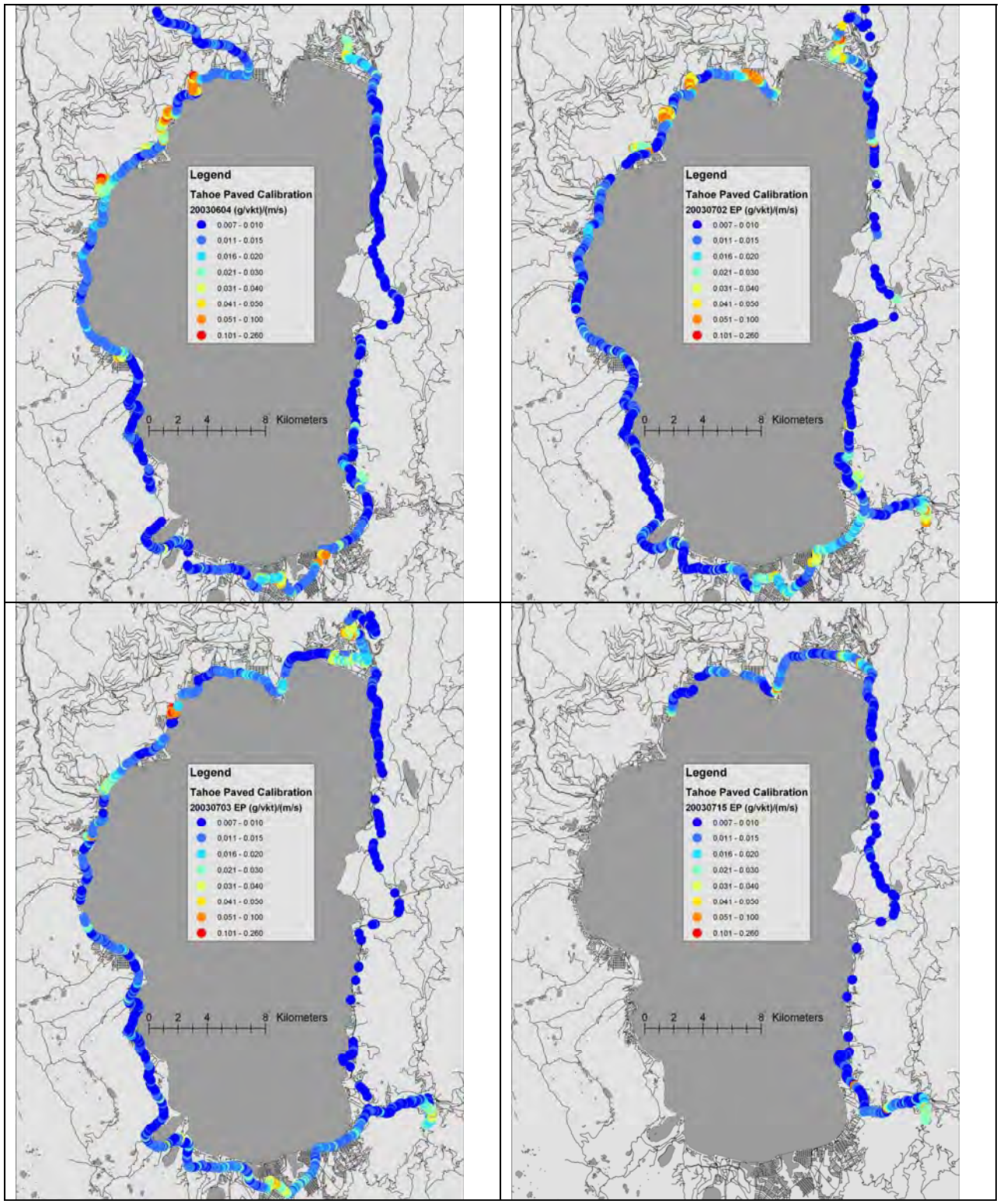
Legend
Tahoe Paved Calibration
20030604 (g/vkt)/(m/s)
0.007 - 0.010
0.011 - 0.015
0.016 - 0.020
0.021 - 0.030
0.031 - 0.040
0.041 - 0.050
0.051 - 0.100
0.101 - 0.260
0 2 4 8 Kilometers
Legend
Tahoe Paved Calibration
20030702 EP (g/vkt)/(m/s)
0.007 - 0.010
0.011 - 0.015
0.016 - 0.020
0.021 - 0.030
0.031 - 0.040
0.041 - 0.050
0.051 - 0.100
0.101 - 0.260
0 2 4 8 Kilometers
Legend
Tahoe Paved Calibration
20030703 EP (g/vkt)/(m/s)
0.007 - 0.010
0.011 - 0.015
0.016 - 0.020
0.021 - 0.030
0.031 - 0.040
0.041 - 0.050
0.051 - 0.100
0.101 - 0.260
0 2 4 8 Kilometers
Legend
Tahoe Paved Calibration
20030715 EP (g/vkt)/(m/s)
0.007 - 0.010
0.011 - 0.015
0.016 - 0.020
0.021 - 0.030
0.031 - 0.040
0.041 - 0.050
0.051 - 0.100
0.101 - 0.260
0 2 4 8 Kilometers

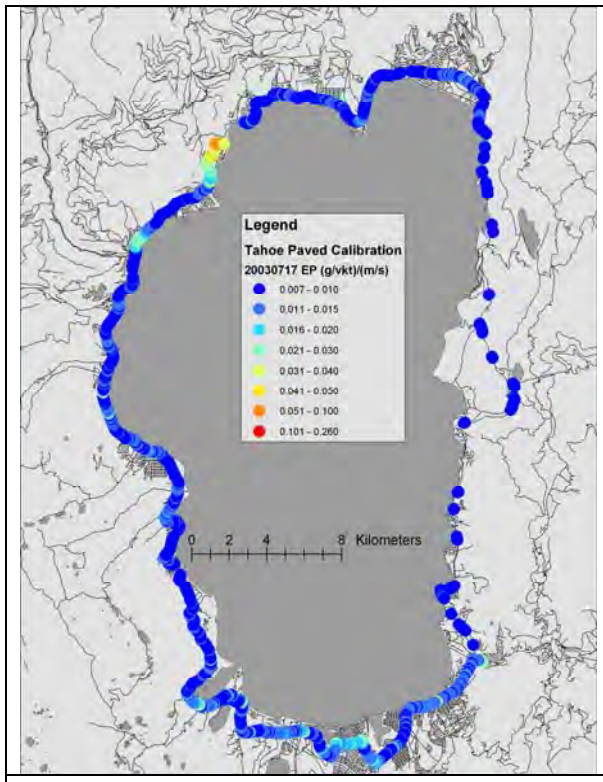 Legend Tahoe Paved Calibration 20030717 EP (g/vkt)/(m/s) 0.007 - 0.010 0.011 - 0.015 0.016 - 0.020 0.021 - 0.030 0.031 - 0.040 0.041 - 0.050 0.051 - 0.100 0.101 - 0.260 0 2 4 8 Kilometers	

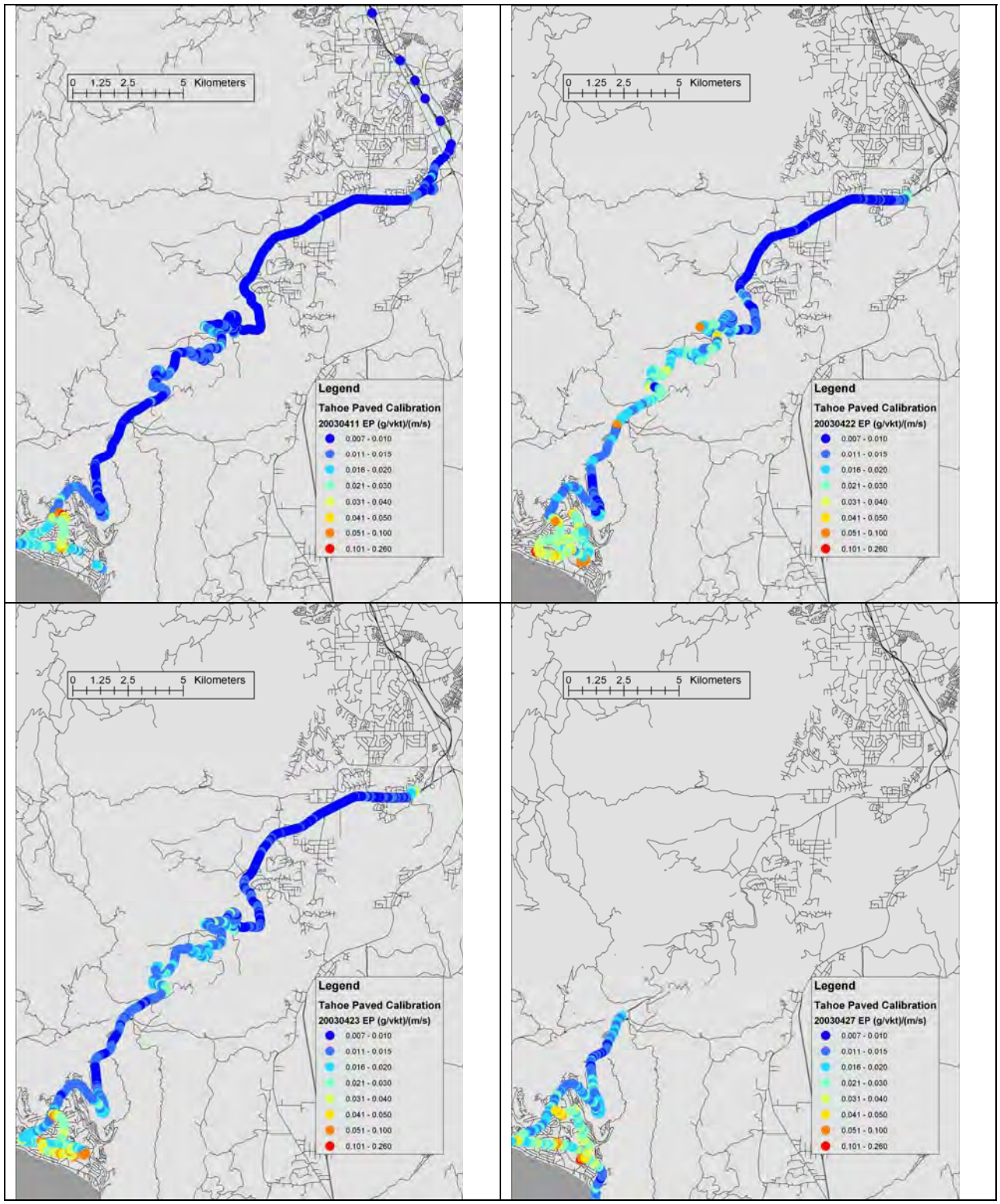
0 1.25 2.5 5 Kilometers
Legend
Tahoe Paved Calibration
20030411 EP (g/vkt)/(m/s)
0.007 - 0.010
0.011 - 0.015
0.016 - 0.020
0.021 - 0.030
0.031 - 0.040
0.041 - 0.050
0.051 - 0.100
0.101 - 0.260
0 1.25 2.5 5 Kilometers
Legend
Tahoe Paved Calibration
20030422 EP (g/vkt)/(m/s)
0.007 - 0.010
0.011 - 0.015
0.016 - 0.020
0.021 - 0.030
0.031 - 0.040
0.041 - 0.050
0.051 - 0.100
0.101 - 0.260
0 1.25 2.5 5 Kilometers
Legend
Tahoe Paved Calibration
20030423 EP (g/vkt)/(m/s)
0.007 - 0.010
0.011 - 0.015
0.016 - 0.020
0.021 - 0.030
0.031 - 0.040
0.041 - 0.050
0.051 - 0.100
0.101 - 0.260
0 1.25 2.5 5 Kilometers
Legend
Tahoe Paved Calibration
20030427 EP (g/vkt)/(m/s)
0.007 - 0.010
0.011 - 0.015
0.016 - 0.020
0.021 - 0.030
0.031 - 0.040
0.041 - 0.050
0.051 - 0.100
0.101 - 0.260

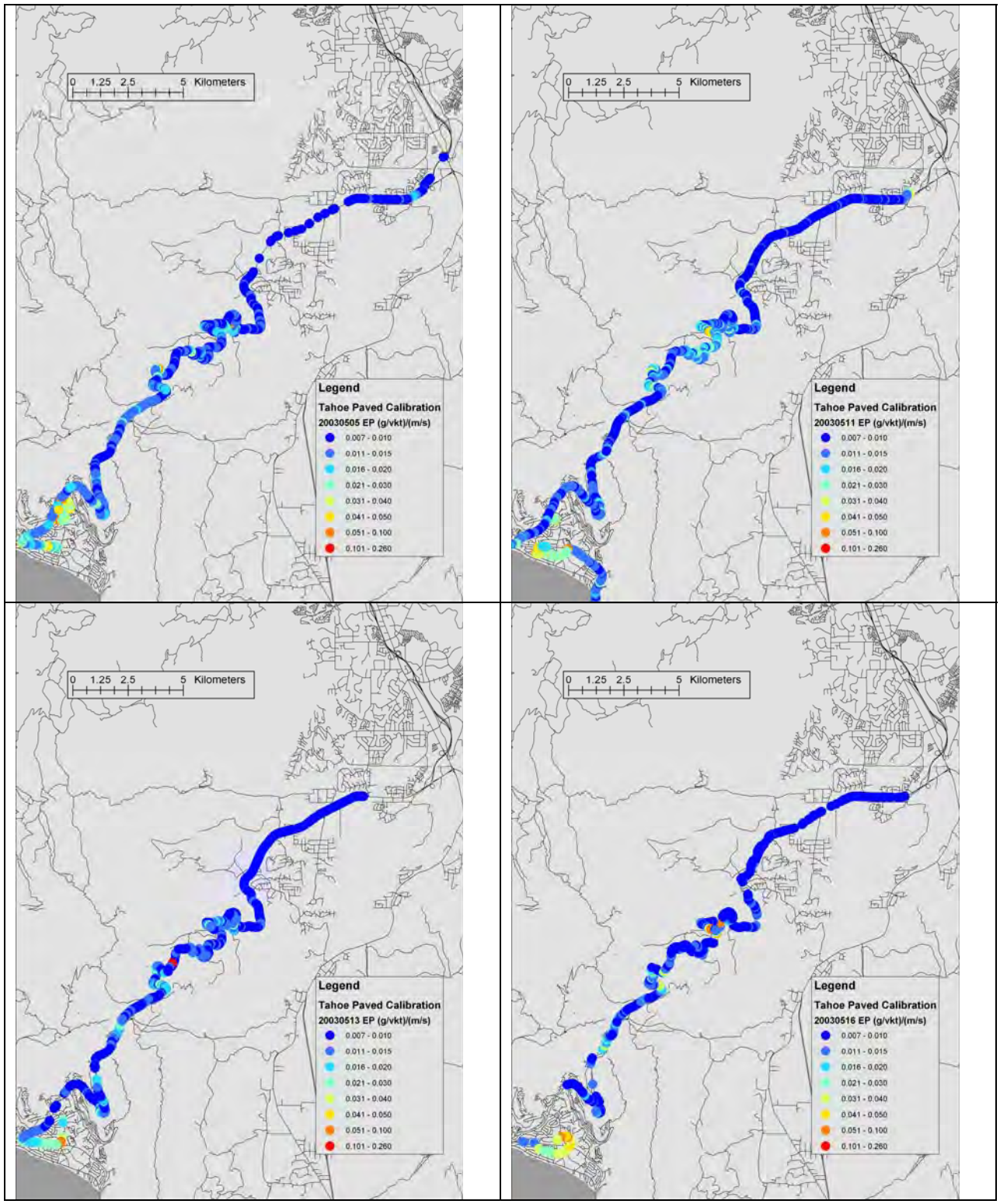
0 1.25 2.5 5 Kilometers
Legend
Tahoe Paved Calibration
20030505 EP (g/vkt)/(m/s)
0.007 - 0.010
0.011 - 0.015
0.016 - 0.020
0.021 - 0.030
0.031 - 0.040
0.041 - 0.050
0.051 - 0.100
0.101 - 0.260
0 1.25 2.5 5 Kilometers
Legend
Tahoe Paved Calibration
20030511 EP (g/vkt)/(m/s)
0.007 - 0.010
0.011 - 0.015
0.016 - 0.020
0.021 - 0.030
0.031 - 0.040
0.041 - 0.050
0.051 - 0.100
0.101 - 0.260
0 1.25 2.5 5 Kilometers
Legend
Tahoe Paved Calibration
20030513 EP (g/vkt)/(m/s)
0.007 - 0.010
0.011 - 0.015
0.016 - 0.020
0.021 - 0.030
0.031 - 0.040
0.041 - 0.050
0.051 - 0.100
0.101 - 0.260
0 1.25 2.5 5 Kilometers
Legend
Tahoe Paved Calibration
20030516 EP (g/vkt)/(m/s)
0.007 - 0.010
0.011 - 0.015
0.016 - 0.020
0.021 - 0.030
0.031 - 0.040
0.041 - 0.050
0.051 - 0.100
0.101 - 0.260

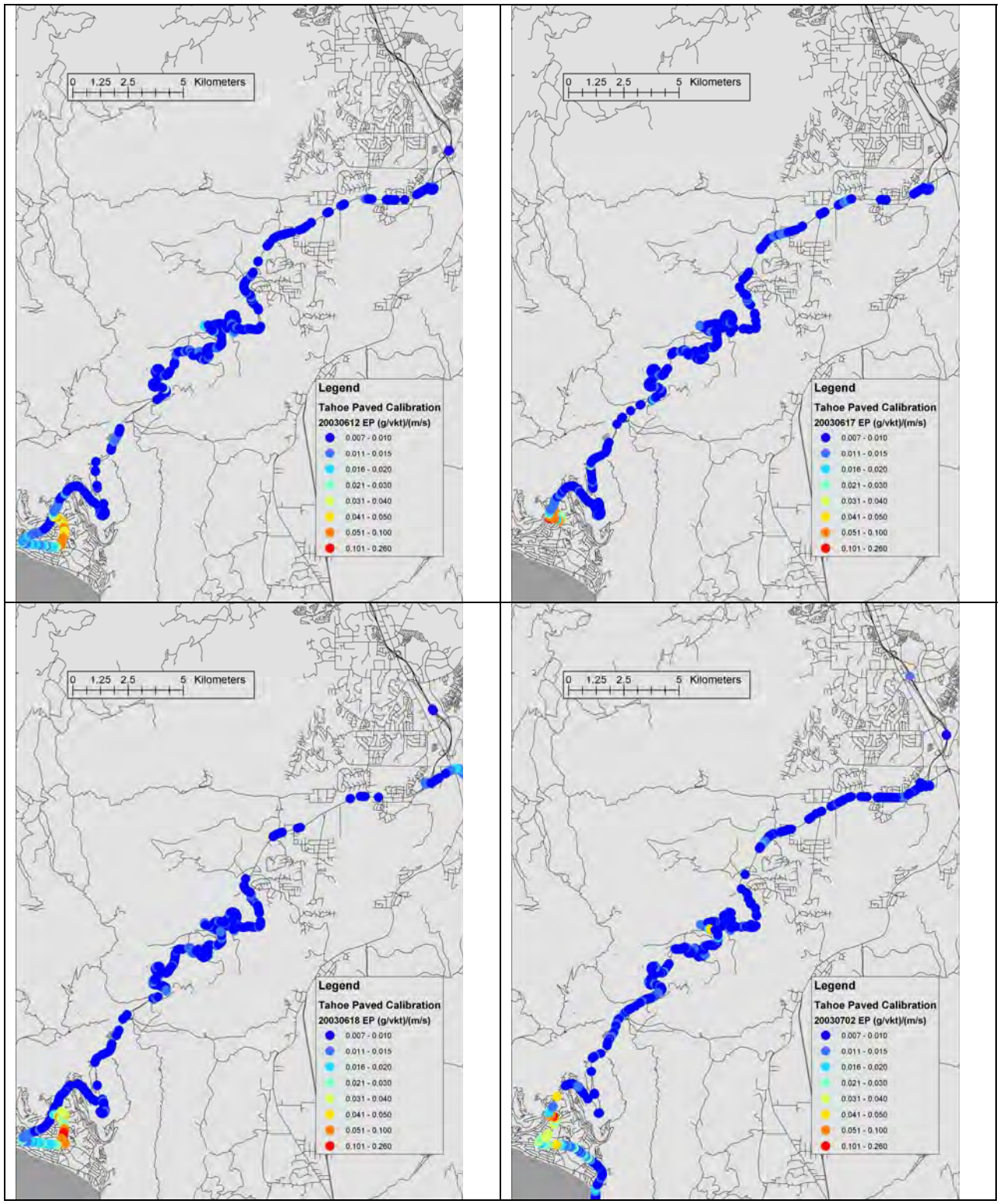
0 1.25 2.5 5 Kilometers
Legend
Tahoe Paved Calibration
20030612 EP (g/vkt)/(m/s)
0.007 - 0.010
0.011 - 0.015
0.016 - 0.020
0.021 - 0.030
0.031 - 0.040
0.041 - 0.050
0.051 - 0.100
0.101 - 0.260
0 1.25 2.5 5 Kilometers
Legend
Tahoe Paved Calibration
20030617 EP (g/vkt)/(m/s)
0.007 - 0.010
0.011 - 0.015
0.016 - 0.020
0.021 - 0.030
0.031 - 0.040
0.041 - 0.050
0.051 - 0.100
0.101 - 0.260
0 1.25 2.5 5 Kilometers
Legend
Tahoe Paved Calibration
20030618 EP (g/vkt)/(m/s)
0.007 - 0.010
0.011 - 0.015
0.016 - 0.020
0.021 - 0.030
0.031 - 0.040
0.041 - 0.050
0.051 - 0.100
0.101 - 0.260
0 1.25 2.5 5 Kilometers
Legend
Tahoe Paved Calibration
20030702 EP (g/vkt)/(m/s)
0.007 - 0.010
0.011 - 0.015
0.016 - 0.020
0.021 - 0.030
0.031 - 0.040
0.041 - 0.050
0.051 - 0.100
0.101 - 0.260

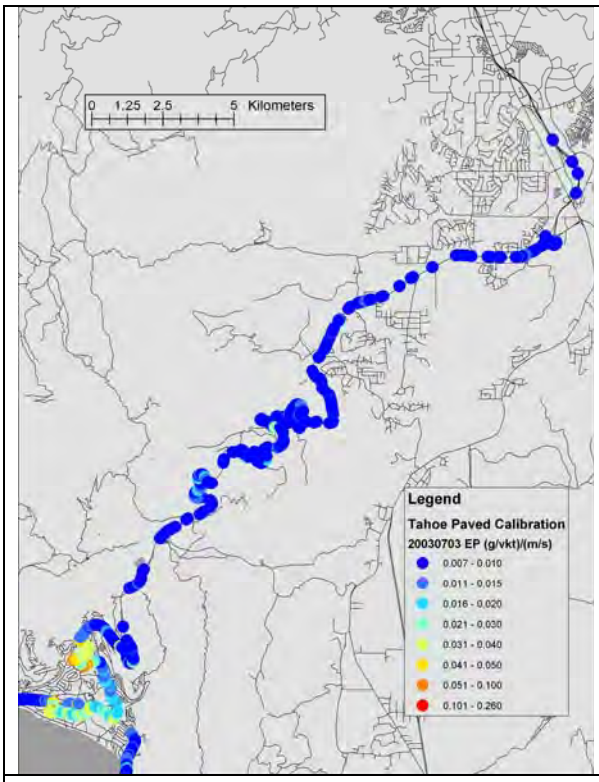
0 1.25 2.5 5 Kilometers
Legend
Tahoe Paved Calibration
20030703 EP (g/vkt)/(m/s)
0.007 - 0.010
0.011 - 0.015
0.016 - 0.020
0.021 - 0.030
0.031 - 0.040
0.041 - 0.050
0.051 - 0.100
0.101 - 0.260

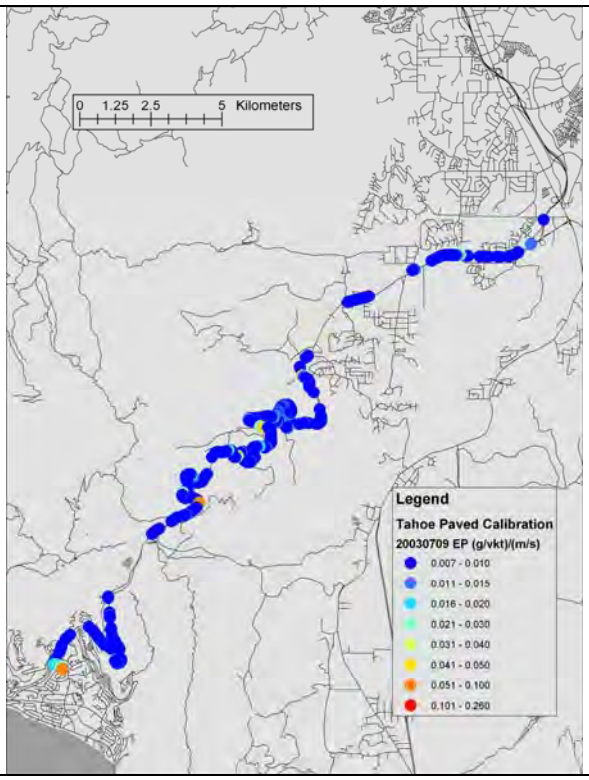
0 1.25 2.5 5 Kilometers
Legend
Tahoe Paved Calibration
20030709 EP (g/vkt)/(m/s)
0.007 - 0.010
0.011 - 0.015
0.016 - 0.020
0.021 - 0.030
0.031 - 0.040
0.041 - 0.050
0.051 - 0.100
0.101 - 0.260